JOURNAL OF CHROMATOGRAPHY

INTERNATIONAL JOURNAL ON CHROMATOGRAPHY, ELECTROPHORESIS AND RELATED METHODS

ELSEVIER

JOURNAL OF CHROMATOGRAPHY

CONTENTS

Contents (continued)

JOURNAL

of

CHROMATOGRAPHY

INTERNATIONAL JOURNAL ON CHROMATOGRAPHY,

ELECTROPHORESIS AND RELATED METHODS

ELSEVIER
AMSTERDAM — OXFORD — NEW YORK — TOKYO

CHROM. 22 643

Synthesis and protein-binding properties of spacer-free thioalkyl agaroses

ANASTASIOS DEMIROGLOU and HERBERT P. JENNISSEN*

Institut für Physiologische Chemie, Universität-GHS-Essen, Hufelandstrasse 55, D-4300 Essen 1 (F.R.G.)

(First received March 29th, 1990; revised manuscript received June 22nd, 1990)

ABSTRACT

Thioalkyl agaroses were synthesized by the tresyl chloride method. Activation of beaded agarose (Sepharose 4B) with tresyl chloride is a non-linear function of the tresyl chloride concentration in the activation mixture. The coupling of alkanethiols to tresyl chloride-activated Sepharose was successful in an alkaline medium containing 0.64 M sodium hydroxide. For the synthesis of thioalkyl agaroses (alkyl-S-Sepharose) with different surface concentrations of immobilized residues the activation time and not the tresyl chloride concentration should primarily be varied. At high tresyl chloride concentrations and long activation times the agarose matrix is destroyed. It was found that optimum concentrations of tresyl chloride lie between 0.05 and 0.15 M if activation times of 60 min are not exceeded. Alkyl-S-Sepharoses differ significantly in their protein adsorption properties from alkyl-N-Sepharoses prepared by the cyanogen bromide or carbonyl diimidazole (CDI) methods. Linkage of the alkyl residue via a thioether bridge enhances the adsorption of proteins by at least an order of magnitude. The results indicate a much stronger influence of the base (sulphur atom) of an immobilized alkyl residue in comparison with its tip (methyl group) than has hitherto been realized. The higher affinity of binding may be due to an interaction of the π-electrons of the sulphur atom with π-electrons in an aromatic amino acid of the protein in addition to the expected hydrophobic interaction between alkyl residue and protein.

INTRODUCTION

Alkyl agarose derivatives have been employed for the chromatographic separation of macromolecules (for reviews, see refs. 1 and 2) and for quantitative protein adsorption studies (for a review, see ref. 3). For the analysis of protein adsorption the interpretation of results is greatly facilitated if the residues are directly coupled to the inert hydrophilic agarose matrix as the interference of spacers with protein binding can never be fully ruled out. As cross-linked agarose gels pose a similar problem as spacer-containing gels only non-cross-linked agarose (Sepharose 4B) was employed.

As an alternative to the cyanogen bromide method of activation of agaroses (which may also introduce some charges [4,5]), the *p*-toluenesulphonyl chloride (tosyl chloride) method of activation [6,7] was introduced. Owing to the relatively low reactivity of tosyl chloride Mosbach and Nilsson [8] later introduced 2,2,2-trifluoroethanesulphonyl chloride (tresyl chloride) as a more potent activator of agarose for

subsequent coupling reactions. Tresylates of agarose (tresyl agarose) can react with primary amino groups or with thiol groups [8]. In the latter instance uncharged agarose derivatives are obtained. Except for preliminary reports [9–11], no method for the preparation of thioalkyl agaroses (alkyl-S-Sepharose) by the tresyl chloride method has been reported, probably owing to the difficulty of bringing alkanethiols into optimum solution for coupling to tresyl agarose. Since our initial report [9], thioether-bonded alkyl derivatives of agarose have been reported by Porath's group [12]. In their work thioalkyl derivatives (C_6–C_{14}) were coupled to Sepharose 6B by the bis-epoxide method via a spacer backbone consisting of ten carbon and three oxygen atoms.

     In this paper we report the coupling of homologous thioalkyl residues (C_2–C_4) without a spacer directly to the agarose matrix leading to alkyl-S-Sepharoses which can be employed for protein adsorption experiments and hydrophobic chromatography. These alkyl-S-agaroses have profoundly different protein-binding properties than the corresponding alkyl-N-agaroses produced by either the cyanogen bromide [13] or the carbonyl diimidazole [14] methods.

EXPERIMENTAL

Preparation of calmodulin
     Bovine testis calmodulin was isolated according to ref. 15 in conjunction with affinity chromatography [16]. The biological activity of purified calmodulin was tested with phosphorylase kinase [17] in the AutoAnalyzer test [18]. The calmodulin concentration necessary or half-maximum activation of phosphorylase kinase was 30–50 nM.

Preparation of alkyl-S-Sepharose
     Synthesis of n-[1-^{14}C]butanethiol. The method is based on the synthesis of thiols via S-alkyl thiuronium salts from thiourea [19].

$['^{14}C]$butyl bromide + thiourea $['^{14}C]$butyl thiuronium salt

$['^{14}C]$butyl thiuronium salt $['^{14}C]$butanethiol
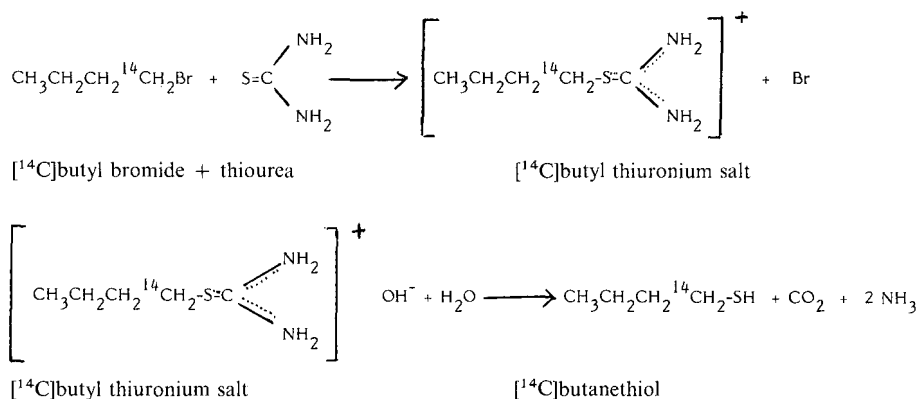
     In a 100-ml spherical flask, 15.5 g (0.2 mol) of thiourea and 10.2 ml of 95% ethanol were mixed with 25.5 g (0.18 mol) of butyl bromide to which *ca.* 2.5 mCi of n-[1-^{14}C]butyl bromide were added and boiled for 6 h in a reflux column. After

cooling, the butyl thiuronium salt crystallized. The liquid was removed by suction and the thiuronium salt was hydrolysed to butanethiol by the addition of 56 ml of 5 M sodium hydroxide solution under nitrogen and heating at 100°C for 2 h under reflux. After cooling, the solution was neutralized with 2 M hydrochloric acid. The thiol phase was isolated, dried with magnesium sulphate and fractionated on a Vigreau column. Finally 6.3 ml (5.48 g) of pure butanethiol was obtained, corresponding to a total yield of *ca.* 33%. The boiling point of the end product was 96–98°C.

Activation of agarose matrix with tresyl chloride. The method of activation of agarose (Sepharose 4B; Pharmacia, Uppsala, Sweden) with tresyl chloride is essentially derived from ref. 8 and can be described by the following reaction:
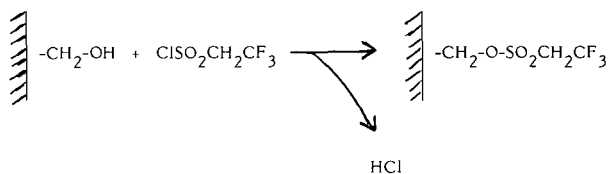
Accordingly, 40 g "wet weight" [4] of Sepharose 4B (Sepharose from which the exterior water had been removed by suction [4]) were washed at very low vacuum on a Büchner funnel with 20 volumes each of water, water–dioxane (3:1), water–dioxane (1:3) and finally water-free (dry) dioxane, which was then removed by suction (suction of air through the gel was avoided), yielding a cake of water-free Sepharose. To 10 g of water-free Sepharose, 0.5 vol. of dioxane and pyridine (2 ml/ml tresyl chloride) were added. Tresyl chloride in an amount of 10–40 μl/g water-free gel was added in the first minute in 3 vol. of dioxane with stirring. The gel was activated for 120 min with the temperature being held constant at 20°C (water-bath). Activation was stopped by washing the gel on a Büchner funnel with 20 volumes each of water-free (dry) dioxane, water–dioxane (1:3), water–dioxane (3:1) and finally water. The activation product, tresyl-Sepharose, can be stored in water at 4°C for several days without loss of reactivity [8].

For the measurement of time curves, 40 g "wet weight" of Sepharose 4B were activated by 0.052, 0.104, 0.156 and 0.208 M tresyl chloride respectively. At the indicated times samples of 1/4 to 1/8 volume of the incubation mixture with the activated gel were taken from the mixture, washed (see above) and incubated for 1 h with the alkaline alkanethiol solution as described below.

Coupling of alkanethiol (C_2–C_4) to tresyl-Sepharose. First experiments showed that tresyl-Sepharose could not be derivatized with butanethiol according to the general procedure described by Mosbach and Nilsson [8]. However, as will be shown (see Results), this problem was overcome by using another medium. The following reaction scheme describes the coupling reaction:
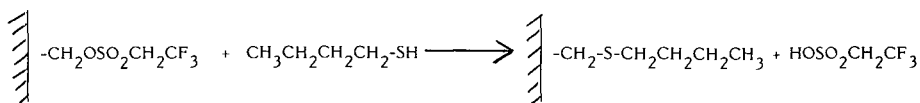
In a typical preparation, 10 g (wet weight) of tresyl-Sepharose were added to 18 ml of a solution containing 0.43 M alkanethiol in 1 M sodium hydroxide solution in a closed flask at room temperature. The final concentrations in the mixture after adding the Sepharose were 0.28 M alkanethiol and 0.64 M sodium hydroxide. The preparations can be scaled up by a factor of 25 without substantial changes in the coupling yield.

For the synthesis of a homologous series, *e.g.*, of three different thioalkyl agaroses of identical degree of substitution, a 3-fold amount (wet weight) of Sepharose 4B was activated with tresyl chloride as described above. After activation and washing (see above), three equal portions of the gel were added at room temperature to the corresponding alkaline alkanethiol solution, one of which was butanethiol solution containing the tracer n-[1-^{14}C]butanethiol. As the degree of substitution with butanethiol corresponded quantitatively to the degree of activation with tresyl chloride (see Results), an identical degree of substitution of the tresyl-Sepharose in the non-tracer-labelled alkanethiol solutions could be concluded from the n-[1-^{14}C]-butanethiol experiment.

After coupling, the gel was washed on a Büchner funnel with *ca.* 20 volumes each of water, acetone–water (1:3, v/v), acetone–water (3:1, v/v) and finally pure acetone until the thiol smell had disappeared. This acetone wash is essential for the removal of disulphides (as will be shown). By a subsequent reversal of the just described washing procedure, the gel was transferred back into an aqueous medium.

As has been discussed [7,20], the S–C bond is very resistant to acidic and alkaline conditions so that stable gel derivatives are obtained. In our experience, butyl-S-Sepharose gels can be stored in neutral aqueous solutions for up to 7 years without a significant loss of immobilized residues.

Micrographs of washed Sepharose 4B and Sepharose 4B derivatives (suspended in water containing bovine serum albumin, 1 mg/ml) were made with a Leitz microscope and a magnification of 140-fold [we thank Dr. F. Mehnert (University of Bochum) for taking the micrographs of Sepharose].

Synthesis of alkyl-N-Sepharoses

Uncharged alkyl-N-Sepharose was prepared according to the carbonyl di-imidazole (CDI) method of Bethell *et al.* [14]. [^{14}C]Butylamine and [^{14}C]ethylamine (New England Nuclear) were employed as tracers, yielding identical substitution results with the CDI method (see also refs. 4 and 21 for results with the cyanogen bromide method).

Solutions and reagents

Dioxane was distilled and subsequently stored in the presence of sodium wire. Highly pure commercial dioxane stored in the presence of sodium wire gave similar results. Water was first deionized and then distilled before use. All other reagents were of analytical-reagent grade. Tresyl chloride was obtained from Fluka.

Analysis of tresyl- and butanethiol-Sepharose

Sulphur determination. Tresyl- and butyl-Sepharose were dried under vacuum at 40°C for *ca.* 2 days (see below). About 20 mg of the dried gel were transferred to a heat stable vial and solid sodium was melted and dripped into the gel. The vial was heated to

a red glow and then transferred into 5 ml of water, where it burst. The aqueous solution of sodium salts was filtered and employed for sulphur determination by iodimetric titration according to Kimball *et al.* [22]. The analyses were done in triplicate.

Radioactive tracer analysis. The degree of substitution was monitored by adding *n*-[1-^{14}C]butanethiol to the coupling mixture in an amount of 0.05–0.25 μCi/ml [4]. The amount coupled was determined after acid hydrolysis [4] of the *n*-[1-^{14}C]butane-thiol-labelled agarose (colourless hydrolysate) followed by liquid scintillation counting [4]. The analyses were done in triplicate.

Determination of gel parameters (packed gel, dry gel, surface area)

The volume of packed gel was determined as previously described [4], giving the degree of substitution in μmol/ml packed gel [4]. The dry weight of the agarose was either determined as described previously [23] or after drying in vacuum for *ca.* 2 days at 40°C (see above). The degree of substitution can then also be expressed in μmol/g dry weight, correcting for errors due to shrinking of the gel during activation or coupling [24]. All analyses were done in triplicate. In general, 1 ml of packed Sepharose leads to *ca.* 30 mg (29–32 mg) of agarose mass after drying [23]. With substituted gels the weight of the dry agarose was normalized, *i.e.*, corrected to net dry weight (= total weight of dried alkyl gel minus the weight of incorporated thioalkyl residues) [24]. Finally, the degree of substitution can either be expressed as a molecular substitution ratio in mol alkyl residue/mol anhydrodisaccharide [24] based on a molecular weight of 306 for an anhydrodisaccharide unit, or as a surface concentration in nmol/m^2 [25,26]. The values for the surface concentration in nmol/m^2 are based on a concentration of anhydrodisaccharide units of *ca.* 100 μmol per 30 mg of dry agarose (see also ref. 23) and a mean surface area of *ca.* 1.3 nm^2 per anhydrodisaccharide unit (with the assumption that this corresponds to the water-accessible surface area) in the final quaternary structure of agarose [27]. From these values a specific surface area of the agarose strands of 2610 m^2/g dry agarose can be calculated. Accordingly, for alkyl-substituted agarose 1 μmol/ml packed gel corresponds to 12.8 nmol/m^2 for non-shrunken agarose [26].

Protein was determined according to Lowry *et al.* [28] on an AutoAnalyzer.

Analytical hydrophobic affinity chromatography of calmodulin [16]

The chromatographic analysis of alkyl agaroses with calmodulin was performed on columns (12 × 0.9 cm I.D.) containing 2 ml of packed gel at room temperature. The gel was washed and equilibrated with buffer A (20 mM Tris–HCl, 1 mM CaCl$_2$, pH 7.0). A sample of 1 mg of purified calmodulin was applied in a volume of 1 ml (buffer A). Unless stated otherwise, fractions of 1.5 ml were collected. The column was then washed with 9 ml of buffer A and subsequently with 9 ml of buffer B (= buffer A + 0.3 M NaCl). Adsorbed calmodulin was eluted with buffer C (20 mM Tris–HCl, 0.3 M NaCl, 10 mM EGTA, pH 7.0). Flow was achieved by gravity. Only fresh, unregenerated gel was used.

RESULTS

Synthesis of butyl-S-Sepharoses

Coupling mixture. Table I demonstrates that even at high tresyl chloride

TABLE I

DEPENDENCE OF THE COUPLING OF [^{14}C]BUTANETHIOL TO TRESYL-SEPHAROSE 4B ON THE COUPLING MEDIUM

Sepharose was activated with tresyl chloride (0.208 M) for 24 h at room temperature as described and then coupled as follows. (a) In the first coupling experiment, 10 g (wet weight) of tresyl-Sepharose were washed with water–dioxane–acetone (1:2:6, v/v/v) and then added to 14.4 ml of solution A (4 ml of [^{14}C]butanethiol plus 10.4 ml of acetone). To the washed gel in solution A were added 3.6 ml of solution B (1.2 ml of 0.5 M Na$_2$CO$_3$ plus 2.4 ml of dioxane) and this mixture was incubated for 15 h at room temperature. (b) In the second experiment, 10 g (wet weight) of tresyl-Sepharose were added to 18 ml of solution C (1 M NaOH, 0.43 M [^{14}C]butanethiol) and incubated for 15 h at room temperature. In both experiments after 15 h the coupled gel was washed with acetone and analysed for incorporation of [^{14}C]butanethiol as described.

Coupling medium	[^{14}C]Butanethiol (mol/l)	Degree of substitution (μmol butyl residues/ml packed gel)
Carbonate–acetone–dioxane	1.3	2
0.64 M NaOH	0.28	56

concentrations (0.208 M) in the incubation mixture, only very little (2 μmol/ml packed gel) butanethiol can be coupled to tresyl-Sepharose in a carbonate–acetone–dioxane medium, a solution which is capable of solubilizing high concentrations (1.3 M) of butanethiol. In contrast, solubilizing butanethiol for coupling in pure 0.64 M sodium hydroxide (= alkaline alkanethiol) leads to a nearly 30-fold increase in the degree of substitution (Table I).

Washing procedure. The "coupling values" obtained can, however, still be misleading as they depend strongly on the washing procedure, as is shown in Table II. Failure to wash with an organic solvent (*e.g.*, acetone) leads to highly erroneous degrees of substitution. This is most easily demonstrated by incubating non-activated,

TABLE II

INFLUENCE OF THE WASHING PROCEDURE ON THE RETENTION OF [^{14}C]BUTANETHIOL ON NON-ACTIVATED SEPHAROSE 4B AND ON THE DEGREE OF SUBSTITUTION OF TRESYL-SEPHAROSE WITH [^{14}C]BUTANETHIOL

5 g (wet weight) of non-activated Sepharose 4B was added to 1.8 vol. of 1 M NaOH–0.43 M [^{14}C]butanethiol (± 0.107 M H$_2$O$_2$) and incubated at room temperature for 7 h. Tresyl-Sepharose (activated with 0.156 M tresyl chloride for 1 h) was coupled by the same method (but without H$_2$O$_2$) for 20 h at room temperature. After coupling the gels were washed either with 20 vol. of 1 M NaOH or 20 vol. of water, water–acetone (3:1), water–acetone (1:3) and acetone (followed by a wash in the reverse order to return to the aqueous medium).

Gel	Degree of substitution (μmol butyl residues/ml packed gel)	
	Wash with 1 M NaOH or KOH	Wash with acetone
Sepharose 4B (non-activated):		
Incubation with [^{14}C]butanethiol + NaOH	10	0.17
Incubation with [^{14}C]butanethiol + NaOH + H$_2$O$_2$	64	0.64
Tresyl-Sepharose: coupling with [^{14}C]butanethiol + NaOH	37	22.2

control Sepharose 4B in alkaline [^{14}C]butanethiol followed by a wash with 1 M sodium hydroxide or potassium hydroxide (Table II). Apparently 10 μmol butyl residues/ml packed gel are coupled. In a second experiment, non-activated Sepharose was incubated in alkaline [^{14}C]butanethiol together with hydrogen peroxide as oxidant of the thiol. The apparent degree of substitution of the gel with butanethiol increases to over 60 μmol/ml packed gel. The non-covalent nature of thiol retention on the gel is easily demonstrated by washing it with acetone, which reduces the amount retained (probably insoluble disulphide) by a factor of 100. Acetone-stable radioactivity was therefore taken as evidence for covalent coupling of the thiol to the tresyl-activated Sepharose. In the present case with tresyl-Sepharose (Table II) a true coupling yield of $ca.$ 22 μmol butyl residues/ml packed gel is obtained.

Time dependence of coupling. Fig. 1 shows the time dependence of the coupling of n-[1-^{14}C]butanethiol to tresyl-Sepharose (activated with 0.208 M tresyl chloride) for 15 h. Maximum coupling is achieved after 1 h. As the amount of butanethiol is in $ca.$ 10-fold excess over the amount of immobilized tresyl leaving groups on the activated gel, a quantitative substitution of these groups and not a limitation of available butanethiol seems likely to be the reason for termination of the reaction. As a consequence of these results, all further coupling mixtures (Tables II–V, Figs. 2–5) were incubated for 60 min at room temperature only.
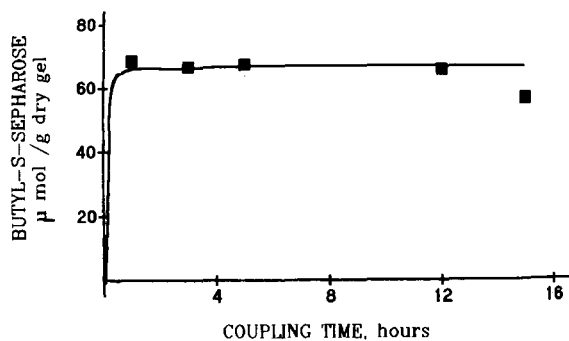
Fig. 1. Time dependence of the coupling of [^{14}C]butanethiol to tresyl-Sepharose at room temperature. 40 g (wet weight) of tresyl-Sepharose (activated by 0.208 M tresyl chloride) was added to 72 ml of 1 M NaOH–0.43 M [^{14}C]butanethiol. At the indicated times $ca.$ one fifth of the coupling mixture was taken as a sample and the reaction was stopped by washing with acetone on a Büchner funnel as described. The degree of substitution was determined by measuring the ^{14}C incorporation (0.028 μCi/ml) as described.

Dependence of activation on tresyl chloride concentration. Table III shows the non-linear dependence of the degree of substitution with tresyl and butyl residues on the initial concentration of tresyl chloride in the activation mixture. The immobilized tresyl chloride and butanethiol were determined in parallel by a determination of sulphur in the activated gel before and after coupling (Table III, series I) and by radioactivity measurements of the coupled gel (Table III, series I and II). The amount of tresyl chloride covalently incorporated into the gel from the incubation mixture was between 3 and 8%. Therefore, the initial concentrations of tresyl chloride only change insignificantly as a result of the activation procedure itself. Table III demonstrates that

TABLE III

DEPENDENCE OF THE DEGREE OF SUBSTITUTION OF SEPHAROSE 4B ON THE TRESYL CHLORIDE CONCENTRATION IN THE INCUBATION MIXTURE

Sepharose 4B was activated with tresyl chloride at the given concentration for 60 min. The degree of substitution was measured by determination of elemental sulphur in tresyl-Sepharose and butyl-S-Sepharose (series I) and by tracer analysis of butyl-S-Sepharose with [14C]butanethiol (series I and II). In series I activation was performed in dioxane distilled and stored over sodium wire; in series II it was performed in commercial dioxane stored over sodium wire.

Tresyl chloride (mol/l)	Sulphur determination (μmol/ml packed gel)		[14C]tracer analysis (μmol/ml packed gel)
	Tresyl-Sepharose	Butyl-Sepharose	
Series I:			
0.052	–	–	2.6
0.104	9.6	9.1	12.6
0.156	21.8	26.4	22.5
0.208	59.0	63.2	54.7
Series II:			
0.040			3.5
0.060			3.0
0.080			1.9
0.090			19.3
0.100			32.0
0.150			37.0

the sulphur and the butyl residue determinations yield almost identical results within the experimental error. From this experiment, coupling yields of *ca.* 100% can be calculated.

Progress curves of tresylation. As the coupling yield is *ca.* 100%, tresylation can be measured via ^{14}C incorporation of alkanethiol into tresyl-Sepharose. The time dependence of tresylation as measured in this manner is shown in Fig. 2. At low tresyl chloride concentrations (Fig. 2A) there is a primary incorporation phase which reaches a plateau region after 40–120 min. However, as the concentration of tresyl chloride is increased (Fig. 2B), a secondary incorporation phase can be seen to occur from the previous plateau phase after *ca.* 80 min, leading to a 2–3-fold additional increase in immobilized butanethiol residues over the plateau region. Finally, at very high tresyl chloride concentrations (0.208 *M*) a true plateau phase is absent and the degree of substitution increases continuously from the onset (Fig. 2B). Tresyl chloride concentrations above *ca.* 0.21 *M* lead to a destruction of the agarose beads (not shown).

Fig. 3 illustrates that the secondary incorporation phase of tresylation and coupling is not due simply to a volume decrease (shrinkage) of the substituted agarose. A recalculation of the original data for the degree of substitution (Fig. 3A) on the basis of the determined dry weight (Table IV) of the agarose leads to lower values but does not abolish the secondary incorporation phase (Fig. 3B).
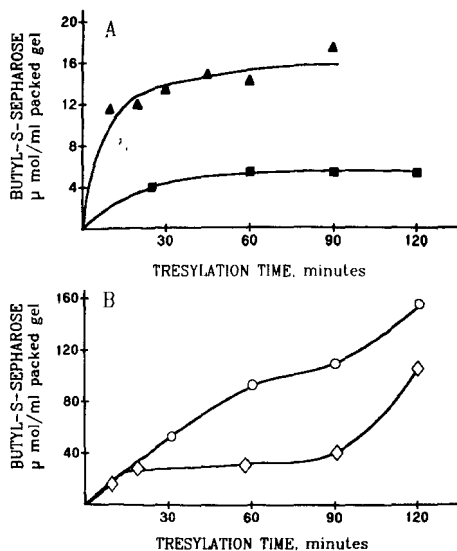
Fig. 2. Progress curves of the tresylation of Sepharose 4B at different concentrations of tresyl chloride in the activation mixture. At each concentration of tresyl chloride (see below) 40 g (wet weight) of Sepharose 4B was activated. At the indicated times *ca.* 1/4–1/8 vol. of the incubation mixture was taken as a sample, washed with dioxane and transferred to aqueous medium as described. The obtained gel (*ca.* 5–10 g, wet weight) was then added to 1.8 vol. of 1 *M* NaOH–0.43 *M* [^{14}C]butanethiol and incubated for 1 h at room temperature. The degree of substitution was determined by measuring the incorporation of [^{14}C]butanethiol. (A) ■ = 0.052 *M*; ▲ = 0.104 *M*. (B) ◇ = 0.156 *M*; ○ = 0.208 *M*.

TABLE IV

SYNTHESIS OF ALKYL-S-SEPHAROSES OF DIFFERENT DEGREES OF SUBSTITUTION AND DIFFERENT ALKYL CHAIN LENGTH IN PREPARATIVE AMOUNTS

For the butyl-S-Sepharose series, *ca.* 210 g (wet weight) of Sepharose 4B were incubated with the given concentration of tresyl chloride for the specified time and then coupled to [^{14}C]butanethiol for 1 h. For the homologous series (C$_2$–C$_4$), *ca.* 50 g (wet weight) of Sepharose 4B were activated and coupled as described. For definition of μmol/ml packed gel, μmol/g dry gel, mol/mol anhydrodisaccharide and nmol/m^2, see Experimental.

Gel	Tresyl chloride (mol/l)	Activation time (min)	Corrected dry weight (mg/ml packed gel)	Degree of substitution			
				μmol butanethiol/ml packed gel	μmol/g dry gel	mol butanethiol/mol anhydrodisaccharide	nmol/m^2
Sepharose 4B			32.0				
Butyl-S-Sepharose	0.052	15	33.6	1.7	50.6	0.015	19.4
	0.156	1	30.1	5.2	172.7	0.053	66.2
	0.156	2	32.0	8.9	278.1	0.085	106.6
	0.156	3.5	37.1	12.0	323.4	0.099	123.9
	0.156	5	33.6	20.7	616.1	0.189	236.1
	0.156	20	38.4	29.0	755.2	0.219	289.3
	0.156	60	36.5	28.4	778.1	0.238	298.1
	0.156	90	37.6	40.7	1082.4	0.331	414.7
	0.156	120	62.4	107.0	1714.7	0.524	657.0
Ethyl-S-Sepharose	0.156	20	34.1	25.0	733.1	0.224	282.0
Propyl-S-Sepharose	0.156	20	36.6	25.0	683.1	0.209	262.7
Butyl-S-Sepharose	0.156	20	36.5	25.0	684.9	0.210	263.4
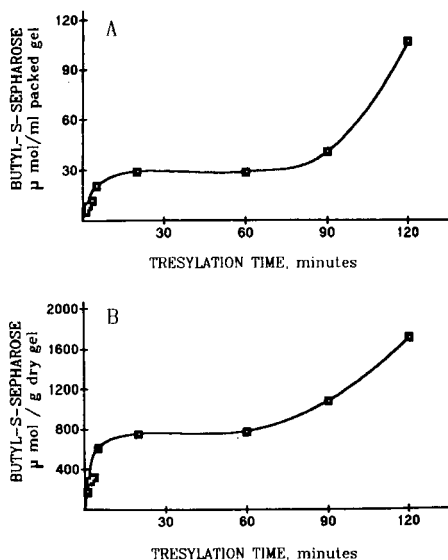
Fig. 3. Biphasic activation of Sepharose 4B by the tresyl chloride method. The degree of substitution with tresyl residues was determined by the quantitative substitution of tresyl leaving groups with [^{14}C]butanethiol as described. The concentration of tresyl chloride in the incubation mixture was 0.156 M. The curves are composed of a primary incorporation phase, a plateau phase and a secondary incorporation phase. The data demonstrate that the secondary incorporation phase is not a result of the dimensions employed for expressing the data and thus is not a result of gel shrinkage. (A) Degree of substitution expressed in μmol/ml packed gel. (B) Degree of substitution expressed in μmol/g dry gel.

Microscopic analysis. Fig. 4 demonstrates that macroscopically tresyl- and butyl-S-Sepharose do not change their morphology significantly in comparison with the unsubstituted gel. At high degrees of substitution polygonal beads occur.

Controlled variation of the degree of substitution. The foregoing data show that the synthesis of butyl-S-Sepharoses with different degrees of substitution is complex and depends non-linearly (Table II) on the tresyl chloride concentration in the activation mixture. Therefore, a series of gels with different degrees of substitution (without disturbance by the secondary incorporation phase) are not easily obtained if the tresyl chloride concentration is varied. These problems can be circumvented by varying the activation time at a constant tresyl chloride concentration of, *e.g.*, 0.156 M (Table III) to obtain any degree of substitution above 5 μmol/ml packed gel. If one adheres to the primary incorporation phase only (*i.e.*, times below the second increment 1–60 min, Fig. 2B), homogeneity of the gels appears to be obtainable.

In order to avoid activation times shorter than 1 min, gels below 5 μmol/ml packed gel were synthesized at a lower tresyl chloride concentration, *e.g.*, 0.052 M. Table III also demonstrates that between 1 and 20 min of activation the mean dry weight of the agaroses (corrected for the weight of the immobilized alkyl residues) increases by 4–6% compared with the control, indicating a negligible gel shrinkage (50–755 μmol/g dry agarose). A maximum gel shrinkage to *ca.* 50% of the initial agarose volume is indicated by a doubling of the dry weight/ml packed gel for the gel
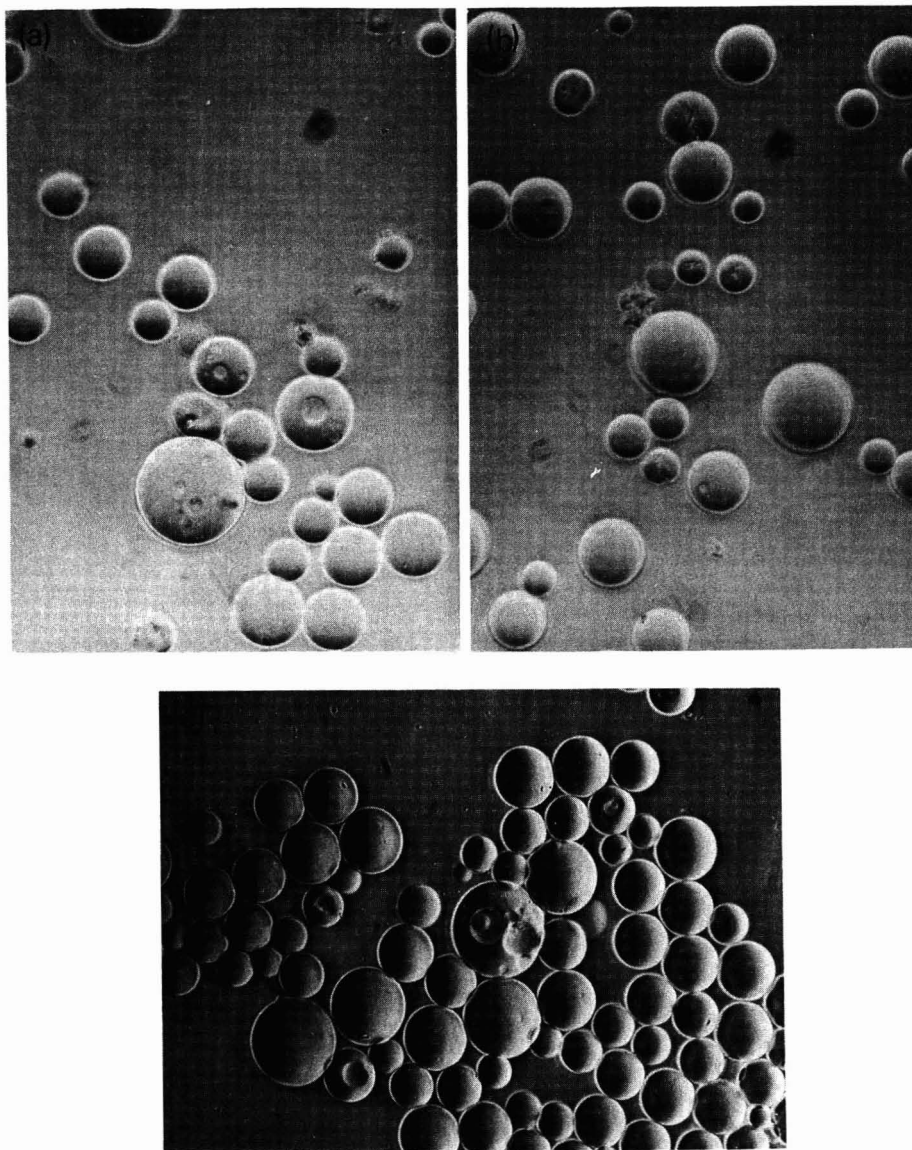
Fig. 4. Micrographs of tresyl- and butyl-S-Sepharose 4B. Magnification *ca.* 140-fold. The diameter of the spheres is between 40 and 140 μm (Pharmacia). About 100 μl of packed gel of the respective Sepharose were suspended in 1 ml of 1% bovine serum albumin to eliminate aggregation of the spheres. The gel suspension was degassed under vacuum for *ca.* 5 min and then spread on a microscope plate for analysis. Photographs were taken with a Leica camera mounted on a Leitz microscope (Agfa-Ortho 25 film). The degrees of substitution were determined by (A) elemental sulphur determination and (B) [^{14}C]butanethiol incorporation. (A) Tresyl-Sepharose 4B (22 μmol/ml packed gel); (B) butyl-S-Sepharose 4B (23 μmol/ml packed gel); (C) control Sepharose 4B.

activated for 120 min (1715 μmol/g dry agarose). Therefore, except for very high degrees of substitution (over 1000 μmol/g dry weight), data can be expressed either on the basis of μmol/ml packed gel or μmol/g dry gel without introducing large errors. A maximum of 0.5 mol alkyl residue/anhydrodisaccharide was introduced into the agarose, indicating that only about half of the available primary OH groups are derivatized on the most highly substituted gel. In Table IV the data are also expressed as surface concentrations (range 19–650 nmol/m^2), making a comparison with other synthetic surfaces possible.
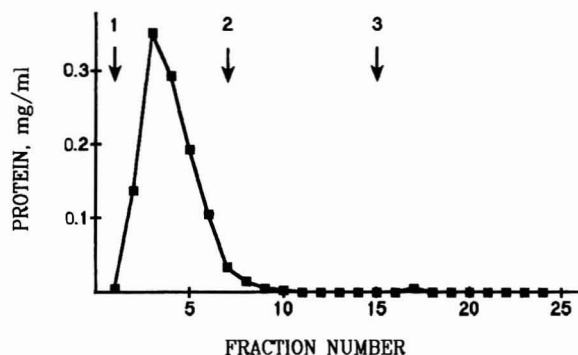
Fig. 5. Adsorption of calmodulin on butyl-N-Sepharose as measured by hydrophobic affinity chromato-graphy. Calmodulin (1 mg) was applied to 2 ml of packed gel of uncharged butyl-N-Sepharose (33 μmol/ml packed gel) on a column (12 cm × 0.9 cm I.D.) in a sample volume of 1 ml in buffer A (with 1 mM CaCl$_2$). Arrow 1, wash with buffer A; arrow 2, wash with buffer B (with 300 mM NaCl); arrow 3, elution with buffer C (with 10 mM EGTA). The fraction volume was 1.5 ml. Flow through the column was driven by gravity.

Protein binding properties of alkyl-S-Sepharoses

Influence of alkyl chain length [29]. Alkyl-S-Sepharoses are very efficient adsorbents of proteins, as can be exemplified by experiments with the Ca^{2+}-binding protein calmodulin. In a control experiment (Fig. 5), calmodulin is not adsorbed on a butyl-N-Sepharose containing 33 μmol/ml packed gel. In the homologous series (C$_2$–C$_4$) of alkyl-S-Sepharose in Fig. 6 (constant degree of substitution: 25 μmol/ml packed gel; Table IV), it can be seen that the adsorption of calmodulin is dependent on the chain length of the immobilized thioalkyl residue. Butyl-S-Sepharose (Fig. 6C) is a very strong adsorbent of calmodulin and even propyl-S-Sepharose (Fig. 6B) adsorbs over 50% of the applied calmodulin (42% "reversibly"). Only ethyl-S-agarose adsorbs poorly at the defined surface concentration and thus has similar properties to the butyl-N-Sepharose control.

Influence of degree of substitution [4,26]. Calmodulin binding also depends strongly on the degree of substitution of Sepharose with thiobutyl residues. Below *ca.* 1 μmol/ml packed gel very little binding occurs (not shown). At 1.7 μmol/ml packed gel significant binding can be measured (Table V). The total amount adsorbed (= difference between applied and recovered amount in eluates) increases *ca.* 5-fold as the degree of substitution increases *ca.* 3-fold from 1.7 to 5.7 μmol/ml packed gel
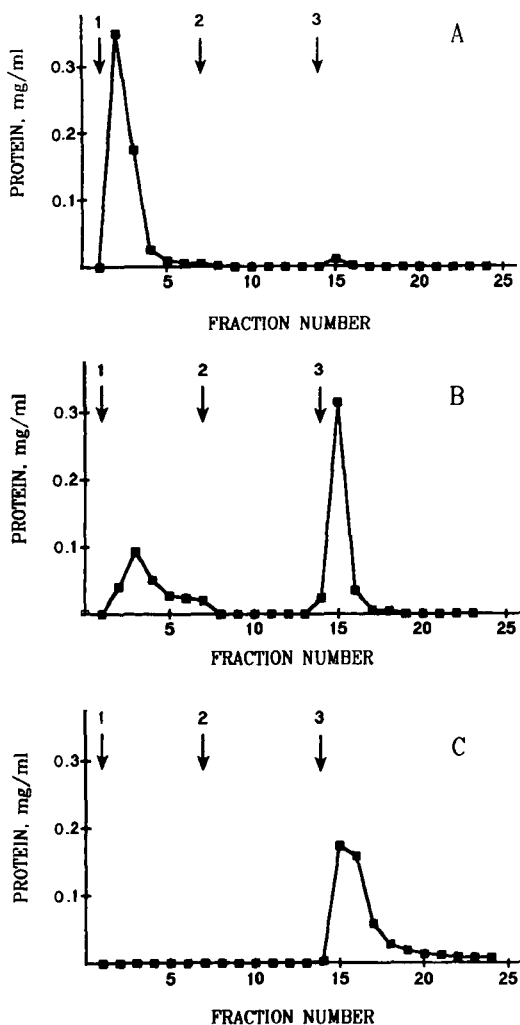
Fig. 6. Adsorption of calmodulin to a homologous series of alkyl-S-Sepharose as measured by hydrophobic affinity chromatography. Calmodulin (1 mg) was applied to 2 ml of packed gel of uncharged butyl-S-Sepharose on a column (12 cm × 0.9 cm I.D.) in a sample volume of 1 ml in buffer A (with 1 mM CaCl$_2$). Arrow 1, wash with buffer A; arrow 2, wash with buffer B (with 300 mM NaCl); arrow 3, elution with buffer C (with 10 mM EGTA). The fraction volume was 1.0 ml. (A) Ethyl-S-Sepharose (25 μmol/ml packed gel); (B) propyl-S-Sepharose (25 μmol/ml packed gel); (C) butyl-S-Sepharose (25 μmol/ml packed gel).

(Table IV). At very high degrees of substitution *ca.* 40% of the adsorbed protein cannot be eluted with EGTA (EGTA-irreversible binding). This fraction of calmodulin can, however, be eluted with detergents (*e.g.*, sodium dodecyl sulphate) (not shown).

TABLE V

QUANTITATIVE HYDROPHOBIC AFFINITY CHROMATOGRAPHY OF CALMODULIN ON ALKYL-AGAROSES

The data were derived from column experiments as described. Calmodulin was applied in buffer A ($+Ca^{2+}$), the column was then washed with buffer B ($+300$ mM NaCl) and finally eluted with buffer C ($+$EGTA). The excluded amount of calmodulin corresponds to the amount washed from the column in buffers A and B. The eluted amount corresponds to the amount eluted with buffer C. The total yield corresponds to the amount recovered in buffers A–C as a percentage of the amount applied. The difference between amount applied and amount recovered is the non-EGTA-elutable fraction ("irreversibly" bound protein), which can, however, be eluted by detergents.

Type of gel	Degree of substitution (μmol/ml packed gel)	Calmodulin			Total yield (%)
		mg applied	mg excluded (unbound)	mg eluted (boud)	
Control:					
Butyl-N-Sepharose	28	1	0.94	0	94
Alkyl-S-Sepharose:					
Homologous series:					
Ethyl-S-	25	1	0.85	0.01	86
Propyl-S-	25	1	0.34	0.42	76
Butyl-S-	25	1	0	0.66	66
Degree of substitution series:					
Butyl-S-	1.7	1	0.79	0.15	94
Butyl-S-	5.2	1	0.19	0.70	89
Butyl-S-	40.7	1	0	0.61	61

DISCUSSION

By working in a strongly alkaline medium, alkanethiols can easily be coupled to tresyl-Sepharose. The method is complicated by the tresylation procedure itself, which is a non-linear function of the tresyl chloride concentration (Table III). This may be due to inactivation of tresyl chloride at low concentrations in the incubation mixture owing to impurities (water?) in the dioxane medium, although this is improbable considering the distillation process employed for the purification of this solvent. The behaviour therefore remains unclear.

In comparison with other activation procedures, the tresylation of agarose as performed here warrants other special considerations. A primary incorporation phase followed by a plateau region is observed (Figs. 2 and 3). As the amount of butanethiol is *ca.* 10-fold in excess of the number of tresyl residues on the activated gel, a limitation of butanethiol cannot be the reason for the plateau region. From this plateau it may be concluded that a single reaction type is involved. At high tresyl chloride concentrations and long activation times a second increment of substitution occurs (secondary incorporation phase). This might be an indication of a second reaction type or possibly of an unfolding of the stacked and double helical agarose structure [27] exposing new reactive hydroxyl groups (possibly also secondary hydroxyl groups) for activation

after a critical exposure time to tresyl chloride. These changes need not be seen on the micrographs of Sepharose 4B, which appears intact after activation and coupling (Fig. 4).

Owing to these abnormal properties of tresyl chloride, the synthesis of structurally homogeneous alkyl-S-Sepharoses with different degrees of substitution poses a special problem. Therefore, a constant, low to intermediate tresyl chloride concentration should be chosen and the time varied to obtain different degrees of tresylation. One should work in the primary incorporation phase and plateau region well below the secondary incorporation phase.

Butyl-S-Sepharose is very efficient in the adsorption of proteins. As measured in batch experiments, the binding capacity of butyl-S-Sepharose for phosphorylase b is over an order of magnitude higher than that of butyl-N-Sepharose (synthesized by the cyanogen bromide method) [9–11] at low degrees of substitution (1–5 μmol/ml packed gel). At high degrees of substitution similar binding capacities for both gel types are obtained (*ca.* 20 mg/ml packed gel at an apparent equilibrium concentration of free enzyme of 0.5 mg/ml) [11].

With calmodulin, C_8-agarose derivatives (octyl- and aminooctyl-) have been reported as strong adsorbents [30,31]. As shown here (Table V, Fig. 6), even a C_3 derivative, propyl-S-Sepharose, is capable of adsorbing calmodulin in a Ca^{2+}-dependent manner. The results also show that the length of the immobilized alkyl residue on the Sepharose is not as decisive as expected, as the shorter propyl-S- derivative is a much better adsorbent than the longer butyl-N- derivative (Table V). This strongly indicates a special function of the sulphur base of the immobilized alkyl residue as compared with its tip (methyl group) and it also makes it very improbable that the dependence of calmodulin adsorption on the surface concentration of immobilized residues is due to changes in their availability (*i.e.*, further extension from the gel of a certain population of residues).

Because of these different protein-binding properties, alkyl-S-Sepharoses should prove useful in hydrophobic chromatography and possibly also in the preparation of selective adsorbent surfaces for biomaterials.

Why do the alkyl-S-Sepharoses bind calmodulin and phosphorylase b [9–11] more tightly than the alkyl-N-Sepharoses? Theoretically, the sulphur in the thioalkyl residue could complex to metals, especially in metal-binding proteins. In fact, a number of sulphur–metal complexes in proteins, *e.g.*, Fe^{2+}, Cu^+ and Zn^{2+}, have been described (for a review, see ref. 32). Comparable complexes between Ca^{2+} and sulphur have to our knowledge not been described for proteins. Experimentally the adsorption of the Ca^{2+}-binding protein fibrinogen to alkyl-S-Sepharose cannot be influenced by Ca^{2+} or EGTA [33]. It is therefore very improbable that complexation between metal and sulphur play an important role in the binding of proteins, specifically Ca^{2+}-binding proteins, to alkyl-S-agaroses.

However, two other possible explanations for the enhanced protein binding to alkyl-S-agaroses exist. In the first it could be reasoned that the sulphur atom displays properties similar to a carbon atom, as sulphur is also non-polar [34]. As sulphur increases the free energy of the system as it is transferred, *e.g.*, from the interior of a protein to water [34] it may have similar water-structuring properties to carbon. Based on the free energies of transfer, neutral oxygen and nitrogen (N/O) belong to a different (polar) class of atoms than the sulphur atom [34], which might explain the different properties of butyl-S- and butyl-N-agaroses.

On the other hand, a major difference between the sulphur atom, a carbon atom and the N/O class atoms lies in the π-electrons of the sulphur atom. A plausible conclusion is therefore that there might be an aromatic amino acid near the hydrophobic pocket or area of calmodulin binding to the base of the thioalkyl residue (this may also hold for other proteins tested in our system, phosphorylase b and fibrinogen). Owing to the large differences in the adsorption properties of the two gel types, we feel that the latter interpretation warrants careful consideration. Similar conclusions have been reached by Porath [35] for other sulphur-bearing agarose derivatives.

ACKNOWLEDGEMENTS

REFERENCES

1 S. Shaltiel, in R. Epton (Editor), *Chromatography of Synthetic and Biological Polymers, Vol. 2, Hydrophobic, Ion Exchange and Affinity Methods*, Ellis Horwood, Chichester, 1976, pp. 13–41.
2 S. Hjertén, *Methods Biochem. Anal.*, 27 (1981) 89–108.
3 H. P. Jennissen, *Makromol. Chem. Macromol. Symp.*, 17 (1988) 111–134.
4 H. P. Jennissen and L. M. G. Heilmeyer, Jr., *Biochemistry*, 14 (1975) 454–460.
5 J. Kohn and M. Wilchek, *Anal. Biochem.*, 115 (1981) 375–382.
6 T. C. J. Gribnau, *Ph.D. Thesis*, University of Nijmegen, 1977.
7 K. Nilsson, O. Norrlöw and K. Mosbach, *Acta Chem. Scand., Ser. B*, 35 (1981) 19–27.
8 K. Mosbach and K. Nilsson, *Biochem. Biophys. Res. Commun.*, 102 (1981) 449–457.
9 A. Demiroglou and H. P. Jennissen, *Abstracts of Communications, 8th International Congress of Biophysics, Bristol, England, July/August, 1984*, p. 49.
10 A. Demiroglou and H. P. Jennissen, *Biol. Chem. Hoppe-Seyler*, 368 (1987) 739.
11 A. Demiroglou, W. Kerfin and H. P. Jennissen, in T. W. Hutchens (Editor), *UCLA Symposia on Molecular and Cellular Biology, New Series, Vol. 80, Protein Recognition of Immobilized Ligands*, Alan R. Liss, New York, 1989, pp. 71–82.
12 F. Maisano, M. Belew and J. Porath, *J. Chromatogr.*, 321 (1985) 305–317.
13 J. Porath, R. Axén and S. Ernback, *Nature (London)*, 215 (1967) 1491–1492.
14 G. S. Bethell, J. S. Ayers, W. S. Hancock and M. T. W. Hearn, *J. Biol. Chem.*, 254 (1979) 2572–2574.
15 F. Autric, C. Ferraz, M.-C. Kilhofer, J.-C. Cavadore and J. G. Demaille, *Biochim. Biophys. Acta*, 631 (1980) 139–147.
16 C. Rochette-Egly, E. Boschetti, P. Basset and J.-M. Egly, *J. Chromatogr.*, 241 (1982) 333–344.
17 H. Boehm and H. P. Jennissen, *J. Muscle Cell Res.*, 6 (1985) 93–94.
18 H. P. Jennissen and L. M. G. Heilmeyer, Jr., *Anal Biochem.*, 57 (1974) 118–126.
19 I. Wenig (Chief Editor), *Organicum*, VEB Deutscher Verlag der Wissenschaften, Berlin, 13th ed., 1974, pp. 234–235.
20 R. L. Burwell, Jr., *Chem. Rev.*, 54 (1954) 615–685.
21 H. P. Jennissen, *J. Colloid Interface Sci.*, 111 (1986) 570–586.
22 J. W. Kimball, R. L. Kramer and E. E. Reid, *J. Am. Chem. Soc.*, 43 (1921) 1199–1202.
23 H. P. Jennissen, *Biochemistry*, 15 (1976) 5683–5692.
24 H. P. Jennissen, *J. Chromatogr.*, 159 (1978) 71–83.

25 H. P. Jennissen, *Adv. Enzyme Regul.*, 19 (1981) 377–406.
26 H. P. Jennissen, *J. Chromatogr.*, 215 (1981) 73–85.
27 S. Arnott, A. Fulmer, W. E. Scott, I. C. M. Dea, R. Moorhouse and D. A. Rees, *J. Mol. Biol.*, 90 (1974) 269–284.
28 O. H. Lowry, N. J. Rosebrough, A. L. Farr and R. J. Randall, *J. Biol. Chem.*, 193 (1951) 265–275.
29 Z. Er-el, Y. Zaidenzaig and S. Shaltiel, *Biochem. Biophys. Res. Commun.*, 49 (1972) 383–390.
30 R. Gopalakrishna and W. B. Anderson, *Biochem. Biophys. Res. Commun.*, 104 (1982) 830–836.
31 T. Tanaka, H. Umekawa, T. Ohmura and H. Hidaka, *Biochim. Biophys. Acta*, 787 (1984) 158–164.
32 L. Ryden, in T. W. Hutchens (Editor), *UCLA Symposia on Molecular and Cellular Biology, New Series, Vol. 80, Protein Recognition of Immobilized Ligands*, Alan R. Liss, New York, 1989, pp. 241–254.
33 A. Demiroglou and H. P. Jennissen, unpublished work.
34 D. Eisenberg and A. D. McLachlan, *Nature (London)*, 319 (1986) 199–203.
35 J. Porath, *Makromol. Chem. Macromol. Symp.*, 17 (1988) 359–372.

High-performance liquid chromatography on silica dynamically modified with hydrazinium derivatives

V. D. SHATZ*, O. V. SAHARTOVA and I. KALVIŅŠ

Institute of Organic Synthesis, Latvian Academy of Sciences, 226006, Riga (U.S.S.R.)

(First received January 8th, 1990; revised manuscript received June 19th, 1990)

ABSTRACT

Chromatographic systems with silica dynamically modified with a series of hydrazine derivatives were studied as a possible alternative to those with chemically bonded stationary phases. The properties of these new systems were compared with those of conventional reversed-phase systems and systems containing silica dynamically modified by cetrimide. As in reversed-phase chromatography on chemically bonded alkylsilicas, solvophobic interactions seem to be the main factor responsible for retention. It is shown that dynamic modification of silica with reagents differing in chemical structure can lead to systems with different selectivity. Betaines and quaternary ammonium and hydrazinium compounds act similarly as modifiers of silica but are very different as ion-pairing agents. The results of experiments performed with modifiers of different hydrophobicity and at various pH values demonstrate that ionic binding is not only mechanism of immobilization on the silica surface. It is shown that the shape of peaks obtained for highly polar and basic solutes is usually better in dynamic modification chromatography than in reversed-phase chromatography on alkylsilicas. Examples of analytical separations of polyfunctional organic substances and some inorganic anions on dynamically modified silica are presented.

INTRODUCTION

High-performance liquid chromatography (HPLC) on dynamically modified silica can be a promising alternative to separations on covalently bonded stationary phases. Owing to its slightly acidic nature, silica can bind organic cations that are added to the mobile phase by way of ion exchange in a certain pH range [1–10]. The organic layer thus generated on the surface can act as a stationary phase in the chromatographic process. Quaternary ammonium salts have so far been the most popular modifiers. It has been · shown that dynamic modification of silica with cetrimide (cetyltrimethylammonium bromide) yields chromatographic systems that are very similar to reversed-phase systems with alkylsilicas as stationary phases. One of the advantages of this method is that dynamic modification is a more reproducible procedure than chemical modification and the properties of the systems obtained are only slightly dependent on the type of silica.

It is obvious that the selectivity of systems with dynamic modification should be dependent on the chemical structure of the modifiers. When one modifier can be easily replaced with another, a broad spectrum of selectivity can be obtained using only one column packed with silica. Nevertheless, only a few organic bases have so far been used

for dynamic modification and no systematic studies on the selectivity of such systems have been published.

The aim of this work was to evaluate the selectivity of a series of new modifiers based on hydrazine derivatives and to demonstrate certain advantages of this separation mode in applied HPLC.

EXPERIMENTAL

Retention was measured in a Gilson HPLC system equipped with a Holochrome spectrophotometric detector set at 254 nm. Dynamic modification was performed on Silasorb 600 silica and Silasorb C_{18} was used as a reference packing (both from Lachema, Brno, Czechoslovakia). Stainless-steel columns (150 mm × 4.6 mm I.D.) were packed by Diagnostikum (Moscow, U.S.S.R.).

The dynamic modifiers included quaternary hydrazinium salts and betaines with different alkyl substituents and functional groups. Cetrimide, the most thoroughly studied modifier, was used as a reference substance. The structures of the modifiers are shown in Fig. 1. The abbreviations used in this work describe the type of modifier ion (Q and B for quaternary salts or betaines, respectively), the nature of basic group (A and H for ammonium and hydrazinium derivatives, respectively) and its hydrophobicity, the number of carbon atoms in the longest alkyl chain in the molecule. For example, the abbreviation for the quaternary salt hexadecyltrimethylammonium bromide is QA16.

The set of test solutes used to characterize the system selectivity included acidic, basic, amphoteric, polar and non-polar substances: isonicotinic acid (PyCOOOH), phenylacetic acid (BzCOOOH), acetanilide (PhNHCOMe), 4-methylpyridine (MePy), acetophenone (PhCOMe), nitrobenzene (PhNO$_2$) and benzene (PhH), where Py = pyridyl, Bz = benzyl, Ph = phenyl and Me = methyl.

The capacity factors, k', were calculated according to the conventional expression:

$$k' = (V_r - V_0)V_0 \tag{1}$$

where V_r is the retention time of the solute under study and V_0 the retention time of an unretained solute. The problem of the correct choice of unretained solutes for

$(CH_3)_3 \overset{+}{N} C_{16} H_{33} \; Br^-$ (Cetrimide, QA16)
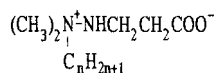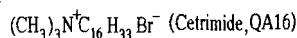
$(CH_3)_2 \overset{+}{N}\text{NHCH}_2\text{CH}_2\text{COO}^-$
     $C_n H_{2n+1}$
n=16 (BH16); n=15 (BH15); n=12 (BH12); n=9 (BH9)

$(CH_3)_2 \overset{+}{N}\text{NHCH}_2\text{CH}_2\text{CN} \; Br^-$ (QH16)
     $C_{16}H_{33}$
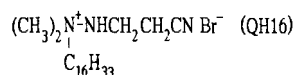
Fig. 1. Structures of the modifiers studied.

conventional modes of chromatography has been discussed in the literature (see, *e.g.*, refs. 11 and 12). This task is even more difficult for dynamic modification chromatography because the amount of the stationary phase is strongly dependent on the composition of the mobile phase. Therefore, accurate measurements of capacity factors and their correct interpretation are highly problematic in this chromatographic mode. We believe that for practical purposes of retention and selectivity comparison it is allowable to assume V_0 to be constant. V_0 was measured for the silica column gravimetrically. The column was filled with water, then placed in the oven of a gas chromatograph set at 120°C and purged with helium for 3 h. V_0 was calculated from the column weight loss in this experiment. Further heating under the same conditions did not lead to an observable weight loss, indicating that all water except the strongly chemisorbed layer on the surface of silica had been removed.

RESULTS AND DISCUSSION

The course of dynamic modification of silica can be easily monitored during column equilibration with an eluent containing a dynamic modifier. For example, the starting eluent can be a buffer containing a certain amount of methanol or acetonitrile. Under these conditions the system can be regarded as a normal-phase system with a very strong mobile phase. Naturally, relatively non-polar solutes (*e.g.*, benzene) should not be retained in such a system. When the system is switched to an eluent containing a modifier, a non-polar stationary phase is generated and the whole system is converted into a reversed-phase type. The retention of the modifiers under study is very strong, and therefore the modifier is almost completely adsorbed during this process. This is accompanied by an increase in the retention time of the test solute. When the dynamic modification is over, capacity factors remain constant provided that the mobile phase composition is constant (Fig. 2). Such curves can be used to determine the approximate amount of adsorbed modifier. It was found that silica adsorbs about 1.1 μmol/m^2 of BH12 and about 0.9 μmol/m^2 of QH16 from an eluent containing 20% of acetonitrile. The latter result was confirmed by an independent
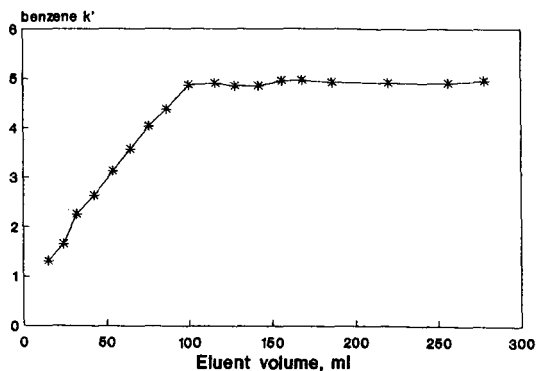
Fig. 2. Equilibration of silica with the dynamic modifier BH12. Mobile phase: 0.01 M BH12, 20% acetonitrile in 0.2 M acetate buffer (pH 6.0).

TABLE I

CAPACITY FACTORS OF BENZENE

Mobile phase: 0.01 M dynamic modifier, 20% acetonitrile in 0.2 M ammonium acetate buffer (pH 6.0).

Column packing	Dynamic modifier	k'
Silasorb C_{18}	None	16.8
	QA16	13.8
	BH16	15.8
Silasorb 600	QA16	8.1
	BH16	13.0
	BH15	12.0
	BH12	5.9
	BH9	0.6
	QH16	10.6

method. The equilibrated column was purged with one volume of water to remove the modifier-containing mobile phase and some packing was removed from the column and dried. Elemental analysis showed the content of carbon to be 11.7%. The content of dynamically immobilized carbon depends primarily on the structure of the modifier and on the concentration of organic solvent. It can reach about 20% in eluents containing no acetonitrile. The mobile phase volume required for complete modification of a given column depends on the concentrations of organic solvent and dynamic modifier. Usually it lies between 50 and 200 ml for 150 mm × 4.6 mm I.D. analytical HPLC columns packed with Silasorb 600 silica.

The retention strength of dynamic modifiers can be evaluated by measuring the k' values of a test solute with a series of mobile phases differing only in the type of dynamic modifier. The data presented in Table I show that with modifiers containing C_{15}–C_{16} alkyl chains the column capacity relative to benzene is slightly lower than that of the chemically bonded alkylsilica column. The system with BH9, containing a C_9 alkyl chain, showed an unexpectedly low retention of benzene.

It is known that retention values in reversed-phase chromatography are dependent on the concentration of organic solvent in the mobile phase. This relationship can be described by several models. We chose the following expression [13]:

$$\log k' = b - p \log C \tag{2}$$

where C is the molar concentration of organic solvent. It has been shown previously [14] in investigations of hundreds of solutes that reversed-phase retention data follow this relationship and the quality of the approximation is not worse than that with other linear models. In contrast, in the experiments on dynamic modification the log k' values did not follow either this relationship (Fig. 3) or other forms of linear models. The typical log k' vs. log C curve is very similar to the curve expressing the relationship between the amount of adsorbed modifier and log C. The observed k' values were divided by the amount of adsorbed hydrazine derivative for each concentration of acetonitrile. The resulting values (log k' per 1 mg of the stationary phase) are shown in
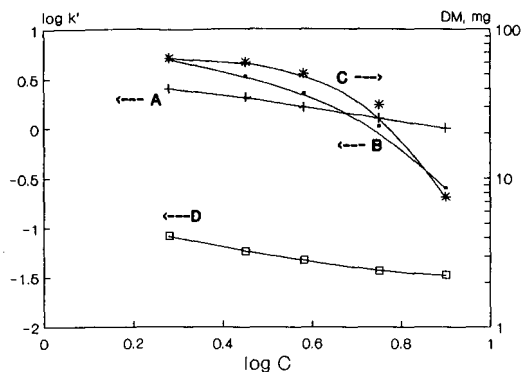
Fig. 3. Influence of acetonitrile concentration in the mobile phase on chromatographic parameters. (A) Capacity factors of benzene in conventional reversed-phase chromatography on Silasorb C_{18}; (B) capacity factors of benzene in dynamic modification chromatography on Silasorb 600 with QA16; (C) amount of adsorbed QA16; (D) capacity factors per 1 mg of adsorbed QA16.

Fig. 3D. The relationship is almost linear and the slope is similar to that in reversed-phase chromatography on Silasorb C_{18} (Fig. 3A). Consequently, the non-linearity of the relationship between log k' and log C is due to the fact that the amount of the active stationary phase (*i.e.*, adsorbed modifier) is not constant in this chromatographic mode but decreases with increasing organic solvent concentration. When the volume fraction of acetonitrile in the mobile phase reaches 40%, the degree of modification becomes negligible and so do the retention values of most solutes.

The selectivity of modifiers was compared in mobile phase consisting of 20% of acetonitrile in 0.2 M ammonium acetate buffer at pH 6.0. The concentration of the dynamic modifiers was 0.01 mol/l. The test solutes were arranged in order of increasing retention in conventional reversed-phase chromatography on Silasorb C_{18}. The "selectivity plots" for silica and octadecylsilica are shown in Fig. 4. It can be seen that the steepness of some segments of the plots is not identical for the nine chromatographic systems used, indicating that the introduction of different modifiers really leads to variations in separation selectivity.

The influence of two typical modifiers on the retention of test solutes on octadecylsilica is demonstrated in Fig. 4a. It can be seen that the elution order of basic and neutral solutes is typical of reversed-phase chromatography in the three systems. On the other hand, solvophobic interactions dominating in the reversed-phase mode are not the only significant interactions in the presence of modifiers. It follows from the comparison of plots for no modifier (N) and QA16 that addition of the quaternary ammonium salt leads to a strongly enhanced (20–50 times) retention of acids owing to the ion-pairing effects. Such effects are less clear when octadecylsilica is modified with the hydrazinium betaine BH16; the only difference between plots N and BH16 is the slightly enhanced retention of phenylacetic acid in the dynamically modified system.

A comparison of chromatographic behaviour on silica and octadecylsilica is presented in Fig. 4b. The experiments were performed on octadecylsilica and unmodified silica in the presence of QA16 and BH16. It can be seen that the chemical nature of the sorbent surface is not a crucial factor. The elution order of basic and
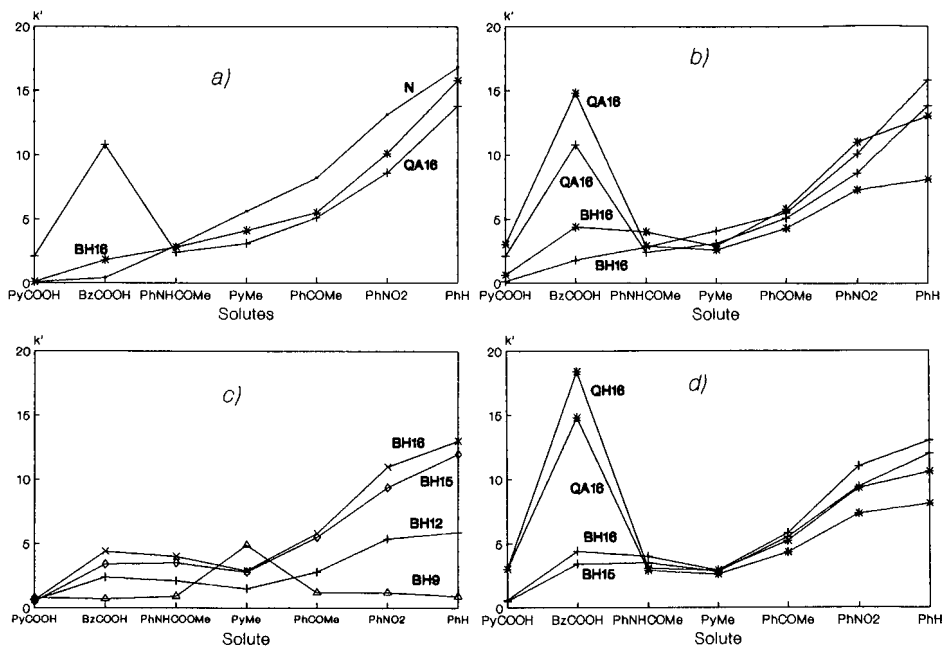
Fig. 4. Selectivity plots. Mobile phase: 0.01 M dynamic modifier, 20% acetonitrile in ammonium acetate buffer (pH 6.0). (a) Retention on Silasorb C_{18} with no modifier (N) and with C_{16} ammonium and hydrazinium modifiers; (b) role of sorbents: $*$, silica Silasorb 600; $+$, octadecylsilica Silasorb C_{18}; (c) role of chain length of hydrazinium betaine derivatives; (d) comparison of properties of ($*$) quaternary and ($+$) betaine modifiers.

neutral solutes on silica dynamically modified with fairly hydrophobic bases was similar to that on the chemically bonded stationary phase, indicating that solvophobic interactions play a dominant role in dynamic modification chromatography similarly to bonded reversed-phase chromatography. Of course, the retention mechanism for acidic solutes in the dynamic modification mode is expected to include ion-pairing effects. This leads to enhanced retention of phenylacetic and isonicotinic acids, as shown in Fig. 4b.

The properties of four hydrazinium betaine modifiers are compared in Fig. 4c. The system capacity with respect to the relatively non-polar acetophenone, nitrobenzene, benzene decreases almost proportionally to the length of the longest carbon chain in the modifier molecules. On the other hand, the retention of most solutes is negligible with the less hydrophobic modifier BH9, containing nine carbon atoms in the longest chain. The only exception is 4-methylpyridine, which is retained even stronger than in the presence of more hydrophobic modifiers. Retention measured on a silica column without modifier showed approximately the same behaviour for all solutes as in the presence of BH9. Consequently, no modification takes place with this substance and the relatively high retention of methylpyridine can be explained by direct interaction of this basic solute with the charged silanols on the surface. This low retention of non-polar solutes with BH9 is unexpected. The degree of modification is believed to be approximately constant for BH16–BH9 because of the very similar

ionogenic properties of these homologues. A possible explanation might be that ion exchange is not the only mechanism responsible for binding of modifier to the silica surface. The ion-exchange binding of the modifier should be suppressed at low pH of the mobile phase because of the negligible extent of silica ionization. No retention should be observed under such conditions. Our experiments with BH16 and a mobile phase of pH 2.5 showed that all the solutes under study still are retained significantly, the capacity factors being about 40% of the values observed at pH 6.0. This is evidence for another mechanism of modifier retention. The polarity of silica is lower than that of the water-rich mobile phase used, and therefore it was assumed that this material can act as a weak reversed-phase sorbent [15]. An example of such a kind of retention of non-ionic solutes, alkylbenzenes from water, has been published previously [16]. We believe that a similar mechanism could be responsible for the sorption of the hydrophobic modifiers under study.

The selectivities obtained with two betaines and two quaternary salts on silica are compared in Fig. 4d. It is clear that the four substances are similar in acting as "reversed-phase dynamic modifiers", whereas the quaternary compounds are much more efficient ion-pairing agents. Obviously, the different properties of these two groups of modifiers can be explained by the presence of a charged carboxylic group in the betaines which partially prevents ion pairing with acidic solutes. Comparison of systems with QH16 and QA16 shows that the quaternary ammonium and quaternary hydrazinium fragments have very similar effects on retention and selectivity towards the test solutes (this may not be the case for groups of closely related substances). The presence of an additional $-NH(CH_2)_2CN$ fragment in the molecule of modifier QH16 does not influence the selectivity very much. Consequently, the hexadecyl group is the main fragment responsible for selectivity.

Certain features of HPLC with dynamic modification are important from a practical point of view. It has been observed that the column efficiency for neutral and acidic solutes is not lower than the efficiency of modern columns for reversed-phase chromatography. It is known that many extremely polar basic solutes show poor
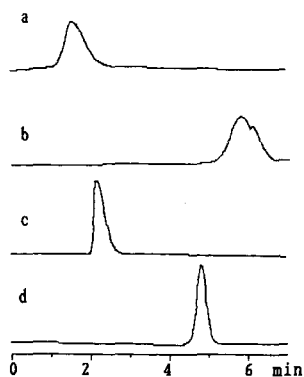
Fig. 5. Chromatograms of pyrazine-2,5-dicarboxylic acid on Silasorb C_{18} (a–c) and Silasorb 600 (d). Mobile phases: (a) 0.01 M sodium dodecylsulphate, 2.5% acetic acid, 97.5% water; (b) 1% tetrabutyl-ammonium phosphate in water (pH 2.5); (c) and (d) 0.01 M QA16 and 23% acetonitrile in 0.2 M acetate buffer (pH 6.0).

peak symmetry and efficiency. The addition of buffers, salts or ion-pairing agents to the mobile phase is not a universal solution to the problem and in many instances the peak shape and symmetry remain unsatisfactory. One of the advantages of dynamic
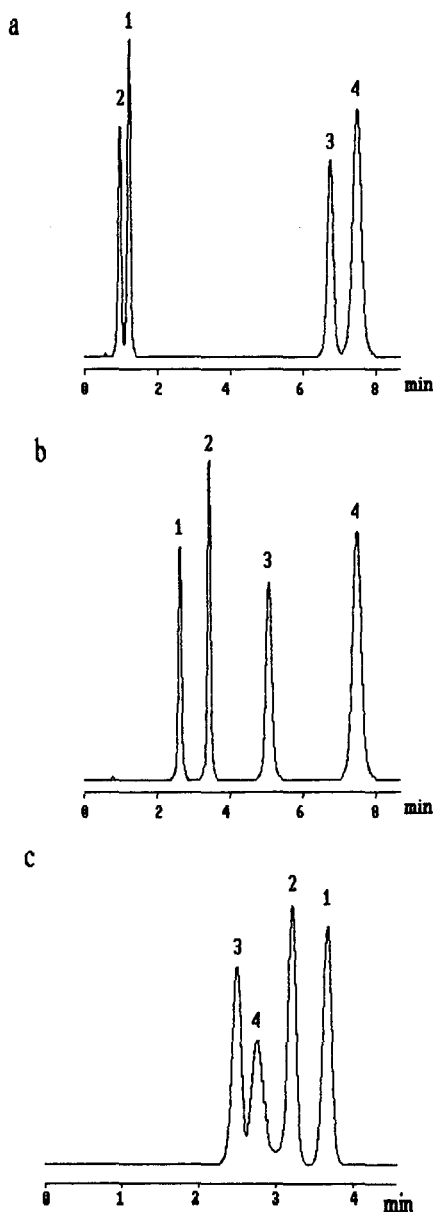
Fig. 6. Chromatography of antibiotics and intermediates. 1 = Aminocephalosporanic acid; 2 = amino-penicillanic acid; 3 = cephalexin; 4 = ampicillin. Mobile phase: (a) 5% acetonitrile in 0.2 M acetate buffer (pH 6.0); (b) 0.01 M QA16, 10% acetonitrile in 0.2 M acetate buffer (pH 6.0); (c) 0.01 M QH16, 7% acetonitrile in 0.2 M acetate buffer (pH 6.0). Columns: (a) Silasorb C_{18}; (b) and (c) Silasorb 600.

modification chromatography is that the column efficiency is usually higher and the peak shape is better than on bonded non-polar stationary phases. This is probably due to the less rigid binding of alkyl chains to the silica matrix and the greater flexibility of stationary phase molecules compared with the bonded stationary phase. An example is the chromatography of pyrazine-2,5-dicarboxylic acid. This highly hydrophilic solute is not retained from the aqueous buffers traditionally used as eluents in reversed-phase chromatography. Addition of the ion-pairing agent sodium dodecylsulphate results in a slight increase in retention, but the peak of the solute is still unacceptably wide (Fig. 5a). Enhanced retention of this solute was achieved by addition of quaternary ammonium modifiers to the mobile phase. Nevertheless, the peak shape remained unsatisfactory when octadecylsilica was used as the column packing (Fig. 5b and c). Consequently, chemically bonded alkylsilica cannot be the optimum sorbent for some classes of solutes. The use of a column packed with unmodified silica resulted in an increased retention volume and simultaneously improved markedly the efficiency and peak symmetry for this solute (Fig. 5d). Similar improvements in peak shapes were observed for many basic solutes. These observations support the opinion that poor peak shape in bonded reversed-phase chromatography in some instances can be explained not by the presence of residual silanol groups on the surface of sorbent but by steric inaccessibility of such groups [17]. This effect may be especially important in the HPLC of multifunctional bases.
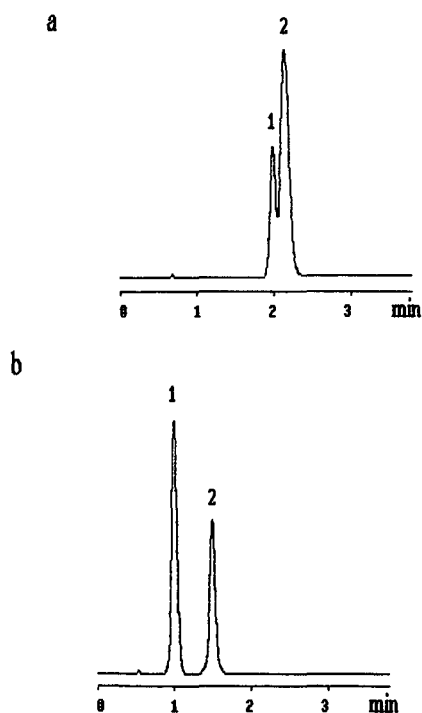
Fig. 7. Separation of (1) uracil and (2) 5-fluorouracil: (a) on Silasorb C_{18}, mobile phase 0.2 M acetate buffer (pH 6.6); b on Silasorb 600, mobile phase 0.01 M QH16 in 0.2 M acetate buffer (pH 6.6).
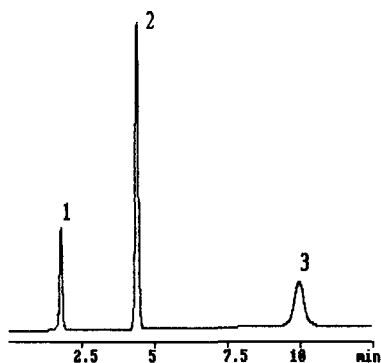
Fig. 8. Separation of anions: 1 = acetate; 2 = nitrite; 3 = nitrate. Mobile phase: 0.037 M BH16, 3% acetonitrile, 97% 0.04 M phosphate buffer (pH 6.9). Column: Silasorb 600.

HPLC in systems dynamically modified with hydrazinium derivatives offers additional possibilities of selectivity control in the separation of some mixtures of practical interest. Two examples are shown in Figs. 6 and 7.

Another area of possible application of hydrazinium derivatives as dynamic modifiers is anion analysis. A possible mechanism of sorption in this simple procedure involves the formation of a dynamically coated layer of the stationary phase and its interaction with the ion pair consisting of the solute anion and modifier cation. A chromatogram for the separation of some UV-absorbing anions is shown in Fig. 8. It is obvious that the column efficiency and peak symmetry are better than those typically observed in ion chromatography.

ACKNOWLEDGEMENTS

REFERENCES

1 Y. Ghaemi and R. A. Wall, *J. Chromatogr.*, 174 (1979) 51.
2 S. H. Hansen, P. Helboe, M. Thomsen and U. Lund, *J. Chromatogr.*, 210 (1981) 453.
3 S. H. Hansen, P. Helboe and U. Lund, *J. Chromatogr.*, 240 (1982) 319.
4 S. Jansson, J. Andersson and M. Johansson, *J. Chromatogr.*, 245 (1982) 45.
5 S. H. Hansen, P. Helboe and U. Lund, *J. Chromatogr.*, 260 (1983) 156.
6 S. H. Hansen, P. Helboe and U. Lund, *J. Chromatogr.*, 270 (1983) 77.
7 S. H. Hansen and P. Helboe, *J. Chromatogr.*, 285 (1984) 53.
8 S. H. Hansen, P. Helboe and M. Thomsen, *J. Chromatogr.*, 360 (1986) 53.
9 S. H. Hansen, P. Helboe and M. Thomsen, *J. Chromatogr.*, 369 (1986) 39.
10 S. H. Hansen, P. Helboe and M. Thomsen, *J. Chromatogr.*, 409 (1987) 71.
11 W. R. Melander, J. F. Erard and Cs. Horváth, *J. Chromatogr.*, 282 (1982) 211.
12 H. Engelhardt, H. Muller and B. Dreyer, *Chromatographia*, 19 (1985) 240.
13 F. Murakami, *J. Chromatogr.*, 178 (1979) 393.
14 V. D. Shatz, O. V. Sahartova and L. A. Brivkalne, *Izv. Akad. Nauk Latv. SSR, Ser. Khim.*, (1987) 459.
15 A. Nahum and Cs. Horváth, *J. Chromatogr.*, 203 (1981) 53.
16 A. N. Ageev, A. V. Kiselev and Ya. I. Yashin, *Chromatographia*, 17 (1983) 545.
17 B. A. Bidlingmeyer, J. K. Del Rios and J. Korpl, *Anal. Chem.*, 54 (1982) 442.

CHROM. 22 633

Gas-phase synthesis, properties and some applications of acylamide stationary phases for high-performance liquid chromatography

V. A. BASIUK* and A. A. CHUIKO

Institute of Surface Chemistry, Academy of Sciences of the Ukrainian S.S.R., Prospekt Nauki 31, Kiev 252028 (U.S.S.R.)

(First received February 19th, 1990; revised manuscript received June 13th, 1990)

ABSTRACT

Acylamide stationary phases for high-performance liquid chromatography were synthesized by a successive gas-phase modification of silica gel with γ-aminopropyltriethoxysilane and benzoyl chloride, benzoic or stearic acid. Derivatization of amino phases with carboxylic acids at temperatures above 150°C requires no activation of carboxyl groups or the use of condensing reagents. The stationary phases produced were studied by IR spectrometry. The formation of amide groups on the aminopropylsilica surface was confirmed and the presence of stable ester-type surface compounds with silanol groups was detected. The effect of the pH of the eluent on the retention of nucleic acid components on acylamide stationary phases was investigated. Examples of the chromatographic separation of nucleosides, amino acid enantiomers and oligomers of N-(2,3-epoxypropyl)carbazole are presented.

INTRODUCTION

Chemically bonded silica stationary phases (SPs) for high-performance liquid chromatography (HPLC) are at present prepared by modification of silica gel with organosilicon or other compounds in a solvent. However, there is an alternative synthetic approach. Wikström *et al.* [1] and Nawrocki and Aue [2] described a gas-phase method for the silanization of SPs for HPLC, consisting in treatment of silica gel with organosilicon compound vapours at reduced pressure. This, owing to the possibility of carrying out the modification at elevated temperatures, considerably shortens the reaction time, which results in a dense monolayer of modified coating, and also requires no organic solvents. Comparison of the chromatographic properties of the prepared materials with those of SPs synthesized by standard methods demonstrated the former to have improved characteristics (high efficiency and good symmetry of peaks).

Hence the capabilities of the gas-phase modification of SPs for HPLC deserve a thorough study. From the cited papers [1,2] it is clear that this method can yield high-quality organosilicon coatings. However, the synthesis of many SPs also includes subsequent stages such as the bonding of molecules of various organic modifiers and derivatives of carboxylic acids [3–5], amino acids [6–8], etc., to active functional groups (amino, halo and epoxyalkyl) of immobilized silanes. In contrast to silanizing reagents,

many of these compounds at ordinary (and sometimes also at elevated) temperatures are in a solid (crystalline) state, which at first glance would seem to preclude their use in the gas-phase method for the derivatization of SPs. However, under a moderate vacuum (of the order of 10^{-1} Torr) and at elevated temperatures (150–300°C), even such almost non-volatile substances as amino acids and nucleic acid bases can sublimate without decomposition [9–11]. We used this property previously in a gas-phase modification of highly dispersed pyrogenic silicas with some amino acids [12] and oxopyrimidines [13]. It was ascertained [12] that the carboxyl groups of amino acids react relatively readily with aminoalkyl groups of silica under vacuum at temperatures above 150°C with the formation of the corresponding surface amides, without the need for condensing reagents. This approach can apparently be employed also for other carboxylic acids, especially monofunctional types.

In this work we employed the gas-phase method for the successive modification of silica gel with γ-aminopropyltriethoxysilane and benzoyl chloride, benzoic or stearic acid and examined the IR spectra and chromatographic properties of the SPs produced for examples of separations of nucleic acid components, enantiomers of amino acids and oligomers of N-(2,3-epoxypropyl)carbazole.

EXPERIMENTAL

Materials and equipment

Materials and compounds used were Silasorb 600 silica gel (5 μm, specific surface area 550 m²/g), adenine, uracil, cytosine and guanine (Chemapol, Prague, Czechoslovakia), L- and D-amino acids, adenosine, uridine, cytidine, guanosine and sodium salts of the corresponding 5'-monophosphates (Reanal, Budapest, Hungary). IR spectra were recorded on a UR-20 spectrophotometer (Karl Zeiss, Jena, G.D.R.) in the range 1400–1900 cm^{-1} for silica gels in the form of a suspension in Nujol and for highly dispersed pyrogenic silica in the form of thin compacted tablets. IR spectra of tablets under vacuum were measured with the use of a cell described elsewhere [14].

Stainless-steel columns (64 × 2 mm I.D.) were packed with SPs by a suspension method (200 bar, isopropanol; HPP-4001 pump, Laboratorní, Přístroje, Prague, Czechoslovakia). A column of Separon C_{18} reversed-phase sorbent (Chemapol, Prague, Czechoslovakia) was commercially available (Nauchpribor, Orel, U.S.S.R.). Chromatographic analyses were performed on Milikhrom 1A microcolumn chromatograph (Nauchpribor) with a UV detector (operating range 190–360 nm). The dynamic modification of reversed-phase sorbents with N-octyl-L-proline was carried out by a procedure similar to those described elsewhere [15,16].

Gas-phase modification of SPs

The conditions for the modification of silica gel with γ-aminopropyltriethoxysilane were similar to those described by Wikström *et al.* [1]. However, we used a reactor of the simplest design possible (Fig. 1). Silica gel was placed on the bottom of the reactor and evacuated for 1 h at 150°C. After cooling to room temperature, the reactor was disconnected from the vacuum system and a tube containing γ-aminopropyltriethoxysilane was placed in it (Fig. 1, stage I). After evacuation at room temperature the stopcock was closed and the bottom zone of the reactor, containing the reagents, was heated for 1 h at 150–170°C (II). Next, the excess of silane and
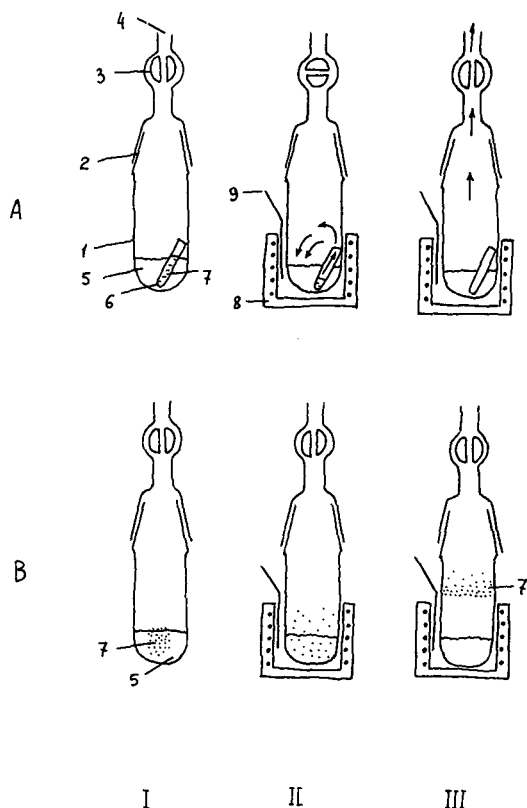
Fig. 1. Scheme of the reactor and sequence of silica gel derivatization with (A) liquid and (B) solid reagents. 1 = Reactor; 2 = joint; 3 = stopcock; 4 = to vacuum pump; 5 = silica gel; 6 = tube; 7 = reagent; 8 = oven; 9 = thermocouple. Steps: (I) preliminary pumping; (II) derivatization; (III) removal of excess of reagent.

volatile reaction products were removed by evacuation at the modification temperature (III). Derivatization of the amino phase obtained with the aid of benzoyl chloride was performed in a similar manner. The treatment was carried out at 170°C for 0.5 h (Fig. 2).
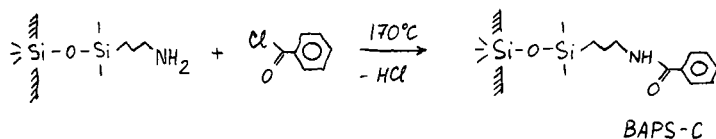
Fig. 2. Gas-phase derivatization of aminopropylsilica (APS) with benzoyl chloride.

The sequence of steps in the modification of aminopropylsilica gel (APS) with solid reagents (benzoic and stearic acids) was the same as above, but the reagents were introduced into the reactor by mixing them with silica gel (Fig. 1). In stage II, evacuation of the reactor was continued. Derivatization (Fig. 3) was conducted at

$$R = C_6H_5 \; (BAPS - A);$$
$$(CH_2)_{16}CH_3 \; (SAPS).$$
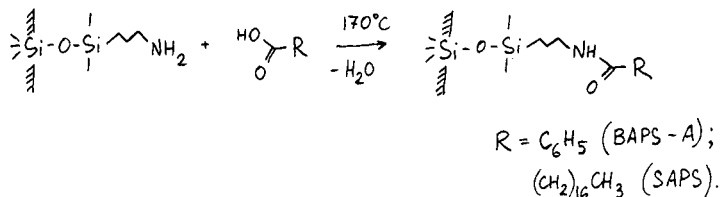
Fig. 3. Gas-phase derivatization of APS with benzoic and stearic acids.

170°C for 0.5 h. After the end of the reaction the excess of the solid reagent condensed in the cold zone of the reactor.

The chemically modified SPs produced were characterized by elemental analysis data (Table I) and IR spectra (in Nujol, Fig. 4). Before packing the columns, residual silanol groups were blocked by treatment with hexamethyldisilazane in toluene (80°C, 1 h).
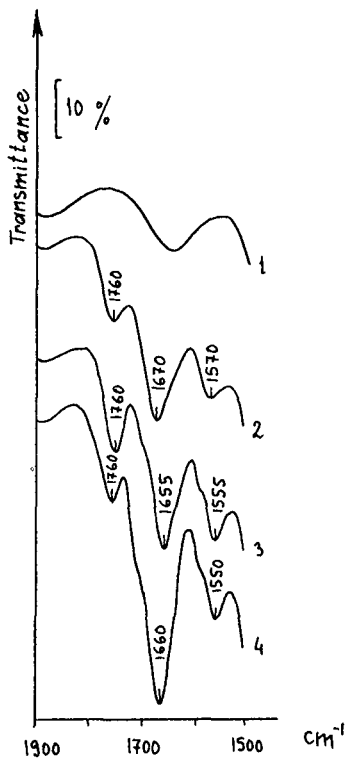
Fig. 4. Infrared spectra of (1) APS, (2) SAPS, (3) BAPS-A and (4) BAPS-C in Nujol.

RESULTS AND DISCUSSION

Modification procedure

As mentioned above, a reactor of the simplest design (Fig. 1) can be used for the gas-phase modification of silica gel. The bottom of the reactor should be as wide as possible so that the sorbent will lie as a thin layer, because highly dispersed silicas (including silica gels with particle size of the order of 10 μm) tend to "boil up" on evacuation, particularly with concurrent heating. A low volatility of stearic and benzoic acids at ordinary temperatures and the impossibility of removing the excess of the reagents from the reactor do not prevent pure materials, *i.e.*, containing no remaining modifier, from being obtained. The excess acid condenses in the reactor cold zone as a dense crust and does not contaminate silica gel when it is unloaded from the reactor. The time needed for APS acylation was less than 0.5 h in all instances (after 0.5 h the acylation yield does not increase with further treatment).

IR spectra of SPs and structure of modifying coating

The formation of amide groups on the APS surface was confirmed by the IR spectrometry. The IR spectra (Fig. 4) for the three acylation products (BAPS-C, BAPS-A and SAPS) exhibit absorption bands typical of secondary amides: amide I ($v_{C=O}$) at 1655–1670 cm^{-1} and amide II (δ_{NH}) at 1550–1570 cm^{-1}. Hence carboxylic acids can be employed for the acylation of amino phases without the use of condensing reagents or activation of carboxyl groups. At the same time, the presence in the IR spectra of absorption bands in the region of 1760 cm^{-1} was unexpected. This absorption also relates to $v_{C=O}$, but is characteristic of esters of carboxylic acids or chemisorption products, formed on condensation of carboxyl (or acid chloride) groups with silanol groups on the silica surface [17] according to Fig. 5.

$$\equiv \overset{\mid}{\underset{\mid}{Si}}-OH \ + \ \overset{X}{\underset{O}{\diagdown}}\!\!-R \ \xrightarrow{-HX} \ \equiv \overset{\mid}{\underset{\mid}{Si}}-O\overset{}{\underset{O}{\diagdown}}\!\!-R \qquad X=OH; \ Hal.$$
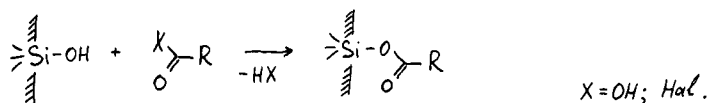
Fig. 5. Formation of ester-type products on chemisorption of carboxylic acids and acyl halides on hydroxylated silica surface.

The presence of residual silanol groups on a silanized surface is not surprising. In our opinion, it is striking that, despite the extreme hydrolytic unstability of $\equiv$SiOCO– bonds [17], bands at 1760 cm^{-1} are observed in the IR spectra of acylamide SPs not only when stored in air (in the presence of water vapour), but also when extracted from columns after obtaining the chromatographic data described below (the work involved end-capping, packing of columns, their elution with phosphate buffer solutions of pH 3–7 and polar organic solvents over a period of 2 months). As a result, no decrease in the intensities of these bands was observed.

These unexpected findings led to more detailed IR spectrometric studies of the behaviour of ester surface compounds both on Silasorb 600 microporous silica gel and on non-porous pyrogenic silica (specific surface area 300 m^2/g). In particular, it was ascertained that, in addition to amide groups, ester chemisorption products also form on the surface of non-porous AP-silica (Fig. 6) as a result of the gas-phase acylation
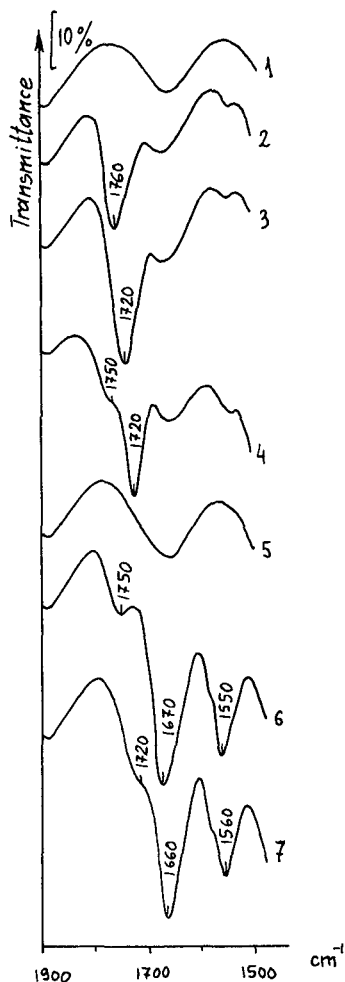
Fig. 6. Infrared spectra of (1) non-porous silica untreated, (2) gas-phase acylated with benzoyl chloride at 170°C and (3) air-exposed for 20 min; (4) microporous silica gel gas-phase acylated with benzoyl chloride at 170°C and air-exposed; (5) non-porous AP-silica untreated, (6) gas-phase acylated with benzoyl chloride at 170°C and (7) air-exposed for 20 min.

with carboxylic acids and benzoyl chloride. However, they turned out to be stable only under vacuum (Fig. 6, curve 6), and in air they hydrolysed in a few minutes (curve 7) to form hydrogen-bonded associations of carboxyl and silanol groups, of which the absorption $v_{C=O}$ at 1720 cm^{-1} is characteristic [17]. Ester surface compounds produced by the gas-phase acylation of dehydrated (unmodified) silica are also hydrolytically unstable (curves 2 and 3). At the same time only part of the ester products are hydrolysed ($v_{C=O}$ at 1720 cm^{-1}) on microporous silica gel (curve 4), both on exposure to a humid atmosphere and on immersion into water, while the $\equiv$SiOCO–band remains as a shoulder at 1750 cm^{-1}. It follows that only those ester products
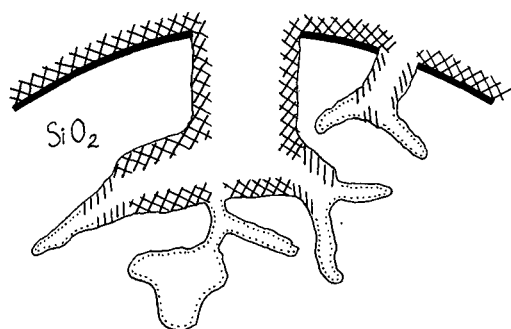
Fig. 7. Schematic diagram of acylamide SP surface fragment: dotted region, micropores inaccessible to reagent molecules; cross-hatched region, silanized surface; and single-hatched region, zones containing hydrolytically stable ester products.

which form in narrow pores of silica gel are hydrolytically stable. Hydrocarbon radicals appear to hydrophobize and "block" these pores, making them inaccessible to water.

On the basis of the above, the structure of the modifying coating of the SPs obtained can be represented schematically as follows. Three types of zones exist on the silica gel surface: (1) surface of micropores inaccessible both to APTES molecules and to the acylating reagents used; (2) surface of narrow pores inaccessible to bulky silane molecules, but permeable to compact molecules of benzoic acid and its chloride and to linear molecules of stearic acid; after formation of ester surface compounds these zones become inaccessible also to water; and (3) surface of broad pores and outside surface of silica gel particles, whereon the silanizing coating forms and its further modification is effected. It is the third type of zone that appears to be responsible for the chromatographic properties of the SPs obtained.

The presence of acylation by-products on the surface of the synthesized SPs prevents an accurate evaluation of the extent of transformation of amino groups into amide groups. Based on the elemental analysis data (Table I), it can only be stated that the resulting concentration of bonded acyl groups with benzoyl chloride used for derivatization is approximately twice that obtained with benzoic and stearic acids.

TABLE I

ELEMENTAL ANALYSIS DATA AND CONCENTRATION OF BONDED GROUPS FOR GAS-PHASE MODIFIED STATIONARY PHASES

SP	Acylating reagent	C(%)	N(%)	H(%)	Concentration of bonded groups, based on C(%)	
					mmol/g	μmol/m^2
APS	—	8.25	1.51	0.84	1.15	2.09
BAPS-C	Benzoyl chloride	18.10	0.95	1.58	1.17	2.13
BAPS-A	Benzoic acid	13.36	1.13	1.21	0.61	1.11
SAPS	Stearic acid	22.52	0.71	3.64	0.66	1.20
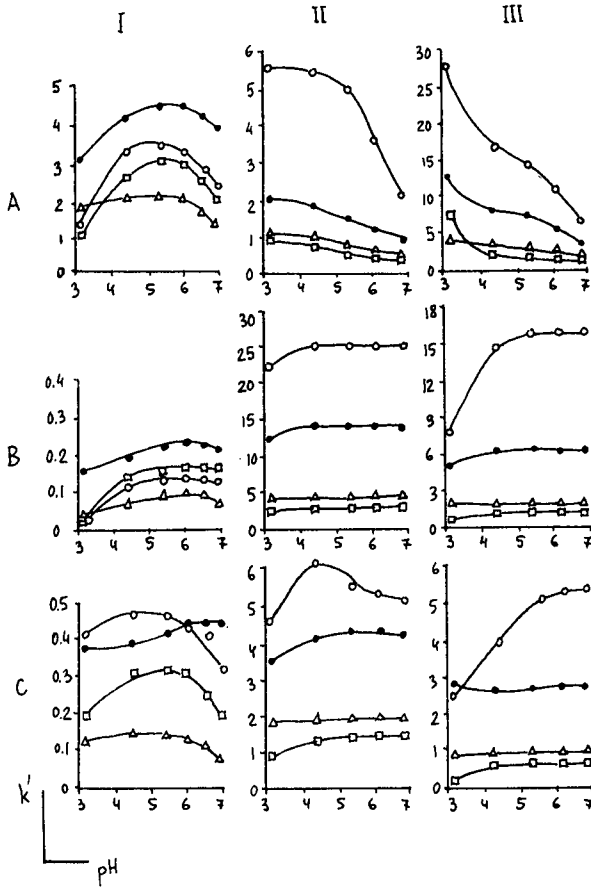
Fig. 8. Plot of retention (k') of nucleic acid constituents by (I) APS, (II) Separon C_{18} and (III) SAPS vs. eluent pH. (A) Nucleoside 5'-monophosphates: O, AMP; ●, GMP; △, UMP; □, CMP. (B) Nucleosides: O, adenosine; ●, guanosine; △, uridine; □, cytidine. (C) Nucleobases: O, adenine; ●, guanine; △, uracil; □, cytosine. Column, 64 × 2 mm I.D.; eluent, phosphate buffer at 100 μl/min; temperature, ambient; detection, UV at 270 nm.

Since in the derivatization of aminoorganosilicas with acyl halides the yield of surface amides is close to 100% (see, e.g., ref. 18), for the carboxylic acids in question it can be assumed to amount to about 50%. According to our results (unpublished), such yields of surface acylation products are observed also with aliphatic dicarboxylic, phthalic, aminobenzoic and α-amino acids.

Retention of nucleic acid components

Bonded SPs, containing amine and amide modifying groups, turned out to be fairly convenient for the fractionation of nucleic acids [4,19]. The separation of these compounds is improved owing to a concurrent action of the ionic and the hydrophobic mechanisms of retention. To evaluate the ion-exchange and reversed-phase (RP) properties of the SPs obtained, we studied the retention on them of nucleosides
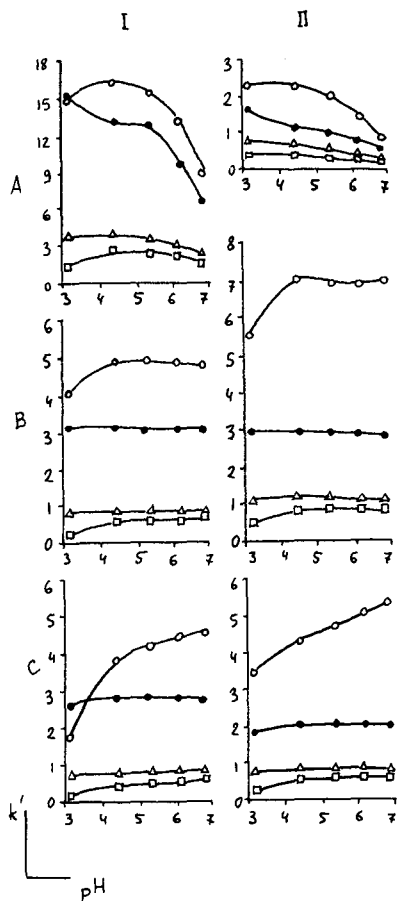
Fig. 9. Plot of retention (k') of nucleic acid constituents on (I) BAPS-A and (II) BAPS-C vs. eluent pH. Symbols and conditions as in Fig. 8.

5'-monophosphates, AMP, GMP, CMP, UMP and of the corresponding nucleosides and free bases at various pH values of the eluent.

The k' versus pH curves of these compounds for SAPS and, for comparison, APS and a traditional ODS sorbent (Separon C_{18}) are presented in Fig. 8. The elution order of bases for SAPS and Separon C_{18} (cytosine, uracil, guanine, adenine, nucleosides and monophosphates) is the same. For APS in the major part of the studied pH range it is uracil, cytosine, guanine, adenine, U, A, C, G, and UMP, CMP, AMP, GMP, respectively. For free bases the maximum k' values (1–6) were obtained with Separon C_{18} and lower values with SAPS. With APS the k' values were less than 0.5 for all bases over the entire pH range of 3–7. The retention of nucleosides on SAPS and Separon C_{18} (maximally) was also approximately one order of magnitude higher than for APS. Finally, the highest k' values for most of monophosphates, differing greatly from those on Separon C_{18} and APS, were obtained on SAPS. Thus, whereas SAPS behaves as a typical ODS sorbent in the separation of electroneutral compounds (nucleosides and
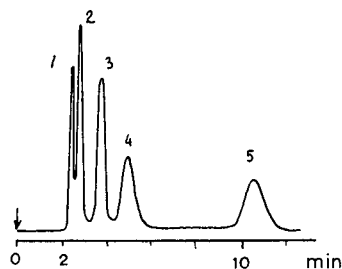
Fig. 10. Separation of nucleosides on BAPS-C: 1 = cytidine; 2 = uridine; 3 = inosine; 4 = guanosine; 5 = adenosine. pH, 4.40; other conditions as in Fig. 8.

corresponding bases), both hydrophobic and ionic interactions with the SP surface contribute to the retention of nucleotides.

BAPS-A also exhibits similar chromatographic properties with respect to nucleic acid components (Fig. 9). There are a number of insignificant differences from SAPS (shape of curves, specific k' values). Deserving more attention, in our opinion, is the fact that this SP, in contrast to BAPS-C, which is close to it in the structure of the bonded layer, exhibits multiphase properties. The ion-exchange properties of BAPS-C turned out to be suppressed because of the use of a very active acylating reagent, benzoyl chloride, in the gas-phase modification and a virtually complete transformation of amino groups into benzamide derivatives. This is evidenced by the fact that the retention of nucleoside 5'-monophosphates on this SP, in contrast to BAPS-A and SAPS, has very low values (Fig. 9) and, moreover, the elution order of the components under analysis remains unchanged over the entire pH range of 3–7. For the rest, BAPS-C is similar to BAPS-A, but exhibits a better selectivity in the separation of nucleosides and free bases. An example of the separation of a mixture of nucleosides is presented in Fig. 10.

Separation of amino acid enantiomers

The following approach is very convenient for the separation of amino acid racemates on ODS sorbents. The C_{18} SP is treated *in situ* with a solution of a derivative of an optically active amino acid, containing a long (C_7–C_{18}) linear hydrocarbon radical [15,16]. Such compounds are strongly sorbed and not washed away by aqueous eluents. Enantiomers of many amino acids can be separated with high selectivity coefficients on the SP thus obtained by ligand-exchange chromatography.

We ascertained that a considerable concentration (about 50% of the initial value) of polar AP groups on the SAPS surface does not affect the capability of bonded stearic acid residues for firm retention of an optically active modifier of such a type, N-octyl-L-proline. This proline derivative is strongly sorbed both on a traditional ODS sorbent (Separon C_{18}) and on SAPS, building in the octyl chain between hydrophobic radicals of the SP (Fig. 11).

After saturation of dynamically modified SPs with copper(II) ions [15,16], we carried out the separation on them of racemates of a number of hydrophobic amino acids. All the steps of modification of both SPs, their saturation with copper(II) ions and the separation of racemates were conducted under identical conditions, in the same sequence and with use of the same reagents.
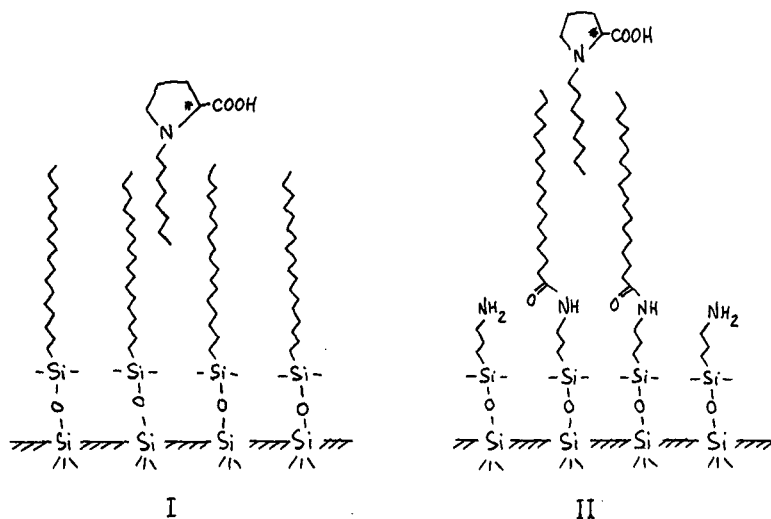
Fig. 11. Coating of (I) Separon C_{18} and (II) SAPS with N-octyl-L-proline.

L-Enantiomers were eluted first in all instances. This is accounted for by the fact that only D-enantiomers are capable of incorporating their side radicals between alkyl groups of reversed phases, whereas α-substituents of L-enantiomers are only attracted to hydrophobic substrate, owing to which the stability of diastereomeric L–L complexes turns out to be lower than that of D–L complexes [15,20].

Retention parameters and selectivity coefficients for some enantiomer pairs are presented in Table II, from which it is seen that a high selectivity of separation is attained on both SPs with the use of the simplest eluent, water with an addition of a copper salt. The minimum $\alpha_{D/L}$ values were obtained for methionine, *viz.*, 1.62 (C_{18}) and 1.68 (SAPS), eluent 10^{-3} M CuSO$_4$, and the maximum values for leucine, *viz.*, 2.51 (C_{18}) and 3.24 (SAPS), eluent 10^{-4} M CuSO$_4$. Higher k' and α values for most enantiomer pairs were obtained on SAPS than on C_{18}. We believe that the k' increase stems from the fact that, apart from complexation with coordination-unsaturated copper ions, hydrophobic interactions with residual AP groups of SAPS (as in the case of nucleotides) contribute to the retention of amino acids. The $\alpha_{D/L}$ increase is probably also associated with a large number of AP groups on this SP, which restrict the reversed-phase capability for retaining molecules of the dynamic modifier. Thus, the N-octyl-L-proline concentration on the SAPS surface turns out to be lower than that on Separon C_{18}; this can appropriately be compared with the "dilution" of chemically bonded chiral groups [21,22], which increases the enantioselectivity. Examples of the separation of enantiomers of some hydrophobic amino acids on SAPS dynamically modified with N-octyl-L-proline are presented in Fig. 12.

Separation of oligomers

As a further example of the application of the acylamide SPs produced by the gas-phase modification, we present the separation of oligomers of N-(2,3-epoxy-propyl)carbazole (EPC), used in xerography. Analysis of the oligomeric composition

TABLE II

COMPARISON OF k' AND α VALUES OF SOME AMINO ACID ENANTIOMERS ON N-OCTYL-L-PROLINE-COATED SEPARON C_{18} AND SAPS

Conditions as in Fig. 12. Mobile phases: (I) 10^{-4} and (II) 10^{-3} M CuSO$_4$.

Amino acid	Mobile phase	Separon C_{18}			SAPS		
		k'_L	k'_D	$\alpha_{D/L}$	k'_L	k'_D	$\alpha_{D/L}$
Norleucine	II	3.63	7.00	1.93	5.00	11.00	2.20
Leucine	I	2.32	5.82	2.51	4.83	15.67	3.24
	II	2.27	5.36	2.36	3.58	8.41	2.35
Norvaline	II	1.13	2.36	2.09	1.46	3.92	2.68
Valine	I	1.50	3.64	2.42	1.50	4.17	2.78
	II	1.05	2.18	2.08	1.50	3.58	2.39
Tyrosine	I	3.40	7.33	2.16	10.17	21.08	2.07
	II	3.05	5.91	1.94	5.50	12.91	2.35
Phenylalanine	II	11.18	18.27	1.63	4.41	12.42	3.22
Methionine	I	3.95	7.45	1.89	3.17	5.33	1.68
	II	1.91	3.09	1.62	2.83	4.75	1.68

of EPC on the ODS SP demonstrates the presence of chains containing 2–13 monomeric units (Fig. 13B). No separation occurs on BAPS-A; all components are retained very weakly. A partial separation is achieved on BAPS-C (Fig. 13C). The application of SAPS, despite the presence of about the same number of residual AP
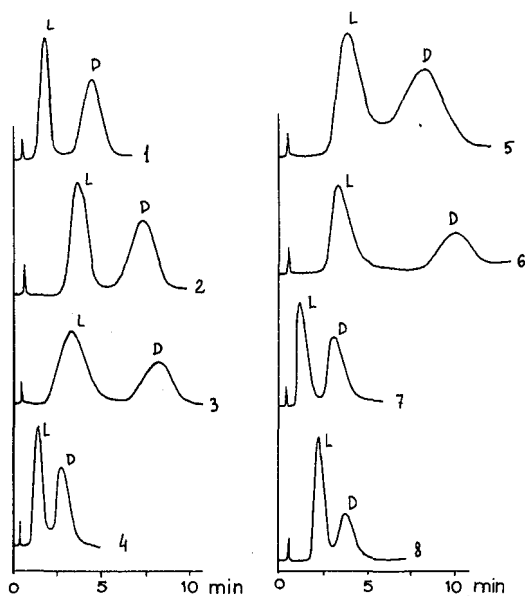
Fig. 12. Enantiomeric resolution of hydrophobic amino acids on N-octyl-L-proline-coated SAPS. 1 = Norvaline; 2 = norleucine; 3 = phenylalanine; 4 and 7 = valine; 5 = tyrosine; 6 = leucine; 8 = methionine. Column, 64 × 2 mm I.D.; eluents, (1–5) 10^{-3} and (6–8) 10^{-4} M CuSO$_4$ at 220 μl/min; temperature, ambient; detection, UV at 240 nm.
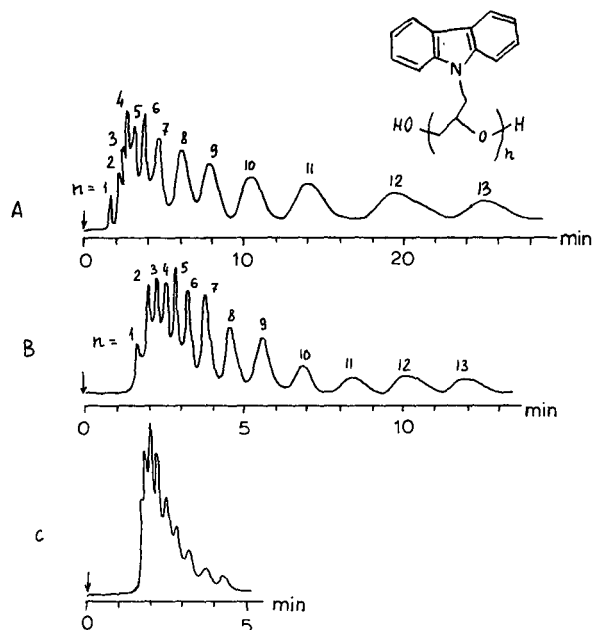
Fig. 13. Separation of EPC oligomers on (A) SAPS, (B) Separon C_{18} and (C) BAPS-C; 1 = N-(2,3-epoxy-propyl)carbazole (monomeric); 2 = dimer; etc. Column, 64 × 2 mm I.D.; eluent, acetonitrile at 100 μl/min; temperature, ambient; detection, UV at 300 nm.

TABLE III

COMPARISON OF k' AND α VALUES OF EPC OLIGOMERS ON SEPARON C_{18} AND SAPS

Conditions as in Fig. 13.

n	Separon C_{18}		SAPS	
	k'_n	$\alpha_{n+1/n}$	k'_n	$\alpha_{n+1/n}$
1 (monomeric)	0.42		0.15	
		1.74		4.33
2	0.73		0.65	
		1.17		1.42
3	0.86		0.92	
		1.30		1.29
4	1.12		1.19	
		1.24		1.16
5	1.39		1.38	
		1.26		1.42
6	1.75		1.96	
		1.28		1.37
7	2.24		2.67	
		1.27		1.40
8	2.85		3.77	
		1.29		1.35
9	3.67		5.08	
		1.26		1.45
10	4.63		7.38	
		1.28		1.32
11	5.92		9.77	
		1.24		1.46
12	7.33		14.23	
		1.23		1.34
13	9.00		19.00	
$\bar{\alpha}_{n+1/n}$		1.26		1.36

groups as on the surface of BAPS-A, yielded good results (Fig. 13A); all the compounds under analysis are well retained and are separated with high selectivity coefficients. The $\alpha_{n+1/n}$ values obtained in the separation of EPC on SAPS exceed the corresponding values for Separon C_{18} by a factor of 1.08 on average (Table III).

Hence the gas-phase modification of amino phases with carboxylic acids is an unlaborious, rapid and efficient method for the synthesis of acylamide SPs, which requires no activation of carboxylic groups or the use of condensing reagents. As the yield of amino groups acylation is about 50%, these phases contain both hydrophobic and anion-exchanging groups, which can contribute to the separation process simultaneously; hence such SPs are convenient for the separation of various classes of compounds.

REFERENCES

1 P. Wikström, C. F. Mandenius and P.-O. Larsson, *J. Chromatogr.*, 455 (1988) 105–117.
2 J. Nawrocki and W. A. Aue, *J. Chromatogr.*, 456 (1988) 337–345.
3 R. Bischoff and L. W. McLaughlin, *J. Chromatogr.*, 270 (1983) 117–126.
4 R. Bischoff and L. W. McLaughlin, *J. Chromatogr.*, 296 (1984) 329–337.
5 H. W. Jarrett, *J. Chromatogr.*, 405 (1987) 179–189.
6 G. Gübitz, F. Juffmann and W. Jellenz, *Chromatographia*, 16 (1982) 103–106.
7 P. Roumeliotis, A. A. Kurganov and V. A. Davankov, *J. Chromatogr.*, 266 (1983) 439–450.
8 L. W. Yu, T. R. Floyd and R. A. Hartwick, *J. Chromatogr. Sci.*, 24 (1986) 177–182.
9 D. Gross and G. Grodsky, *J. Am. Chem. Soc.*, 77 (1955) 1678–1680.
10 A. B. Teplitsky and I. K. Yanson, *Biofizika*, 20 (1975) 189–193.
11 L. B. Clark, G. G. Peschel and I. Tinoco, *J. Phys. Chem.*, 69 (1965) 3615–3619.
12 V. A. Basiuk, V. I. Bogomaz, V. G. Golovatyi and A. A. Chuiko, *Zh. Prikl. Khim. (Leningrad)*, 60 (1987) 1092–1096.
13 V. A. Basiuk, V. I. Bogomaz and A. A. Chuiko, *Teor. Eksp. Khim.*, 22 (1986) 495–499.
14 V. A. Nikitin, A. N. Sidorov and A. V. Karyakin, *Zh. Fiz. Khim.*, 30 (1956) 117–128.
15 V. A. Davankov, A. S. Bochkov, A. A. Kurganov, P. Roumeliotis and K. K. Unger, *Chromatographia*, 13 (1980) 677–685.
16 A. P. Sidorov, T. A. Belousova, Yu. P. Belov, M. N. Chumachenko and I. V. Martynov, *Zh. Anal. Khim.*, 42 (1987) 727–729.
17 R. P. Young, *Can. J. Chem.*, 47 (1969) 2237–2247.
18 L. Horner and H. Ziegler, *Z. Naturforsch.*, 42 (1987) 643–660.
19 H. Engelhardt and E. Schweinheim, *Chromatographia*, 22 (1986) 425–429.
20 V. A. Davankov, A. A. Kurganov and A. S. Bochkov, *Adv. Chromatogr.*, 22 (1983) 71–116.
21 L. R. Gelber, B. L. Karger, J. L. Neumeyer and B. Feibush, *J. Am. Chem. Soc.*, 106 (1984) 7729–7734.
22 B. Feibush, M. J. Cohen and B. L. Karger, *J. Chromatogr.*, 282 (1983) 3–26.

Purification of the subunits of pea mitochondrial F_1-ATPase by high-performance liquid chromatography

DACHENG GUO[a] and ARNOST HORAK*

Department of Plant Science, University of Alberta, Edmonton, Alberta T6G 2P5 (Canada)

(First received March 6th, 1990; revised manuscript received June 25th, 1990)

ABSTRACT

The subunits of the F_1-ATPase from pea cotyledon mitochondria were purified by reversed-phase chromatography. The resolution of the subunits was affected by several chromatographic parameters: a reversed-phase C_8 column was superior to the less hydrophobic Bio-Gel TSK Phenyl-5-PW column for the resolution of the subunits, acetonitrile was more suitable for good separation of the subunits than 2-propanol and the flow-rate had a significant effect on peak height but little effect on the column resolving power. Tandem chromatography on two reversed-phase chromatography columns with different hydrophobicities was used in an attempt to isolate F_1-ATPase subunits directly from soluble proteins extracted from submitochondrial particles.

INTRODUCTION

The proton-translocating ATPase reversibly couples ATP synthesis and hydrolysis to the translocation of protons across energy-transducing membranes. The enzyme contains two sectors: a hydrophilic portion, F_1, and a hydrophobic membrane portion, F_0. The F_1 sector contains the binding sites for nucleotides and phosphate and is responsible for catalytic activity. Depending on the biological source of the enzyme, the isolated F_1 sector can contain five or six different subunits. Current interest is focused on the structure and function of these subunits. Several procedures have been reported for the isolation of the subunits. The δ and ε subunits of *Escherichia coli* F_1-ATPase have been purified to homogeneity by treating the enzyme with pyridine and using molecular sieve chromatography [1,2]. The use of ion-exchange celluloses (DEAE- and CM-cellulose) has been applied to resolve all five subunits of the F_1-ATPase from the thermophilic bacterium PS3 [3,4]. A similar procedure, reported by Dunn and Futai [5], involves the use of the hydroxyapatite–DEAE-Sepharose method to isolate the α, β and γ subunits of the *E. coli* coupling factor ATPase [5]. Unfortunately, the procedures used are time consuming and problems of poor resolution and low protein yields are often associated with these traditional techniques. Saishu *et al.* [6] used reversed-phase high-performance liquid chromato-

_____

[a] Present address: Department of Physiology, University of Alberta, Edmonton, Alberta T6G 2H7, Canada.

graphy (RP-HPLC) to isolate the ε subunit from the thermophilic F_1-ATPase, but the separation of the other subunits was poor.

In this paper, we describe the use of RP-HPLC columns for the purification of F_1-ATPase subunits. The F_1-ATPase was isolated from pea cotyledon mitochondrial membranes. The purified enzyme contained six subunits, designated α, β, γ, δ, δ' and ε in order of decreasing molecular weight [7]. The subunits from the purified pea cotyledon F_1-ATPase were separated by RP-HPLC on a SynChropak C_8 column and an attempt was also made to isolate the subunits directly from the proteins extracted from submitochondrial particles by a low-ionic strength sucrose solution.

EXPERIMENTAL

Reagents

Unless stated otherwise, chemicals and solvents were of analytical-reagent grade. HPLC-grade trifluoroacetic acid (TFA) and acetonitrile were purchased from Pierce (Rockford, IL, U.S.A.) and Fisher Scientific (Fairlawn, NJ, U.S.A.), respectively, and HPLC-grade 2-propanol from Caledon Labs. (Georgetown, Canada). Doubly distilled water was purified by passing it through Milli-Q water purification system (Millipore, Bedford, MA, U.S.A.).

Apparatus

The instrumentation consisted of a Vista Series 5000 liquid chromatograph (Varian, Walnut Creek, CA, U.S.A.) combined with a Varian CS401 data system and coupled to a Varian UV-50 variable-wavelength detector. Three different HPLC columns were used: (1) SynChropak RP-8, 250 × 4.6 mm I.D., particle size 6.5 μm, pore size 300 Å, carbon loading *ca.* 7.5% (SynChrom, Linden, IN, U.S.A.); (2) Bio-Gel TSK Phenyl RP+ reversed-phase, 75 × 4.6 mm I.D. (Bio-Rad Labs., Richmond, CA, U.S.A.); and (3) Bio-Gel TSK Phenyl-5-PW, 75 × 7.5 mm I.D. (Bio-Rad Labs.).

Purification of F_1-ATPase prior to HPLC

The pea mitochondrial F_1-ATPase was isolated as described by Horak and Packer [7]. Mitochondrial membranes were extracted with low-ionic strength sucrose solution (300 mM sucrose–2 mM tricine, pH 7.4). After centrifugation for 45 min at 100 000 g at 20°C, the supernatant was collected and the F_1-ATPase was purified by DEAE-cellulose column chromatography and by sucrose density gradient centrifugation [7]. The purified F_1-ATPase was subjected to HPLC.

High-performance liquid chromatography

The purified F_1-ATPase was incubated in 0.5% TFA in water for 2 h before injection. The samples were chromatographed at 22°C using a linear gradient of 1% B/min (solvent A was 0.1% TFA in water; solvent B was either 0.1% TFA in acetonitrile or 0.1% TFA in 2-propanol). The polypeptides collected from HPLC were dialysed against 50 mM Tris buffer containing 0.5% sodium dodecyl sulphate (SDS) (pH 7) to remove TFA and acetonitrile and then concentrated using Centricon membranes (Centricon microconcentrator; Amicon, Danvers, MA, U.S.A.).

Electrophoresis

SDS polyacrylamide gel electrophoresis (SDS-PAGE) was carried out according to Laemmli [8] on a 1.5-mm slab gel consisting of a 13% separating gel and a 4% stacking gel. The gels were stained for protein with Coomassie Blue R250.

RESULTS AND DISCUSSION

Purification of F$_1$-ATPase subunits by reversed-phase HPLC

The native F$_1$-ATPase from pea cotyledon mitochondria was purified by DEAE-cellulose column chromatography and by sucrose density gradient centrifugation [7]. The enzyme, the molecular weight of which is *ca.* 400 000 daltons, is too large to be loaded into most commercially available reversed-phase columns. Therefore, a method for dissociating the enzyme complex into subunits was needed. The subunits of the F$_1$-ATPase were dissociated at room temperature in a 0.5% TFA–water solution (pH 2.0). The polypeptides were separated on a SynChropak C$_8$ column with a linear gradient of acetonitrile (1% B/min) at a flow-rate of 1 ml/min. The TFA–water to TFA–acetonitrile gradient has proved to be an excellent system for the RP-HPLC of peptides and proteins [9]. Under the chromatographic conditions used, the enzyme was well resolved into five peaks (Fig. 1). As shown in Fig. 1, all polypeptides were eluted from the reversed-phase column by a high concentration of acetonitrile, suggesting that the subunits are hydrophobic.

Because of their hydrophobic nature, the subunits recovered by lyophilization following HPLC purification were difficult to dissolve even in buffers containing detergents such as SDS or Tween 20. Therefore, an alternative method was used to improve the polypeptide recovery. The materials collected from the HPLC column were dialysed extensively against 50 m*M* Tris buffer containing 0.5% SDS (pH 7.0). The purpose of this step was to replace the TFA–acetonitrile solution directly with the Tris–SDS buffer.

The peaks on the chromatogram were labelled A, B, C, D and E in order of elution of the polypeptides (Fig. 1). The purity of the materials corresponding to peaks
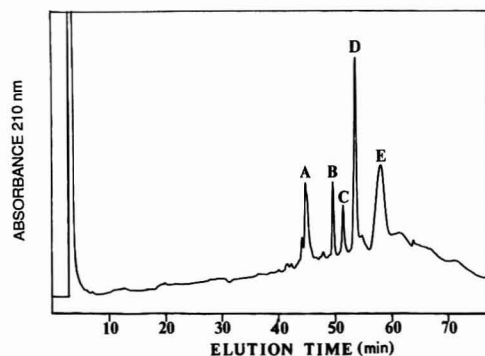
Fig. 1. Separation of subunits of the pea mitochondrial F$_1$-ATPase on a reversed-phase SynChropak C$_8$ column. Conditions: linear gradient (1% B/min) where solvent A was 0.1% TFA in water and solvent B was 0.1% TFA in acetonitrile; flow-rate, 1 ml/min; sample load, 60 μg of the native F$_1$-ATPase which had been incubated in 0.5% TFA–water for 2 h prior to injection.
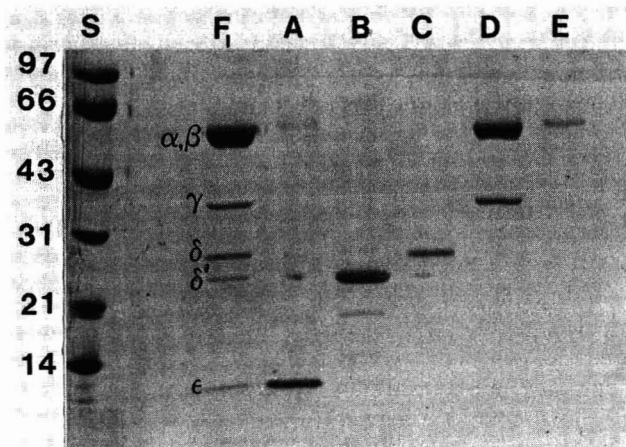
Fig. 2. SDS-PAGE of the subunits separated on the reversed-phase column in Fig. 1. Lanes: S = 10 μg of low-molecular-weight protein standards (Bio-Rad Labs.); F_1 = 10 μg of pea mitochondrial F_1-ATPase; A–C = 5 μg of the materials collected from peaks A–C in Fig. 1; D = 10 μg of the material from peak D; E = 2 μg of the material from peak E.

A–E was determined by SDS-PAGE (Fig. 2). The results indicate that the δ and α subunits are essentially pure after purification by RP-HPLC (lanes C and E, Fig. 2). The ε and δ′ subunits contained minor impurities (lanes A and B, Fig. 2). Peak D contained two polypeptides corresponding to the β and γ subunits of the F_1-ATPase. To test the possibility of a disulphide link between these two subunits, the native enzyme was incubated in 5% β-mercaptoethanol and in 0.5% TFA before injection into the SynChropak column. The resulting chromatograms were identical, suggesting that a disulphide link was not responsible for the co-chromatography of these two subunits.

Comparison of reversed-phase columns which differ in their hydrophobicities

The TFA-treated F_1-ATPase was chromatographed on three different HPLC columns using identical eluting conditions. The three columns differ in their hydrophobicities in the following order: SynChropak RP-8 > TSK Phenyl RP+ > TSK Phenyl-5-PW. The SynChropak and TSK Phenyl RP+ columns showed much better overall resolution than the TSK Phenyl-5-PW column (Fig. 3). The SynChropak column was superior to the TSK Phenyl RP+ column for the resolution of the larger F_1-ATPase subunits (peaks D and E in Fig. 3).

Effect of the organic solvent on subunit separation

In our RP-HPLC system the protein samples were applied in water and eluted with a linear gradient of the organic solvent (acetonitrile or 2-propanol). Addition of a counter ion (TFA) in both water and organic solvent helped to minimize interactions between the silanol groups of the column and the positively charged groups of the protein [10,11]. Of the two organic solvents used, 2-propanol has a higher eluotropic strength than acetonitrile [12–14]. As seen in Fig. 4, the subunit elution times were
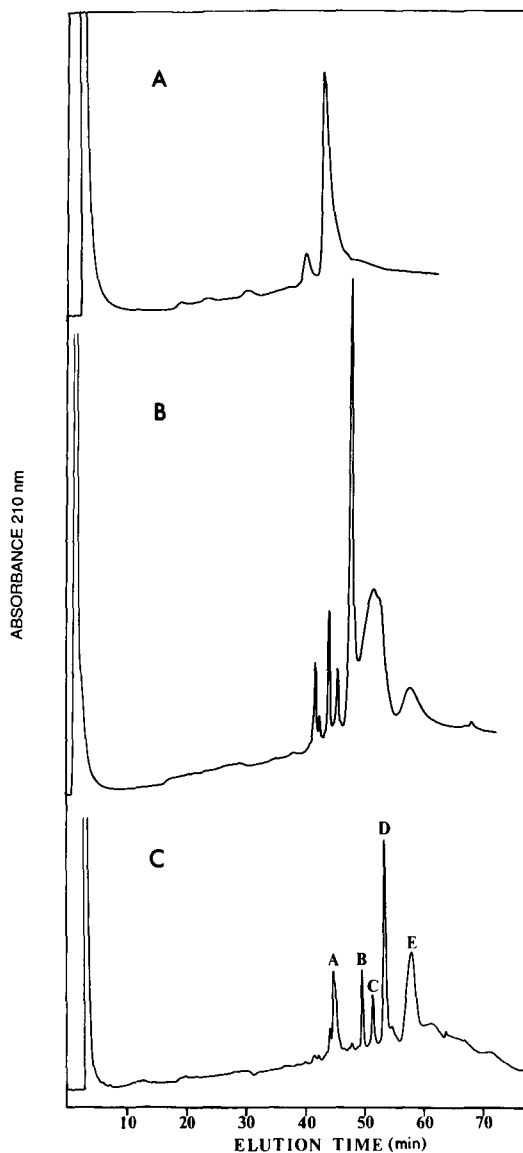
Fig. 3. Separation of subunits of the pea mitochondrial F$_1$-ATPase on three HPLC columns. Top, Bio-Gel TSK Phenyl-5-PW column; middle, Bio-Gel TSK Phenyl RP+ column; bottom, SynChropak C$_8$ column. Conditions: linear gradient (1% B/min) where solvent A was 0.1% TFA in water and solvent B was 0.1% TFA in acetonitrile; flow-rate, 1 ml/min; sample load, 60 μg of the F$_1$-ATPase (top and bottom) and 160 μg of the F$_1$-ATPase (middle).

significantly reduced when acetonitrile was replaced with 2-propanol as the organic solvent. However, much better resolution of the subunits was obtained when acetonitrile was used.
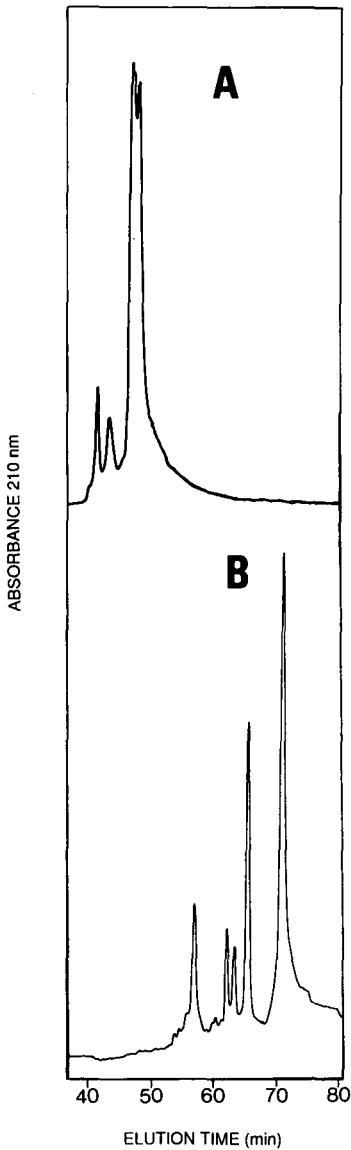
Fig. 4. Effect of the organic solvent on the separation of F_1-ATPase subunits on reversed-phase SynChropak C_8 column. Organic solvent: top, 2-propanol; bottom, acetonitrile. Conditions: linear gradient (1% B/min), where A was 0.1% TFA in water and B was 0.1% TFA in one of the above organic solvents; flow-rate, 0.5 ml/min; sample load, 60 μg of the F_1-ATPase for each injection.

Effect of flow-rate on subunit separation

F_1-ATPase subunits were separated on the SynChropak column using a linear gradient of 1% B/min at a flow-rate of 0.5 ml/min (Fig. 4B) or 1 ml/min (Fig. 1). The resolution of the polypeptides was similar when the flow-rate was changed from 1 to 0.5 ml/min, but the peak height was significantly increased.

Purification of the F$_1$-ATPase subunits from the soluble proteins extracted from submitochondrial particles

Approximately 30% of the ATPase activity present in the low-ionic strength extract of mitochondrial membranes is recovered as the purified enzyme after sucrose density gradient centrifugation [7]. In view of the high resolving power of reversed-phase HPLC, we hoped that by using RP-HPLC the F$_1$-ATPase subunits could be purified with a higher recovery directly from the mitochondrial membrane extracts. However, we found that RP-HPLC on the SynChropak C$_8$ column alone was not sufficient to resolve the ATPase subunits from the complex mixture of polypeptides present in the extract (results not shown). To reduce the complexity of the polypeptide mixture applied to the SynChropak column, a preliminary fractionation of the mitochondrial extracts was performed on a Bio-Gel TSK Phenyl RP+ column (Fig. 5). The extracts were applied to the column directly without pretreatment with 0.5% TFA–water. Five protein fractions were eluted using conditions described in Fig. 5. The polypeptide composition of these fractions was analysed by SDS-PAGE. Fraction No. 4 contained all the subunits of the F$_1$-ATPase in addition to other polypeptides. The proteins from this fraction were incubated for 2 h in 0.5% aqueous TFA (pH 2) and then rechromatographed on the SynChropak column as described in Fig. 6A. Purified F$_1$-ATPase was also chromatographed on this column (Fig. 6B). The elution times of the subunits of purified F$_1$-ATPase were used to identify the corresponding peaks of the chromatogram of fraction No. 4. It is evident from Fig. 6A that the α, β and γ subunits of F$_1$-ATPase (peaks E and D, respectively; see also Figs. 1
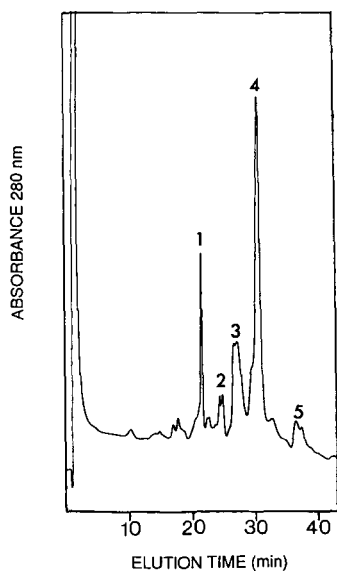
Fig. 5. Fractionation of soluble proteins extracted from pea mitochondrial membranes on a Bio-Gel TSK Phenyl RP+ column. Conditions: a linear gradient from 0 to 30% B in the first 20 min, then a gradient from 30 to 50% B from 20 to 60 min and a final gradient from 50 to 80% B from 60 to 80 min; solvent A was 0.1% TFA in water and solvent B was 0.1% TFA in acetonitrile; flow-rate, 1 ml/min; sample load, 440 μg of soluble proteins extracted from pea mitochondrial membranes.
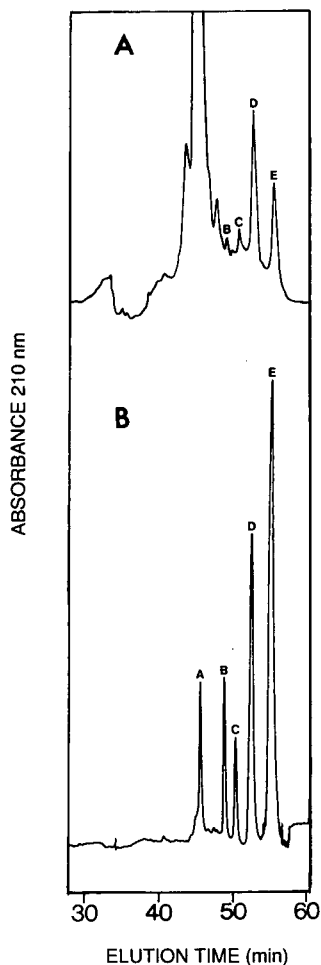
Fig. 6. Rechromatography of the proteins collected from peak 4 in Fig. 5 on a reversed-phase SynChropak C_8 column. Sample: top, proteins collected from peak 4 in Fig. 5; bottom, purified F_1-ATPase. Conditions: linear gradient (1% B/min), where solvent A was 0.1% TFA in water and solvent B was 0.1% TFA in acetonitrile; flow-rate, 1 ml/min.

and 2) are well resolved from the remaining polypeptides. The smaller F_1-ATPase subunits (δ, δ' and ε in peaks C, B and A, respectively) did not separate sufficiently from the other polypeptides that were present in fraction No. 4.

The results indicate that utilizing the HPLC methods described above, only the three larger subunits (α, β and γ) could be purified directly from mitochondrial extracts. However, we have shown that the smaller δ and δ' and ε subunits could be separated by RP-HPLC of the purified F_1-ATPase.

REFERENCES

1 J. B. Smith and P. C. Sternweis, *Biochemistry*, 16 (1977) 306.
2 P. C. Sternweis and J. B. Smith, *Biochemistry*, 19 (1980) 526.
3 M. Yoshida, N. Sone, H. Hirata and Y. Kagawa, *J. Biol. Chem.*, 252 (1977) 3480.
4 M. Yoshida, H. Okamoto, N. Sone, H. Hirata and Y. Kagawa, *Proc. Natl. Acad. Sci. U.S.A.*, 74 (1977) 936.
5 S. D. Dunn and M. Futai, *J. Biol. Chem.*, 255 (1980) 113.
6 T. Saishu, H. Nojima and Y. Kagawa, *Biochim. Biophys. Acta*, 867 (1986) 97.
7 A. Horak and M. Packer, *Biochim. Biophys. Acta*, 810 (1985) 310.
8 U. K. Laemmli, *Nature (London)*, 227 (1970) 680.
9 D. Guo, C. T. Mant, A. K. Taneja and R. S. Hodges, *J. Chromatogr.*, 359 (1986) 499.
10 D. Guo, C. T. Mant and R. S. Hodges, *J. Chromatogr.*, 386 (1987) 205.
11 S. Y. M. Lau, A. K. Taneja and R. S. Hodges, *J. Chromatogr.*, 317 (1984) 129.
12 W. C. Mahoney and M. A. Hermodson, *J. Biol. Chem.*, 255 (1980) 11199.
13 M. Hermodson and W. C. Mahoney, *Methods Enzymol.*, 91 (1983) 352.
14 L. Fausnaugh, L. A. Kennedy and F. E. Regnier, *J. Chromatogr.*, 317 (1984) 141.

Alkanesulphonates as eluents for the determination of nitrate and nitrite by ion chromatography with direct UV detection

JENS K. THOMSEN* and RAYMOND P. COX

Institute of Biochemistry, Odense University, Campusvej 55, DK-5230 Odense M (Denmark)

(First received February 27th, 1990; revised manuscript received May 13th, 1990)

ABSTRACT

A homologous series of alkanesulphonates were investigated for use as eluents in the ion chromatography of nitrate and nitrite with direct UV detection. The alkyl chain length has a large positive effect on elution strength when a poly(styrene–divinylbenzene)-based ion-exchange column is used. This effect is much less apparent with silica-based columns. Sulphonates from methane- to 1-hexanesulphonate gave excellent separations of nitrate and nitrite, allowing the determination of either without interference in the presence of a 1000-fold molar excess of the other, and making a 1-min assay for nitrate and nitrite possible. The alkanesulphonates can also be used with conductivity detection, allowing the specificity of UV detection to be combined with the versatility of conductivity measurements.

INTRODUCTION

High-performance liquid chromatography (HPLC) is a widely used technique for the determination of inorganic anions [1,2]. As only a few anions show appreciable UV absorbance in the available region of the spectrum, conductivity detection has most commonly been used. A variety of anion-exchange columns are available which give excellent resolution with aromatic eluents such as phthalate, which are commonly used in single-column ion chromatography with conductivity detection. However, the use of optical detection for direct measurements of UV-absorbing ions such as nitrate and nitrite is prevented by the high background absorbance of aromatic eluents. Direct measurements have two advantages in the determination of nitrate and nitrite: they allow the use of standard HPLC apparatus with UV detectors, and they avoid potential interferences from other ions with low UV absorbance. There is therefore a need for information about alternative eluents that can be used with optical detection. Ideally these would be effective at low concentrations so that they could also be used with conductivity detection.

The alkanesulphonates provide a series of potential eluents with low UV absorbance and a number of other desirable properties. They are anionic over a wide pH range and form a homologous series with varying degrees of hydrophobic character. They are non-volatile and readily available in pure form.

Methanesulphonate was used together with a silica-based anion-exchange column as an eluent for the HPLC of anions by Ivey [3], who reported the separation of

several anions, including nitrite and nitrate, using low concentrations (2–10 mM), and was able to use both conductivity and absorbance measurements. However, higher concentrations were necessary in subsequent investigations with different columns, varying from 11 mM chloromethanesulphonate [4] and 12–20 mM methanesulphonate [5] to 200 mM methanesulphonate [6] with silica-based columns of different capacities. The highest concentrations were reported to cause column damage [6]. High concentrations of methanesulphonate (30 mM) were also used with a poly-methacrylate-based column [7]; in contrast, Jackson [8] obtained a good separation of nitrate and nitrite with low concentrations (ca. 3 mM) of 1-heptane- and 1-octane-sulphonate using the same type of column. This suggests that the longer chain alkanesulphonates might be valuable eluents for ion chromatography.

We report here a comparison of the effects of a series of alkanesulphonates with different alkyl chain lengths on the separation of nitrate and nitrite on commercially available low-capacity resin- and silica-based anion-exchange columns.

EXPERIMENTAL

HPLC system

An HPLC system with a Kontron 420 pump, a Kontron 460 autosampler and a Kontron 432 UV–visible detector set at 210 nm was used. In experiments with conductivity detection the pump and autosampler were connected in series with a Kontron 430 UV–visible detector and a Tecator 6200 ion analyzer. In both instances a Kontron 450 data system was used for control of the apparatus and collection and treatment of the results. The autosampler was operated with the injection volume set at 5, 10 or 50 μl.

Columns

A Wescan Anion/R column (250 mm × 4.6 mm I.D.), the material being a poly(styrene–divinylbenzene)-based anion exchanger with a capacity of 0.2 mequiv./g, was used together with an Alltech Anion/R precolumn (10 mm × 4.6 mm I.D.). For comparison, a Tecator Anion/Si silica-based anion-exchange column (250 mm × 4.6 mm I.D.) with an Alltec Anion/S precolumn (10 mm × 4.6 mm I.D.) and a Vydac 300IC polymer-protected silica-based anion-exchange column (50 mm × 4.6 mm I.D.) were used with some eluents. A Wescan Anion/R precolumn (30 mm × 4.6 mm I.D.) was used as an analytical column for the development of a rapid assay for nitrate and nitrite. The column temperature was maintained at 30°C in all instances.

Mobile phases

Methanesulphonic acid and the sodium salts of methane-, 1-butane-, 1-hexane- and 1-octanesulphonic acid were obtained from Aldrich; the last three were of the quality recommended for use as ion-pairing reagents. Sodium ethanesulphonate was of the highest quality available from TCI Tokyo Kasei. 2-(N-Morpholino)ethane-sulphonic acid (MES) and tris(hydroxymethyl)aminomethane (Tris) were obtained from Sigma. All eluents used with the resin column were buffered with 0.5 mM Tris–0.25 mM methanesulphonic acid (pH ≈ 8.2). Eluents for use with the silica-based columns were buffered with 0.5 mM MES–0.25 mM NaOH (pH ≈ 6.2.). Distilled water for eluent preparation was filtered through a Millipore Milli-Q system with

a 0.22-μm exit filter before the addition of sodium sulphonates, as vacuum filtration of the eluents after the addition of the long-chain sulphonates results in excessive foam formation. All eluents were degassed under vacuum on an ultrasonic bath before use.

Analysis of results

For singly charged eluents and analytes the expected relationship between eluent concentration, C, and capacity factor, k', is given by $Ck' = $ constant [9]. From this it is possible to derive a relationship between retention time, t_R, and C:

$$t_R = (a\ t_M)/C + t_M \tag{1}$$

with two unknowns, a, which is equal to Ck', and t_M, which is the time for transit of the mobile phase. Values of Ck' for different eluents were calculated by fitting the experimental values for retention time at different eluent concentrations to eqn. 1 using non-linear regression.

RESULTS

The chain length of alkanesulphonates has a large effect on the efficiency with which anions can be eluted from the poly(styrene–divinylbenzene) anion-exchange column. Fig. 1 shows the effects of the concentration of methane-, ethane-, 1-butane- and 1-hexanesulphonate on the retention times of nitrate and nitrite at a fixed flow-rate. Octanesulphonate was even more effective than hexanesulphonate, but the concentrations required were so low that deformation of the peak shape was observed as a result of column overloading when 5 nmol nitrate and 5 nmol nitrite were injected (results not shown). Perchlorate was a slightly weaker eluent than butanesulphonate but more effective than ethanesulphonate.
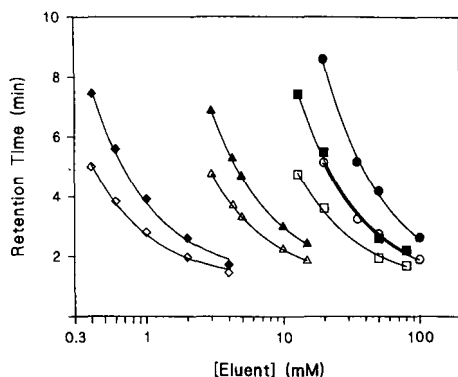
Fig. 1. Retention times for nitrate (solid symbols) and nitrite (open symbols) at different sodium alkanesulphonate concentrations; the flow-rate was 2 ml/min. The column used was a 25-cm Wescan Anion/R with an Alltec Anion/R precolumn. In addition to sodium alkanesulphonate, the eluent contained 0.5 mM Tris–0.25 mM methanesulphonic acid. $\bigcirc$,$\bullet$ = Methanesulphonate; $\square$,$\blacksquare$ = ethanesulphonate, $\triangle$,$\blacktriangle$ = 1-butanesulphonate; $\Diamond$,$\blacklozenge$ = 1-hexanesulphonate. The lines through the experimental points were obtained by fitting the results to the theoretical relationship (eqn. 1) between retention time and eluent concentration.

The greater elution strength of the higher homologues can be explained by interactions between the hydrophobic alkyl chain and the poly(styrene–divinyl-benzene) matrix, and might not be observed with other kinds of column material. The behaviour of methane- and 1-hexanesulphonate was therefore investigated with two different types of silica-based column. Table I shows the elution strength of the alkanesulphonates as the product of eluent concentration and the capacity factor for nitrate. This product was found by fitting experimental results to the theoretical relationship between retention time and eluent concentration (eqn. 1), and is a measure of the eluent concentration needed to obtain a capacity factor of 1 for the anion considered. While 1-hexanesulphonate as eluent was 68 times stronger than methane-sulphonate when the poly(styrene–divinylbenzene)-based column was used, the elution strength was increased only 1.2 times when the silica-based column was used and 2.0 times with the polymer-protected silica column.

The resolution of nitrate and nitrite obtained with the poly(styrene–divinyl-benzene) column also depends on the type and concentration of the eluent. Fig. 2 shows the relationship between the capacity factor obtained with different eluent concentrations and the resolution obtained. The best resolution was obtained with either methanesulphonate or with ethanesulphonate (results not shown). The results for 1-butanesulphonate (not shown) were between those for methane- and 1-hexane-sulphonate. In addition to the effect of chain length on the resolution, there was also the expected increase in resolution when the capacity factor was increased by lowering the concentration of the eluent. However, even in the worst cases, the resolution observed was always more than adequate, and other criteria such as the analysis time and the eluent concentration can be considered when selecting analytical conditions.

The use of high concentrations of eluent produces the risk of greater contamination by impurities present in the reagents; this was a problem with the quality of the ethanesulphonate used, which gave rise to a higher background absorbance that than with the other eluents investigated. It is also possible that high eluent concentrations could lead to column damage and microbial growth, although

TABLE I

ELUTION STRENGTH OF ALKANESULPHONATES WITH DIFFERENT TYPES OF COLUMN

Results were obtained by fitting the data from a series of experiments with different eluent concentrations to the theoretical relationship between retention time and concentration as described under Experimental.

Column	Type	Product of eluent concentration and capacity factor for nitrate (mM)	
		Methanesulphonate[a]	1-Hexanesulphonate
Wescan Anion/R	Resin	130	1.9[b]
Vydac 300IC	Silica	113	56[c]
Tecator Anion/Si	Silica	14	12[d]

[a] Eluent concentrations from 15 to 100 mM were used.

[b] Eluent concentrations from 0.4 to 4 mM were used.

[c] Ck' was calculated using the observed capacity factor from a single experiment where the eluent concentration was 10 mM.

[d] Ck' was calculated from a single experiment where the eluent concentration was 5 mM.
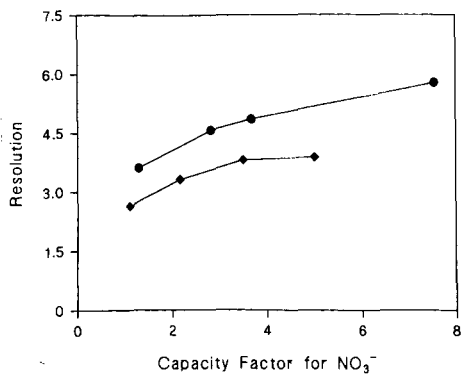
Fig. 2. Relationship between capacity factor for nitrate and resolution of the nitrate and nitrite peaks obtained with different concentrations of ($\bullet$) methanesulphonate and ($\blacklozenge$) 1-hexanesulphonate. The capacity factor (k') was calculated from the retention time (t_R) and the transit time for the mobile phase (t_M) according to the expression $k' = (t_R - t_M)/t_M$; t_M was taken as the time when the negative peak from the water injection was observed in the chromatogram; in the case of 1-hexanesulphonate the measured t_M with 4 mM eluent was used in all instances.

we did not experience such problems. In contrast, low eluent concentrations can give rise to peak deformation as a result of overloading, as we observed with 1-octane-sulphonate and concentrations of 1-hexanesulphonate under 1.0 mM. As a reasonable compromise we selected 5 mM 1-butanesulphonate for further investigations. Using this eluent, we obtained the chromatograms shown in Fig. 3 for two nitrate and nitrite standard mixtures differing a 1000-fold in concentration. The retention times and resolution obtained under these conditions are given in Table II. Some analogous results for the performance of the polymer-protected silica column are also given in Table II. The resolution obtained is excellent with both methane- and 1-hexane-sulphonate.
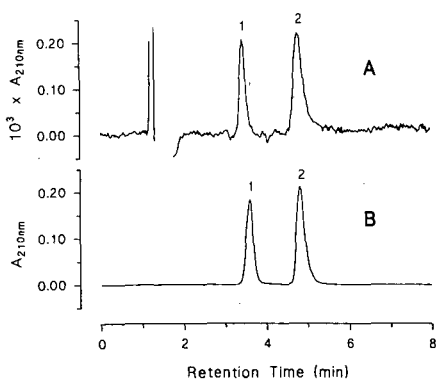
Fig. 3. Chromatograms of two standard mixtures of nitrate and nitrite. The eluent was 5 mM sodium 1-butanesulphonate containing 0.5 mM Tris–0.25 mM methanesulphonic acid and the column was a 25-cm Wescan Anion/R analytical column with an Alltec Anion/R precolumn. The flow-rate was 2 ml/min. (A) 50 μl of 1 μM NaNO$_3$–1 μM NaNO$_2$; (B) 50 μl of 1 mM NaNO$_3$–1 mM NaNO$_2$. Peaks: 1 = nitrite; 2 = nitrate.

TABLE II

EXAMPLES OF ANALYTICAL RESULTS OBTAINED WITH ALKANESULPHONATES USING DIFFERENT COLUMNS

The eluent flow-rate was 2 ml/min with the Wescan column and 3 ml/min with the Vydac column.

Eluent	Concentration (mM)	25-cm Wescan Anion/R column			5-cm Vydac 300IC column		
		t_R (min)		Resolution	t_R (min)		Resolution
		NO_2^-	NO_3^-		NO_2^-	NO_3^-	
Methanesulphonate	20	5.1	8.6	5.8	2.1	3.2	3.3
1-Butanesulphonate	5	3.3	4.7	3.7	—	—	—
1-Hexanesulphonate	10	--	--	—	1.6	2.3	3.0
1-Hexanesulphonate	1	2.8	3.9	3.3	—	—	—

One practical effect of a high resolution of two components is the ability to determine either without interference in the presence of a large excess of the other. This is illustrated in Fig. 4, which shows the effect of increasing concentrations of the other ion on the apparent peak height and peak area of nitrate or nitrite. The results show that with the eluent used, either anion can be determined without interference in the presence of a 1000-fold molar excess of the other. These measurements were performed in the absence of interfering components. High concentrations of ions such as chloride in the sample are likely to influence the resolution obtained. This was investigated in a serie of experiments (not shown) analogous to those in Fig. 4. Samples with 1 nmol of nitrate and nitrite containing up to 1 mg (17 μmol) of sodium chloride were injected. The area of the nitrate peak was constant at chloride-to-nitrate molar ratios up to about 5000, whereas baseline distortion affected the area of the nitrite peak at chloride-to-nitrite ratios over about 500. High chloride concentrations also caused the
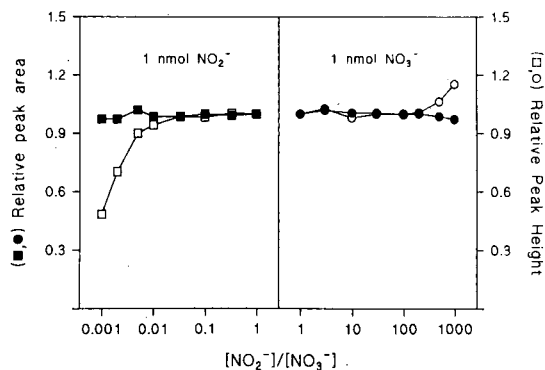
Fig. 4. Interference between nitrite and nitrate when measuring one in the presence of an excess of the other. Left, peak height and area obtained for 1 nmol of nitrite in the presence of various amounts of nitrate between 1 μmol and 1 nmol; right, corresponding heights and areas obtained with 1 nmol nitrate and various amounts of nitrite between 1 nmol and 1 μmol.
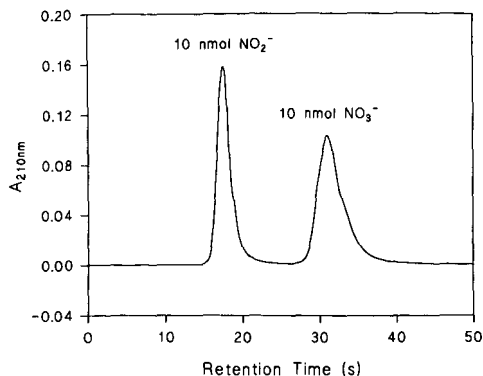
Fig. 5. Rapid assay of nitrate and nitrite using a 3-cm Wescan Anion/R precolumn as an analytical column. The eluent was 40 mM sodium methanesulphonate containing 0.5 mM Tris–0.25 mM methanesulphonic acid at a flow-rate of 4 ml/min. A volume of 10 μl of 1 mM nitrate and 1 mM nitrite was injected.

nitrite peak to be displaced in the direction of the nitrate peak, and the two peaks were only partially resolved when the injected sample contained 1 mg of sodium chloride.

Another advantage of high resolution is the possibility of using shorter columns. Veuthey *et al.* [10] used a 3-cm resin-based ion-exchange precolumn as the analytical column with sodium hydrogenphthalate as eluent to reduce the analysis time for several inorganic anions. As resolution is proportional to the square root of the column length, whereas transit time is proportional to the length, 50% of the resolution can be maintained when the column length and thus the analysis time at a given flow-rate are reduced by 75%. As the back-pressure depends on the length of the column, it is possible to decrease the analysis time further by increasing the flow-rate when shorter columns are used. Thus the choice of methanesulphonate, which gives the optimum peak separation, as the eluent at a concentration of 40 mM and increasing the flow-rate from 2 to 4 ml/min with a 3-cm column results in a 1-min assay with a resolution of 2.5, as shown in Fig. 5.
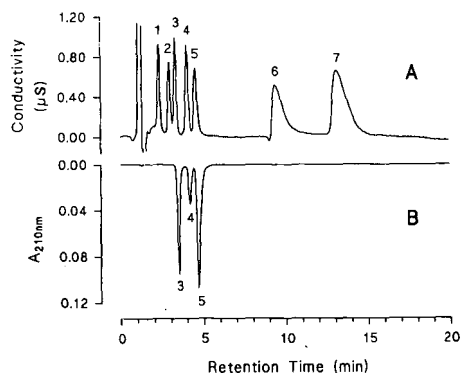
Fig. 6. Chromatograms of a standard mixture of seven anions using both (A) conductivity detection and (B) UV detection. Conditions as in Fig. 3. Injection volume, 50 μl. The sample contained (1) 1 mM F$^-$, (2) 0.5 mM Cl$^-$, (3) 0.5 mM NO$_2^-$, (4) 0.5 mM Br$^-$, (5) 0.5 mM NO$_3^-$, (6) 2 mM HPO$_4^{2-}$ and (7) 1 mM SO$_4^{2-}$.

Long-chain sulphonates can also be used with coupled conductivity and UV detection as a powerful method for determining both UV-absorbing and UV-transparent anions. Fig. 6 shows the separation of seven anions using 1-butanesulphonate as eluent. It is noteworthy that with conductivity detection the water peak from injection is the only system peak observed, and that the injection peak using UV detection is negligible.

The position of the phosphate peak in the seven anions standard depends on the pH of the eluent. In the chromatogram in Fig. 6 this was buffered at about pH 8.2, so that phosphate is present in the HPO_4^{2-} form. In general, buffering the eluent at different pH values was found to have little effect on nitrate and nitrite [as long as nitrite ($pK_a = 3.4$) is not appreciably protonated] but changes the position of elution of weak acids and the zwitterionic buffers commonly used in biochemistry. This can be useful in separating nitrate or nitrite from interfering components of this type.

DISCUSSION

The choice of a method for the determination of nitrate and nitrite by HPLC depends on a number of factors. The detector and column types available will usually be a major consideration, together with the concentrations expected in the sample and the nature of interfering compounds. Other considerations include the number of samples to be analysed and hence the significance of the cost and time of the assays, and the possible interest of simultaneous measurements of other components.

Although ion-pair chromatography on reversed-phase columns [11,12] may have advantages in particular situations, ion-exchange chromatography on specialized columns for inorganic anions is the most straightforward approach. Direct UV detection for nitrate and nitrite is probably the method of choice unless it is desired to measure other non-absorbing anions at the same time. This approach is sensitive, straightforward and uses the most commonly available detector, and interference is essentially limited to other UV-absorbing anions. However, when non-absorbing anions are to be measured in the same sample, it is necessary to use conductivity or indirect UV detection with absorbing eluents [13].

Of the potential eluents available for use with direct UV detection, the results presented here show that the alkanesulphonates have several advantages. The existence of a homologous series means that for a wide range of types of resin-based column, conditions can be found allowing elution within reasonable times without the use of excessively high eluent concentrations. The high elution strength of the longer chain homologues means that eluent concentrations giving a low background in conductivity measurements can be used. This opens up the possibility of combining the selectivity of UV detection with the universality of conductivity detection. For maximum detector response in conductivity measurements, the use of alkanesulphonates will be inferior to weakly acidic eluents because of the signal enhancement resulting from the use of a mixture of charged and uncharged forms of the eluent [14]. However, this enhancement is associated with the presence of system peaks which are not observed with alkanesulphonates.

With silica-based columns the hydrophobicity of the eluent is of minor importance, and the retention of nitrate and nitrite is mostly affected by the concentration of the eluent and the capacity of the column. Rapid elution with low

eluent concentrations depends on a low column capacity, leading to the danger of column overloading if the sample contains high concentrations of interfering ions. The advantages of alkanesulphonates as eluents allowing the use of low concentrations are thus most apparent when columns with hydrophobic carrier material are used.

Although this investigation was concerned with nitrate and nitrite, UV detection can also be used for the measurement of other inorganic anions, including bromide and chloride [5]. We have found alkanesulphonates to be useful in simultaneous determinations of chloride by measurement of absorbance at 190 nm and sulphate by measurement of conductivity in sea-water samples, where the chloride peak in conductivity detection was obscured by the injection peak.

The separations obtained with alkanesulphonates appear to be at least as good as those obtained with the aromatic compounds commonly used for ion chromatography, and they are therefore of considerable potential interest as eluents for the determination of inorganic anions using HPLC.

REFERENCES

1 P. R. Haddad and A. L. Heckenberg, *J. Chromatogr.*, 300 (1984) 357.
2 P. R. Haddad, in H. A. McKenzie and L. E. Smythe (Editors), *Quantitative Trace Analysis of Biological Materials*, Elsevier, Amsterdam, 1988, p. 51.
3 J. P. Ivey, *J. Chromatogr.*, 267 (1983) 218.
4 P. E. Jackson, P. R. Haddad and S. Dilli, *J. Chromatogr.*, 295 (1984) 471.
5 G. P. Ayers and R. W. Gillett, *J. Chromatogr.*, 284 (1984) 510.
6 L. Eek, *J. Chromatogr.*, 322 (1985) 491.
7 N. J. Eggers and D. L. Cattle, *J. Chromatogr.*, 354 (1986) 490.
8 P. E. Jackson, personal communication.
9 P. R. Haddad and C. E. Cowie, *J. Chromatogr.*, 303 (1984) 321.
10 J. L. Veuthey, J. P. Senn and W. Haerdi, *J. Chromatogr.*, 45 (1988) 183.
11 M. Lookabaugh and I. S. Krull, *J. Chromatogr.*, 452 (1988) 295.
12 M. L. Marina, J. C. Diez-Masa and M. V. Dabrio, *J. Liq. Chromatogr.*, 12 (1989) 1973.
13 N. Chauret and J. Hubert, *J. Chromatogr.*, 469 (1989) 329.
14 J. S. Fritz, D. L. DuVal and R. E. Barron, *Anal. Chem.*, 56 (1984) 1177.

Capillary supercritical fluid chromatography of explosives

Investigations on the interactions between the analytes, the mobile phase and the stationary phase

ALBRECHT MUNDER[a], STEPHEN N. CHESLER and STEPHEN A. WISE*

Organic Analytical Research Division, Center for Analytical Chemistry, National Institute of Standards and Technology (formerly National Bureau of Standards), Gaithersburg, MD 20899 (U.S.A.)

(First received January 10th, 1990; revised manuscript received July 24th, 1990)

ABSTRACT

The independent effects of pressure and temperature in supercritical fluid chromatography on the capacity ratio on chromatographic resolution of some polar organic model compounds were investigated. Increasing the pressure isothermally leads to a steady decrease in retention and resolution. With changing temperature, a maximum in the capacity ratio as well as the resolution was observed. These observations may be related to a combination of gas chromatographic (GC) and liquid chromatographic (LC) theories of solute interactions with the mobile and stationary phases. However, pure GC- or LC-like behavior was not observed either below or above the critical point of the mobile phase. Capacity ratios for various explosives, propellants and related compounds were determined on capillary open tubular columns coated with either a non-polar methyl- or a polar cyanopropyl–phenyl-substituted siloxane stationary phase. The mobile phase for all studies was carbon dioxide. On the polar column, many of the solutes exhibited a good correlation between their bulk dipole moment and chromatographic retention. Deviations from this correlation could be explained by means of the physical or steric properties of these solutes. The elution order of the compounds on the non-polar column was similar to the order achieved using GC rather than LC.

INTRODUCTION

Due to the complex interactions present in supercritical fluid chromatography (SFC), there is still no straightforward explanation of the phenomena occurring. However, many authors have performed theoretical and experimental investigations to study the effects of pressure, temperature and density of the fluid on the chromatographic behavior of test compounds [1–18]. In most cases the test solutes were a homologous series of alkanes, phthalates or polycyclic aromatic hydrocarbons. Our intention was to compare the findings of previous authors with our results obtained on a set of more polar species. In our selection of polar test compounds,

---

[a] Present address: Degussa AG, VTC-A, 6450 Hanau 1, Postfach 1345, F.R.G.

a polar stationary phase and a non-polar mobile phase, we tried to achieve a better understanding of the solute–stationary phase interactions.

EXPERIMENTAL[a]

A Model 501 capillary supercritical fluid chromatograph (Lee Scientific, Salt Lake City, UT, U.S.A.) was used, which was equipped with a split injector and both UV and flame ionization detectors. A bonded methylpolysiloxane column (SB methyl-100, 5 m × 100 μm I.D., 0.25 μm film thickness, Lee Scientific) and a bonded 50% cyanopropyl–phenylpolysiloxane column (DB 225, 10 m × 50 μm I.D., 0.05 μm film thickness, J & W Scientific, Folsom, CA, U.S.A.) were used for the studies described.

Nitroglycerine, nitrocellulose, 2,4,6,N-tetranitro-N-methylaniline (tetryl) and 1,3,5,7-tetranitro-1,3,5,7-tetraazacyclooctane (HMX) were obtained from the U.S. Army Explosives Repository (Dover, NJ, U.S.A.). Ethylene glycol dinitrate, diethylene glycol dinitrate, 1,3,5-trinitro-1,3,5-triazacyclohexane (RDX) and pentaerythritol tetranitrate (PETN) were received from the Bureau of Alcohol, Tobacco & Firearms (Rockville, MD, U.S.A.). SFC-grade carbon dioxide and additional reference chemicals were obtained in the highest purity available from commercial sources.

RESULTS AND DISCUSSION

Interaction with the mobile phase

First, we investigated the effects of pressure and temperature on the capacity ratio as well as the chromatographic resolution of a set of test compounds, the three isomeric of mononitrotoluene (NT). The first inflection of the baseline from the UV detector response was generally taken as the chromatographic void volume for retention measurements. Chromatographic resolution (R_s) was calculated as follows:

$$R_s = 1.177 \, [t_{s(2)} - t_{s(1)}]/[b_{0.5(2)} + b_{0.5(1)}]$$

where t_s is the retention time and $b_{0.5}$ is the peak width at half height of the compounds under consideration. The instrument was used in the pressure control mode and was equipped with a cyanopropyl–phenylpolysiloxane column. The column was maintained at a constant temperature while a range of different pressures was applied. Increasing the column pressure led to a steady decrease in capacity ratio (k') (Fig. 1). Similar behavior using different separation systems has been reported by other authors [1–7]. At even higher pressures (*e.g.*, greater than 250 atm), k' is reported to increase [8].

The fluid density increases with increasing pressure as does the solubility of the analytes in the mobile phase. Therefore, the decrease in k' of the analytes can be explained by the increase in their solubility with increasing pressure. The minimum observed in the k' *versus* pressure plot arises from intermolecular repulsion forces in the
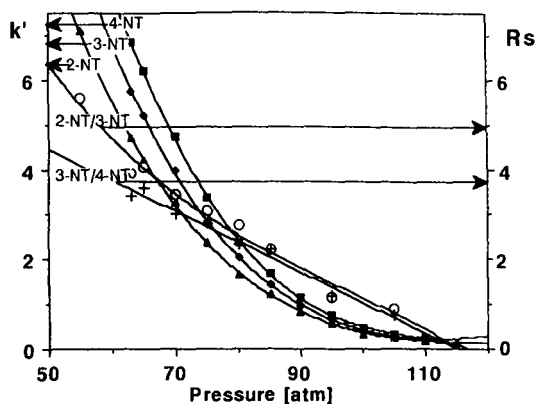
Fig. 1. Effect of pressure in SFC on the capacity ratio and the chromatographic resolution of the three nitrotoluenes. Column: DB 225 (10 m × 50 μm I.D., 0.05 μm film thickness), at 60°C. ■ = 4-NT; ◆ = 3-NT; ▲ = 2-NT; ○ = 2-NT/3-NT; + = 3-NT/4-NT.

bulk fluid. These forces appear with increasing density or pressure [9], thus decreasing the solubility of the solutes. This minimum also coincides with a maximum in a solubility–pressure plot [19,20]. In this context, "solvent strength" of the fluid, rather than solubility of a test compound, might be the appropriate term to use. Others have applied thermodynamic models to predict the dependence of k' on the pressure yielding results that were in good agreement with the experimental data [1,2,4,5,9–12].

Chromatographic resolution of the three compounds decreased steadily as the pressure increased (see Fig. 1). This observation is similar to the results reported by others [3,7]. Evidently, at low densities the diffusion coefficients in the mobile phase were high, which led to high effective plate numbers and thus to high R_s [3]. It should be emphasized that, as the system turned from the subcritical to the supercritical state (at 73 atm), no discontinuity in either the plots of k' or R_s versus pressure was observed, as reported by others [12].
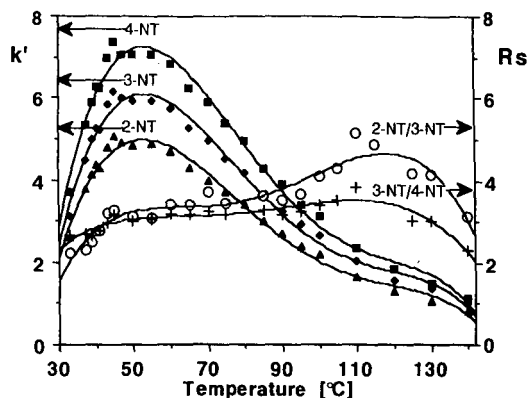
Fig. 2. Effect of temperature in SFC on the capacity ratio and the chromatographic resolution of the three nitrotoluenes. Column as in Fig. 1; 63 atm.; symbols as in Fig. 1.
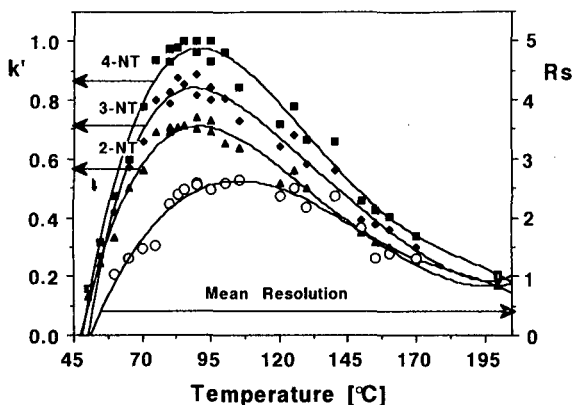
Fig. 3. Effect of temperature in SFC on the capacity ratio and the chromatographic resolution of the three nitrotoluenes. Column as in Fig. 1; 100 atm; $\square$, $\blacklozenge$ and $\blacktriangle$ as in Fig. 1; $\bigcirc$ = mean resolution.

Next, the density was changed under isobaric conditions by varying the temperature. In contrast to the isothermal change of the density, maxima were present for both the capacity ratio as well as the chromatographic resolution (Figs. 2 and 3). In the case of subcritical pressure (63 atm, Fig. 2), the maxima for the capacity ratios were observed at a lower pressure than the maxima in the chromatographic resolution. Under supercritical conditions, however (100 atm, Fig. 3), the maxima of the two different kinds of chromatographic variables almost coincide. The mean resolution was calculated as the mean of the chromatographic resolution of 2-NT/3-NT and 3-NT/4-NT, respectively, at the respective temperature.

Maxima of both capacity ratio and chromatographic resolution, as determined in the isobaric experiments (Figs. 2 and 3), appeared at three different densities. These same densities were encountered in the isothermal experiments (Fig. 1), where no maxima were observed. Therefore, the appearance of such maxima cannot be due to changes in density alone. Several authors, who also observed such maxima in capacity factors (e.g., [3,6,10–18]), interpreted this effect as a superposition of both volatilization and solvation of the compounds. Increasing temperature decreases density and therefore increases retention. At even higher temperature, the volatility of the components becomes more important, leading to a gas chromatographic (GC)-like decrease in retention with increasing temperature.

Although the maxima in plots of capacity ratios *versus* temperature have been described by other authors for a broad range of phase systems as well as analytes, it has not been emphasized that, with homologous series of isomers, the maxima occur at the same temperature for all components. In other words, the onset of the "GC behavior" evidently is not influenced by the nature of the analyte. Because the series investigated covered a broad range of boiling points, the appearance of the descending section of the plot cannot be attributed solely to volatilization of the test components at elevated temperatures. Other, less straightforward retention mechanisms are likely to occur.

With more strongly retained compounds than the nitrotoluenes (such as polycyclic aromatic hydrocarbons), additional minima in the capacity ratio [3,4,7,16,17] and the chromatographic resolution [3,16,17] have been reported. This

correlates with the maxima occurring when solubility of a test compound in a fluid is plotted *versus* temperature [19,20]. Because these minima in the k'–temperature and R_s–temperature plots were observed when the temperature was lowered further, they might be related to the effect of the density on k', as are the minima observed in the k' *versus* pressure plots [8]. This would be in contrast to the maxima that occurred only in the case of isobaric changes in density.

Determination of the extrema of k' at several different pressures showed that at higher pressure both minima and maxima were shifted towards a higher temperature (lower density) and became less pronounced, as has also been reported by others [3,12–18]. The same holds true for the solubility–temperature plots [19]. Although the positions of the extrema are linked to the density of the mobile phase, there is generally no absolute value of the density where those extrema appear. For example, there is an absence of maxima in the plots of capacity factor *versus* pressure shown in Fig. 1. Components with stronger retention and higher boiling points also show stronger extrema than their less-retained, lower-boiling isomers or homologues (Figs. 2 and 3, [13–18]). Those observations summarized above may be generalized in the following manner: the more intense the analyte–stationary phase interactions (reflected in relatively long retention times), the more sensitive is their chromatographic behavior to changes both in pressure and temperature. It is interesting that neither the choice of the phase system used for the separation, nor the nature of the test compounds has any impact on those general findings. This could be concluded from our data as well as those cited earlier.

Although some of the phenomena have been treated theoretically on a thermo-dynamic basis [1–5,9–12,16], there is still a need for an explanation of the complex effects observed and described above.

Interaction with the stationary phase

To investigate the interactions between the analytes and the stationary phase, the retention behavior of a large set of compounds, namely a variety of explosives, propellants and related compounds, was determined on two columns with phases of totally different selectivity. The non-polar methyl column should display a separation following partition phenomena, whereas the cyanopropyl–phenyl column is expected to show evidence of polar interactions. For the two different columns, the capacity ratios of the compounds investigated are listed in Table I.

Whereas the elution order of the dinitrotoluenes on the polar DB 225 column is similar to that observed in reversed-phase liquid chromatography (LC) [21], RDX is much less retained in the LC system. The elution orde of various explosives in our SFC separations is very different from that observed in other reversed-phase LC separations [22–25].

There are apparently more similarities between GC and SFC [26–28]; *e.g.*, the elution order of the different mono- and dinitrotoluenes is the same in GC (irrespective of the column used) as in SFC on the methyl column. This observation suggests that, in the case of this non-polar column, a partition-type retention mechanism is effective.

There are only a few publications on SFC of explosives [29–35]. Nevertheless, the elution order of the limited number of compounds investigated by those authors agrees well with our results.

We next focused on investigating a likely retention mechanism for the

TABLE I

CAPACITY RATIOS OF ALL EXPLOSIVES, PROPELLANTS AND RELATED COMPOUNDS
CONSIDERED IN THE PRESENT STUDY

Compound	SB Methyl-100 (60°C, 83 atm, 11 min, 3 atm/min, 95 atm)	DB 225 (85°C, 100 atm, 11 min, 3 atm/min, 180 atm)
2-Nitrotoluene (2-NT)	0.62	0.32
3-Nitrotoluene (3-NT)	0.70	0.38
4-Nitrotoluene (4-NT)	0.77	0.52
2,6-Dinitrotoluene (2,6-DNT)	1.48	1.38
2,3-Dinitrotoluene (2,3-DNT)	1.98	3.08
2,4-Dinitrotoluene (2,4-DNT)	2.06	2.17
3,4-Dinitrotoluene (3,4-DNT)	2,36	4.19
2,4,6-Trinitrotoluene (TNT)	2.52	4.71
Picric acid (PA)	3.76	n.e.[a]
Tetryl	5.20	11.00
1-Nitronaphthalene (1-NN)	2.67	2.06
1,5-Dinitronaphthalene (1,5-DNN)	4.41	5.67
1,3-Dinitronaphthalene (1,3-DNN)	4.93	6.23
2,7-Dinitronaphthalene (2,7-DNN)	6.13	7.59
1,8-Dinitronaphthalene (1,8-DNN)	7.39	10.90
Ethyleneglycoldinitrate (EGDN)	n.r.[b]	0.46
Diethyleneglycoldinitrate (DEGDN)	n.r.	1.25
Nitroglycerine (NG)	1.53	2.48
Diphenylamine (DPA)	3.35	2.20
PETN	3.36	6.98
N-Nitroso diphenylamine (NNDPA)	3.61	2.16
Dibutylphthalate (DBP)	4.52	1.46
RDX	4.57	13.30
Diethyldiphenylurea (DEDPU)	4.83	1.40
2-Nitrodiphenylamine (2-NDPA)	5.77	4.40
HMX	n.e.	n.e.
Nitroquinoline (NQ)	n.e.	n.e.

[a] n.e. = Not eluted under the conditions applied.
[b] n.r. = Not retained under the conditions applied.
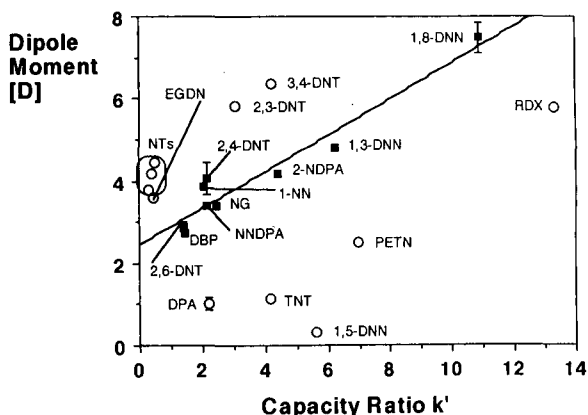
Fig. 4. Dipole moment *versus* capacity ratio in SFC for various explosives. Column: DB-225 (10 m × 50 μm I.D., 0.05 μm film thickness); see Table I for conditions. ■ Indicates data used for generation of correlation line. Error bars represent standard deviation of the mean of dipole moment data found in the literature.
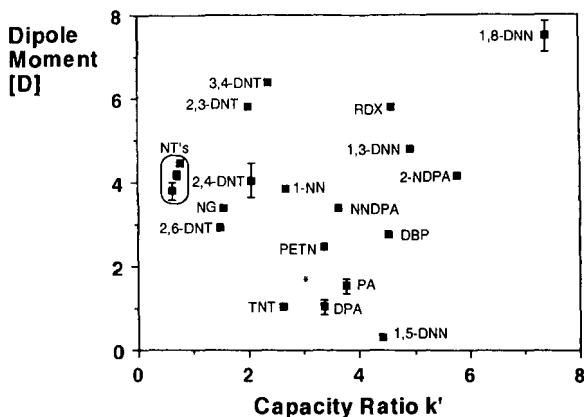
Fig. 5. Dipole moment *versus* capacity ratio in SFC for various explosives. Column: SB Methyl-100 (5 m × 100 μm I.D.,, 0.25 μm film thickness); see Table I for conditions.

compounds on the polar DB 225 column, *i.e.*, the effect of dipole moment. Fig. 4 shows the elution order of the analytes on the DB 225 column plotted *versus* their dipole moment. For those compounds not appearing in the graph, data on their dipole moment were not available. About half of the points are on a straight line (obtained by linear correlation calculations) correlating polarity of the compound and retention on the polar column.

Some compounds showed weaker retention than expected considering their dipole moment, thus falling above the line. Those compounds were either more volatile species (nitrotoluenes, ethyleneglycol dinitrate) or there was some steric hindrance of the polar substituents (as in 2,3-dinitrotoluene and 3,4-dinitrotoluene), which influenced the retention. The other group of compounds that did not follow the simple correlation between dipole moment and retention exhibited stronger retention than predicted. In other words, their bulk dipole moment was lower than expected based on retention. Most members of this group contained highly polar groups, but in highly symmetrical positions, leading to a low bulk dipole moment, (*e.g.*, 2,4,6-trinitro-toluene, 1,5-dinitronaphthalene, PETN and RDX). Diphenylamine is a very polar-izable compound, and therefore was more strongly retained than would be expected based on its low dipole moment. Consequently, the retention of the compounds in SFC on the DB 225 column may be generally understood as a polar interaction between sterically free polar sections of the analyte molecule and the cyanopropyl–phenyl stationary phase.

A similar plot of the elution order *versus* the dipole for the methyl column is shown in Fig. 5. No obvious correlation is observed, which suggests that the retention mechanism is not based on a polar interaction of the compounds with the stationary phase.

ACKNOWLEDGEMENTS

REFERENCES

1 P. J. Schoenmakers, *J. Chromatogr.*, 315 (1984) 1.
2 C. R. Yonker and R. W. Gale, *J. Phys. Chem.*, 91 (1987) 3333.
3 E. Klesper, *Fresenius Z. Anal. Chem.*, 330 (1988) 200.
4 C. R. Yonker, R. W. Wright, S. L. Frye and R. D. Smith, *ACS Symp. Ser.*, 329 (1987) 172.
5 C. R. Yonker and R. D. Smith, *J. Chromatogr.*, 459 (1988) 183.
6 I. K. Barker, J. K. Kithinji, K. D. Bartle, A. A. Clifford, M. W. Raynor, G. F. Shilstone and P. A. Halford-Maw, *Analyst (London)*,114 (1989) 41.
7 D. Leyendecker, D. Leyendecker, F. P. Schmitz and E. Klesper, *J. Chromatogr.*, 371 (1986) 93.
8 R. G. Christensen, *J. High Resolut. Chromatogr. Chromatogr. Commun.*, 8 (1985) 824.
9 D. E. Martire and R. E. Boehm, *J. Phys. Chem.*, 91 (1987) 2433.
10 C. R. Yonker and R. D. Smith, in B. A. Charpentier and M. M. Sevenants (Editors), *Supercritical Fluid Extraction and Chromatography*, American Chemical Society, Washington, DC, 1988, p. 161.
11 C. R. Yonker, B. W. Wright, R. C. Petersen and R. D. Smith, *J. Phys. Chem.*, 89 (1985) 5526.
12 T. A. Berger, *J. Chromatogr.*, 478 (1989) 311.
13 T. Takeuchi, Y. Hashimoto and D. Ishii, *J. Chromatogr.*, 402 (1987) 328.
14 T. L. Chester and D. P. Innis, *J. High Resolut. Chromatogr. Chromatogr. Commun.*, 8 (1985) 561.
15 P. J. Schoenmakers and L. G. M. Uunk, in J. C. Giddings, E. Grushka, P. R. Brown (Editors), *Advances in Chromatography*, Vol. 30, 1989, p. 1.
16 D. Leyendecker, D. Leyendecker, F. P. Schmitz and E. Klesper, *J. Liq. Chromatogr.*, 10 (1987) 1917.
17 F. P. Schmitz, D. Leyendecker and E. Klesper, *Ber. Bunsenges. Phys. Chem.*, 88 (1984) 912.
18 T. Takeuchi, K. Ohta and D. Ishii, *Chromatographia*, 25 (1988) 125.
19 M. A. McHugh and V. J. Krukonis, *Supercritical Fluid Extraction. Principles and Practice*, Butterworth, Stoneham, MA, 1986.
20 E. Stahl, K. W. Quirin, A. Glatz, D. Gerard and G. Rau, *Ber. Bunsenges. Phys. Chem.*, 88 (1984) 900.
21 E. P. Meier, L. G. Taft, A. F. Graffeo and T. B. Stanford, *4th Int. Conf. Sens. Environ. Pollut., New Orleans, November, 1977*, Paper 132.
22 K. Bratin, P. T. Kissinger, R. C. Briner and C. S. Bruntlett, *Anal. Chim. Acta*, 130 (1981) 295.
23 M. P. Maskarinec, D. L. Manning, R. W. Harvey, W. H. Griest and B. A. Tomkins, *J. Chromatogr.*, 302 (1984) 51.
24 A. H. Lyter, *J. Forens. Sci.*, 28 (1983) 446.
25 J. B. F. Lloyd, *J. Chromatogr.*, 261 (1983) 391.
26 T. Tamiri and S. Zitrin, *J. Energ. Mater.*, 4 (1986) 215.
27 I. S. Krull, M. Swartz, K. H. Xie and J. N. Driscoll, *Proc. Int. Symp. Anal. Detect. Explos.*, Fed. Bur. Invest., Washington, DC, 1988, p. 107.
28 J. M. F. Douse, *J. Chromatogr.*, 328 (1985) 155.
29 F. Belkin, R. W. Bishop and M. V. Sheely, *J. Chromatogr. Sci.*, 23 (1985) 532.
30 J. M. F. Douse, *J. Chromatogr.*, 445 (1988) 244.
31 K. Grolimund, in M. L. Lee and K. E. Markides (Editors), *SFC-Applications*, Brigham Young University Press, Provo, UT, 1988, p. 175.
32 E. C. Huang, in M. L. Lee and K. E. Markides (Editors), *SFC-Applications*, Brigham Young University Press, Provo, UT, 1988, p. 177.
33 P. Sandra, in M. L. Lee and K. E. Markides (Editors), *SFC-Applications*, Brigham Young University Press, Provo, UT, 1988, p. 176.
34 M. Ashraf-Khorassani and L. T. Taylor, *J. High Resolut. Chromatogr. Chromatogr. Commun.*, 12 (1989) 40.
35 W. H. Griest, C. Guzman and M. Dekker, *J. Chromatogr.*, 467 (1989) 423.

Theory of temperature-programmed gas chromatography

The method of moment analysis

JIAN YING ZHANG*, GUANG MIN WANG and RONG QIAN

608-Group, Dalian Institute of Chemical Physics, Chinese Academy of Sciences, Dalian (China)
(First received December 28th, 1989; revised manuscript received June 1st, 1990)

ABSTRACT

For temperature-programmed gas chromatography, it is shown that the first original, the second and the third central moments of a moving zone are additive along all parts of the component passing through in a linear system. Trace expressions for zones moving along the column and expressions for the calculation of the first three moments (retention time, peak variance and third central moment related to peak skew) of peaks according to isothermal data are derived. It is also shown that the definition of local plate height and related equations for peak variance in the literature are not correct. Reasonable definitions of local plate height and related equations are then developed appropriately.

INTRODUCTION

The theory of temperature-programmed gas chromatography (TPGC) was developed by several workers [1–5] and equations for the retention time and peak variance were derived and optimization procedures developed. However, in the literature, trace expressions for components moving along the column length with time have not been considered in detail. Also, the third central moment, which reflects the skew of peaks, and higher order moments have not previously been studied. Additionally, the definition of local plate height and related equations for peak variance in the literature [1,6–8] are not correct, as the actual peak variance in TPGC could not be calculated using these equations with isothermal data.

In the present treatments, equations for the retention time and traces of components moving along the column length are derived. Reasonable definitions of local plate height and related equations for the calculations of peak variance in TPGC are then developed.

In this paper, a new method, moment analysis, is developed for TPGC, in which the retention time, peak variance and higher order moments are dealt with by a common, general, strict and simple method. By using this method, equations for the calculation of different order of moments, including retention time, peak variance and third central moment, in TPGC using isothermal data are developed. Decompression effects of the carrier gas are taken into account.

RETENTION TIME AND TRACE

In this treatment, only systems which satisfy the following assumptions are discussed: columns are homogeneous; columns, or more generally systems, are linear; and carrier gas pressures at the column inlet and column outlet remain constant during analysis.

Considering a component, the position of its zone centre at time t is $z = z(t)$ and the velocity of the zone centre is

$$dz/dt = Rv = v/(1+k) \tag{1}$$

where $k = k(t)$ is the capacity factor and v is the local velocity of the carrier gas.

Darcy's Law is expressed as

$$v = -(K/\eta)dP/dz \tag{2}$$

where K and η are the permeability and viscosity, respectively, of the carrier gas and P is the local pressure of the carrier gas. As the column is homogeneous, at any moment there is no temperature gradient along the column length, and we can write

$$pv = P_i v_i = P_o v_o = \bar{P}\bar{v} \tag{3}$$

where P_i and P_o are the carrier gas pressure at column inlet and column outlet, respectively and v_i and v_o are the corresponding carrier gas velocities. $\bar{P}$ is the distance average of P, i.e.,

$$\bar{P} = (\int_0^L Pdz)/L = P_o/j \tag{4}$$

where

$$j = \frac{3}{2} \cdot \frac{(\alpha^2 - 1)}{(\alpha^3 - 1)} \tag{5}$$

and

$$\alpha = P_i/P_o \tag{6}$$

are constants.

From eqns. 2 and 3, we have

$$\frac{z}{L} = \frac{\alpha^2 - (P/P_o)^2}{\alpha^2 - 1} = \frac{\alpha^2 - (v_o/v)^2}{\alpha^2 - 1} \tag{7}$$

and the time average of v with time is given by

$$\frac{1}{t_0}\int_0^{t_0} vdt = \frac{1}{t_0}\int_0^L dz = \frac{L}{t_0} \tag{8}$$

where

$$t_0 = \int_0^L dz/v = \int_0^L \frac{\sqrt{\alpha^2 - (\alpha^2 - 1)z/L}}{v} \cdot dz = \frac{L}{jv_o} \tag{9}$$

Noting that $\bar{v}$ in eqn. 3 can be written as

$$\bar{v} = v_o P_o/\bar{P} = j \, v_o \tag{10}$$

then $\bar{v}$ is just the time average of v within the dead time t_0, and it is only related to the column temperature, *i.e.*,

$$\bar{v} = L/t_0 \tag{11}$$

On the other hand, the distance average of v along the column is

$$\bar{\bar{v}} = \frac{1}{L} \int_0^L v dz \tag{12}$$

It can be derived that

$$\bar{\bar{v}} = \frac{2 \, \bar{v}}{j(\alpha + 1)} \tag{13}$$

Combining eqns. 10 and 7 leads to

$$v = \frac{\bar{v}}{j\sqrt{\alpha^2 - (\alpha^2 - 1)z/L}} \tag{14}$$

This equation relates v (local value) and $\bar{v}$ at an appropriate column temperature.
    By combining eqns. 1 and 14, the retention time t_R in TPGC (in this text, subscripts R and r denote TPGC and isothermal processes, respectively) is obtained by the expression

$$\int_0^{t_R} \frac{dt}{t_0 \, (1+k)} = 1 \tag{15}$$

This is consistent with the equation derived by Harris and Habgood [3].
    The procedure for the calculation of t_R according to isothermal data can be outlined as follows. Experimentally, the dead time can be written as

$$t_0(T) = (A' + B'T)/(P_i - P_o) \tag{16}$$

Recalling that P_i and P_o are constants, this reduces to

$$t_0(T) = A_0 + B_0 T \tag{17}$$

The linear heating programme can be expressed as

$$T = T_0 + rt \tag{18}$$

where T_0 and r are the initial temperature and the heating rate, respectively. It is well known that

$$\ln k = C_0 + D_0/T \tag{19}$$

If the constants A_0, B_0, C_0 and D_0 above are determined by regression to several (more than two) isothermal data, then from eqns. 17, 18, 19 and 15, for any values of T_0 and r, the retention time t_R of each component with temperature programming can be calculated immediately.

The trace expression in TPGC can be obtained by combining eqns. 1 and 14, i.e.,

$$z(t)/L = \frac{\alpha^2}{\alpha^2 - 1} - \frac{1}{\alpha^2 - 1}\left(\alpha^3 - \frac{\alpha^3 - 1}{L}\int_0^t \frac{\bar{v}}{1 + k} \cdot dt\right)^{2/3} \tag{20}$$

Eqn. 14 is then rewritten as

$$v(t) = \frac{\bar{v}}{j}\left(\alpha^3 - \frac{\alpha^3 - 1}{L}\int_0^t \frac{\bar{v}}{1 + k} \cdot dt\right)^{-1/3} \tag{21}$$

Similarly to the calculation of t_R, the position of the zone centre and its velocity (Rv) at any time t can be calculated by eqns. 20 and 21.

As a simple example, in Fig. 1 we give the trace for isothermal processes. The trace expression is obtained according to eqn. 20 as

$$z(t)/L = \frac{\alpha^2}{\alpha^2 - 1} - \frac{1}{\alpha^2 - 1}\left[\alpha^3 - (\alpha^3 - 1)\frac{t}{t_r}\right]^{2/3} \tag{22}$$

As in Fig. 1, actual traces for isothermal processes always fall between the two limiting curves, i.e., the curve $z/L = t/t_r$ ($\alpha \to 1$) and the curve $z/L = 1 - (1 - t/t_r)^{2/3}$ ($\alpha \to \infty$).

MOMENTS OF LINEAR SYSTEMS

It is well known that moments play an important role in chromatography [9–15], as they are directly related to factors of practical importance, e.g., M_0, peak area; M_1, peak average retention time ($\approx t_r$); M_2, peak variance ($= \tau^2$); M_3, peak asymmetry (skew $= M_3/M_2^{3/2}$); M_4, peak flattening (excess $= M_4/M_2^2 - 3$); where M_1 denotes the first original (absolute) moment and M_2, M_3 and M_4 denote the second, third and fourth central moment, respectively.

Basic relationships for moments
    The properties of moments are generally discussed as follows [16–18]. First we discuss the moments created by the column itself.
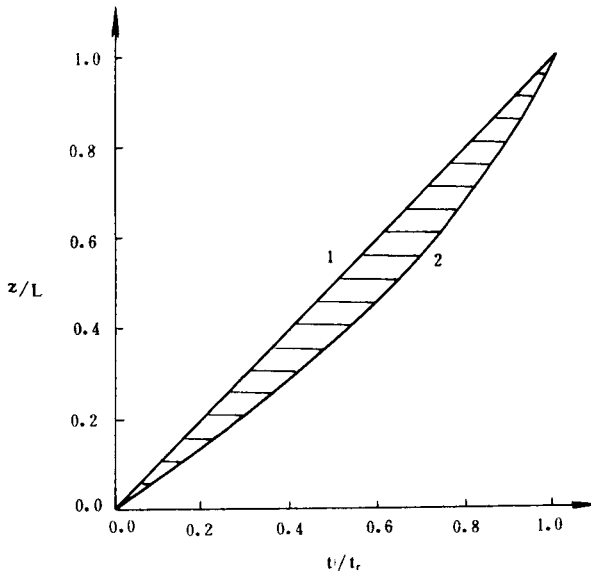
Fig. 1. Traces of components (including air peak) along the column length for isothermal processes. Actual traces always fall between the two limiting curves (shaded area), i.e., curve 1, $z/L = t/t_r$ $(\alpha \rightarrow 1)$ and curve 2, $z/L = 1 - (1 - t/t_r)^{2/3}$ $(\alpha \rightarrow \infty)$.

The whole column can be regarded as many successive short lengths, Δl_1, Δl_2, Δl_3, etc., and we consider the variation of the peak profiles along these column intervals. Suppose individual responding functions of the column intervals are represented by $f_1(t), f_2(t), f_3(t)$, etc., respectively, that is, if a sharp [Dirac $\delta(t)$ function] injection is performed at the inlet of intervals Δl_i $(i = 1,2,3,...)$, the profile at the outlet of intervals Δl_i will be depicted by the corresponding function $f_i(t)$.

If the $\delta(t)$ function sampling proceeds at the inlet of the whole column, the profile at the outlet of length interval Δl_i will be $g_i(t)$, where $g_i(t)$ is the convolution of $f_1(t)$, $f_2(t), f_3(t), \ldots$, and $f_i(t)$, as the column is assumed to be linear. In the following, we use $\Delta_s M_{ni}$ and M_{ni} denoting the nth moment ($n = 1$ for original moment, $n > 1$ for central moment) corresponding to $f_i(t)$ and $g_i(t)$, respectively, that is,

$$\Delta_s M_{1i} = \int_0^\infty f_i(t) t \, \mathrm{d}t \tag{23}$$

$$\Delta_s M_{ni} = \int_0^\infty f_i(t)(t - \Delta_s M_{1i})^n \mathrm{d}t \qquad (n = 2,3,...) \tag{24}$$

$$M_{1i} = \int_0^\infty g_i(t) t \, \mathrm{d}t \tag{25}$$

$$M_{ni} = \int_0^\infty g_i(t)(t - M_{1i})^n \mathrm{d}t \qquad (n = 2,3,...) \tag{26}$$

In TPGC, $f_i(t)$ is a complex function related to the temperature of the interval, because the column temperature is varying during elution and different parts of a zone pass through the column interval at different moments in time, and hence at different temperatures. However, in practice, the time interval is very short when a peak is passing through a very short (infinitesimal) column length interval, provided that the column efficiency is not too low. For example, if the plate number $N = 5.54\,(t_R/w_{\frac{1}{2}})^2 = 5.54 \times 10^4$, $w_{\frac{1}{2}} = 1\% \, t_R$. Assuming that column temperature increases by 100 K during the retention time t_R, the range of temperature variation for the peak passing through an infinitesimal column length will be *ca.* 1 K. Therefore, to a good approximation, we assume that, during the process of a peak moving through an infinitesimal column length interval, the local temperature remains at a certain value that is approximately equal to the temperature of the zone centre passing through. Hence the column can be regarded as many successive length intervals in which each remains at an isothermal temperature while the zone passes through. The time gradient of temperature is then changed into the space gradient of temperature along the column length.

For simplicity, we first consider two intervals, Δl_1 and Δl_2. For a sharp injection into the inlet of the column, *i.e.*, the inlet of the length interval Δl_1, the profile at the outlet of Δl_1 will be $g_1(t) = f_1(t)$, and the profile at the outlet of Δl_2 will be $g_2(t)$, where $g_2(t)$ is the convolution of $g_1(t)$ and $f_2(t)$:

$$g_2(t) = \int_0^t g_1(t')\,f_2(t-t')\mathrm{d}t' \tag{27}$$

Similarly, the profile at the outlet of Δl_3 will be $g_3(t)$, which is the convolution of $g_2(t)$ and $f_3(t)$, etc.

For the first length interval Δl_1,

$$M_{11} = \Delta_s M_{11} \tag{28}$$

$$M_{n1} = \Delta_s M_{n1} \qquad (n=2,3,\ldots) \tag{29}$$

The first original moment of $g_2(t)$ is (referring to Fig. 2)

$$M_{12} = \int_0^\infty g_2(t)t\mathrm{d}t = \int_0^\infty \int_0^t g_1(t')\,f_2(t-t')t\mathrm{d}t'\mathrm{d}t$$

$$= \int_0^\infty \int_{t'}^\infty g_1(t')\,f_2(t-t')t\mathrm{d}t\mathrm{d}t'$$

$$= \int_0^\infty \int_0^\infty g_1(t')\,f_2(x)\,(x+t')\mathrm{d}x\mathrm{d}t'$$

$$= \int_0^\infty g_1(t')\,(\Delta_s M_{12} + t')\mathrm{d}t'$$

$$= M_{11} + \Delta_s M_{12} \tag{30}$$
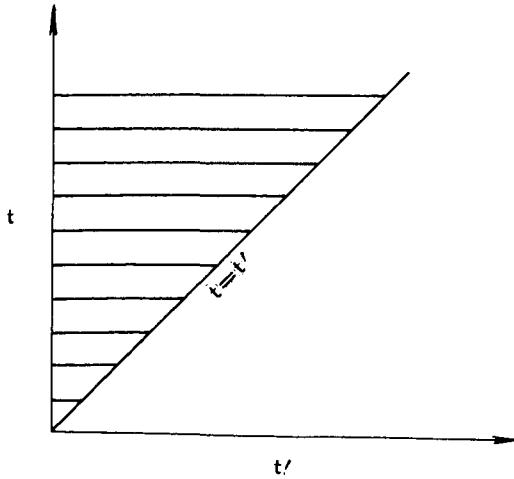
Fig. 2. Integrated field transformation.

The nth central moments of $g_2(t)$ are

$$M_{n2} = \int_0^\infty g_2(t) \, (t - M_{12})^n \mathrm{d}t$$

$$= \int_0^\infty \int_0^t g_1(t') f_2(t-t') \, (t - M_{12})^n \, \mathrm{d}t' \mathrm{d}t$$

$$= \int_0^\infty \int_{t'}^\infty g_1(t') f_2(t-t') \, (t - M_{11} - \Delta_s M_{12})^n \, \mathrm{d}t \mathrm{d}t'$$

$$= \int_0^\infty \int_0^\infty g_1(t') f_2(x)(x + t' - M_{11} - \Delta_s M_{12})^n \, \mathrm{d}x \mathrm{d}t'$$

$$= \int_0^\infty \int_0^\infty g_1(t') f_2(x) \left[\sum_{k=0}^n C_n^k \, (t' - M_{11})^k \, (x - \Delta_s M_{12})^{n-k} \right] \mathrm{d}x \mathrm{d}t' \qquad (31)$$

where $n = 2, 3, \ldots$,

$$C_n^k = \frac{n!}{k! \, (n-k)!}$$

and $x = t - t'$ (see Fig. 2).

In eqn. 31, for $n = 2, 3, \ldots$, we have

$$M_{22} = M_{21} + \Delta_s M_{22} \qquad (32)$$

$$M_{32} = M_{31} + \Delta_s M_{32} \tag{33}$$

$$M_{42} = M_{41} + \Delta_s M_{42} + 6M_{21}\Delta_s M_{22} \tag{34}$$

$$M_{52} = M_{51} + \Delta_s M_{52} + 10(M_{21}\Delta_s M_{32} + M_{31}\Delta_s M_{22}) \tag{35}$$

$$M_{62} = M_{61} + \Delta_s M_{62} + 15(M_{21}\Delta_s M_{42} + M_{41}\Delta_s M_{22}) + 20M_{31}\Delta_s M_{32} \tag{36}$$

The same results can be derived by using the Laplace transformation method.

The first three moments

From eqns. 30, 32 and 33, it can be shown that the first three moments for the whole column are

$$M_1 = \sum_i \Delta M_{1i} = \sum_i \Delta_s M_{1i} \tag{37}$$

$$M_2 = \sum_i \Delta M_{2i} = \sum_i \Delta_s M_{2i} \tag{38}$$

$$M_3 = \sum_i \Delta M_{3i} = \sum_i \Delta_s M_{3i} \tag{39}$$

where the sums are for all column length intervals and Δ is the generally used symbol for increments, *i.e.*,

$$\Delta M_{ni} = M_{ni} - M_{n(i-1)} \tag{40}$$

This illustrates that the first original, the second central and the third central moments are additive along the column length. It is concluded that, for homogeneous conditions along the column length, the moments M_1, M_2 and M_3 are directly proportional to the column length L. This has been confirmed by the results of Grubner [11], Grushka [9] and Chen and Peng [10].

Similarly, the first three moments for the whole system can be shown to be the sums of the appropriate order of moments created by the column itself and that caused by the extra-column devices, that is, the first three moments are additive for every part the component passing through. In the following, we mainly discuss the moments related to the column.

For the original moment, according to eqn. 37,

$$t_R = M_{1R} = \lim_{\Delta z \to 0} \sum_i \Delta_s M_{1i} = \int_0^{t_R} dt = \int_0^L \frac{dz}{Rv} \tag{41}$$

This is only a formal expression. In practice, eqn. 15 is used for calculations.

For the second central moment, for isothermal processes it can be theoretically expressed as

$$M_{2r}^{the} = \sum_{pq} F_{2pq}(k) \, \bar{v}^{-p} [D_g(\bar{v})]^q L \tag{42}$$

where $\sum_{pq}$ denotes the summation for all pairs of p and q and

$$D_g(v) = D_{g0}(T/T_{00})^{1.75} P_o/P = D_{gT} P_o/P = D_{gT} \, jv/\bar{v} \tag{43}$$

in which T_{00} is an arbitrary temperature corresponding to the constant D_{g0}.

The appropriate local expression for M_2 (with $\bar{v}$ and L changed into v and Δz) is

$$\Delta_s M_{2z} = \sum_{pq} F_{2pq}(k) v^{-p} [D_g(v)]^q \, \Delta z \tag{44}$$

According to eqn. 32, when $\Delta z \rightarrow 0$, this leads to

$$dM_2 = \lim_{\Delta z \rightarrow 0} \Delta M_{2z} = \lim_{\Delta z \rightarrow 0} \Delta_s M_{2z}$$
$$= \sum_{pq} F_{2pq}(k) v^{-p} [D_g(v)]^q dz \tag{45}$$

Hence the second central moment (observed) for TPGC is

$$M_{2R} = \sum_{pq} \int_0^L F_{2pq}(k) v^{-p} [D_g(v)]^q dz$$
$$= \sum_{pq} \int_0^{t_R} F_{2pq}(k) v^{1-p} [D_g(v)]^q/(1+k) dt \tag{46}$$

where v is expressed as in eqn. 21.

According to eqn. 46, for isothermal processes (i.e., the special temperature programme with $r=0$), we obtain the expression for the experimentally observed second central moment, viz.,

$$M_{2r}^{obs} = \sum_{pq} F_{2pq}(k) \bar{v}^{-p} \, j^q D_{gT}^q \, L \, \varphi_{p-q} \tag{47}$$

where φ_{p-q} is the pressure calibration factor, which is defined as

$$\varphi_n = (\bar{v}^n/L) \int_0^L v^{-n} \, dz \tag{48}$$

with

$$\varphi_0 = 1 \tag{49}$$

$$\varphi_1 = 1 \tag{50}$$

$$\varphi_2 = \frac{1}{2} \cdot j^2 \cdot \frac{\alpha^4 - 1}{\alpha^2 - 1} = \frac{9}{8} \cdot \frac{[(P_i/P_o)^4 - 1] \, [(P_i/P_o)^2 - 1]}{[(P_i/P_o)^3 - 1]^2} \tag{51}$$

$$\varphi_3 = \frac{2}{5} \cdot j^3 \cdot \frac{\alpha^5 - 1}{\alpha^2 - 1} \tag{52}$$

$$\varphi_4 = \frac{1}{3} \cdot j^4 \cdot \frac{\alpha^6 - 1}{\alpha^2 - 1} \tag{53}$$

$$\vdots$$

$$\varphi_n = \frac{2}{n+2} \cdot j^n \cdot \frac{\alpha^{n+2} - 1}{\alpha^2 - 1} \tag{54}$$

Similarly, for the third central moment, if the theoretical expression is

$$M_{3r}^{the} = \sum_{pq} F_{3pq}(k) \, \bar{v}^{-p} \, [D_g(\bar{v})]^q L \tag{55}$$

then the third central moment (observed) for TPGC is

$$M_{3R} = \sum_{pq} \int_0^{t_R} F_{3pq}(k) \, v^{1-p} \, [D_g(v)]^q/(1+k) \, \mathrm{d}t \tag{56}$$

The expression for the observed third central moment is

$$M_{3r}^{obs} = \sum_{pq} F_{3pq}(k) \, \bar{v}^{-p} j^q \, D_{gT}^q \, L \, \varphi_{p-q} \tag{57}$$

As an example, we take the theoretical expressions for the second and third central moments in ref. 9, *i.e.* (note: for normal conditions $2D_g/v \ll L$),

$$M_{2r}^{the} = [2\bar{v}^{-3} \, D_g(\bar{v}) \, (1+k)^2 + J_1 k/\bar{v}]L \tag{58}$$

$$M_{3r}^{the} = [12\bar{v}^{-5} \, [D_g(\bar{v})]^2 \, (1+k)^3 + J_2 \, \bar{v}^{-3} D_g(\bar{v})k(1+k) + J_3 k/\bar{v}]L \tag{59}$$

where J_1, J_2 and J_3 are constants related to the parameters of the column.
Under these conditions,

$$M_{2R} = \int_0^{t_R} [2\bar{v}^{-1} jD_{gT} (1+k)/v + J_1 \, k/(1+k)]\mathrm{d}t \tag{60}$$

$$M_{2r}^{obs} = [2\bar{v}^{-3} jD_{gT} (1+k)^2 \, \varphi_2 + J_1 k/\bar{v} \, \varphi_1]L \tag{61}$$

and

$$M_{3R} = \int_0^{t_R} [12 \, \bar{v}^{-2} j^2 \, D_{gT}^2 \, (1+k)^2/v^2 + J_2 \, \bar{v}^{-1} jD_{gT} \, k/v + J_3 \, k/(1+k)]\mathrm{d}t \tag{62}$$

$$M_{3r}^{obs} = [12\bar{v}^{-5} \, j^2 D_{gT}^2 \, (1+k)^3 \, \varphi_3 + J_2 \, \bar{v}^{-3} \, jD_{gT} \, k(1+k) \, \varphi_2 + J_3 k/\bar{v}]L \quad (63)$$

In practice, the moments may be regressed to isothermal data as

$$M_{2r} = A_2 + B_2 t_r + C_2 t_r^2 \tag{64}$$

$$M_{3r} = A_3 + B_3 t_r + C_3 t_r^2 + D_3 t_r^3 \tag{65}$$

where $t_r = t_0 \, (1+k)$. Additionally, if the decompression effects of the carrier gas are neglected, then we have approximately

$$M_{2R} = (1/L) \int_0^L M_{2r} dz = \int_0^{t_R} (M_{2r}/t_r) \, dt \tag{66}$$

and

$$M_{3R} = (1/L) \int_0^L M_{3r} \, dz = \int_0^{t_R} (M_{3r}/t_r) \, dt \tag{67}$$

The fourth and fifth central moments

For the fourth central moment, according to eqn. 34 we can write

$$M_{41} = \Delta_s M_{41}$$
$$M_{42} = M_{41} + \Delta_s M_{42} + 6M_{21}\Delta_s M_{22}$$
$$M_{43} = M_{42} + \Delta_s M_{43} + 6M_{22}\Delta_s M_{23}$$
$$M_{44} = M_{43} + \Delta_s M_{44} + 6M_{23}\Delta_s M_{24}$$
$$\vdots$$
$$M_{4(i-1)} = M_{4(i-2)} + \Delta_s M_{4(i-1)} + 6M_{2(i-2)}\Delta_s M_{2(i-1)}$$
$$M_{4i} = M_{4(i-1)} + \Delta_s M_{4i} + 6M_{2(i-1)}\Delta_s M_{2i}$$

Adding these equations, we obtain

$$M_{4i} = \sum_{j=1}^{i} \Delta_s M_{4j} + 6 \sum_{j=1}^{i-1} \left(\sum_{k=1}^{j} \Delta_s M_{2k} \right) \Delta_s M_{2(j+1)} \tag{68}$$

Similarly, for the fifth central moment it can be shown that (referring to eqn. 35),

$$M_{5i} = \sum_{j=1}^{i} \Delta_s M_{5j} + 10 \sum_{j=1}^{i-1} [M_{2j} \Delta_s M_{3(j+1)} + M_{3j} \Delta_s M_{2(j+1)}]$$
$$= \sum_{j=1}^{i} \Delta_s M_{5j} + 10 \sum_{j=1}^{i-1} \left[\left(\sum_{k=1}^{j} \Delta_s M_{2k} \right) \Delta_s M_{3(j+1)} \right.$$
$$\left. + \left(\sum_{k=1}^{j} \Delta_s M_{3k} \right) \Delta_s M_{2(j+1)} \right] \tag{69}$$

Referring to eqns. 68 and 69, theoretical expressions for the fourth and fifth central moments may reasonably be written as

$$M_{4r}^{the} = F_{41} [k,\bar{v},D_g \, (\bar{v})] \, L + F_{42} [k,\bar{v},D_g(\bar{v})] \, L^2 \tag{70}$$

$$M_{5r}^{the} = F_{51} [k,\bar{v},D_g \, (\bar{v})] \, L + F_{52} [k,\bar{v},D_g(\bar{v})] \, L^2 \tag{71}$$

Appropriate local expressions can then be written as

$$\Delta_s M_{4z} = F_{41}[k,v,D_g(v)]\Delta z + F_{42}[k,v,D_g(v)]2z\Delta z \tag{72}$$

and

$$\Delta_s M_{5z} = F_{51}[k,v,D_g(v)]\Delta z + F_{52}[k,v,D_g(v)]2z\Delta z \tag{73}$$

According to eqns. 68 and 69, the moments for TPGC will be

$$
\begin{aligned}
M_{4R} = &\int_0^L F_{41}[k,v,D_g(v)]\mathrm{d}z + \int_0^L F_{42}[k,v,D_g(v)]2z\mathrm{d}z \\
&+ 6\int_0^L \left\{\int_0^z F_2[k',v',D_g(v')]\mathrm{d}z'\right\} F_2[k,v,D_g(v)]\mathrm{d}z
\end{aligned}
\tag{74}
$$

and

$$
\begin{aligned}
M_{5R} = &\int_0^L F_{51}[k,v,D_g(v)]\mathrm{d}z + \int_0^L F_{52}[k,v,D_g(v)]2z\mathrm{d}z \\
&+ 10\int_0^L \left\{\int_0^z F_2[k',v',D_g(v')]\mathrm{d}z'\right\} F_3[k,v,D_g(v)]\mathrm{d}z \\
&+ 10\int_0^L \left\{\int_0^z F_3[k',v',D_g(v')]\mathrm{d}z'\right\} F_2[k,v,D_g(v)]\mathrm{d}z
\end{aligned}
\tag{75}
$$

where $k' = k(z')$, $v' = v(z')$, and

$$F_2[k,v,D_g(v)] = \sum_{pq} F_{2pq}(k)v^{-p}[D_g(v)]^q$$

$$F_3[k,v,D_g(v)] = \sum_{pq} F_{3pq}(k)v^{-p}[D_g(v)]^q$$

PLATE HEIGHT AND PEAK VARIANCE

Fundamental aspects of plate height

For arbitrary chromatographic processes (here we still use subscripts R), the plate height for the whole column is defined as

$$H_R = \frac{LM_{2L}}{M_{1L}^2} = \frac{L\tau_L^2}{t_R^2} = \left(\frac{L}{t_R}\right)^2 \frac{\tau_L^2}{L} \tag{76}$$

Similarly, the local plate height should be defined as

$$H_z = \lim_{\Delta z \to 0} \frac{\Delta z \Delta_s M_{2z}}{(\Delta_s M_{1z})^2} = \frac{\mathrm{d}z\mathrm{d}M_2}{(\mathrm{d}M_1)^2} = R^2 v^2 \cdot \frac{\mathrm{d}\tau^2}{\mathrm{d}z} \tag{77}$$

which can also be written as

$$H_z = \lim_{\Delta z \to 0} \frac{R^2 v^2 \Delta_s \tau_z^2}{\Delta z} = \lim_{\Delta z \to 0} \frac{\Delta_s \sigma_z^2}{\Delta z} \tag{78}$$

According to the additivity of the second central moment along the column length, the observed plate height H_R and the local plate height H_z are related by the following expression:

$$H_R = \frac{L}{t_R^2} \int_{(0)}^{(L)} d\tau^2 = \frac{L}{t_R^2} \int_0^L \frac{H_z}{R^2 v^2} \cdot dz \tag{79}$$

For isothermal chromatography, a similar expression was derived by Giddings [6].

In TPGC (or general processes), it is not correct to define the local plate height as [1,6–8]

$$H_z' = \frac{d\sigma^2}{dz} = \lim_{\Delta z \to 0} \frac{\Delta \sigma^2}{\Delta z} \tag{80}$$

because, at any position z, $\sigma = Rv\tau$, where $\sigma = \sigma(z)$, $\tau = \tau(z)$, $Rv = R(z)v(z)$ and

$$\frac{d\sigma^2}{dz} = R^2 v^2 \cdot \frac{d\tau^2}{dz} + \tau^2 \cdot \frac{d(R^2 v^2)}{dz} \quad \text{corrected 26 may 3'}\! \tag{81}$$
$$d\sigma^2/dz$$

in TPGC, $d(R^2 v^2)/dz \neq 0$, and hence $\underline{d\sigma^2} \neq R^2 v^2 d\tau^2/dz$. Only when the system is under isothermal conditions and the decompression effects of the carrier gas are neglected are the two definitions in eqns. 77 and 80 equivalent to each other.

Since H_z in eqn. 77 and H_r ($= H_R$ for $k = $ constant in eqn. 76) have the same form of definitions (only for different column lengths), an expression for H_z can then be deduced from that for H_r just as that for $\Delta_s M_{2z}$ in eqn. 44 and M_{2r}^{the} in eqn. 42. However, the expression for H_z' in eqn. 80 cannot be deduced from that for H_r; because of their different definitions they are only related in form by the following relationship [1,7,8], which cannot be used for practical calculations:

$$H_R = \frac{L}{t_L^2 R_L^2 v_L^2} \int_0^L H_z' dz \tag{82}$$

It should be made clear that σ^2 discussed above is different from σ'^2 in the equation

$$H_R = \sum_j \sigma_j'^2 / L \tag{83}$$

where $\sigma_j'^2$ is the variance created by independent dispersion processes (ordinary diffusion, eddy diffussion and local non-equilibrium, etc.) of the whole column. However, σ_i^2 discussed above is the variance for different length intervals, and each

involves the effects created by all independent dispersion processes, so certainly they are not independent of each other, that is,

$$\sigma_L^2 = \sum_j \sigma_j'^2 \tag{84}$$

According to eqn. 76, eqn. 83 is valid only for isothermal processes in which the decompression effects are neglected.

Eqn. 79 is a fundamental equation, that is suitable for both TPGC and isothermal processes. This equation is discussed below.

In isothermal chromatography, the variance in distance at the column end is

$$\sigma_L^2 = R_L^2 v_L^2 \tau_L^2 = \int_0^L (v_L/v)^2 \, H_z dz$$
$$= \int_0^L (P/P_o)^2 \, H_z dz = \int_0^L [\alpha^2 - (\alpha^2 - 1)z/L] H_z dz \tag{85}$$

This result is the same as that derived by Giddings et al. [19]. Under this condition, we have

$$\frac{d\sigma^2}{dz} = [\alpha^2 - (\alpha^2 - 1)z/L] H_z \tag{86}$$

In TPGC, the variance in distance at the column end is

$$\sigma_L^2 = R_L^2 v_L^2 \int_0^L \frac{H_z}{R^2 v^2} \cdot dz \tag{87}$$

which is equivalent to

$$\frac{d\sigma^2}{dz} = R_L^2 \, v_L^2 \cdot \frac{H_z}{R^2 v^2} \tag{88}$$

Obviously, only for isothermal processes and when the decompression effects of the carrier gas are neglected does

$$\frac{d\sigma^2}{dz} = H_z \tag{89}$$

when H_z is equal to H_z'.

Calculations of plate height and peak variance

A theoretical expression for the plate height for the whole column can be written as

$$H_r^{the} = A + B \cdot \frac{D_g(\bar{v})}{\bar{v}} + C \cdot \frac{\bar{v}}{D_g(\bar{v})} + D\bar{v} \tag{90}$$

The local plate height, H_z, will be ($\bar{v} \rightarrow v$ in eqn. 90)

$$H_z = A + B \cdot \frac{jD_{gT}}{\bar{v}} + C \cdot \frac{\bar{v}}{jD_{gT}} + Dv \tag{91}$$

The observed plate height in TPGC can then be calculated by eqn. 79.

The observed plate height under appropriate isothermal conditions can be derived as

$$H_r^{obs} = \left(A + B \cdot \frac{j\,D_{gT}}{\bar{v}} + C \cdot \frac{\bar{v}}{jD_{gT}} \right) \varphi_2 + D\bar{v} \tag{92}$$

which was also derived by Giddings *et al.* [19].

The appropriate expressions for peak variance are as follows:

$$M_{2r}^{the} = \frac{M_{1r}^2 H_r^{the}}{L} = \frac{L\,H_r^{the}}{R^2 v^{72}} \quad \text{corrected } 2\,\delta\,n\upsilon\,3\,\omega \quad R^2 v^{-2} \tag{93}$$

$$M_{2R} = \int_{(0)}^{(L)} dM_2 = \int_0^L \frac{H_z}{R^2 v^2} \cdot dz = \int_0^{t_R} \frac{H_z}{Rv} \cdot dt \tag{94}$$

$$M_{2r}^{obs} = \frac{L\,H_r^{obs}}{R^2 \bar{v}^2} \tag{95}$$

The above illustrates that discussions based on plate height and peak variance are equivalent for calculations.

As an example, for a capillary, we outline the procedures for the calculation of plate height and peak variance in TPGC. Under these conditions, eqn. 90 becomes the Golay equation. Substituting

$$A = 0$$

$$BD_{gT} = B_c T^{1.75}$$

$$\frac{C}{D_{gT}} = C_c \cdot \frac{1 + 6k + 11k^2}{(1+k)^2} \cdot \frac{1}{T^{1.75}}$$

$$D = D_c \cdot \frac{k}{(1+k)^2}$$

into eqn. 92, and regressing to more than three different isothermal data, the regression coefficients B_c, C_c and D_c can be determined. Substituting them into eqns. 91, 79 and 94, the plate height and peak variance in TPGC can then be calculated.

The plate height and peak variance can also be calculated based on other formulations for $H(T,v)$; for example, the deWet and Pretorius [20] formulation may be used for such a purpose.

DISCUSSION

For the Van Deemter equation, some contradictions occur between theory and experiment. For example, experimentally the term A in H may be negative [21,22], and $H-v$ plot as different curves for columns of different length [23]. The reasons may be as follows. $W_{\frac{1}{2}}^2$ is used to replace M_2 and peaks are assumed to be symmetrical; pressure decompression effects are not considered, especially for long columns; extra-column effects are neglected; the systems are not homogeneous; the systems are not linear; and the relationships between H and other factors (v,k,L,D_g, etc.) are only approximately correct.

In practice, extra-column effects generally exist and further it is difficult to determine higher order moments correctly [12–15], so these factors must be considered during confirmation of the theory just developed.

From the above considerations, in TPGC retention time can be calculated by eqn. 15 and peak variance by eqn. 94, 46 or 66. The third central moment can be calculated by eqn. 56 or 67. Plate height and higher order moments can also be calculated by appropriate expressions just developed. The trace for the moving zone position at any moment in time is given by eqn. 20. From these, optimization procedures can then be carried out for TPGC, that is, the optimum initial temperature and heating rate for any temperature programme under the conditions of a given sample and a given column can be predicted according to isothermal data.

ACKNOWLEDGEMENTS

REFERENCES

1 J. C. Giddings, in N. Brenner, J. E. Callen and M. D. Weiss (Editors), *Gas Chromatography*, Academic Press, New York, 1962, p. 57.
2 A. S. Said, in N. Brenner, J. E. Callen and M. D. Weiss (Editors), *Gas Chromatography*, Academic Press, New York, 1962, p. 79.
3 W. E. Harris and W. H. Habgood, *Programmed Temperature Gas Chromatography*, Wiley, New York, 1966.
4 A. S. Said, *Theory and Mathematics of Chromatography*, Hüthig, Heidelberg, 1981, Ch. 10.
5 V. Bartu, *J. Chromatogr.,* 260 (1983) 255.
6 J. C. Giddings, *Dynamics of Chromatography*, Marcel Dekker, New York, 1965.
7 G. H. Stewart, *Anal. Chem.,* 32 (1960) 1205.
8 H. W. Habgood and W. E. Harris, *Anal. Chem.,* 32 (1960) 1206.
9 E. Grushka, *J. Phys. Chem.,* 76 (1972) 2586.
10 S. Y. Chen and S. Y. Peng, in P.-C. Lu and E. Bayer (Editors), *Proceedings of Sino–West German Symposium on Chromatography*, Science Press, Beijing, 1983, p. 313.
11 O. Grubner, *Adv. Chromatogr.,* 6 (1968) 173.
12 E. Grushka, M. N. Myers, P. D. Schettler and J. C. Giddings, *Anal. Chem.,* 41 (1969) 889.
13 J. Skopp, *AIChE J.,* 30 (1984) 151.
14 D. J. Anderson and R. R. Walters, *J. Chromatogr. Sci.,* 22 (1984) 353.
15 W. W. Yau, *Anal. Chem.,* 49 (1977) 395.
16 J.-Y. Zhang, *J. High Resolut. Chromatogr. Chromatogr. Commun.,* 10 (1987) 418.
17 J.-Y. Zhang, B.-C. Lin and P.-C. Lu, *Chromatographia,* 23 (1987) 487.
18 J.-Y. Zhang, *M.S. Thesis*, Dalian, 1985.

19 J. C. Giddings, S. L. Seager, L. R. Stucki and G. H. Stewart, *Anal. Chem.,* 32 (1960) 867.
20 W. J.deWet and V. Pretorius, *Anal. Chem.,* 30 (1958) 325.
21 C.-J. Sun, *Principles and Technology of Gas Chromatography*, Chemical Industry Publishing House, Beijing, 1979, p. 84.
22 H. Purnell, *Gas Chromatography*, Wiley, New York, 1962, p. 162.
23 K. Yabumoto and W. J. A. Vandenheuvel, *J. Chromatogr.,* 140 (1977) 197.

Gas chromatographic–mass spectrometric identification of the fatty acids in borage oil using the picolinyl ester derivatives

INGER WRETENSJÖ* and LENNART SVENSSON

Department of Analytical Chemistry, R&D, Kabi Nutrition, S-112 87 Stockholm (Sweden)

and

W. W. CHRISTIE

Hannah Research Institute, Ayr KA6 5HL (U.K.)

(First received February 2nd, 1990; revised manuscript received June 22nd, 1990)

ABSTRACT

When subjected to capillary gas chromatography, picolinyl ester derivatives of fatty acids were shown to have as good chromatographic properties as the corresponding methyl esters. By using a capillary column of medium polarity (Supelcowax 10), excellent resolution with respect to chain length, degree of unsaturation and positional isomers was obtained without any serious problems with a disturbed background due to column bleed in the mass spectrometric interpretation of diagnostic ions. These features permitted a simple one-step procedure to be carried out for the characterization of fatty acids with respect to molecular weight, number of double bonds and positional isomers. The usefulness of the technique for the identification of the fatty acids in borage seed oil (*Borago officinalis*) was demonstrated. In addition to γ-linolenic acid, the most important fatty acid in borage seed oil from a commercial standpoint, a further fourteen different fatty acids could be positively identified.

INTRODUCTION

Gas chromatography (GC) of methyl ester derivatives on fused-silica capillary columns of medium polarity is generally considered as the method of choice for the quantitative analysis of complex fatty acid mixtures of natural origin. However, although having excellent GC properties, the methyl esters are less suitable as derivatives for structural determination by mass spectrometry (MS), mainly because isomerization of the unsaturated fatty acids occurs during ionization. Several different methods to overcome the problem of double bond migration have been extensively reviewed [1,2].

One commonly used approach involves the fixation of the double bond by chemical means such as hydroxylation followed by trimethylsilylation. However, although this is a powerful technique for the identification of pure fatty acids, the large increase in molecular weight and retention times makes the procedure less suitable for the analysis of natural fatty acid mixtures containing polyenoic acids. Another

approach to the problem is the preparation of pyrollidide [3,4], picolinyl ester [5–8] or oxazoline [9,10] derivatives, which stabilize the double bonds during ionization in the mass spectrometer, resulting in well recognizable diagnostic ions. However, in these procedures packed columns or capillary columns coated with non-polar stationary phases have generally been used, which might cause problems with respect to low resolution and increased risk of peak overlapping.

One approach to overcome this problem has been fractionation of the methyl esters with respect to unsaturation by silver ion high-performance liquid chromatography before GC–MS [8]. In this study the usefulness of capillary GC of picolinyl ester derivatives on a medium-polarity column for the mass spectrometric identification of the fatty acids in borage oil is demonstrated. The results obtained confirm previous identifications of γ-linolenic acid based on other techniques such as equivalent chain length values [11] and permanganate–periodate oxidation [12]. Further, most of the other fatty acids in borage oil were identified by using this technique.

EXPERIMENTAL

Materials

Refined borage seed oil (*Borago officinalis*) was obtained from Kabi Nutrition, (Stockholm, Sweden). 3-(Hydroxymethyl)pyridine, dimethylaminopyridine and trifluoroacetic anhydride were purchased from Sigma (Poole, U.K.), potassium hydroxide from EKA (Bohus, Sweden), ethanol from Kemetyl (Stockholm, Sweden) and all other reagents and solvents from Merck (Darmstadt, F.R.G.). Sepralyte (Bond-Elut) NH_2 (aminopropyl-bonded silica) sorbent was purchased from Analytichem International (Atlanta, GA, U.S.A.).

Preparation of picolinyl esters

After saponification of the oil (100 mg), the free fatty acids were converted into their picolinyl derivatives essentially as described by Christie and Stefanov [13]. In order to obtain a higher yield of free fatty acids in the extraction step, the hydrochloric acid concentration was increased to 6 M. For the removal of unreacted free fatty acids after the derivatization step, Bond-Elut NH_2 was used instead of purification by Florisil column chromatography. To the derivatives dissolved in diethyl ether a few milligrams of Bond-Elut NH_2 were added. After 10 min the mixture was vortex mixed and centrifuged. The isolated supernatant was evaporated and the dried residue dissolved in hexane.

Preparation of fatty acid methyl esters

The oil (100 mg) was transesterified using 0.5 M methanolic sodium methoxide and the methyl esters were extracted into hexane.

Gas chromatography of fatty acid methyl esters

A Hewlett-Packard 5880 gas chromatograph equipped with flame ionization detector, a split injection system and a Supelcowax 10 fused-silica capillary column, (30 m × 0.25 mm I.D.) was used. The carrier gas (helium) flow-rate was 0.9 ml/min and the splitting ratio was 1:100. The oven temperature was held at 180°C for 8 min

and then programmed at 10°C/min to 225°C, at which it was held for 23 min. The injection and detection temperatures were 250°C.

Gas chromatography of picolinyl ester derivatives

The same equipment and analytical conditions were used as in the analysis of fatty acid methyl esters except for the temperature settings. The oven temperature was held isothermally at 260°C throughout and the injection and detection temperatures were 280°C.

Gas chromatography–mass spectrometry of picolinyl ester derivatives

A Hewlett-Packard Model 5890 gas chromatograph equipped with a split/splitless injection system in combination with a Hewlett-Packard 5970 mass-selective detector was used. The column was the same as for the GC analysis. The helium flow-rate was set at 1 ml/min and the oven temperature was 260°C. The injection and ion source temperatures were 280 and 250°C, respectively. The spectra were recorded at an ionization energy of 70 eV.

RESULTS AND DISCUSSION

A comparison of the gas chromatograms obtained for methyl esters and picolinyl derivatives of the fatty acids in borage oil is show in Fig. 1. In order to elute the picolinyl derivatives within a reasonable period of time, a higher column temperature was needed. A temperature of 260°C, 20°C below the recommended maximum temperature of the column, was chosen as a satisfactory compromise with respect to column bleeding and analysis time. Despite the differences in retention times, the elution patterns are very similar and the picolinyl derivatives seem to have as good GC properties as the methyl esters. The small peak appearing on the shoulder of peak 8 in the chromatogram of the picolinyl esters might be an artefact introduced during the preparation of the picolinyl esters.

The fatty acid composition of borage oil as obtained by analysis of the methyl esters is shown in Table I. The distribution is similar to previously published results [11]. In an attempt to use the peak-area distribution of the picolinyl derivatives instead of the methyl esters as a measure of the fatty acid composition, it was observed that polyunsaturated and late-eluting fatty acids were discriminated against to some extent (cf., Table I).

The mass spectra of the fatty acid picolinyl ester derivatives of borage oil contained good molecular ions and distinct diagnostic ions, which facilitated identification of the fatty acid moieties. As expected, a certain degree of bleeding from the medium-polarity column could be observed. As a consequence, disturbing background peaks interfered to some extent in the interpretation of the mass spectra of minor constituents. By increasing the sample size and by using background subtraction, these problems were essentially eliminated as could be demonstrated by the very informative mass spectrum of 18:4 $(n-3)$, a minor fatty acid in borage oil comprising only 0.2% (Fig. 4). The negative intensities of some peaks in Figs. 2, 3 and 4 are due to background subtraction.

In Table II, all the fatty acids which could be identified in the borage oil are given together with the most important diagnostic ions.
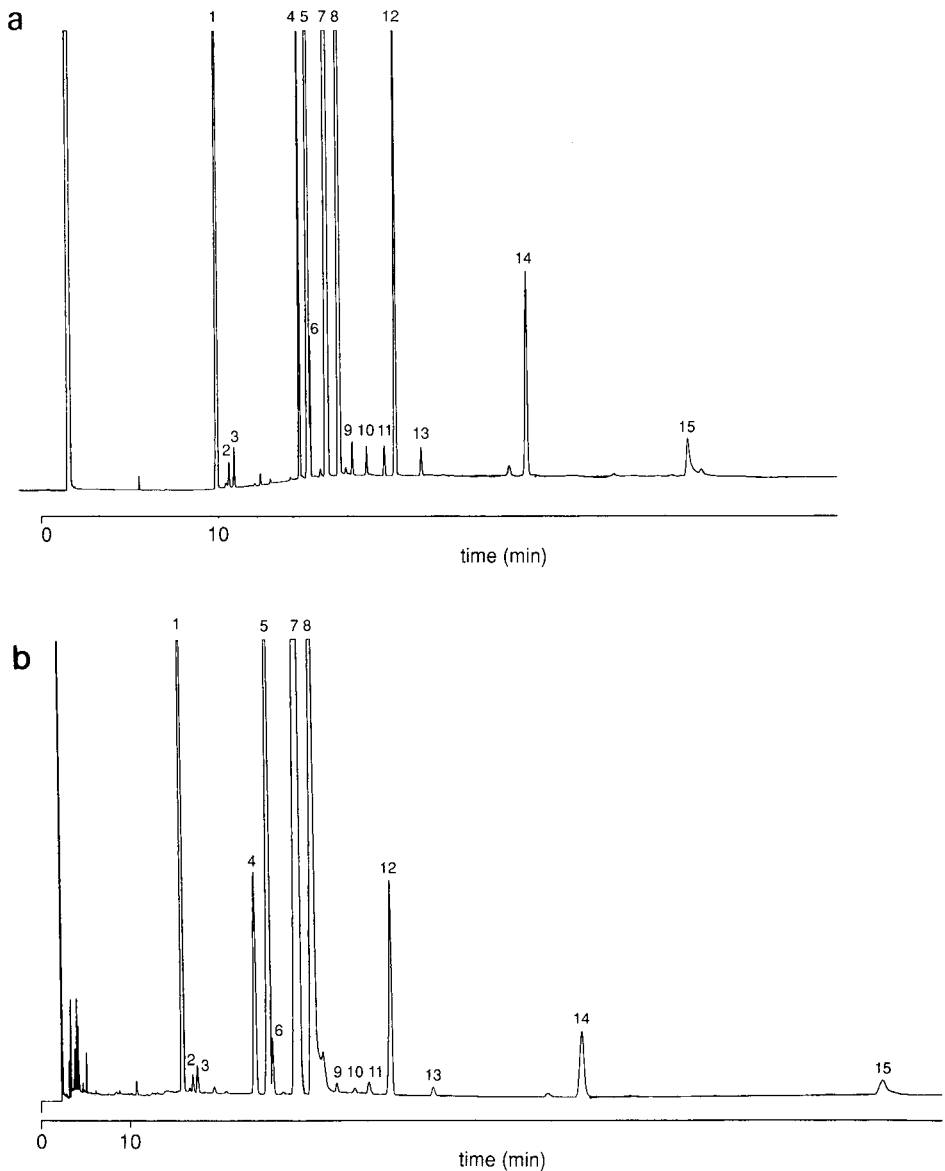
Fig. 1. Chromatograms showing separation of fatty acids in borage oil as (a) methyl esters and (b) picolinyl esters on a fused-silica capillary column coated with a polyethylene glycol phase (Supelcowax 10). For detailed analytical conditions, see Experimental. Peaks: $1 = 16:0$; $2 = 16:1$ $(n-7)$; $3 = 16:1$ $(n-5)$; $4 = 18:0$; $5 = 18:1$ $(n-9)$; $6 = 18:1$ $(n-7)$; $7 = 18:2$ $(n-6)$; $8 = 18:3$ $(n-6)$; $9 = 18:3$ $(n-3)$; $10 = 18:4$ $(n-3)$; $11 = 20:0$; $12 = 20:1$ $(n-9)$; $13 = 20:2$ $(n-6)$; $14 = 22:1$ $(n-9)$; $15 = 24:1$ $(n-9)$.

The mass spectra of the picolinyl esters of saturated fatty acids showed a regular pattern of fragments 14 a.m.u. apart, representing cleavage at each methylene group. Among the monoenoic fatty acids, two 16:1 isomers could be found, *i.e.*, the

TABLE I

THE FATTY ACID DISTRIBUTION IN BORAGE OIL DETERMINED BY GC ANALYSIS OF FATTY ACIDS AS METHYL AND PICOLINYL ESTERS

Peak No.	Component	Methyl esters (area %)	Picolinyl esters (area %)
1	16:0	9.77	12.35
2	16:1 $(n-7)$	0.14	0.16
3	16:1 $(n-5)$	0.21	0.26
4	18:0	3.44	3.92
5	18:1 $(n-9)$	14.80	16.60
6	18:1 $(n-7)$	0.52	0.63
7	18:2 $(n-6)$	37.51	38.22
8	18:3 $(n-6)$	24.58	19.18
9	18:3 $(n-3)$	0.20	0.13
10	18:4 $(n-3)$	0.18	0.07
11	20:0	0.22	0.21
12	20:1 $(n-9)$	4.18	4.12
13	20:2 $(n-6)$	0.22	0.17
14	22:1 $(n-9)$	2.51	2.03
15	24:1 $(n-9)$	1.11	0.71

$(n-7)$ and $(n-5)$ isomers, the occurrence of the latter not having been reported previously in borage seed oil. Except for the gap of 26 a.m.u., or sometimes better a gap of 40 a.m.u., being indicative of the position of the double bond, each monoenoic fatty acid as a general rule shows a doublet of peaks representing hydrogen abstraction allylic to the double bond [6]. For instance, 16:1 $(n-5)$ could be identified partly
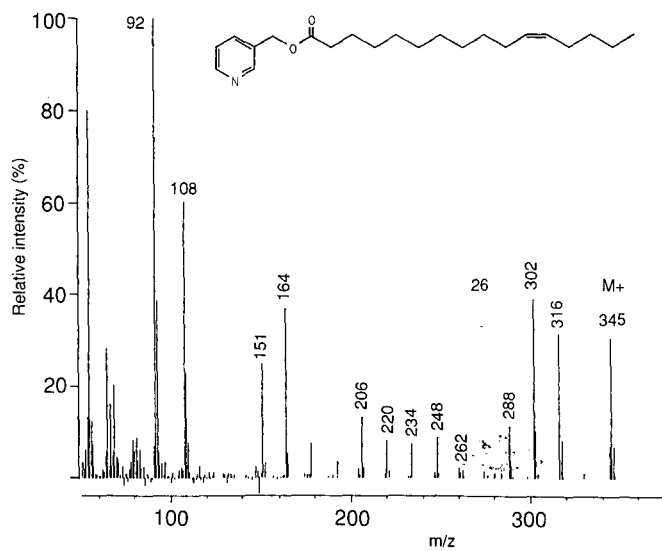
Fig. 2. Mass spectrum of 11-hexadecenoic acid picolinyl ester [16:1 $(n-5)$] in borage oil.

TABLE II

GC–MS ANALYSIS OF FATTY ACID PICOLINYL ESTERS IN BORAGE OIL

Peak No.	Component	Retention time (min)	Molecular ion m/z	Base ion m/z	Other useful or diagnostic ions m/z (%)							
1	16:0	12.35	347	92	318(13)	304(15)	290(15)	276(16)	262(17)	248(13)	234(11)	220(10)
2	16:1 $(n-7)$	13.35	345	92	316(8)	302(10)	288(39)	274(32)	260(6)	234(4)	220(11)	206(10)
3	16:1 $(n-5)$	13.61	345	92	316(31)	302(39)	288(11)	262(2)	248(9)	234(7)	220(8)	206(13)
4	18:0	19.21	375	92	346(10)	332(13)	318(14)	304(14)	290(15)	276(17)	262(16)	248(13)
5	18:1 $(n-9)$	20.28	373	92	316(10)	302(9)	288(38)	274(33)	260(10)	234(4)	220(12)	206(8)
6	18:1 $(n-7)$	21.63	373	92	330(9)	316(27)	302(35)	288(15)	262(4)	248(11)	220(10)	206(16)
7	18:2 $(n-6)$	22.87	371	92	328(12)	314(15)	300(7)	274(12)	260(17)	234(4)	220(8)	206(6)
8	18:3 $(n-6)$	24.18	369	92	312(11)	298(7)	272(9)	258(11)	232(3)	218(3)	192(2)	178(3)
9	18:3 $(n-3)$	27.43	369	92	340(7)	314(8)	300(26)	274(8)	260(8)	234(4)	220(9)	206(8)
10	18:4 $(n-3)$	28.59	367	92	338(3)	312(6)	298(7)	272(5)	258(9)	232(3)	218(1)	178(2)
11	20:0	30.63	403	92	374(9)	360(10)	346(10)	332(13)	318(16)	304(17)	290(17)	276(20)
12	20:1 $(n-9)$	32.12	401	92	344(7)	330(7)	316(31)	302(40)	288(11)	262(3)	248(10)	234(8)
13	20:2 $(n-6)$	35.67	399	92	356(9)	342(13)	328(8)	302(13)	288(30)	262(5)	248(10)	234(7)
14	22:1 $(n-9)$	45.98	429	92	358(7)	344(27)	330(39)	316(13)	290(4)	276(13)	262(9)	248(9)
15	24:1 $(n-9)$	64.36	457	92	386(11)	372(23)	358(33)	344(13)	318(4)	304(14)	290(13)	276(13)
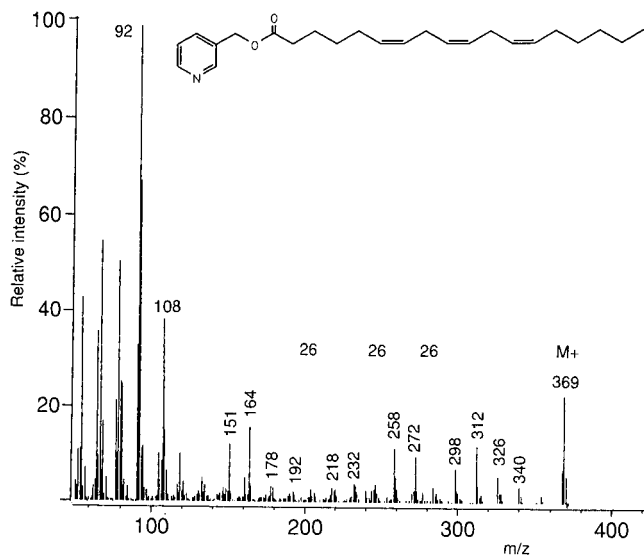
Fig. 3. Mass spectrum of 6,9,12-octadecatrienoic acid picolinyl ester [18:3 $(n-6)$] in borage oil.

because of a gap of 26 a.m.u. between the fragments 262 and 288 or of 40 a.m.u. (m/z = 248–288) and partly because of a doublet of ions at m/z 302 and 316 (Fig. 2). The spectrum of the analogous C_{18} fatty acid derivative has been published elsewhere [5].

The structures of the dienoic fatty acids could be determined in the same way as for the monoenoic compounds. For instance, in the spectrum of linoleic acid the position of the double bond could be determined by a gap of 26 a.m.u. between the
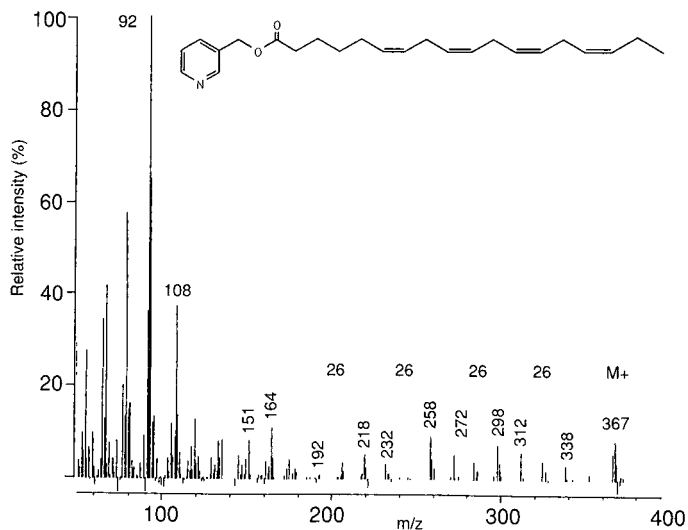
Fig. 4. Mass spectrum of 6,9,12,15-octadecatetraenoic acid picolinyl ester [18:4 $(n-3)$] in borage oil.

peaks of m/z 274 and 300. After a gap of 14 a.m.u., representing a methylene group, another gap of 26 a.m.u., representing the second double bond, appears. Three diagnostic ions representing hydrogen abstraction allylic to the double bonds could also be found at m/z 274, 314 and 328. The spectrum was similar to that obtained by Harvey [6].

All the trienoic and tetraenoic fatty acids in borage seed oil could be identified. None of the double bonds of these fatty acids were close to the carboxyl group, which could lead to difficulties in identification [7]. The pattern 26–14 a.m.u. indicating double bonds could be seen and also a strong diagnostic ion representing cleavage by loss of an allylic radical adjacent to the terminal double bond [6]. In the spectrum of the picolinyl ester of γ-linolenic acid ions 14 a.m.u. apart, counted from the methyl end, were found (Fig. 3). The first double bond is reached at the gap of 26 a.m.u. between the fragments of m/z 272 and 298. After 14 a.m.u. ($-CH_2$) another gap of 26 a.m.u. is reached, representing the second double bond. Finally, the third double bond is found between C_6 and C_7. The third gap of 26 a.m.u. was not as distinct as the others, the gap of 40 a.m.u. between the fragments of m/z 178 and 218 being more indicative of the double bond. The strong diagnostic ion of this trienoic acid is, according to the schemes of Harvey [6], at m/z 258. The fatty acid octadecatetraenoic acid or 18:4 ($n-3$), previously identified by Kleiman et al. [11] by means of equivalent chain-length values, was also confirmed by GC–MS. The spectrum is shown in Fig. 4. The positions of the three double bonds closest to the methyl end are determined by the pattern 26–14 a.m.u.. The fourth double bond closest to the carboxyl group does not give very distinct ions, but again a gap of 40 a.m.u. between the fragments of m/z 178 and 218 is found. The diagnostic ion representing cleavage adjacent to the terminal double bond is found at m/z 298 [6].

Picolinyl ester derivatives have been shown to be very useful for the structure determination of fatty acids by GC–MS, also reported elsewhere [5–8], because of their good mass spectrometric qualities. For the GC separation, non-polar columns have mostly been chosen because of the high molecular weight and also the polarity of picolinyl esters. However, on non-polar columns overlapping of peaks might be expected, especially with the ($n-6$) and ($n-3$) families of fatty acids. When a medium-polarity column was used, as in this instance, positional isomers could be separated easily. Linoleic acid and α-linoleic acid were also well resolved which might not be the case on non-polar columns [13]. An early attempt to use such a column was not successful [7], but there have been improvements in manufacturing techniques recently to give polar phases of great stability. Although the picolinyl esters of fatty acids were run isothermally at 260°C and the corresponding methyl esters according to a temperature programme from 80 to 225°C, their gas chromatograms were very similar (Fig. 1). This circumstance would facilitate identification. This technique, involving only one instrumental step, is very suitable for the identification of fatty acids in oils of moderate complexity. For more complex oils, such as fish oils, probably a liquid chromatographic prefractionation is required [8]. Positive identification of the fatty acids in oil of *Borago officinalis* by GC–MS was achieved previously by Craig and Bhutty [12] by means of permanganate–periodate oxidation after the isolation of each of the fatty acids. In that work, 11-hexadecenoic acid [16:1 ($n-5$)], α-linolenic acid [18:3 ($n-3$)] and 6,9,12,15-octadecatrienoic acid [18:4 ($n-3$)] were not identified. These three fatty acids were probably not detectable by the procedures available at that

time. According to the present work, 16:1 $(n-5)$, 18:3 $(n-3)$ and its corresponding tetraene, 18:4 $(n-3)$, are present but in small amounts, *viz.*, 0.21%, 0.20% and 0.18%, respectively (Table I).

REFERENCES

1 D. E. Minnikin, *Chem. Phys. Lipids*, 21 (1978) 313–347.
2 B. Schmitz and R. A. Klein, *Chem. Phys. Lipids*, 39 (1986) 285–311.
3 B. Å. Andersson and R. T. Holman, *Lipids*, 9 (1974) 185–190.
4 V. K. S. Shukla, J. Clausen, H. Egsgaard and E. Larsen, *Fette Seifen Anstrichm.*, 82 (1980) 193–199.
5 D. J. Harvey, *Biomed. Mass Spectrom.*, 9 (1982) 33–38.
6 D. J. Harvey, *Biomed. Mass Spectrom.*, 11 (1984) 340–347.
7 W. W. Christie, E. Y. Brechany, S. B. Johnson and R. T. Holman, *Lipids*, 21 (1986) 657–661.
8 W. W. Christie, E. Y. Brechany and K. Stefanov, *Chem. Phys. Lipids*, 46 (1988) 127–135.
9 J. Y. Zhang, Q. T. Yu, B. N. Liu and Z. H. Huang, *Biomed. Environ. Mass Spectrom.*, 15 (1988) 33–44.
10 Q. T. Yu, B. N. Liu, J. Y. Zhang and Z. H. Huang, *Lipids*, 24 (1989) 79–83.
11 R. Kleiman, F. R. Earle and I. A. Wolff, *J. Am. Oil Chem. Soc.*, 41 (1964) 459–462.
12 B. M. Craig and M. K. Bhutty, *J. Am. Oil Chem. Soc.*, 41 (1964) 209–211.
13 W. W. Christie and K. Stefanov, *J. Chromatogr.*, 392 (1987) 259–265.

Gas chromatographic determination of traces of light hydrocarbons and sulphur compounds in gases at low pressure by the simultaneous use of flame ionization and flame photometric detectors

GIANRICO CASTELLO*, GIUSEPPINA D'AMATO and MARIO NICCHIA

Istituto di Chimica Industriale, Università di Genova, Corso Europa 30, 16132 Genova (Italy)

(First received March 28th, 1990; revised manuscript received June 26th, 1990)

ABSTRACT

Flame ionization and flame photometric detectors were used for the determination of light hydrocarbons and sulphur compounds in low-pressure (20–130 Pa) gases formed in radiofrequency plasma reactors. The method can be easily extended to many types of samples, such as controlled atmospheres for microelectronic processes and polluted air. The separation of C_1–C_5 hydrocarbons, hydrogen sulphide, carbonyl sulphide, sulphur dioxide, carbon disulphide, thiols and sulphides was tested on various columns: Carbopack BTH-100, Chromosil 330, Supelpak S, Chromosorb 105 and 107. The best results for the particular application, in terms of analysis speed and peak resolution, were obtained by using a short (80 cm × 2 mm I.D.) PTFE column filled with Chromosorb 105, connected by means of a 50:50 splitter to the two detectors operated in parallel. The analysis of the products formed in an ethane–sulphur dioxide plasma discharge takes about 5 min and sensitivities of 10^{-12} g/s for hydrocarbons and 10^{-10} g/s for sulphur compounds were achieved.

INTRODUCTION

The application of radiofrequency plasma discharges to the surface modification of polymers and inorganic materials, by using as the feed gas mixtures of organic and inorganic compounds, has been investigated by many workers, and the determination of gaseous compounds formed in the gas phase was accomplished by using mass spectrometric and gas chromatographic techniques [1–4]. A knowledge of the purity of the gases used and the determination of the compounds formed during the reaction, which can exert catalytic or inhibitory effects on the surface reactions, is of great importance for the interpretation of the results and the study of the reaction kinetics.

Gas chromatography (GC) with specific detectors can assist in the determination of traces of organic compounds containing heteroatoms: electron-capture detector for halogens and nitro compounds, thermionic detector for nitrogen and phosphorus, flame photometric detector for sulphur and phosphorus.

In the series of experiments described here, a flame photometric detector was used to determine the amounts of hydrogen sulphide, carbonyl sulphide, thiols and

sulphides formed in a plasma discharge carried out in a feed gas composed of ethane and sulphur dioxide, which were submitted to the plasma action alone or on the surface of various polymers. The reaction of the excited species formed in the discharge with the polymer surface can yield various organic compounds containing sulphur atoms. Their identification and determination must be carried out in a low-pressure environment (between 0.2 and 1 T; 25–133 Pa) and therefore special equipment is necessary in order to deliver the sample to the analytical system.

The same methods can also be applied in the analysis of controlled atmospheres used in microelectronic production processes and, in general, when low-pressure samples have to be analysed. With some modification and simplification, the same technique can be applied to the analysis of gas mixtures at normal pressures.

EXPERIMENTAL AND RESULTS

Plasma discharge unit
        Fig. 1 is a schematic diagram of the discharge unit that permitted the treatment of polymeric films with different reactive gases or the direct deposition on inert surfaces of thin layers of compounds formed in the gas phase.
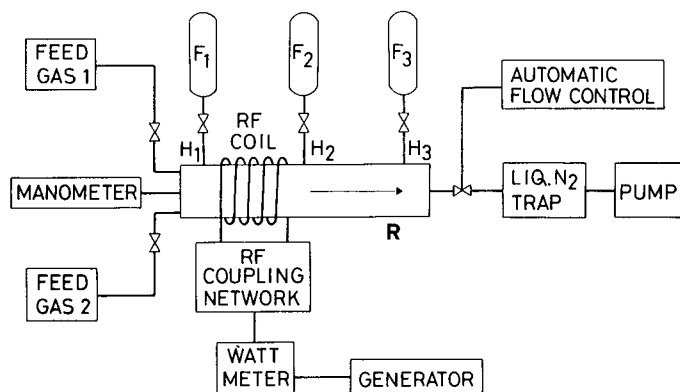
Fig. 1. Schematic diagram of the plasma generation apparatus (see text). H_1, H_2, H_3: pick-up points for the collection of samples in vials F or direct connection to vacuum manifold of Fig. 2.

        The system was operated at a pressure of about 50 Pa with a flow-rate of 10–20 cm^3/min, obtained by continuously feeding the gas mixture at one end of the reaction tube, R, and by extracting the products and the unreacted gases at the other end with suitable vacuum pump. The plasma discharge was obtained by inductive coupling with an RF generator at a frequency of 13.5 MHz. Continuous and instantaneous samples can be taken from small tubes H_1–H_3 connected at various points of the reaction tube R. Samples averaged over minutes or hours of continuous discharge can be collected in evacuated vials F_1–F_3.

Sample concentration and injection
        Fig. 2 shows the vacuum manifold used for the extraction of the gas from the
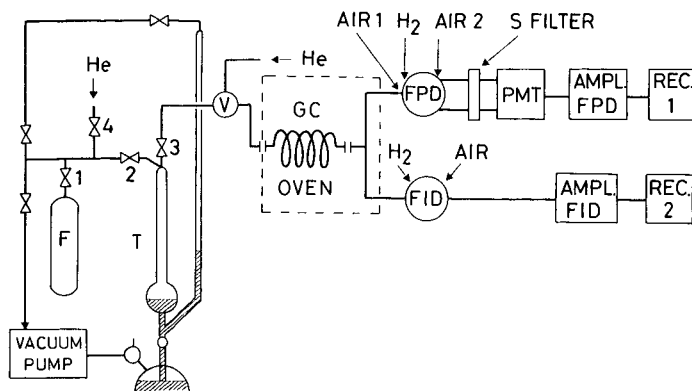
Fig. 2. Vacuum manifold used to extract low-pressure samples from vial F or directly from the RF discharge unit in Fig. 1, and to deliver them to the GC column and detectors (see text).

reaction tube or from the vials. It consists of a Toepler pump, T, where the gases can be aspirated through stopcocks 1 and 2 by lowering the mercury level.

Stopcock 2 was then closed and the mercury level raised to concentrate the gases in the upper part of T and pressurize them in order to permit the determination of their volume under known conditions of temperature and pressure, and their introduction into the gas chromatograph valve V. Pure helium supplies through stopcock 4 can be used to dilute the reaction gases in order to remain within the linearity range of the detector or pressurize them to facilitate sampling.

Stopcock 1 can be connected directly to the plasma discharge unit or to vials where the reaction products were previously collected. This manifold can therefore be used for analysis of low-pressure gas samples of any origin.

Pressurized samples (gas cylinders, gas-tight syringes, etc.) can be directly injected through valve V. Through the same valve can be injected constant volumes of standard gases prepared by using an exponential dilution flask [5,6], in order to permit an absolute calibration of the detector response.

Gas chromatographic analysis

The separation of sulphur compounds at low concentration was carried out previously by other workers by using different stationary phases: silica gel [7], graphitized carbon black treated with phosphoric acid [8], commercially available Carbopack BHT [9] or Porapak QS specially treated by washing with acetone [10], equivalent to Supelpak-S commercial phase [11]. All these phases were tested in our experiments and found to be more or less satisfactory for the separation of sulphur compounds. An additional problem arises because the selected phase must at the same time perform an efficient separation of light hydrocarbons and a fast analysis to permit a frequent check of the composition of the system under study during the evolution of the plasma discharge phenomena.

Therefore, other commercially available porous polymer bead stationary phases, (Porapak and Chromosorb Century Series) were tested by injecting standard mixtures containing both types of compounds.

As the method can be of general interest for the analysis of mixtures differing from plasma gases but containing hydrocarbon and sulphur compounds in trace amounts (refinery and paper mill effluents, waste gases, polluted industrial and town air, etc.), in the analysed samples were incorporated some gases that are probably not formed in plasma reactions but can be found in environmental samples (Table I).

The columns were made with inert tubing (PTFE) of I.D. 2 mm, filled with the following stationary phases, operated at different temperatures and flow-rates of the carrier gas: (1) Carbopack BHT-100 (Supelco, Bellefonte, PA, U.S.A.), 1.5 m, held isothermally at room temperature (30°C), carrier gas flow-rate 30 ml/min; (2) Chromosil 330 (Supelco), 1.5 m, operated isothermally at 40°C, carrier gas flow-rate 30 ml/min; (3) Supelpak-S (Supelco), 5 m, held isothermally at room temperature (30°C), carrier gas flow-rate 30 ml/min, temperature programme 1 min at 30°C, increased at 20°C/min to 200°C; (4) Chromosorb 105 (Johns-Manville, Denver, CO, U.S.A.), 80 cm, carrier gas flow-rate 30 ml/min, temperature programme 1 min at 60°C, increased at 20°C/min to 180°C, held for 2 min; and (5) Chromosorb 107 (Johns-Manville), same length and conditions as for column 4.

The adjusted retention times, t'_R (min), on the various columns are given in Table I. Column 1 (Carbopack BHT-100), a graphitized carbon black material [8,9], permitted a satisfactory separation of both sulphur compounds and hydrocarbons. Long retention times were observed for hydrocarbons $>C_5$ and for sulphur compounds heavier than n-propanethiol. Under the conditions shown in Table I the following t'_R values were obtained: dimethyl sulphide, 38 min; diethyl sulphide, 56 min; n-butanethiol, 65 min; and n-hexane, 81 min; the peaks were wide, which decreased the detectivity of small amounts of substance. The overall analysis time on this column is generally too long for practical use in the rapid analysis of plasma gases.

Column 3 (Supelpak-S) is a specially washed and treated Porapak QS packing, as described by de Souza et al. [10,11], originally suggested for the separation of craft pulp mill exhaust gases. This packing permitted a good resolution of sulphur compounds with retention times that, under our experimental conditions, are about half of these reported by de Souza et al. for light compounds (hydrogen sulphide, carbonyl sulphide) and approximate the previously reported values for slow-eluting substances (dimethyl disulphide, butanethiol). Unfortunately, this column gave several interfering peaks in the hydrocarbon region.

The same effect was observed by using column 2, Chromosil 330. In this instance the rapid elution of hydrocarbons with grouped peaks may be an advantage when very small amounts of flame ionization detector-sensitive compounds have to be detected, as the minimum detectable amount increases with decrease in the peak width. Obviously, only the total amount of C_2 or C_4 hydrocarbons can be measured.

Columns 2 and 3 showed poor efficiency in the separation of C_2 hydrocarbons, which were important components of the plasma gases used in our experiments. The separation of these compounds together with a sufficient resolution of higher hydrocarbons and sulphur compounds was carried out by using short PTFE columns (80 cm × 2 mm I.D.) filled with Chromosorb 105 porous polymer beads. This phase is an acrylic ester polymer with a surface area of 400–500 m^2/g and an average pore diameter of 500 Å [12,13] and permits a rapid separation of sulphur gases with symmetrical peaks while giving an acceptable resolution between light hydrocarbons up to pentane isomers. Some inversion of the elution order of saturated and

TABLE I

ADJUSTED RETENTION TIMES t'_R (min) OF LIGHT HYDROCARBONS AND SULPHUR COMPOUNDS ON DIFFERENT COLUMNS

For column preparation and analysis conditions, see text.

Compound	Column				
	(1) Carbopack BHT-100	(2) Chromosil 330	(3) Supelpak-S	(4) Chromosorb 105	(5) Chromosorb 107
Ethane	0.67	0.58	0.32	0.45	0.45
Ethylene	0.49	0.58	0.30	0.37	0.41
Acetylene	1.52	0.65	0.32	0.52	0.60
Propane	2.22	0.97	0.60	1.44	1.39
Propene	2.05	1.02	0.95	1.33	1.38
Isobutane	5.58	1.42	1.60	2.50	2.41
n-Butane	7.46	1.63	2.12	2.73	2.88
1-Butene	6.23	1.72	2.12	3.20	3.31
2-Butene (cis)	9.02	1.77	2.14	3.60	3.57
2-Butene (trans)	9.02	1.77	2.14	3.40	3.36
Isobutene	7.10	1.62	1.64	3.12	3.45
n-Pentane	24.60	2.80	3.10	4.28	4.45
Isopentane	18.50	2.56	3.07	4.10	4.17
Hydrogen sulphide	0.49	1.02	0.60	0.72	0.86
Carbonyl sulphide	1.30	0.95	0.84	1.01	1.07
Sulphur dioxide	1.22	3.93	1.62	2.03	4.18
Methanethiol	2.16	1.90	2.10	3.46	3.82
Ethanethiol	6.68	3.42	2.12	4.13	4.41
Dimethyl sulphide	7.03	3.06	5.05	4.00	4.17
Carbon disulphide	8.00	2.39	5.10	4.06	4.11
n-Propanethiol	22.20	7.61	4.30	12.50	13.70

unsaturated branched-chain compounds was observed with different batches of polymer and therefore the identification of these compounds should always be confirmed by injecting authentic samples. This problem has also been found with the other gas–solid or gas–gel chromatographic phases, were the mesh size, pore diameter, treatments and activation of the column may change the performance of different batches of products and their selectivity [14]. Therefore, the retention times for the fast-eluting compounds in Table I are averages from different analyses on various columns.

Moreover, the Chromosorb 105 columns showed some difficulty in separating small amounts of acetylene in the presence of a large excess of ethane. The retention time of acetylene increases with respect of that of ethane on decreasing the column temperature [15], but the slope coefficient as a function of temperature is small and therefore the separation of small amounts of acetylene from ethane is difficult. If the separation of these two gases is necessary, a column filled with Chromosorb 107 (acrylic ester polymer, surface area 400–500 m^2/g, average pore diameter 80 Å) can be used.

On Chromosorb 107 acetylene has a retention index [16] ranging between 220
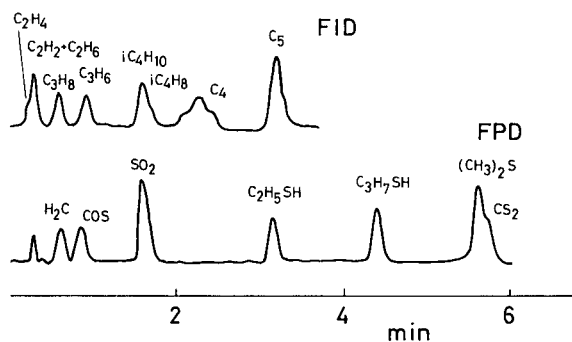
Fig. 3. Analysis of standard mixture of hydrocarbons and sulphur compounds on column 3 (Supelpak-S) with simultaneous analysis with flame ionization (FID) and flame photometric detection (FPD). For column parameters and analysis conditions, see text.

and 230 in the temperature interval used and therefore its peak is reasonably separated from that of ethane. The separation of ethylene and ethane is lightly less than that obtained on Chromosorb 105 (the retention index of ethylene is 185 on Chromosorb 105 and 190 on Chromosorb 107) but is sufficient for practical purposes [17].

Figs. 3 and 4 show the analyses of standard mixtures on Supelpak S and Chromosorb 105 (columns 3 and 4).

Fig. 5 shows a fast-eluting chromatogram obtained from an ethane–sulphur dioxide plasma. The separation of the main components of the mixture is satisfactory. Some other compounds were also detected.

Longer columns (up to 3 m) permitted a better separation of C_4 compounds, but with longer retention times (up to 20 min), acceptable for the analysis of environmental samples but sometimes unsuitable for the analysis speed required to follow the evolution of the product concentrations in the RF plasma reactor.

Faster programming rates or higher final column temperatures were also to be avoided owing to the excessive noise and baseline drift on the flame photometric
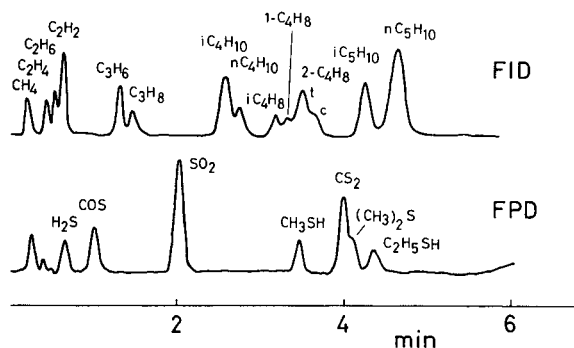
Fig. 4. Analysis of standard mixture of hydrocarbons and sulphur compounds on column 4 (Chromosorb 105) with simultaneous analysis with flame ionization (FID) and flame photometric detection (FPD). For column parameters and analysis conditions, see text.
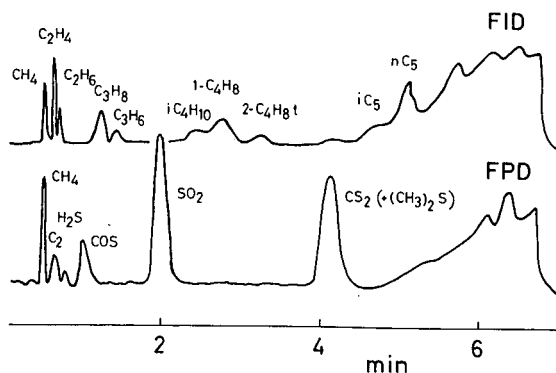
Fig. 5. Analysis of reactor plasma gas obtained from RF discharge with a 50:50 mixture of ethane and sulphur dioxide at 0.75 Torr.

detector. The use of different detectors connected in parallel (flame ionization, electron-capture, flame photometric) was previously suggested for the determination of organic pollutants in open air [18].

Detectors

As shown in Fig. 2, a 50:50 splitter at the end of the column, made with a Swagelok 1/8-in. T-piece connected to two short PTFE tubes (I.D. 0.8 mm), leads the eluting gases to the two detectors installed in the two bases of the heated detector oven of the Varian 3700 gas chromatograph. No differential flow control is necessary if the length of the two connecting tubes is properly adjusted in order to give the same flow-rate through the two detectors. If necessary, a variable restrictor (high-temperature needle valve; Nupro, Willoughby, OH, U.S.A.) can be installed on the flame ionization detector side of the splitter, where decomposition or reaction of sulphur compounds has a negligible effect on the detector response.

A dual flame photometric detector (Varian) was used for the determination of sulphur compounds. The first flame, used to decompose the eluting compounds and convert them into combustion products consisting of relatively simple molecules, is a "reversed" flame where a flow of air (air 1) mixed with the carrier gas coming from the column burns in a hydrogen atmosphere. The exhaust gases of the first flame, which is hydrogen rich, burn on the top of the second concentric burner, where combustion is sustained by a second air flow (air 2).

The flow-rates were air 1, 80 cm^3/min; hydrogen, 80 cm^3/min; and air 2, 170 cm^3/min; the sum of the two air supplies is sufficient to consume approximately 50% of the hydrogen supplied to the burner and flame 2 is also a hydrogen-rich environment, where the emission of sulphur light, centred around the wavelength of 400 nm, takes place with reduced interference due to the combustion of hydrocarbons, mainly decomposed in the first flame. The light emitted was filtered through a broad-bandpass glass filter with peak transmission at 365 nm that transmitted to the photomultiplier (PMT) the low-wavelength portion of the S_2 emission spectra, thus reducing the interference with the CH emission lines due to thiols and residual hydrocarbons not completely decomposed in the first flame.
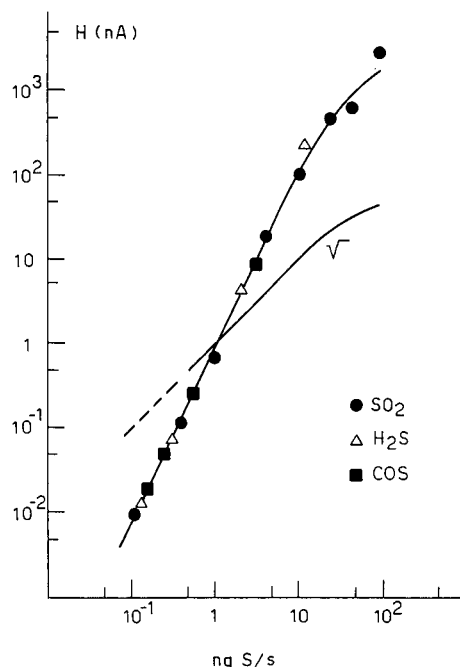
Fig. 6. Calibration graphs for the flame photometric detector obtained with an exponential dilution flask for sulphur dioxide, carbonyl sulphide and hydrogen sulphide. The line with the square-root symbol shows the response with slope = 1 obtained by using the linearizing circuit of the GC amplifier.

The detector response for hydrogen sulphide, carbonyl sulphide and sulphur dioxide was linear with slope 2.0 on a bilogarithmic plot (Fig. 6) in the range between 0.1 and 20 ng/s of sulphur.

The linear responses to other sulphur compounds (thiols, sulphides) were not tested over a wide concentration range, but the available data lie on the same straight line and therefore the calibration with a dual flame arrangement could be used for all the analysed compounds on the basis of their content of sulphur atoms. In the range 0.5–20 ng/s the quadratic attenuator built in the gas chromatograph amplifier permitted a linear response with slope 1 (shown with a square-root symbol in Fig. 6) to be obtained, thus permitting direct integration by the data system (Varian Vista 402).

For amounts smaller than 0.5 ng/s the square-root output cannot be used because it performs the square-root operation on the total detector signal, i.e., the peak plus the baseline offset, which become significant with respect to small peak areas. Further, the signal processor ignores minimum signal amplitudes, and a signal and noise cutoff occurs at about a 0.5 nA detector signal at the maximum sensitivity. Amounts of sulphur below 0.5 ng/s (dashed line in Fig. 6) are therefore better measured by interpolation of the output signal on a slope 2.0 bilogarithmic plot similar to that shown in Fig. 6 but where the peak area is plotted as a function of the amount of sulphur in the sample.

Single flame operation, obtained by turning off the air supply to flame 1, was

also tested. This mode of operation decreased the linearity of the square-law dependence of the signal on the concentration and increased the quenching of the sulphur signal due to simultaneous elution of any hydrocarbon. Further, the sensitivity to sulphur atoms was dependent on the type of sulphur compound, and the advantage of a calibration that is nearly independent of the molecular structure and depends only on the number of sulphur atoms in the molecule was lost. Dual flame operation was therefore used for quantitative analysis.

Sensitivities below the ppm range were easily obtained with samples at atmospheric pressure. Concentrations of about 0.01% of sulphur compounds were found in low-pressure plasma gases.

Minimum detectable amounts of 10^{-12} g/s for hydrocarbons with the flame ionization detector and 10^{-10} g/s for sulphur with the flame photometric detector were found.

ACKNOWLEDGEMENTS

REFERENCES

1 G. Smolinsky and M. J. Vasile, *J. Mass Spectrom. Ion Phys.*, 21 (1976) 171.
2 M. J. Vasile and G. Smolinsky, *J. Mass Spectrom. Ion Phys.*, 24 (1977) 11.
3 G. Castello, P. Canepa and M. Nicchia, *Ann. Chim. (Rome)*, 67 (1977) 149.
4 G. Castello, *J. Chromatogr.*, 244 (1982) 271.
5 J. E. Lovelock, in R. Scott (Editor), *Gas Chromatography 1960*, Butterworths, London, 1960.
6 C. H. Hartmann and K. P. Dimick, *J. Gas Chromatogr.*, 6 (1966) 163.
7 W. L. Thornsberry, Jr., *Anal. Chem.*, 43 (1971) 452.
8 F. Bruner, A. Liberti, M. Possanzini and I. Allegrini, *Anal. Chem.*, 44 (1972) 2070.
9 F. Bruner, P. Ciccioli and F. di Nardo, *J. Chromatogr.*, 99 (1974) 661.
10 T. L. C. de Souza, D. C. Lane and S. P. Bhatia, *Anal. Chem.*, 47 (1975) 543.
11 T. L. C. de Souza, *J. Chromatogr. Sci.*, 22 (1984) 470.
12 S. B. Dave, *J. Chromatogr. Sci.*, 7 (1969) 389.
13 S. B. Dave, *Ind. Eng. Chem., Prod. Res. Dev.*, 14 (1975) 85.
14 G. Castello and G. D'Amato, *J. Chromatogr.*, 349 (1985) 189.
15 G. Castello and G. D'Amato, *J. Chromatogr.*, 212 (1981) 261.
16 E. Kovats, *Helv. Chim. Acta*, 4 (1968) 1915.
17 G. Castello and G. D'Amato, *J. Chromatogr.*, 243 (1982) 25.
18 P. Ciccioli, G. Bertoni, E. Brancaleoni, R. Fratarcangeli and F. Bruner, *J. Chromatogr.*, 126 (1976) 757.

Gas chromatographic separation of diastereomeric esters of α-alkyl-α-amino acids on dimethylpolysiloxane[a]

HANS BRÜCKNER* and MATTHIAS LANGER[b]

Institute of Food Technology, University of Hohenheim, D-7000 Stuttgart 70 (F.R.G.)

(First received March 13th, 1990; revised manuscript received May 28th, 1990)

ABSTRACT

The separation of 28 (R,S)-α-alkyl-α-amino acids (AAAs) with the structure $H_2NC(R^1)(R^2)COOH$ (R^1,R^2 = alkyl, aralkyl, which may be further substituted; R^1, $R^2 \neq H$) was systematically investigated by capillary gas chromatography on the stationary phase dimethylpolysiloxane (CP-Sil 5); the AAAs were used as their N(O)-pentafluoropropionyl (PFP)-AAA $(S)(+)$-2-alkyl esters (alkyl = 2-butyl to 2-octyl and 3-methyl-2-butyl). In selected cases, (R,S)-3,3-dimethyl-2-butyl esters, (R,S)-3-octyl esters, (R,S)-2-dodecyl esters and $(-)$-menthyl esters were also employed. Baseline resolution was achieved for these AAAs by derivatization with suitable alcohols. By using AAAs of known absolute configuration, it was possible to establish the order of emergence as (S)-AAAs before (R)-AAAs for PFP-(R,S)-AAA $(S)(+)$-2-alkyl esters. This is the opposite elution order to that of α-amino acids having a C^α-hydrogen atom. In spite of their opposite elution orders on achiral stationary phases, conformational analysis of PFP $(S)(+)$-2-alkyl esters of (S)-α-amino acids and (S)-AAAs shows that they have the same bulkiness chirality.

INTRODUCTION

As a consequence of the substitution of the C^α-hydrogen atom of protein amino acids by alkyl or alkaryl groups, the resulting chiral α-alkyl-α-amino acids (AAAs) of the type $H_2NC(R^1)(R^2)COOH$ ($R^1 \neq R^2 \neq H$) show different chemical and chromatographic behaviours to their parent compounds [1,2]. In spite of the increasing interest in the use of chiral and non-chiral AAAs as sterically constrained, non-protein amino acids, *e.g.*, for peptide drug design [3,4], the systematic investigation of their chiral analytical properties is still hampered by the fact that only a few racemic and no optically pure AAAs are currently commercially available (see Experimental), although stereoselective syntheses [5] and enzymic scaled-up resolutions of (R,S)-AAA amides [6] have been described.

The natural microheterogeneity of the 20-mer peptide antibiotic paracelsin served as a possible model for reversed-phase interaction mechanisms in high-per-

---

formance liquid chromatography (HPLC) [7,8] and, in the case of synthetic *homo*-Aib oligopeptides, the thin-layer chromatographic recognition of 3_{10}-helical conformations of these peptides [9] has been realized. Further, by using α-aminoisobutyric acid (α-methylalanine, 2-methylalanine, Aib) and isovaline (2-ethylalanine, Iva) as highly specific marker compounds for the detection of a unique group of polypeptide antibiotics of the peptaibol family, it was shown that these AAAs are common metabolites of certain genera of fungi [10,11,12] and that Aib and Iva, therefore, are neither exceedingly rare amino acids in the biosphere nor, if occurring in sediments, necessarily of extraterrestrial origin [13].

     Using capillary gas chromatography (GC) and the diastereomeric approach, Pollock [14] demonstrated that (*R,S*)-Iva was partly separated as the N-trifluoroacetyl (TFA)-Iva (*S*)(+)-2-alkyl esters (alkyl = *n*-pentyl to *n*-octyl) but not as the TFA-Iva (*S*)(+)-2-butyl ester. The formation of N-pentafluoropropionyl (PFP)-(*R,S*)-Iva (*S*)(+)-3-methyl-2-butyl esters was used for the revison of the configuration of Iva in the peptide antibiotic antiamoebin [15]. Chang *et al.* [16] demonstrated that a number of (*R,S*)-AAAs are separable as N-TFA isopropyl esters on optically active diamide stationary phases and we have reported the separation of derivatives of selected (*R,S*)-AAAs using the chiral stationary phases Chirasil–L-Val and XE-60–L-Val–(*S*)-α-phenylethylamide [17]. Further, it was shown that the resolution of (*R,S*)-AAAs is also possible by chiral ligand-exchange HPLC using either chiral additives, such as N-dialkyl-L-amino acids together with Cu^{II} salts [18,19], to eluents or by employing chiral stationary phases such as Chiral ProCu [19,20–24]. Moreover, HPLC and precolumn derivatization of (*R,S*)-AAAs with *o*-phthaldialdehyde together with N-acyl-L-cysteine (acyl = acetyl, *tert.*-butyloxycarbonyl) [22,23,25], derivatization of (*R,S*)-AAAs using Marfey's reagent [21,24] and thin-layer chromatography using Chiralplate [26] have also made the separation of (*R,S*)-AAAs possible.

EXPERIMENTAL

Gas chromatography
     A Hewlett-Packard Model 5880 A gas chromatograph equipped with a flame ionization detector and a 26 m × 0.22 mm I.D. wall-coated open-tubular (WCOT) fused-silica column coated with 0.21-μm dimethylpolysiloxane (CP-Sil 5) (Chrompack, Middelburg, The Netherlands) was used. The carrier gas was helium at 100 kPa (1.0 bar), the splitting ratio was *ca.* 1:30 and the injector and detector temperatures were 250°C.

Abbreviations and sources of α-alkyl-α-amino acids
     In order to have simple nomenclature and abbreviations, in this work AAAs are considered as being formally derived by substitution of a $C^{α}$-hydrogen atom in α-amino acids by an alkyl group. Substitution of the $C^{α}$-hydrogen atom of Ala by an *n*-alkyl group (alkyl = ethyl to *n*-octyl) thus leads to the homologous series α-Et-Ala to α-Oct-Ala (for abbreviations of alkyl groups, see the next paragraph) and substitution of the $C^{α}$-hydrogen atom in α-amino-*n*-butyric acid (Abu) by an *n*-alkyl group (alkyl = *n*-propyl to *n*-hexyl) leads to the homologous series α-Prop-Abu to α-Hex-Abu (see also Fig. 1).

     Derivatives of the following AAAs were investigated {for racemic AAAs the

prefix DL- is used as given by the manufacturers, for enantiomers (R,S)- is used in this paper in order to avoid ambiguities [24]} DL-α-methylaspartic acid (α-Me-Asp), DL-α-methylglutamic acid (α-Me-Glu), DL-α-methylornithine (α-Me-Orn), DL-α-methylserine (α-Me-Ser), DL-α-methyl-*m*-methoxyphenylalanine (α-Me-*m*-PheOMe), DL- and L-α-methyltyrosine (α-Me-Tyr) and DL- and L-α-methyl-(3,4-dihydroxyphenyl)alanine (α-Me-Dopa) were purchased from Sigma (St. Louis, MO, U.S.A.), DL-α-methylleucine (α-Me-Leu) from Bachem (Bubendorf, Switzerland) and DL-α-ethylphenylglycine (α-Et-Phg) from EMKA Chemie (Markgröningen-Talhausen, F.R.G.).

Commercially unavailable AAAs were synthesized in our laboratory according to the Strecker procedure by reaction of the respective ketones (from Fluka, Buchs, Switzerland) with potassium cyanide and ammonium chloride and subsequent saponification of the nitriles with hydrochloric acid. The AAAs were liberated from the hydrochlorides by treatment with tributylamine and purified by crystallization from methanol–water. The following AAAs were synthesized (abbreviations and other names used in the relevant literature are given in parentheses): DL-α-ethylalanine (α-Et-Ala or isovaline, Iva), DL-α-propylalanine (α-Prop-Ala, α-methylnorvaline), DL-α-butylalanine (α-But-Ala, α-methylnorleucine), DL-α-pentylalanine (α-Pent-Ala, 2-methyl-2-aminoheptanoic acid), DL-α-hexylalanine (α-Hex-Ala, 2-methyl-2-aminooctanoic acid), DL-α-heptylalanine (α-Hept-Ala, 2-methyl-2-aminononanoic acid), DL-α-octylalanine (α-Oct-Ala, 2-methyl-2-aminodecanoic acid), DL-α-nonylalanine (α-Non-Ala, 2-methyl-2-aminoundecanoic acid), DL-α-propyl-α-amino-*n*-butyric acid (α-Prop-Abu, α-ethylnorvaline), DL-α-butyl-α-amino-*n*-butyric acid (α-But-Abu, α-ethylnorleucine), DL-α-pentyl-α-amino-*n*-butyric acid (α-Pent-Abu, 2-ethyl-2-aminoheptanoic acid) and DL-α-hexyl-α-amino-*n*-butyric acid (α-Hex-Abu, 2-ethyl-2-aminooctanoic acid). Pure enantiomers of α-Et-Ala and α-Prop-Ala were obtained by digestion of the respective N-chloroacetyl- or N-trifluoroacetyl derivatives with acylase I or carboxypeptidase [21]. L-α-Me-Leu, L-α-Me-Phg, L-α-Me-Tyr-Ome, L-α-Et-Phe, DL-α-Et-Phe, L-α-Me-*homo*-Phe and DL-α-Me-*homo*-Phe were gifts from Dr. J. Kamphuis (DSM Research, Geleen, The Netherlands) (configuration as designated by the supplier). $(S)(+)$-2-Butanol, $(S)(+)$-2-pentanol, $(S)(+)$-2-octanol, (R,S)-2-dodecanol, (R,S)-3-octanol and (R,S)-3,3-dimethyl-2-butanol (pinacolic alcohol) were obtained from Fluka, $(S)(+)$-3-methyl-2-butanol, $(S)(+)$-2-hexanol and $(S)(+)$-2-heptanol from Chemical Dynamics (EHEMALOG) (South Plainfield, NJ, U.S.A.) and $(1R,2S,5R)(-)$-menthol from Aldrich (Steinheim, F.R.G.). $(S)(+)$-3-Methyl-2-butanol and $(S)(+)$-2-pentanol were also synthesized in our laboratory according to procedures described in the literature [27]. Pentafluoropropionic anhydride (PFPA) was obtained from Pierce (Rockford, IL, U.S.A.), acetyl chloride of pro analysi (p.a.) grade from Fluka and dichloromethane (p.a.) from Merck (Darmstadt, F.R.G.).

Procedures for derivatization of amino acids for GC

Aliphatic and aromatic AAAs. About 0.6 mg of the AAAs in 0.1 ml of a 20% (v/v) solution of acetyl chloride in the respective alcohol was sonicated and heated for 1 h in a 1-ml Reacti-vial (Wheaton, Milleville, NJ, U.S.A.). The mixture was evaporated to dryness in a stream of dry nitrogen, the residue was dissolved in 100 μl of dichloromethane (DCM) and 25 μl of PFPA were added. After 20 min at 100°C the reagents were removed in a stream of nitrogen, the residue was dissolved in 50 μl ml of DCM and 0.8-μl portions were subjected to GC in the split mode.

TABLE I

COMPARISON OF NET RETENTION TIMES, t (min), AND RESOLUTION FACTORS, α, AT THE TEMPERATURE T (°C) OF N(O)-PENTAFLUOROPROPIONYL DERIVATIVES OF (R,S)-α-ALKYL-α-AMINO ACID (S) $(+)$-2-ALKYL ESTERS [(R,S)-AAAs] ON DIMETHYLPOLYSILOXANE (CP-SIL 5)

Carrier gas, helium (100 kPa). Resolution factors in italics are highest factors in the series of alcohols.

(R,S)-AAA	2-Butyl ester			3-Methyl-2-butyl ester			2-Pentyl ester		
	t	T	α	t	T	α	t	T	α
α-Et-Ala	12.20 12.40	80	1.016	7.30 7.45	100	1.021	7.81 8.00	100	*1.024*
α-Prop-Ala	10.97 11.13	90	1.015	8.37 8.53	105	1.019	6.87 7.13	110	*1.038[+a]*
α-But-Ala	7.24 7.40	110	1.022	8.52 8.78	115	1.031[+]	7.06 7.43	120	*1.052[+]*
α-Pent-Ala	7.64 7.83	120	1.025	8.71 9.01	125	1.034[+]	5.90 6.21	135	1.053[+]
α-Hex-Ala	7.94 8.16	130	1.028	8.93 9.24	135	1.035[+]	7.48 7.90	140	1.056[+]
α-Hept-Ala	8.21 8.43	140	1.027	9.08 9.38	145	1.033[+]	7.61 8.02	150	1.054[+]
α-Oct-Ala	6.84 7.01	155	1.025	9.28 9.58	155	1.032[+]	6.39 6.69	165	1.047[+]
α-Non-Ala	6.89 7.09	165	1.029	9.20 9.46	165	1.028[+]	5.12 5.33	180	1.041[+]
α-Prop-Abu	8.23 —	105	n.r.[b]	9.91 —	110	n.r.	10.36 10.54	110	*1.017*
α-But-Abu	8.44 —	115	n.r.	9.93 —	120	n.r.	10.20 10.53	120	1.032[+]
α-Pent-Abu	8.65 8.78	125	1.015	9.94 10.08	130	1.014	10.25 10.67	130	1.041[+]
α-Hex-Abu	8.87 9.02	135	1.017	9.96 10.13	140	1.017	10.27 10.70	140	1.042[+]
α-Me-Leu	7.49 7.66	105	1.023	7.15 7.37	115	1.031[+]	7.44 7.72	115	*1.038[+]*
α-Me-Met	6.58 6.77	135	1.029	7.48 7.79	140	1.041[+]	7.41 7.86	140	1.061[+]
α-Me-Ser	8.53 8.81	95	1.033	7.79 8.06	105	1.035[+]	6.44 6.81	110	1.057[+]
α-Me-Asp	10.50 10.65	130	1.014	—[c]			8.85 9.14	150	*1.033[+]*
α-Me-Glu	8.04 8.17	150	1.016	8.08 8.21	165	1.016	6.79 7.05	170	1.038[+]
α-Me-Orn	6.57 6.75	145	1.027	8.95 9.22	145	1.030[+]	5.78 6.14	155	1.062[+]

2-Hexyl ester			2-Heptyl ester			2-Octyl ester		
t	T	α	t	T	α	t	T	α
8.56 8.73	110	1.020	9.16 9.32	120	1.017	9.72 9.86	130	1.014
7.35 7.59	120	1.033[+]	6.32 6.51	135	1.030[+]	8.07 8.30	140	1.029[+]
7.32 7.64	130	1.044[+]	7.41 7.77	140	1.049[+]	7.48 7.84	150	1.048[+]
5.91 6.20	145	1.049[+]	7.26 7.71	150	*1.062[+]*	7.15 7.58	160	1.060[+]
5.86 6.16	155	1.051[+]	5.73 6.08	165	1.061[+]	6.90 7.36	170	*1.067[+]*
5.93 6.25	165	1.054[+]	5.64 6.00	175	1.064[+]	6.62 7.09	180	*1.071[+]*
5.93 6.25	175	1.054[+]	5.51 5.85	185	1.062[+]	6.37 6.80	190	*1.068[+]*
6.98 7.35	180	1.053[+]	6.46 6.87	190	1.063[+]	6.05 6.46	200	*1.068[+]*
10.98 11.08	120	1.009	11.26 11.45	130	*1.017*	9.15 9.31	145	*1.017*
10.51 10.82	130	1.029[+]	10.42 10.85	140	*1.041[+]*	8.38 8.72	155	*1.041[+]*
10.28 10.71	140	1.042[+]	9.89 10.45	150	1.057[+]	9.68 10.26	160	*1.060[+]*
9.98 10.44	150	1.046[+]	9.47 10.08	160	1.064[+]	9.09 9.72	170	*1.069[+]*
7.82 8.05	125	1.029[+]	8.15 8.40	135	1.031[+]	8.24 8.46	145	1.027[+]
7.38 7.83	150	1.061[+]	7.50 8.00	160	*1.067[+]*	7.16 7.63	170	1.066[+]
6.64 7.03	120	1.059[+]	6.75 7.22	130	*1.070[+]*	7.10 7.60	140	*1.070[+]*
8.01 8.20	170	1.024	7.17 7.30	190	1.018	9.56 9.87	200	1.032
7.01 7.34	185	1.047[+]	7.44 7.86	200	1.056[+]	9.26 9.84	210	*1.063[+]*
5.41 5.81	165	1.074[+]	5.12 5.57	175	*1.088[+]*	— [c]		

TABLE I *(continued)*

(R,S)-AAA	2-Butyl ester			3-Methyl-2-butyl ester			2-Pentyl ester		
	t	T	α	t	T	α	t	T	α
α-Me-Phg	6.37 6.52	140	1.024	7.06 7.25	145	1.027[+]	7.12 7.60	145	1.067[+]
α-Et-Phg	8.75 8.89	140	1.016	9.66 9.78	145	1.012	7.98 8.42	150	1.055[+]
α-Me-Phe	9.60 9.83	140	1.024	8.60 8.93	150	*1.038*[+]	8.96 9.12	150	1.018
α-Et-Phe	8.72 8.88	150	1.018	7.86 8.05	160	*1.024*	8.05 8.14	160	1.011
α-Me-*homo*-Phe	7.53 7.69	160	1.021	8.17 8.38	165	1.026	8.24 8.64	165	1.049[+]
α-Me-*p*-Tyr	6.79 6.92	160	1.019	8.82 9.06	160	*1.027*	7.39 7.47	165	1.011
α-Me-*m*-Tyr	6.21 6.40	160	1.031	8.08 8.46	160	*1.047*[+]	6.95 7.06	165	1.016
α-Me-*p*-TyrOMe	7.29 7.43	170	1.019	9.59 9.85	170	*1.027*[+]	9.90 —	170	n.r.
α-Me-*m*-PheOMe	6.65 6.77	170	1.018	7.25 7.45	175	*1.028*[+]	8.90 8.97	170	1.008
α-Me-Dopa	7.97 8.15	160	1.023	8.01 8.25	165	*1.030*[+]	8.51 —	165	n.r.

[a] Baseline resolution is indicated by a superscript "plus" sign.
[b] n.r. = Not resolved.
[c] No derivatization achieved under the conditions used.

Acidic and basic AAAs. About 0.6 mg of the amino acid in 300 μl of 2.5 M hydrochloric acid in methanol were heated in a 1-ml Reacti-vial at 100°C for 1 h. The reagents were removed in a stream of nitrogen and the resulting methyl ester was transesterified by addition of 100 μl of acetyl chloride in the respective alkanol by heating at 100°C for 1 h. Acylation with PFPA was carried out as described above. Derivatization of sparingly soluble AAAs was performed by stirring with a PTFE-coated, triangular stirring bar. Derivatization procedures and treatment with nitrogen were carried out in a heating/stirring module from Pierce equipped with an aluminium block.

2-Hexyl ester			2-Heptyl ester			2-Octyl ester		
t	T	α	t	T	α	t	T	α
7.09 7.52	155	1.061[+]	6.97 7.45	165	*1.069[+]*	5.82 6.20	180	1.065[+]
7.95 8.36	160	1.052[+]	7.63 8.12	170	1.064[+]	7.45 7.95	180	*1.067[+]*
8.96 9.12	160	1.018	8.70 8.87	170	1.020	8.45 8.59	180	1.017
7.79 7.93	170	1.018	9.17 9.38	175	1.023	10.93 11.18	180	1.023
7.89 8.28	175	1.049[+]	7.45 7.90	185	1.060[+]	8.73 9.29	190	*1.064[+]*
8.45 8.61	170	1.019	9.63 9.83	175	1.021	8.97 9.19	185	1.025
7.78 7.95	170	1.022	7.25 7.42	180	1.023	8.47 8.68	185	1.025
11.38 —	175	n.r.	12.95 —	180	n.r.	14.79 —	185	n.r.
10.33 10.42	175	1.009	11.99 12.13	180	1.012	13.68 13.80	185	1.009
7.30 7.40	175	1.014	8.29 8.42	180	1.016	7.63 7.78	190	1.020

RESULTS AND DISCUSSION

Selection of derivatives, stationary phase and GC conditions
In a previous paper [17], it was shown that satisfactory resolution of N(O)-perfluoroacyl-(S)(+)-2-alkyl esters of selected (R,S)-AAAs was achieved by use of capillary columns coated with CP-Sil 19 CB (Chrompack). In order to investigate systematically the influence of the respective alkyl esters on the resolution factors, we used the N(O)-PFP esters exclusively and 100% dimethylpolysiloxane (CP-Sil 5) as a standard stationary phase. Suitable isothermal temperatures (80–190°C) and carrier gas pressures were selected in order to obtain about equal retention times of *ca.* 7–12 min and the highest resolution factors for the various derivatives.

Resolution of N(O)-pentafluoropropionyl-α-alkyl-α-amino acid 2-alkyl esters

Derivatives of 28 AAAs were investigated. Retention times, isothermal temperatures and resolution factors (α) are given in Table I and for selected AAAs in Table II. AAAs are grouped as the α-alkylalanines and the α-alkyl-α-amino-*n*-butyric acids with increasing alkyl chain lengths, and then as neutral, acidic, basic and aromatic side-chain α-methyl amino acids (Table I; for nomenclature of AAAs, see Fig. 1 and Experimental). Derivatives of (*R,S*)-AAAs for which baseline resolution was achieved are indicated by a superscript "plus" sign on the resolution factors in the tables. Sections of gas chromatograms of PFP-(*R,S*)-AAA (*S*)(+)-2-octyl esters are shown in Fig. 2. Gas chromatograms of PFP-(*R,S*)-AAA (*S*)(+)-3-methyl-2-butyl esters [19] and selected gas chromatograms of the series (*S*)(+)-2-pentyl to (*S*)(+)-2-heptyl esters have been published elsewhere [21,22,24]. The influence of the structures of the 2-alkanols on the α values of the diastereomeric PFP-AAA 2-alkyl esters is discussed below.

(S)(+)-2-Butyl esters [14,27–30]. Most AAAs were separated more or less satisfactorily, but in no case was complete baseline resolution achieved. α-Prop-Abu and α-But-Abu were not resolved. In most instances the use of these esters is less advantageous in comparison with those described below.

(S)(+)-3-Methyl-2-butyl esters [27,29–31]. In comparison with the (*S*)(+)-2-butyl esters an increase of α was achieved in most instances together with baseline resolution of the enantiomers in many instances. However, α-Prop-Abu and α-But-Abu were again not resolved. α-Me-Phg, α-Me-Phe, α-Et-Phe, α-Me-*m*-PheOMe and Me-Dopa were baseline resolved and the best resolution of α-Me-Tyr and analogs was also obtained by use of this reagent. The significantly increased resolution of AAAs by esterification with branched 2-alkanols is also demonstrated for (*R,S*)-3,3-dimethyl-2-butanol (pinacolic alcohol) in some selected cases (Table II). This reagent provides the highest resolution factors for α-Et-Ala and α-Me-Phe. However, this alcohol also shows significant kinetic discrimination [30,32].

(S)(+)-2-Pentyl esters [14,27,29,30]. Most aliphatic side-chain AAAs showed baseline resolution with this reagent. α-Me-Phg, α-Et-Phg and α-Me-*homo*-Phe showed baseline resolution, in contrast to α-Me-Phe, α-Et-Phe and hydroxylated aromatic AAAs, which exhibited incomplete separation. This behaviour was also found for the (*S*)(+)-2-hexyl, (*S*)(+)-2-heptyl and (*S*)(+)-2-octyl esters of these aromatic AAAs.
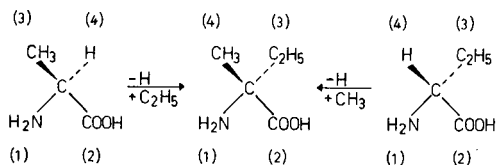
Fig. 1. (*R*)-α-Ethylalanine (α-Et-Ala, isovaline), as an example of an α-alkyl-a-amino acid, might be *formally* derived from either L-Ala [= (*S*)-Ala] by Cα-hydrogen substitution by an ethyl group, or from D-Abu [= (*R*)-Abu] (Abu, α-amino-*n*-butyric acid) by Cα-hydrogen substitution by a methyl group. Numbers indicate the priority of Cα substituents according to the Cahn–Ingold–Prelog rule. Formal substitution of the Cα-hydrogen by alkyl groups in Ala and Abu leads to the series α-alkyl-Ala and α-alkyl-Abu, respectively, or, in general, to α-alkyl-α-amino acids.
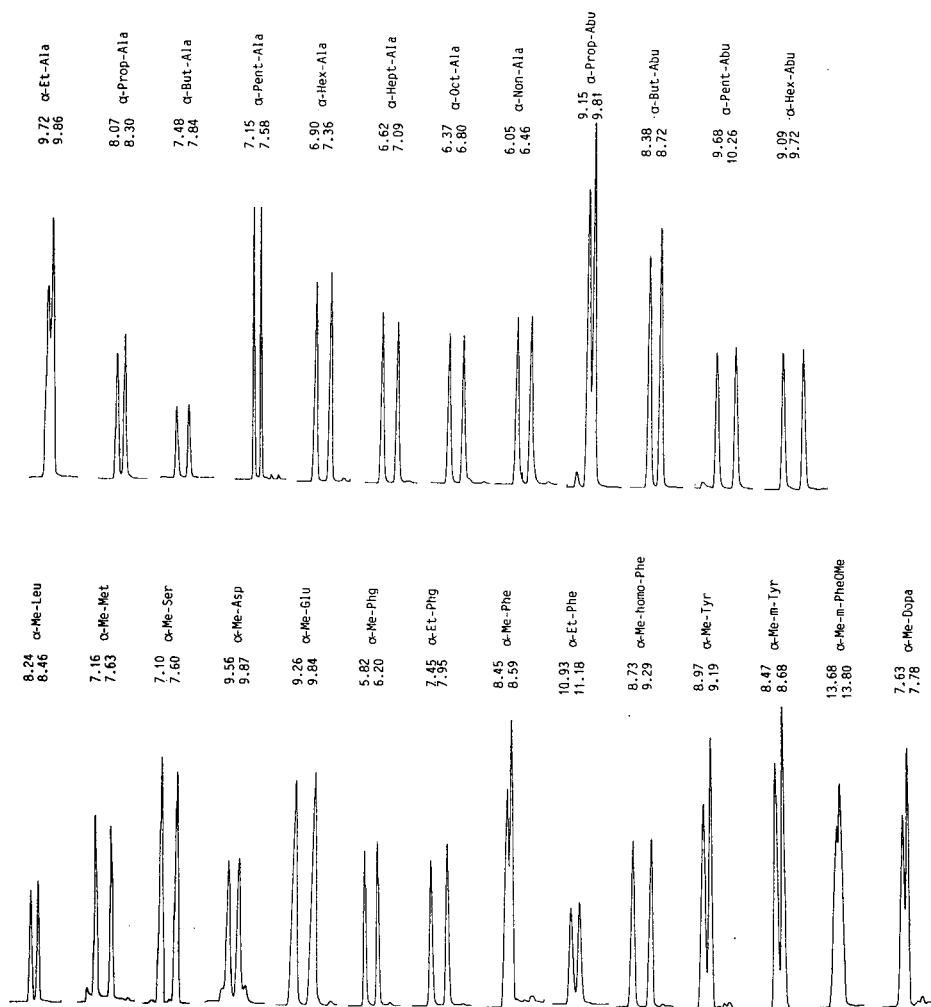
Fig. 2. GC of N(O)-pentafluoropropionyl-(R,S)-α-alkyl-α-amino acid (S)(+)-2-octyl esters on dimethyl-polysiloxane (CP-Sil 5). Net retention times (min) at isothermal temperatures (cf., Table I) are given. Carrier gas, helium at 100 kPa (1.0 bar).

(S)(+)-2-Hexyl [14,29], (S)(+)-2-heptyl [14] and (S)(+)-2-octyl esters [14,28,30]. In comparison with the pentyl esters, higher α were found for these esters for aliphatic AAAs. α-Me-Phg, α-Et-Phg and α-Me-*homo*-Phe were baseline resolved and the other aromatic AAAs were partially resolved by use of these alcohols, with the exception of α-Me-Tyr-OMe, which remained unresolved. In most instances increasing α values were found in the series of pentyl to octyl esters, with the highest α values for (S)(+)-2-octyl esters (Fig. 2). An exception is α-Et-Ala, which exhibited decreasing α values on going from the pentyl to the octyl ester.

(R,S)-2-Dodecyl, (R,S)-3-octyl [30] and (R,S)-3,3-dimethyl-2-butyl esters [27,29,30]. [It is understood that by derivatization of (S)-AAAs with (R,S)-2-alka-

TABLE II

COMPARISON OF NET RETENTION TIMES, t (min), AND RESOLUTION FACTORS, α, AT THE TEMPERATURE T (°C) OF N(O)-PENTAFLUOROPROPIONYL DERIVATIVES OF (S)-α-AL-KYL-α-AMINO ACID (R,S)-2-ALKYL ESTERS [(S)-AAAs] ON CP-SIL 5

Carrier gas, helium (100 kPa).

(S)-AAA	2-Dodecyl ester			3-Octyl ester			3,3-Dimethyl-2-butyl ester		
	t	T	α	t	T	α	t	T	α
α-Et-Ala	10.16 —	170	n.r.[a]	8.75 —	130	n.r.	9.26 9.48	100	1.024[+b]
α-Me-Leu	8.31 8.51	185	1.024[+]	7.84 7.94	145	1.013	7.69 7.86	120	1.022
α-Me-Phe	7.15 7.36	220	1.029[+]	7.90 —	180	n.r.	10.97 11.59	150	1.057[+]
α-Me-Tyr	8.05 8.41	220	1.045[+]	8.37 —	185	n.r.	7.18 7.56	170	1.053[+]

[a] n.r. = not resolved.
[b] Baseline resolution is indicated by a superscript "plus" sign.

nols actually the 2-alkanols are resolved. As α does not change when (R,S)-AAAs are resolved with (R) or (S)-2-alkanols, respectively, for simplicity the terminology that follows is used]. This tendency for higher α values with increasing chain length of the 2-alkanols is exemplified by (R,S)-2-dodecanol for selected (S)-AAAs, giving baseline resolution for α-Me-Leu, α-Me-Phe and α-Me-Tyr (Table II). α-Et-Ala was not resolvable with (R,S)-2-dodecanol. (R,S)-3-Octanol, in striking contrast to (R,S)-2-octanol, gave no resolution for α-Et-Ala, α-Me-Phe and α-Me-Tyr and low resolution for α-Me-Leu (Table II). Remarkably, (R,S)-3,3-dimethyl-2-butanol gave the highest α values for all derivatives investigated of α-Et-Ala, α-Me-Phe and α-Me-*homo*-Phe, but not for α-Me-Leu (*cf.*, Tables I and II). α-Prop-Abu was partially resolved by 3,3-dimethyl-2-butanol, but the resolution coefficient (α = 1.014) was lower than that with 2-pentanol (α = 1.017) under the same conditions (*cf.*, Table I). By analogy with protein amino acids, significant diastereomeric fractionation would be expected for AAAs by esterification with this sterically highly constrained alkanol [30,32].

($1R,2S,5R$)($-$)-*Menthyl esters [27,33].* Excellent resolution was achieved for aromatic AAAs by esterification with ($-$)-menthol, in particular for those which were unsatisfactorily resolved by (S)($+$)-2-alkanols (Table III). However, no separation was obtained for α-alkylalanines by esterification with ($-$)-menthol and, as a major disadvantage, low derivatization yields were obtained with this reagent, which did not increase on transesterification of the respective methyl esters.

Relative derivatization yields of AAAs with alcohols

The relative derivatization yields of the isomeric amino acids (assumed to give equal flame ionization detector responses) valine (Val), norvaline (Nva) and isovaline (Iva) were investigated on CP-Sil 5 by derivatization with 1- and 2-propanol. With

TABLE III

COMPARISON OF NET RETENTION TIMES, t (min), AND RESOLUTION FACTORS, α, AT THE TEMPERATURE T (°C) OF N(O)-PENTAFLUOROPROPIONYL-(R,S)-α-ALKYL-α-AMINO ACID (1R,2S,5R)($-$)-MENTHYL ESTERS [(R,S)-AAAs] ON CP-SIL 5

Carrier gas, helium (100 kPa).

(R,S)-AAA	t	T	α	(R,S)-AAA	t	T	α
α-Et-Phg	7.10 7.31	195	1.030[+a]	α-Me-p-Tyr	7.74 8.11	200	1.048[+]
α-Me-Phe	9.73 10.11	190	1.039[+]	α-Me-m-Tyr	7.55 8.03	200	1.064[+]
α-Et-Phe	8.36 8.70	200	1.041[+]	α-Me-p-TyrOMe	9.02 9.31	210	1.032[+]
α-Me-*homo*-Phe	10.23 10.39	200	1.016	α-Me-m-PheOMe	8.32 8.71	210	1.047[+]

[a] Baseline resolution is indicated by a superscript "plus" sign.

1-propanol, Nva (unbranched side-chain) and Val (branched side-chain), both having C^α-hydrogen atoms, gave equal peak areas in GC, and are therefore assumed to give 100% relative derivatization yields (r.d.y.), whereas Iva (alkyl-substituted C^α-hydrogen atoms) gave 80% r.d.y. With 2-propanol, Nva gave 100%, Val 77% and Iva 37% r.d.y. This clearly shows the steric hindrance resulting from the side-chain branching of the amino acids and from the branching of the alcohols. Further, by analogy with protein amino acids [30], for the determination of the ratios of enantiomers of AAAs using the diastereomeric approach a possible kinetic discrimination [30,32] in the esterification process has to be evaluated, in particular for highly branched alcohols such as 3,3-dimethyl-2-butanol.

Elution order and assignment of absolute configuration of AAAs

As pure or enriched enantiomers of AAAs (*cf.*, Experimental) were available, the elution order of enantiomers as their PFP-AAA $(S)(+)$-2-alkyl esters was determined unambiguously for these AAAs. In all instances the (S)-AAAs eluted before the (R)-AAAs when using $(S)(+)$-2-alkanols, and (R)-AAAs before (S)-AAAs after esterification with $(R)(-)$-2-butanol. By analogy this is assumed to be valid for all AAAs investigated and also for AAAs which are structurally related. This elution order of AAAs is the opposite of that of amino acids having a C^α-hydrogen atom. The elution order, optical rotation and absolute configuration of AAAs have also been correlated by chiral ligand-exchange chromatography [20].

Configuration and elution order of α-alkyl-α-amino acids as compared with protein amino acids

Feibush and Gil-Av [34] presented a model for the elution order of enantiomeric N-TFA-amino acid esters of the general type $CF_3CONHCHRCOOR'$ on a chiral "ureido" phase. They postulated that the order of emergence is dependent on the relative effective size of the substituents H, R and COOR' at the asymmetric carbon
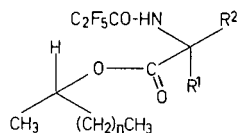
Fig. 3. Scheme of spatial arrangement and bulkiness chirality of N-PFP-(S)-α-amino acid (S)( )-2-alkyl esters for α-amino acids (R^1 = H, R^2 = alkyl, alkaryl) and for α-alkyl-α-amino acids (R' = Me, Et; R^2 = alkyl, alkaryl, bulkiness of $R^2 > R^1$).

atom. Feibush [35] applied a similar model to the separation of diastereomeric α-acetoxypropionic 2-alkyl esters and found for the LD (= S,S) isomers, which showed the longer retention time of the LD–DD pair, that the substituents on both asymmetric carbon atoms are arranged in the same direction with regard to their size in decreasing order ("bulkiness chirality") when viewing the molecule along its long axis.

This is also true for diastereomeric esters of proteinogenic amino acids, but the corresponding α-methyl-α-amino acids show the opposite order of elution, although the respective derivatives of amino acids and AAAs do have the same bulkiness chirality (Fig. 3). On chiral stationary phases, however, enantiomeric esters of amino acids and AAAs, such as N-TFA-1-propyl esters, show the same elution order for R- and S-enantiomers, respectively.

CONCLUSIONS

Systematic investigation of the separation of 28 diastereomeric N(O)-PFP-(R,S)-AAA (S)(+)-2-alkyl esters [series (S)(+)-2-butanol to (S)(+)-2-octanol and (S)(+)-3-methyl-2-butanol; with in selected instances the use of 3,3-dimethyl-2-butanol, (R,S)-3-octanol, (R,S)-2-dodecanol and (−)-menthol] by GC on dimethylpolysiloxane showed that no one alcohol made the baseline separation of all AAAs possible, but that baseline resolution could be achieved for most AAAs by use of an appropriate alcohol (see tables and Fig. 2). The most difficult AAA to resolve as diastereomeric esters on CP-Sil 5 are those which have the relatively smallest differences in sizes of the *geminal* alkyl groups, i.e., α-Et-Ala (Iva) and α-Prop-Abu (*cf.*, Tables I and II).

For determinations of the ratios of enantiomers in a certain (R,S)-AAA, not only the optical purity of the alkanol employed but also the kinetic discrimination in the esterification process as a function of the branching of the alcohol and of the side-chains of AAAs have to be determined.

(S)-AAAs are eluted before (R)-AAAs in the cases of diastereomeric PFP-(R,S)-AAA (S)(+)-alkyl esters and the use of achiral stationary phases. This is the opposite elution order to that of α-amino acids having a C^α-hydrogen atom, where R-(= D) enantiomers elute before S-(= L) enantiomers. However, with respect to their bulkiness chirality [35] (i.e., arrangement of alkyl and aryl substituents in decreasing order; *cf.*, Fig. 3), PFP-(S)-AAA (S)(+)-2-alkyl esters show the same elution order as PFP-(R)-AA (S)(+)-2-alkyl esters.

REFERENCES

1 J. R. Cronin, *Anal. Biochem.*, 81 (1977) 151.
2 H. Brückner, I. Bosch, T. Graser and P. Fürst, *J. Chromatogr.*, 386 (1987) 251.
3 C. Toniolo and E. Benedetti, *ISI Atlas Sci. Biochem.*, (1988) 225.
4 G. R. Marshall, J. D. Clark, J. B. Dunbar, G. D. Smith, J. Zabrocki, A. S. Redlinski and M. T. Leplawy, *Int. J. Pept. Protein Res.*, 32 (1988) 544.
5 R. M. Williams, *Synthesis of Optically Active α-Amino Acids*, Pergamon Press, Oxford, 1989.
6 W. H. Kruizinga, J. Bolster, R. M. Kellogg, J. Kamphuis, W. H. J. Boesten, E. M. Meijer and H. E. Schoemaker, *J. Org. Chem.*, 53 (1988) 1826.
7 K. D. Lork, K. K. Unger, H. Brückner and M. T. W. Hearn, *J. Chromatogr.*, 476 (1989) 135.
8 B. Pfleiderer, K. Albert, K. D. Lork, K. K. Unger, H. Brückner and E. Bayer, *Angew. Chem.*, 101 (1989) 336; *Angew. Chem., Int. Ed. Engl.*, 28 (1989) 327.
9 H. Brückner, in W. A. König and W. Voelter (Editors), *Chemistry of Peptides and Proteins*, Vol. 4, Attempto Verlag, Tübingen, 1989, p. 79.
10 H. Brückner and C. Reinecke, *J. High Resolut. Chromatogr. Chromatogr. Commun.*, 11 (1988) 735.
11 H. Brückner and C. Reinecke, *J. High Resolut. Chromatogr.*, 12 (1989) 113.
12 H. Brückner, N. Nuber and C. Reinecke, *Fresenius' Z. Anal. Chem.*, 333 (1989) 777.
13 M. Zhao and J. L. Bada, *Nature (London)*, 339 (1989) 463.
14 G. E. Pollock, *Anal. Chem.*, 44 (1972) 2368; correction, 46 (1974) 614.
15 H. Brückner, G. J. Nicholson, G. Jung, K. Kruse and W. A. König, *Chromatographia*, 13 (1980) 209.
16 S. C. Chang, R. Charles and E. Gil-Av, *J. Chromatogr.*, 288 (1982) 20.
17 H. Brückner, I. Bosch, T. Graser and P. Fürst, *J. Chromatogr.*, 395 (1987) 569.
18 S. Weinstein and N. Grinberg, *J. Chromatogr.*, 318 (1985) 117.
19 H. Brückner, M. Langer, A. Esna-Ashari, A. Labudda, Z. J. Kamiński and M. T. Leplawy, in G. Lubec and G. A. Rosenthal (Editors), *Amino Acids: Chemistry, Biology and Medicine*, ESCOM Science, Leiden, 1990, p. 159.
20 H. Brückner, *Chromatographia*, 24 (1987) 725.
21 H. Brückner, S. Kühne, S. Zivny and M. Currle, in T. Shiba and S. Sakakibara (Editors), *Peptide Chemistry 1987*, Protein Research Foundation, Mino Osaka, 1988, p. 175.
22 H. Brückner, I. Bosch, S. Kühne and S. Zivny, in G. R. Marshall (Editor), *Peptides, Chemistry and Biology*, ESCOM Science, Leiden, 1988, p. 195.
23 Z. J. Kamiński, M. T. Leplawy, A. Esna-Ashari, S. Kühne, S. Zivny, M. Langer and H. Brückner, in G. Jung and E. Bayer (Editors), *Peptides 1988*, Walter de Gruyter, Berlin, New York, 1989, p. 298.
24 H. Brückner, S. Kühne, S. Zivny, M. Langer, Z. J. Kamiński and M. T. Leplawy, in A. Aubry, M. Marraud and B. Vitoux (Editors), *Second Forum on Peptides*, John Libbey Eurotext, London, Paris, 1989, p. 291.
25 A. Duchateau, M. Crombach, J. Kamphuis, W. H. J. Boesten, H. E. Schoemaker and E. M. Meijer, *J. Chromatogr.*, 471 (1989) 263.
26 J. Martens and R. Bhushan, *Int. J. Pept. Protein Res.*, 34 (1989) 433.
27 B. Halpern and J. W. Westley, *Aust. J. Chem.*, 19 (1966) 1533.
28 E. Gil-Av, R. Charles and G. Fischer, *J. Chromatogr.*, 17 (1965) 408.
29 J. W. Westley, B. Halpern and B. L. Karger, *Anal. Chem.*, 40 (1968) 2046.
30 G. S. Ayers, R. E. Monroe and J. H. Mossholder, *J. Chromatogr.*, 63 (1971) 259.
31 W. A. König, W. Rahn and J. Eyem, *J. Chromatogr.*, 133 (1977) 141.
32 G. G. Smith and D. M. Wonnacott, in P. E. Hare, T. C. Hoerning and K. King (Editors), *Biogeochemistry of Amino Acids*, Wiley, New York, 1980, p. 203.
33 M. Hasegawa and I. Matsubara, *Anal. Biochem.*, 38 (1975) 308.
34 B. Feibush and E. Gil-Av, *J. Gas Chromatogr.*, (1967) 257.
35 B. Feibush, *Anal. Chem.*, 43 (1971) 1098.

Note

Chiral stationary phase for the facile resolution of β-adrenoceptor blocking agents

MASAKI OHWA*, MIYAKO AKIYOSHI and SHUICHI MITAMURA

Chemicals Research Laboratory, R & D Laboratories-1, Nippon Steel Co., 1618 Ida, Nakahara-ku, Kawasaki, 211 (Japan)

(Received April 24th, 1990)

The relationship between molecular chirality and the pharmaceutical activity of various drugs is of great interest [1]. The separation of a racemic mixture of β-adrenoceptor blocking agents (β-blockers), in particular, has attracted considerable attention [2]. For instance, propranol, a typical β-blocker, has been widely used in the treatment of a variety of cardiovascular disorders and its (S)-(−)-isomer is 100 times more potent than its antipode, the (R)-(−)-isomer [3]. In addition to the different pharmacological activities, recent studies have shown that the absorption, metabolism and disposition kinetics of drugs also depend greatly on molecular chirality [4]. Therefore, the development of a facile procedure capable of separating and quantifying the enantiomers of of β-blockers is important.

The chromatographic separation of a racemic mixture has been recognized as one of the most effective methods for the above purpose [5]. In addition to the conventional indirect separation method using diastereomeric derivatives, there are two different direct separation approaches, a chiral stationary phase (CSP) method and a chiral ion-pair method. Several kinds of CSPs for the direct chromatographic separation of enantiomeric β-blockers, such as α_1-acid glycoprotein [6], cyclodextrins [7] and cellulose derivatives [8] have been developed recently. An ion-pair chromatographic method for the separation of a racemic mixture of various drugs [9] was developed by Petterson and co-workers, who found (+)-10-camphorsulphonic acid [10] and N-benzyloxycarbonylglycyl-L-proline [11] to be particularly effective as chiral counter ions for a number of β-blockers. These results prompted us to develop a new CSP for the separation of a racemic mixture of β-blockers by immobilizing glycyl-L-proline (GPr) on modified silica gel.

In this paper, the synthesis of a novel chiral stationary phase and the results of the separation of a series of β-blockers are presented.

EXPERIMENTAL

Materials

All chemicals were analytical-reagent grade, except where indicated otherwise, and were used without further purification.

Develosil 100-5 (5 μm) silica gel, purchased from Nomura Chemical (Aichi, Japan) was used as a support. 3-Glycidoxypropyltrimethoxysilane was obtained from Shin-Etsu (Tokyo, Japan), glycyl-L-proline from the Peptide Institute (Osaka, Japan) or Sigma (St. Louis, MO, U.S.A.), Propranolol, pindolol and atenolol from Sigma, carteolol from Kanto (Tokyo, Japan) and metoprolol from Sterochim (Milan, Italy).

Preparation of the CSP–GPr chiral stationary phase

To a suspension of Develosil 100-5 (20.0 g), dried for 4 h at 120°C, in dry toluene (100 ml) was added 3-glycidoxypropyltrimethoxysilane (12.0 ml) and the resulting mixture was heated under reflux for 20 h with the removal from the mixture of the methanol formed. After cooling, the modified silica gel was filtered with a glass filter (G-4), washed with dry toluene (2 × 50 ml) and dried under vacuum to give 23.6 g of the product. A portion of this modified silica gel (3.70 g) was suspended in dry methanol (20 ml) and then the monosodium salt of glycyl-L-proline (0.512 g) was added and the mixture was allowed to stand for 7 days with occasional stirring under nitrogen at room temperature. The resulting chiral stationary phase, CSP–GPr was collected by filtration and washed exhaustively with methanol. Elemental analysis gave C 7.38, H 1.43, N 0.57; required for silanized silica gel, C 7.28, H 1.47, N <0.1%.

Chromatography

A stainless-steel column (150 mm × 0.46 mm, I.D.) was packed with the modified silica gel using conventional slurry packing techniques. Chromatography was carried out at room temperature at a flow-rate of 1.0 ml/min using a mixture of methanol and dichloromethane containing an amine (1.0 mM) as the mobile phase. A Shimadzu (Kyoto, Japan) Model 6A, high-performance liquid chromatograph equipped with a Rheodyne Model 7120 injector with a 20-ml loop and a Shimadzu SPD-6A UV detector measuring at 280 nm was used.

RESULTS AND DISCUSSION

The chiral stationary phase, CSP–GPr was prepared from glycyl-L-proline and Develosil 100-5 (5 μm), pretreated with 3-glycidoxypropyltrimethoxysilane as a coupler, as shown in Fig. 1.

The separation of a racemic mixture of β-blockers on the prepared CSP was first conducted under the conditions used by Pettersson and co-workers with a solution of triethylamine in dichloromethane (1.0 mM) as the mobile phase [10]. Pindolol (separation factor, α = 1.15), propranolol (α = 1.15) and carteolol (α = 1.18) were well separated into enantiomers. However, the retention time of these peaks varied with time so that the reproducibility of an analysis was poor. Addition of methanol to the mobile phase solved this problem. Amines added to the mobile phase compete with the β-blocker (β-amino alcohol) for ion pair formation with the carboxyl groups
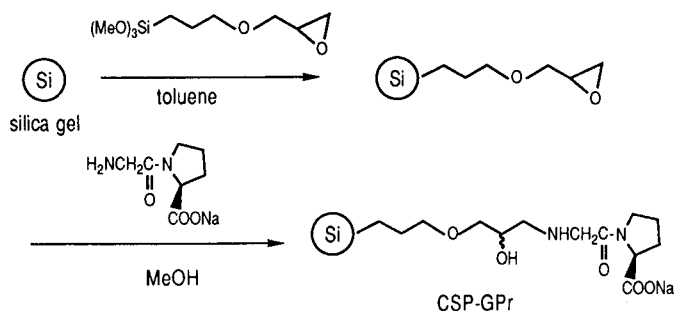
Fig. 1. Synthesis of the chiral stationary phase. Me = methyl.

of CSP–GPr, hence the retention time and separation factor will be affected by the amine structure and basicity. The effects of alcohols and amines added to the mobile phase were further investigated to elucidate the characteristics of CSP–GPr.

Organic solvent in a mobile phase
The results of the separation of propranolol with various mobile phases are given in Table I. When 2-propanol was added instead of methanol, the peaks exhibited tailing, even though the selectivity remained the same as with methanol. Chloroform separated the enantiomers of pindolol better than dichloromethan (Table II).

TABLE I

EFFECT OF ALCOHOLS IN THE MOBILE PHASE ON THE RESOLUTION OF PROPRANOLOL

Chiral stationary phase: CSP–GPr. Mobile phase: alcohol–dichloromethane (3:97) containing 1.0 mM triethylamine. Flow-rate: 1.0 ml/min. Temperature: 25°C. UV detection at 280 nm.

Alcohol	δ^a	$k_1{}^b$	$k_2{}^b$	α^c	$R_s{}^d$
Methanol	14.4	1.01	1.11	1.10	0.63
Ethanol	12.7	15.3	17.4	1.13	1.52
2-Propanol	11.5	3.30	3.66	1.11	0.60

  [a] δ = Hildebrand's solubility parameter.
  [b] Capacity factor of the first eluted enantiomer: k_1 = (retention time − dead time)/dead time.
  [c] Separation factor $\alpha = k_2 / k_1$.
  [d] Resolution factor R_s = 2 (distance between the two peaks) / (sum of the band widths of the two peaks).

TABLE II

EFFECT OF ORGANIC SOLVENTS IN THE MOBILE PHASE ON THE RESOLUTION OF PINDOLOL

Conditions as in Table I. Mobile phase: methanol–halogenated solvent (3:97) containing 1.0 mM triethylamine.

Solvent	δ	k_1	k_2	α	R_s
Dichloromethane	9.7	4.00	4.29	1.07	0.88
Chloroform	9.3	3.80	4.26	1.12	1.17

TABLE III

EFFECT OF VARIOUS AMINES ON THE RESOLUTION OF PINDOLOL

Mobile phase: methanol–dichloromethane (3:97) containing 1.0 mM amine. Conditions as in Table I.

Amine	pK_a[a]	k_1	α	R_s	
Triethylamine	11.01	1.01	1.11	1.10	0.63
Diethylamine	11.09	4.68	5.22	1.12	1.05
Diisopropylamine	11.13	6.56	6.99	1.07	0.59
Butylamine	10.78	4.58	4.92	1.08	0.93
Pyrrolidine	11.27	2.33	2.49	1.07	0.71
Piperidine	11.12	5.74	6.07	1.12	1.63
Morpholine	8.33	26.21	27.90	1.06	0.91
2-Aminoethanol	9.52	1.91	2.10	1.10	0.99
2-(Ethylamino)ethanol	–	5.45	5.84	1.07	1.04

[a] These data were taken from ref. 12.

TABLE IV

RESOLUTION OF VARIOUS β-BLOCKERS ON CSP–GPr

Conditions as in Table I. Mobile phase: methanol–chloroform (2:98) containing 1.0 mM diethylamine.

$$R_1OCH_2CHCH_2NHCCH_3$$

with OH and CH₃ and R₂ substituents on the chain:

$$\underset{OH}{R_1OCH_2\overset{|}{C}HCH_2NH\overset{R_2}{\overset{|}{C}}\underset{CH_3}{\overset{|}{C}}CH_3}$$
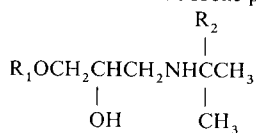
Solute	R_1	R_2	k_1	k_2	α	R_s
Propranolol	naphthyl	H	1.77	2.06	1.16	1.09
Pindolol	indolyl	H	8.24	9.55	1.16	1.02
Compound I[a]	indoline	H	11.7	16.1	1.37	2.12
Compound II[a]	dihydroindolyl	H	2.30	2.77	1.21	1.13
Carteolol	dihydroquinolinone	CH₃	4.04	4.82	1.19	1.21
Metoprolol	$CH_3OCH_2CH_2$–C₆H₄–	H	1.18	1.31	1.12	0.41
Atenolol	H_2NCCH_2–C₆H₄– (C=O)	H	11.2	12.3	1.10	0.58

[a] These compounds are β-blocker analogues.
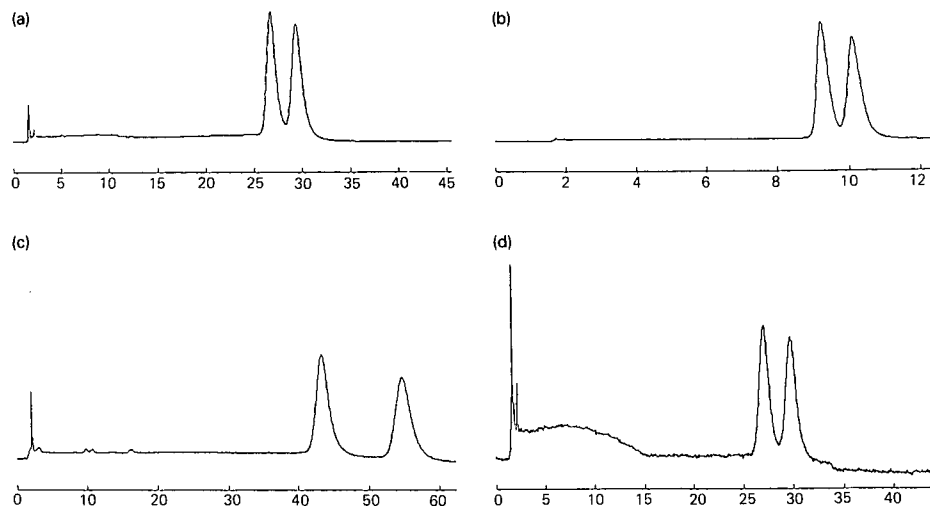
Fig. 2. Chromatograms of (a) pindolol, (b) propranolol, (c) compound I and (d) carteolol using CSP–GPr as a chiral stationary phase. Mobile phase: methanol–dichloromethane (3:97) containing 1.0 mM diethylamine. Flow-rate: 1.0 ml/min. Temperature: 25°C. UV detection at 280 nm. Time axis in min.

Influence of amine additives

The separation of a racemic mixture of propranolol was carried out using mobile phase containing nine types of amines, and the results are summarized in Table III. The retention time is greatly affected by the concentration of amines. As the amine concentration in the mobile phase increases, the β-blocker is eluted in a shorter time. Addition of sterically bulky diisopropylamine reduced the separation factor. The relationship between the basicity and the separation factor is not clear at this stage, but triethylamine, diethylamine and piperidine gave optimum separation factors among the nine amines investigated.

A series of β-blockers were separated on CSP–GPr using methanol–dichloromethane (3:97) containing diethylamine (1.0 mM) and the results are summarized in Table IV. Typical chromatograms are shown in Fig. 2.

In conclusion, an effective and readily prepared chiral stationary phase has been developed that has potential for application to other adrenergic drugs and other groups of pharmaceuticals with similar chemical structures.

Further studies are in progress to improve the resolution by changing the immobilized peptide structure and the results will be presented elsewhere.

REFERENCES

1 I. W. Wainer and D. E. Drayer (Editors), *Drug Stereochemistry: Analytical Methods and Pharmacology*, Marcel Dekker, New York, 1988.
2 T. Walle and U. Walle, in V. Marko (Editor), *Determination of β-Blockers in Biological Matrices*, Elsevier, Amsterdam, 1988, Ch. 7.
3 A. M. Barret and V. A. Cullum, *Br. J. Pharmacol.*, 34 (1968) 43.
4 T. Walle, J. Webb, E. Bagwell, U. Walle, H. Daniell and T. Gattney, *Biochem. Pharmacol.*, 37 (1988) 115.
5 S. G. Allenmark, *Chromatographic Enantioseparation, Methods and Applications*, Wiley, New York, 1988.
6 G. Schill, I. W. Wainer and S. A. Barkan, *J. Liq. Chromatogr.*, 9 (1986) 641.
7 D. W. Armstrong, T. W. Ward, R. D. Armstrong and T. E. Beesley, *Science (Washington, D.C.)*, 232 (1986) 1132.
8 Y. Okamoto, M. Kawashima, R. Aburatani, K. Hatada, T. Nishiyama and M. Masuda, *Chem. Lett.*, (1986) 1237.
9 C. Pettersson and G. Schill, in M. Zief and L. J. Crane (Editors), *Chromatographic Chiral Separations*, Marcel Dekker, New York, 1988, p. 283.
10 C. Pettersson and G. Schill, *J. Chromatogr.*, 204 (1981) 179.
11 C. Pettersson and M. Josefsson, *Chromatographia*, 21 (1986) 321.
12 D. D. Perrin, *Dissociation Constants of Organic Bases*, Plenum Press, New York, 1965.

Note

Poly(crown ether) stationary phase for open-tubular capillary column chromatography

AIQIN ZHANG, JILONG GE, ZHENXI GUAN, JINHUI DENG, HUWEI LIU, JIYA ZHU and RUONONG FU*

Department of Chemical Engineering, Beijing Institute of Technology, P.O. Box 327, Beijing 100081 (China)

and

ZAIFU HUANG and BIN ZHANG

Department of Environmental Science, Wuhan University, Wuhan (China)

(First received February 23rd, 1990; revised manuscript received June 27th, 1990)

Applications of crown ethers and cryptands in analytical chemistry have been extensively developed [1], one of the most important being in high-performance liquid chromatography (HPLC) for the separation of ionic species [2]. Some low-molecular-weight crown ethers, *e.g.*, dibenzo-24-crown-8, were used as packed column stationary phases by Li [3,4] for the separation of alcohols, phenols, amines, aromatic compounds and halides. Fine *et al.* [5] prepared and characterized open-tubular columns coated with three types of poly(crown ether), poly(vinylbenzo-15-crown-5), vinylmethyl-sila-17-crown-6 and vinylmethylsila-14-crown-5. Zagorevskaya and Kovaleva [6] used dibenzo-18-crown-6 and dinitrodibenzo-18-crown-6 as gas chromatographic station-ary phases coated on a carbon sieve for the separation of paraffinic and aromatic hydrocarbons. More recently, Rouse *et al.* [7] synthesized an oligo (ethylene oxide)-substituted polysiloxane and 18-crown-6-substituted polysiloxane as open-tubular column stationary phases and compared them with Carbowax 20M. In our previous work [8], two kinds of crown ethers were used as capillary column stationary phases.

In this work, 3-allylbenzo-15-crown-5-substituted polysiloxane was synthesized and coated on fused-silica capillary columns. The retention behaviour was studied and compared those of three columns coated with low-molecular-weight crown ethers. The crown ethers investigated are shown in Fig. 1.

EXPERIMENTAL

Model SP-2305 and SP-3700 gas chromatographs (Beijing Analytical In-strument Factory, Beijing, China) equipped with flame ionization detectors were used for evaluation of retention behaviour. Glass capillary columns statically coated with dibenzo-24-crown-8 were prepared as described previously [8]. Fused-silica capillary
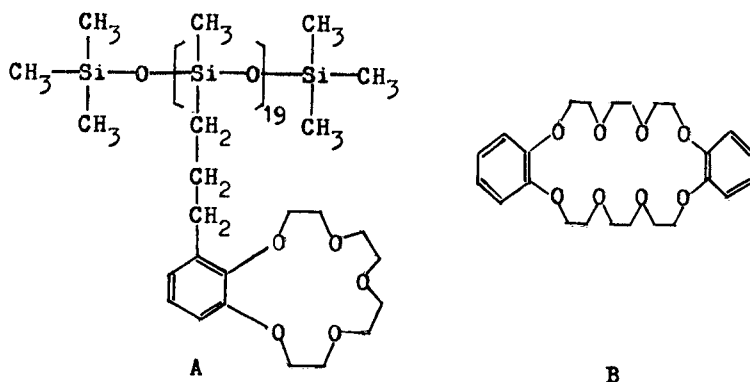
Fig. 1. Structure of crown ether stationary phases studied. A = PAB15C5S; B = DB24C8.

columns (0.25 mm I.D.) (Yongnian Optical Fibre Factory, Hebei, China) were purged with dry nitrogen at 250°C for 2 h before coating, then filled with a solution of poly(crown ether) stationary phase in dichloromethane and sealed at one end, evaporating the solvent under vacuum at 35°C from the other end. After solvent evaporation, the column was dried with dry nitrogen at room temperature for 1 h, then connected to the gas chromatograph and conditioned at 180°C. Allylbenzo-15-crown-5 and dibenzo-24-crown-8 were obtained from the Department of Environmental Science, Wuhan University (Wuhan, China). Poly(methylhydrosiloxane) (PHMS) was obtained from the Second Beijing Chemicals Factory (Beijing, China). All other chemicals used for synthesis or characterization purpose were of analytical-reagent grade. Benzo-15-crown-5-substituted (crown) polysiloxane was synthesized from allylbenzo-15-crown-5 and PHMS by a procedure similar to that in the literature [7].

RESULTS AND DISCUSSION

Table I gives the characteristics of three fused-silica capillary columns coated

TABLE I

CHARACTERISTICS OF THE CAPILLARY COLUMNS STUDIED

Column No.	Column dimension (length × I.D.)	Stationary phase[a]	Column efficiency (plate/m)	Column temperature (°C)	Test compound
1	8.5 m × 0.25 mm	PAB15C5S	2675	140	$n\text{-}C_{13}$
2	15 m × 0.25 mm	PAB15C5S	3578	140	$n\text{-}C_8\text{-OH}$
3	10 m × 0.25 mm	PAB15C5S	4705	150	$n\text{-}C_1$
4	20 m × 0.29 mm[b]	DB24C8	350	120	$n\text{-}C_{15}$
5	20 m × 0.22 mm	DSU30C10	2680	165	$n\text{-}C_{13}$
6	20 m × 0.22 mm	SU15C5	2770	170	$n\text{-}C_{13}$

[a] PAB15C5S and DB24C8, see Fig. 1; DSU30C10 = 4,4-dipentadecyl- or 4,3′-dipentadecyl-30-crown-10; SU15C5 = 3-pentadecylbenzo-15-crown-5.
[b] Glass capilary column.

TABLE II

SELECTIVITIES AND POLARITIES OF THE CROWN ETHERS STUDIED

X' = Benzene; Y' = butanol; Z' = 2-pentanone; U' = nitropropane; S' = pyridine.

Stationary phase	McReynolds constants (ΔI)						b
	X'	Y'	Z'	U'	S'	Mean	
DB24C8	301	448	355	526	479	422	0.2340
SU15C5	121	218	165	242	195	189	0.2730
DSU30C10	82	116	128	213	166	141	0.2720
PAB15C5S	198	390	196	371	434	318	0.2563
SE-30[a]	15	44	53	64	41	43	0.2495
PEG-20M[a]	322	536	368	572	510	461	0.2235

[a] From ref. 9.

with PAB15C5S and a glass capillary column coated with dibenzo-24-crown-8, and two columns coated with SU15C5 and DSU30C10 for comparison. The results indicate that the efficiency of the glass capillary column coated with DB24C8 is the lowest, and those of the fused-silica capillary columns with PAB15C5S are the highest.
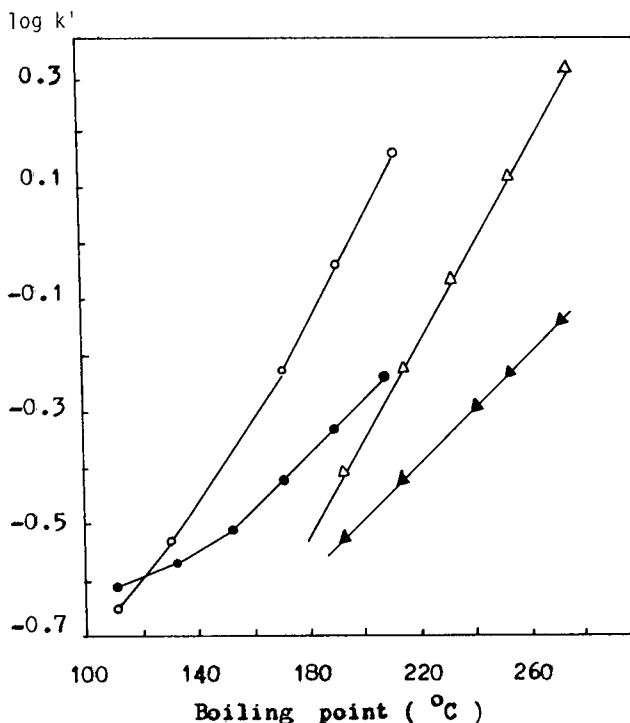
Fig. 2. Plot of log k' against boiling point for (○) alcohols at 140°C, (●) alcohols at 180°C, (△) alkanes at 140°C and (▲) alkanes at 180°C on column 3.

This occurs mainly because DB24C8 cannot form an even film on the wall of a glass capillary column, whereas PAB15C5S is a polysiloxane polymer, which can easily form a thin film on the wall of a fused-silica capillary column. Therefore, the use of a poly(crown ether) as a stationary phase in an open-tubular column gives a higher column efficiency than a low-molecular-weight crown ether.

The selectivity and polarity of PAB15C5S and DB24C8 are represented by McReynolds constants and b (the slope of the curve obtained when the logarithm of the adjusted retention times of n-alkanes are plotted as a function of the number of carbon atoms). These parameters and average polarities are listed in Table II. These parameters are also listed for SU15C5, DSU30C10, SE-30 and PEG-20M for comparison. The average polarity of PAB15C5S is higher than that of SU15C5 and DSU30C10, but is lower than that of DB24C8 and PEG-20M. It is surprising that the average polarity of PVB15C5, which was used as stationary phase for capillary columns by Fine *et al.* [5], is much higher than that of PAB15C5S (526 for PVB15C5 and 318 for PAB15C5S), and even higher than that of PEG-20M.

Of the six stationary phases in Table II, SU15C5 and DSU30C10 have the highest b values, owing to the long alkane chains, and therefore they are suitable for the separation of apolar compounds. On the other hand, PAB15C5S has a medium b value, similar to that of SE-30, so PAB15C5S is suitable for the separation not only of apolar compounds but also of hydroxyl compounds owing to the high selectivity for alcohols.

Fig. 2 shows the plots of log k' (capacity factor) *vs.* boiling points of homologous alkanes and alcohols, wich demonstrates the above-mentioned explanation about the selectivity of PAB15C5S. The slopes of the plots (Fig. 2) at the same temperature are
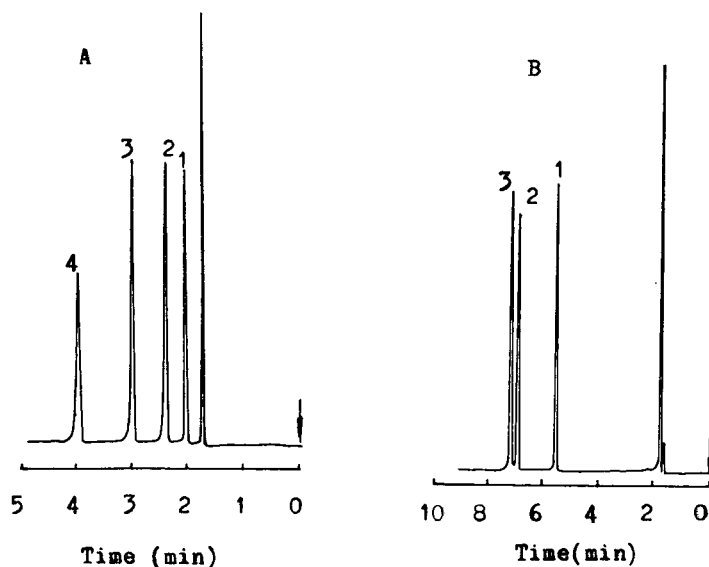
Fig. 3. Chromatograms of (A) alcohols (n-C$_4$–n-C$_7$) and (B) cresols on column 1 (PAB15C5S). (A) Column temperature = 146°C; 1 = n-butanol; 2 = n-heptanol; 3 = n-hexanol; 4 = n-heptanol. (B) Column temperature = 136.6°C; 1 = o-cresol; 2 = m-cresol; 3 = p-cresol.
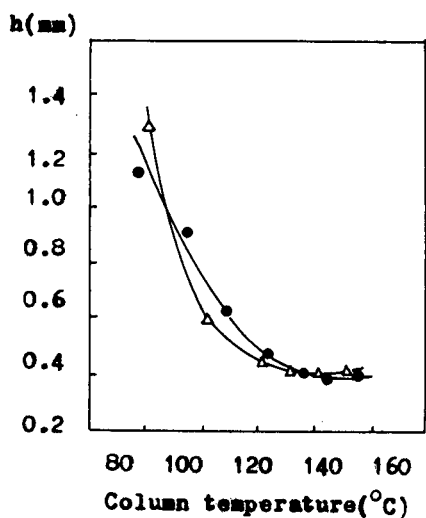
Fig. 4. Plots of column efficiency vs. column temperature. (●) Column 2; (△) column 3.
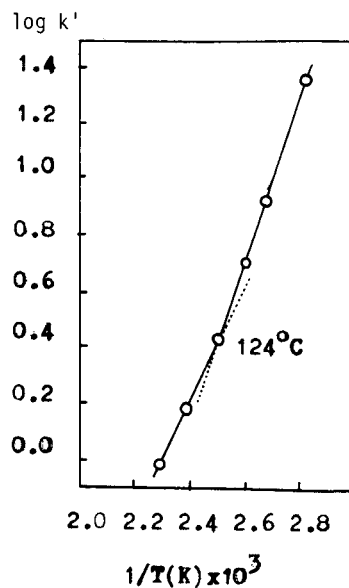
Fig. 5. Plot of log k' vs. reciprocal of column temperature for octanol on column 2.
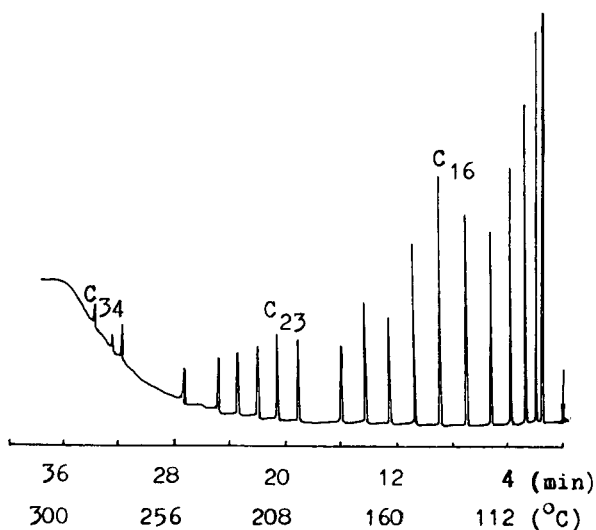
Fig. 6. Gas chromatogram of n-alkane mixture on column 3. Column temperature: 100°C for 2 min then programmed to 300°C at 6°C/min. Injection temperature: 350°C.

similar, which means that PAB15C5S stationary phase has a similar resolving power. On the other hand, at the same boiling point, the k' values of alcohols are higher than those of the corresponding alkanes. This demonstrates that crown ether stationary phases undergo a special interaction with alcohols. A fused-silica capillary column coated with PAB15C5S is suitable especially for the separation of phenols; e.g., the cresol isomers can be separated completely. Fig. 3 shows chromatograms for the separation of phenols and alcohols.

To test the effect of temperature on the column efficiency, the height equivalent to a theoretical plate (HETP) was determined at different temperatures and a constant flow-rate of the carrier gas. Fig. 4 illustrates a plot of HETP (k) vs. column temperature (t) for n-octanol on the three poly(crown ether) capillary columns. It is clear that the column efficiency increases with increasing temperature and has a maximum value at about 150°C, which is higher than the transition temperature (discussed below). This behaviour is different from that of SU15C5 and DSU30C10 columns, on which the plot of HETP vs. t has a maximum [8]. As with other crown ether columns, PAB15C5S columns also have a liquid–liquid transition temperature point (Fig. 5) at about 124°C.

To investigate the thermal stability of the PAB15C5S capillary columns, an n-alkane mixture was separated on column 3, which was cross-linked with V4 [tetra(methylvinyl)cyclotetrasiloxane] and DCUP (dicumyl perioside), and the chromatogram is shown in Fig. 6. The baseline drift was $1.1 \cdot 10^{-12}$ A when the column temperature was programmed from 100 to 300°C at 6°C/min. Therefore, it can be concluded that the fused-silica capillary column coated with PAB15C5S possesses high thermal stability, and it is better than that of low-molecular-weight crown ether stationary phases and PEG-20M.

Fused-silica capillary columns coated with PAB15C5S were used to separate polar and apolar compounds, such as isomers of cresol, mono- and dinitrotoluene, nitrohalogenated benzenes and dimethoxybenzene, and excellent results were obtained.

REFERENCES

1 K. Kimura and T. Shono, J. Liq. Chromatogr., 5 (1982) 223.
2 T. M. Kolthoff, Anal. Chem., 51 (1979) 1R.
3 R.-S. Li, Wuhan Daxue Xuebao, Ziran Kexueban, 4 (1985) 121.
4 R.-S. Li, Sepu, 4 (1986) 304.
5 D. D. Fine, H. L. Gearhart, II, and H. A. Mottola, Talanta, 32 (1985) 751.
6 E. V. Zagorevskaya and N. Y. Kovaleva, J. Chromatogr., 365 (1986) 7.
7 C. A. Rouse, A. C. Finlinson, B. J. Tarbet, J. C. Pixton, N. M. Djordjevic, K. E. Markides and M. L. Lee, Anal. Chem., 60 (1988) 901.
8 Y. Jin, R. Fu and Z. Huang, J. Chromatogr., 469 (1989) 153.
9 W. O. McReynolds, J. Chromatogr. Sci., 8 (1970) 685.

Note

Resolution of free aromatic amino acid enantiomers by host–guest complexation using reversed-phase liquid chromatography

J.-P. JOLY* and N. MOLL

Laboratoire de Chimie Organique III (UA 486 CNRS), Université de Nancy I, B.P. 239, 54506 Vandoeuvre-lès-Nancy Cedex (France)

(First received March 2nd, 1990; revised manuscript received June 26th, 1990)

The determination of the enantiomeric composition of amino acids can be accomplished in one of three basic ways: prederivatization of the enantiomers with a chiral reagent [1], addition of a chiral reagent to the mobile phase [2] or use of a chiral stationary phase (CSP) [3]. Although the first method is still the most efficient, it seems to be limited to analytical purposes. The second, especially the ion-exchange systems with chiral mobile phases on an achiral stationary phase, allows the direct separation of underivatized amino acids but requires additional steps to isolate the desired enantiomer from the components of the mobile phase [4].

A wide variety of CSPs have been studied in the attempt to resolve racemic amino acids but none has yet been able to resolve all of the common amino acids. Early attempts with CSPs involved ligand-exchange chromatography on covalently bonded copper(II) ion–L-proline complexes [5]. Kyba *et al.* [6] developed the synthesis of optically active crown ethers bearing binaphthyl units. By anchoring covalently some of these compounds, called hosts, on silica gel or polystyrene resin, they were able to resolve many amino acids as guests mainly as their methyl ester salts in mixtures of organic solvents as eluents [7]. More recently, Shinbo *et al* [8] extended the *in situ* or dynamic coating procedure first introduced by Kirkland and Dilks in 1973 [9] to the preparation of chiral crown ether packings for the chromatographic separation of many racemic underivatized amino acids with dilute perchloric acid as the eluent at 2°C.

However, the synthesis of such chiral crown ethers as highly pure enantiomers always requires extra resolution of racemic mixtures by recrystallization of diastereomeric species [10] or by liquid chromatography on a CSP [11]. For future separations of amino acids on CSPs preparative-scale systems should ideally use cheap aqueous mobile phases without any prederivatization. With the same approach we recently reported the synthesis of new chiral macrocyclic ethers derived from D-mannitol as a source of an inexpensive chiral framework and their immobilization on an

octadecylsilanized silica [12]. We describe here the preparation and some of the chromatographic characteristics of a similarly designed CSP.

EXPERIMENTAL

Reagents

All common chemicals and solvents were purchased from Aldrich (Strasbourg, France) or Prolabo (Paris, France) and were used without further purification. DL-α-Phenylglycine and D-tryptophan were obtained from Fluka (Buchs, Switzerland), (R)-(−)- and (S)-(+)-2-phenylglycine, DL-4-chlorophenylalanine and p-nitro-DL-phenylalanine from Aldrich, and p-nitro-L-phenylalanine, DL-tryptophan and DL-phenylalanine from Sigma (St. Louis, MO, U.S.A.). Rapid chromatography [13] was performed using Merck 9385 silica gel (40–63 μm). The chiral crown ether **2** was immobilized by dynamic coating on a reversed-phase column (Merck 19637; LiChrospher 100 RP-18, end-capped, $d_p = 5$ μm).

General

^{1}H and ^{13}C NMR spectra were recorded using a Bruker AM 400 spectrometer at 400.13 and 100.58 MHz, respectively, with tetramethylsilane or chloroform as internal references. Optical rotations were measured at 293 K using a Perkin-Elmer 141 polarimeter and a 1-dm cell. Analytical chromatography was performed using a Waters Assoc. Model 6000 pump, a Rheodyne Model 7125 injector, a Waters Model 440 UV detector (254 nm) and a Spectra-Physics Model 4290 integrator.

1,2:5,6-Di-O-isopropylidene-3,4-bis-O-[(2-chloroethoxy)ethyl]-D-mannitol (1)

A 5.25-g (20.0-mmol) amount of 1,2:5,6-diisopropylidene-D-mannitol (from D-mannitol, methoxy-2-propene and p-toluenesulphonic acid [14]) was reacted in a two-phase system with 100 ml of bis(2-chloroethyl) ether as solvent and reagent, 100 ml of 50% sodium hydroxide solution and 13.60 g of tetrabutylammonium hydrogensulphate (2 equiv) below 20°C for 14 h [15]. The mixture was diluted with water (100 ml) and dichloromethane (100 ml), decanted and the aqueous phase was washed with dichloromethane (2 × 50 ml). The organic extracts were combined, washed with water (2 × 50 ml), dried and concentrated. After evaporation of excess chloroethyl ether the resulting material was purified by rapid chromatography [25 × 5 cm I.D. column, ethyl acetate-n-hexane (1:2, v/v) as eluent to afford 7.13 g (75%) of **1** as a colourless oil: $[\alpha]_D = +14.9^0$ ($c = 16$; CCl$_4$). Microanalysis: calculated for C$_{20}$H$_{36}$O$_8$Cl$_2$, C 50.53, H 7.63, Cl, 14.91; found, C 50.30, H 7.54, Cl 15.41%.

1,2:5,6-Di-O-isopropylidene-3,4-O-[1,2-(4-tert.-butylbenzenediyl)bis(oxyethoxy-ethyl)]-D-mannitol (2)

A solution of 4-*tert.*-butylcatechol (1.03 g, 6 mmol) in n-butanol (40 ml) was stirred for 30 min at room temperature under argon. To this solution was added dry potassium carbonate (0.992 g, 6 mmol) and then, after having heated the resulting mixture to a gentle reflux, 2.282 g (4.8 mmol) of **1** were added. The resulting solution was boiled for 5 h, allowed to cool to room temperature and the butanol was evaporated under reduced pressure. The residue was dissolved in dichloromethane (50 ml), washed with distilled water (2 × 20 ml) and the organic phase was dried and

prepurified by elution through a neutral alumina column (about 30 g) with 100 ml of ethyl acetate. After evaporation, the resulting gum was purified by rapid chromatography [15 × 5 cm I.D column, ethyl acetate–n-hexane (3:2, v/v) as eluent to afford 1.73 g (63%) of **2** as a homogeneous gum: $[\alpha]_D$ = +3.4°, $[\alpha]_{435}$ = +11.6° (c = 2; CCl_4). ^{1}H NMR (C^2HCl_3):δ1.28 (s, 12 H, t-butyl + 1-methylisopropylidene), 1.30 (s, 3 H, 1-methylisopropylidene), 1.38 (2 s, 6 H, 2-methylisopropylidene), 3.48 (m, 2 H), 3.65–3.73 (m, 4 H), 3.74–3.99 (m, 4 H), 4.02 (dd, 2 H, H-1a/H-6a), 4.04–4.19 (m, 4 H, H-1e/H-6e + 2 H), 4.32 (m, 2 H, H-2/H-5), 6.80 (d, 1 H, H-5 of catechol), 6.90 (dd, 1 H, H-4 of catechol, 1 H), 6.93 (d, 1 H, H-2 of catechol). ^{13}C NMR (C^2HCl_3) : δ 148.30 (C-4 of catechol), 146.78 (C-2 or C-1 of catechol), 144.33 (C-1 or C-2 of catechol), 117.83 (C-3 or C-5 of catechol), 113.45 (C-5 or C-3 of catechol), 112.42 (C-6 of catechol), 108.57 (ketal), 80.61 (C-3/C-4 of mannitol), 75.11 (C-2 or C-5 of mannitol), 75.10 (C-5 or C-2 of mannitol), 72.60 (C-1 or C-6 of mannitol), 72.44 (C-6 or C-1 of mannitol), 70.76, 69.87, 69.19, 68.89 and 66.53 (crown methylenes), 34.16 (t-butyl), 31.45 (t-butyl *methyls*), 26.57 and 25.31 (isopropylidenes). Microanalysis: calculated for $C_{30}H_{48}O_{10}$, C 63.36, H 8.51; found, C 63.49, H 8.76%.

In situ coating of the crown ether 2

Commercial octadecylsilanized silica (*ca.* 2.3 g) was packed into a 250 × 4.6 mm I.D. stainless-steel column as a toluene–isopropanol–96% ethanol (1:1:1, v/v/v) slurry under a pressure of 450 bar [16]. The column was then washed with chloroform (50 ml) and methanol (50 ml) and equilibrated with 100 ml of methanol–water (55:45, v/v). To a solution of 250 mg of **2** in 55 ml of dry methanol were added 45 ml of distilled water, leading to a slight opalescence without any precipitation. Immobilization of the crown ether on the packing was carried out by pumping the above solution at 0.5 ml/min at 25°C. To achieve a regular coating, the proportion of methanol was decreased stepwise from 55% to 15% by passing 5 × 50 ml of appropriate methanolic aqueous solution at 0.5 ml/min. Finally, the column was carefully equilibrated with distilled water (300 ml at 0.1 ml/min) and the amount of crown ether immobilized on the silica (*ca.* 200 mg) was calculated from the difference between the initial 250 mg and the recovered amount of **2** after combination and evaporation of the eluted methanolic solutions.

RESULTS AND DISCUSSION

Synthesis of the crown ether 2 and its immobilization on C_{18} silica

The synthesis of crown ether **2** according to Fig. 1 allowed us to investigate the effects of the bulky *tert.*-butyl group on the catechol on chiral separation. Earlier results with related crown ethers where the 4-position on the catechol was substituted by a methyl or a nitro group led to the conclusion that a π-donor or π-acceptor group on the stationary phase could increase the separation factor of certain free aromatic amino acid enantiomers. A more lipophilic crown ether was also expected to enhance hydrophobic interactions with the alkyl groups of the silanized silica. A *tert.*-butylcatechol dipotassium salt in 25% excess was used to cyclize **1** with maximum template effect in boiling n-butanol; no starting material could be seen after 5 h of reaction by thin-layer chromatography. No attempt was made to improve the moderate 63% yield (*e.g.*, by using neutral alumina instead of silica for the final purification).
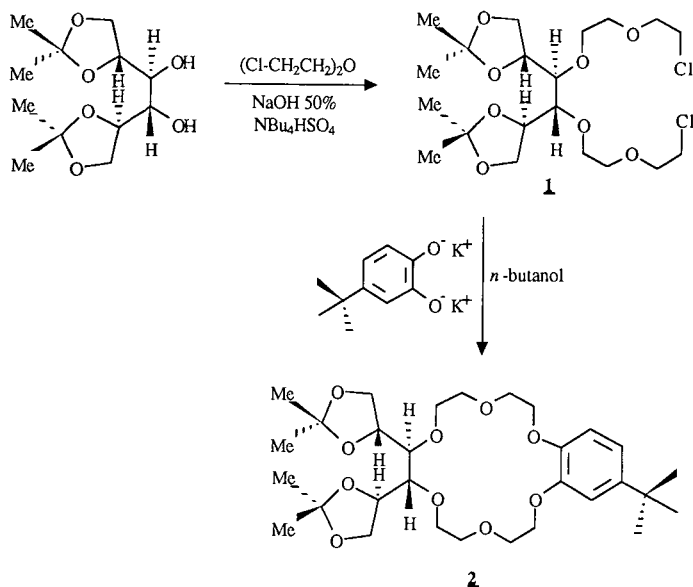
Fig. 1. Two-step synthesis of crown ether **2** from diisopropylidene-D-mannitol. Bu = Butyl; Me = methyl.

Replacement of methanol with acetonitrile as a miscible organic solvent for *in situ* coating led to very slow loading as **2** was either insufficients soluble or not retained on the C_{18} packing, depending on the proportion of acetonitrile. Attention was paid to careful equilibration of the packing before and after the dynamic coating. Reduced equilibration times or by-passing some dilution steps afforded less effective packings with the same amount of crown ether immobilized on the silica. Therefore, the lack of homogeneity in the distribution of the adsorbed crown ether throughout the column can lead to different overall thermodynamic behaviour of the resulting CSP.

Liquid–liquid extraction experiments

Chiral differentiation in complexation of the enantiomers of phenylglycine by crown ether **2** was classically measured by ^1H NMR after partitioning phenylglycine methyl ester perchlorate between water and chloroform [6]. For this purpose, 28.44 mg of **2** (0.05 mM) were dissolved in 1.0 ml of C^2HCl_3 and shaken for 1 min at 0°C with 1.0 ml of lithium perchlorate (4 M) in ^2H_2O containing 40.33 mg (0.2 mM) of racemic phenylglycine methyl ester hydrochloride. The mixture was allowed to settle for 30 min at 0°C and, the organic layer was then carefully separated, dried over lithium perchlorate, filtered and its ^1H NMR spectrum immediately taken at 27°C. The most obvious change was the splitting of the singlet of the benzylic proton on the asymmetric centre of the guest into two broad overlapping singlets around 4.95 ppm, which did not allow separated integration. The ratio of expanded aromatic signal surfaces (10 Hz/cm) up- and downfield from 7.00 ppm led to a guest/host (G/H) stoichiometry of 1.15. The splitting of the diastereomeric methyl groups of the guest into two well separated singlets at 3.73 ppm for the R and at 3.64 ppm for the S enantiomer with an approximate ratio of 63:37 in favour of the R isomer was unexpected.

In order to establish the ability of chiral recognition of **2** towards free racemic

phenylglycine, a more polar organic phase (23.1% C^2H_3CN in C^2HCl_3) was used at 0°C and led to variable results in relation to the proportion of perchloric acid initially added to the aqueous phase. An excess of acid (initial pH < 1) caused partial hydrolysis of the isopropylidene groups but also important complexation (G/H around 1). Duplication of the run with an aqueous phase of initial pH 3 did not cause any hydrolysis of ketal but only a modest extraction (G/H < 0.2). Triplication with an aqueous phase of initial pH 2 did not improve significantly the extraction rate of free phenylglycine but caused a slight measurable hydrolysis of the protective groups (around 5%). No splitting of the singlet around 4.95 ppm could be observed, even on heating the isolated and dried chloroform solution to 40°C.

In brief, host **2** was able to extract phenylglycine as a free acid or as its related methyl ester when associated with the perchlorate anion. Major changes in chemical shifts and multiplicity in the ^1H NMR spectra and unusually low solubilities in C^2HCl_3 were proof of the rapid formation of highly structured 1:1 complexes with an enantiomeric excess of at least 26% in the case of the methyl ester salt.

Chromatographic experiments

Earlier results showed that no resolution of racemic phenylglycine methyl ester could be observed with such a related crown ether immobilized on a C_{18} silica when dilute perchloric acid was used as the eluent, although a high capacity factor was measured for this compound (capacity factor, $k' = 17$). No attempt was made to study other amino acid methyl esters or different mobile phases as the final aim was the resolution of free amino acids which were tested as received, without any prederivatization.

Baseline resolution of racemic phenylglycine was obtained with pure water as the eluent with an α value of 1.92 at 0°C and 1.69 at 20°C. The R enantiomer was eluted after the S enantiomer. As a stoichiometry of 1:1 was measured for this complexation according to the results of the one-plate extraction, one can use the general equation $\Delta(\Delta G^0) = -RT \ln \alpha$ to determine the free-energy differences at the two temperatures, which were -354 and -305 cal/mol, respectively. The temperature dependance of $\Delta(\Delta G^0)$ indicates that the more stable complex (corresponding to the most retained R enantiomer) depends to a large extent on the enthalpic term, whereas the less stable complex (corresponding to the least retained S enantiomer) is mostly determined by the entropic term [17]. A maximum α value of 2.2 was measured when acetonitrile–water (20:80, v/v) was used as the eluent at 20°C. The retention time of the most retained R enantiomer was only half that measured with pure water but the peak symmetry was poorer, suggesting slower complexation–decomplexation kinetics.

The best results for basic tryptophan were obtained when water was replaced with 10^{-4} M perchloric acid in a 80:20 mixture with acetonitrile at 0°C; in this instance the capacity factors were twice as large with an almost total separation in about 49 min (see Fig. 2). In contrast, the selectivity was significantly reduced from 1.32 to 1.24. Also, the L enantiomer was eluted first.

Racemic phenylalanine gave only a single peak whether pure water, water–acetonitrile or dilute perchloric acid was used as the eluent.

Racemic p-nitro-DL-phenylalanine was totally resolved when 10^{-4} M perchloric acid–acetonitrile (80:20) was used as the eluent with an α value of 1.35 (see Fig. 3). Only partial separation was observed under neutral conditions. As for phenylglycine, the D enantiomer was eluted after the L enantiomer.

Fig. 2. Chromatographic resolution of 8 μg of racemic tryptophan on a C_{18} packing coated with *ca.* 200 mg of **2**. Mobile phase: 10^{-4} *M* perchloric acid–acetonitrile (80:20) at 0°C; flow-rate, 0.8 ml/min.
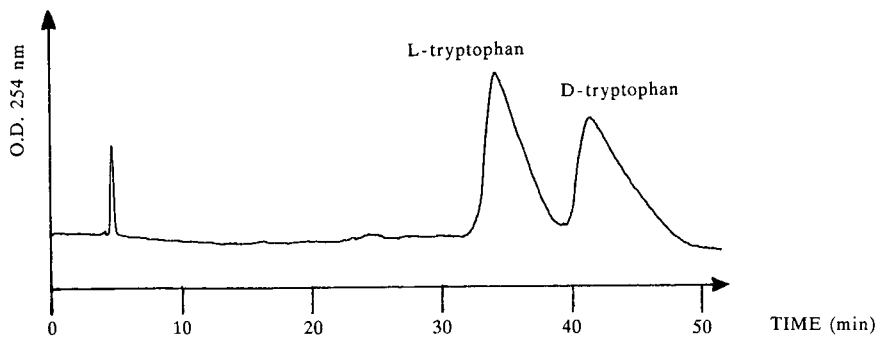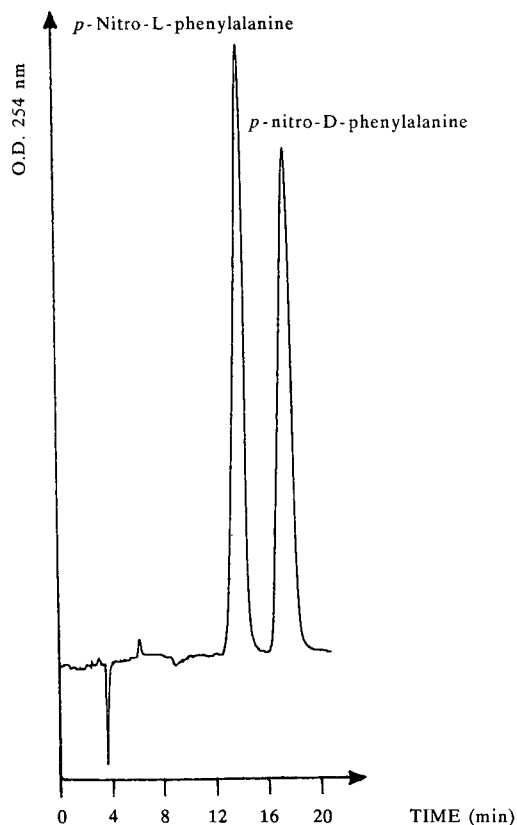

Fig. 3. Chromatographic resolution of 5 μg of racemic *p*-nitrophenylalanine on a C_{18} packing coated with *ca.* 200 mg of **2**. Mobile phase: 10^{-4} *M* perchloric acid–acetonitrile (80:20) at 0°C; flow-rate, 1.0 ml/min.

DL-4-Chlorophenylalanine was not eluted within 1 h when acetonitrile-water (25:75) was used as the mobile phase. Neither higher proportions of acetonitrile nor other organic solvents in the eluent were tested as it was feared that the crown ether could be leached out from the packing by less polar mobile phases.

CONCLUSION

It can be assumed that the magnitude of chiral recognition depends mainly on the steric bulk around the chiral centre, as the best selectivity was observed with racemic phenylglycine. If we consider the NH_3^+ group anchored in the centre and on the top of the heterotopic cavity of the host the three others groups on the stereogenic centre differ greatly in bulk, in the order $C_6H_5 > CO_2H > H$. On the other hand, π-stacking interactions are able to stabilize one of the two diastereoisomeric adsorbates; p-nitro-D-phenylalanine was perfectly separated from its antipode but not D-phenylalanine. Formation of an additional hydrogen bond between the hydrogen atom of the carboxylic acid function and one of the oxygen atoms of the ketal may provide a third useful interaction according to the classical three-point model. Lastly, an acidic medium or the addition of acetonitrile to the mobile phase favours strong pole–dipole interactions between the organic cation and the oxygens of the cavity but does not always increase selectivities. In brief, at least three semi-independent interactions are involved in the chiral recognition process.

We are now checking systematically the chromatograhic behaviour of host **2** and related compounds towards aliphatic amino acids in various mobile phases to improve our understanding of the chiral recognition process.

REFERENCES

 1 S. Einarsson, B. Josefsson, P. Möller and D. Sanchez, *Anal. Chem.*, 59 (1987) 1191.
 2 H. Franck, G. J. Nicholson and E. Bayer, *J. Chromatogr. Sci*, 15 (1977) 174.
 3 E. Gil-Av, B. Feibush and R. Charles-Siegler, *Tetrahedron Lett.*, 10 (1966) 1009.
 4 A. Dobashi and S. Hara, *J. Chromatogr.*, 349 (1985) 143.
 5 S. V. Rogozhin and V. A. Davankov, *Dokl. Akad. Nauk SSSR*, 192 (1970) 1288.
 6 E. B. Kyba, K. Koga, L. R. Sousa, M. G. Siegel and D. J. Cram. *J. Am. Chem. Soc.*, 95 (1973) 2692.
 7 L. R. Sousa, G. D. Y. Sogah, D. H. Hoffmann and D. J. Cram, *J. Am. Chem. Soc.*, 100 (1978) 4569.
 8 T. Shinbo, T. Yamaguchi, K. Nishimura and M. Sugiura, *J. Chromatogr.*, 405 (1987) 145.
 9 J. J. Kirkland and C. H. Dilks, Jr., *Anal. Chem.*, 45 (1973) 1778.
10 R. C. Helgeson, J. M. Timko, P. Moreau, S. C. Peacock, J. M. Mayer and D. J. Cram, *J. Am. Chem. Soc.*, 96 (1974) 6762.
11 K. Yamamoto, T. Kitsuki and Y. Okamoto, *Bull. Chem. Soc. Jpn.*, 59 (1986) 1269.
12 J.-P. Joly and B. Gross, *Tetrahedron Lett.*, 30 (32) (1989) 4231.
13 W. C. Still, M. Kahn and A. Mitra, *J. Org. Chem.*, 43 (1978) 2923.
14 J.-L. Debost, J. Gelas and D. Horton, *J. Org. Chem.*, (1983) 1381.
15 P. Di Cesare and B. Gross, *Synthesis*, (1979) 458.
16 N. Moll and J.-P. Joly, *J. Chromatogr.*, 405 (1987) 347.
17 E. P. Kyba, J. M. Timko, L. J. Kaplan, F. de Jong, G. W. Gokel and D. J. Cram, *J. Am. Chem. Soc.*, 100 (1978) 4555.

Note

Liquid chromatographic determination of felypressin using a column-switching technique and post-column derivatization

MATS SVENSSON* and KERSTIN GRÖNINGSSON

Pharmaceutical R&D, Analytical Department, Astra Pain Control AB, S-151 85 Södertälje (Sweden)

(First received March 23rd, 1990; revised manuscript received June 27th, 1990)

Felypressin (Fig. 1), which is a nonapeptide with a vasopressoric effect, is often present in odontological local anaesthetic formulations.

In the pharmacopoeias [1,2], felypressin is determined by bioassay, measuring the increase in blood pressure of rats. Felypressin-like nonapeptides have also been determined by high-performance liquid chromatography (HPLC) with UV detection at 210–220 nm [3,4]. A chromatographic method for the determination of oxytocin has also been described [5]. This method includes an on-line preconcentration and reversed-phase chromatography with post-column derivatization and fluorescence detection.

In a pharmaceutical formulation containing about 0.5 μmol/l (0.5 μg/ml) of felypressin and *ca.* 0.1 mol/l (30 mg/ml) of the local anaesthetic prilocaine hydrochloride (Fig. 2), felypressin has been determined after removal of prilocaine by extraction, precolumn derivatization with fluorescamine and fluorescence detection after reversed-phase chromatography [6]. As this method includes an extraction step, precolumn derivatization and manual injection, it is time consuming and not easily automated.

From studies of the retention behaviours of felypressin and prilocaine on different reversed-phase stationary phases, an automated method, including a column-switching technique and post-column derivatization, has been developed. In this method, felypressin is retained on a short column (extraction column), while other irrelevant components (*e.g.*, large amounts of prilocaine) are eluted. The final purification of felypressin is performed on a second column (separation column). Fluorescence detection after post-column derivatization with fluorescamine gives a detection limit of 0.6 ng (0.6 pmol).
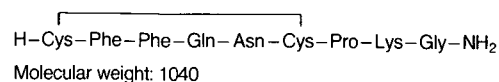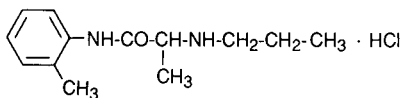
H–Cys–Phe–Phe–Gln–Asn–Cys–Pro–Lys–Gly–NH$_2$

Molecular weight: 1040

Fig. 1. Sequence of felypressin.

Molecular weight: 256.8

Fig. 2. Structure of prilocaine hydrochloride.

EXPERIMENTAL

Apparatus

The LC equipment consisted of an SP 8770 pump (Spectra-Physics, San Jose, U.S.A.) to deliver eluent I, an LDC/Milton Roy Constametric III pump (Laboratory Data Control, Riviera Beach, FL, U.S.A.) to deliver eluent II, both at a flow-rate of 1.0 ml/min, and an LDC/Milton Roy 4711 pump (Laboratory Data Control) to deliver the post-column reagent, at a flow-rate of 0.25 ml/min. The samples and standards were injected with a Spectra-Physics SP 8780 XR autosampler and the vials were obtained from Chromacol (London, U.K.).

The eluate was mixed with the reagent in a 5 m × 0.5 mm I.D. knitted Teflon tube [7] and detected with a RF-535 fluorescence detector (Shimadzu, Kyoto, Japan) with an excitation wavelength of 390 nm and an emission wavelength of 470 nm. A Shimadzu SPD-6A UV detector set at 210 nm was used in testing the different stationary phases and to monitor the effluent from the extraction column.

An automated switching valve (Waters Assoc. Milford, MA, U.S.A.), controlled by a Spectra-Physics SP 4270 integrator was used to perform the column-switching procedure. The fluorescence was recorded with a Nelson Analytical (Cupertino, CA, U.S.A.) Model 600 reintegration data system. UV absorbance was recorded on a Spectra-Physics SP 4270 integrator.

Stationary phases

The stationary phases and columns tested were a LiChrospher 60 RP-Select B (150 × 4.0 mm I.D.) stainless-steel column with 5-μm particles, a Superspher 60 RP-8e (50 × 4.0 mm I.D.) cartridge column with 4-μm particles, both from E. Merck (Darmstadt, F.R.G.), a Supelcosil LC-18 DB (150 × 4.6 mm I.D.) stainless-steel column with 5-μm particles (Supelco, Bellefonte, PA, U.S.A.), a Nucleosil C_{18} (125 × 4.0 mm I.D.) stainless-steel column with 3-μm particles (Macherey, Nagel & Co., Düren, F.R.G.) and a Zorbax-CN (150 × 4.6 mm I.D.) stainless-steel column with 5-μm particles (DuPont, Wilmington, DE, U.S.A.). The extraction column used in the method was a Superspher 60 RP-8 (25 × 4.0 mm I.D.) cartridge column with 4-μm particles (E. Merck).

Chemicals

The eluents used were prepared from acetonitrile and phosphate buffers of different pH (ionic strength 0.05 or 0.1), all degassed with helium for at least 10 min before use.

Acetonitrile was of chromatographic purity grade and all other chemicals were

TABLE I

STEPS IN THE CHROMATOGRAPHIC PROCEDURE

Step[a]	Time (min)	Eluent No.[b]	Column	Dimensions (length × I.D.) (mm)
1	0–14	I	Superspher 60 RP-8	25 × 4
2	14–23	II	Superspher 60 RP-8	25 × 4
			+ Superspher 60 RP-8e	50 × 4
3	23–30	I	Superspher 60 RP-8	25 × 4

[a] 1 = removal of prilocaine; 2 = chromatography of felypressin; 3 = re-equilibration of the extraction column (see Fig. 3).

[b] I = acetonitrile–phosphate buffer (pH 6.0) (12:88); II = acetonitrile–phosphate buffer (pH 6.0) (20:80).

of analytical-reagent grade and were obtained from E. Merck.

Fluorescamine was obtained from Fluka (Buchs, Switzerland) and was dissolved in acetonitrile at a concentration of 0.30 g/l. This reagent also contained 0.1% (v/v) of Brij-35 (Technicon, Tarrytown, NY, U.S.A.).

Felypressin was obtained as a concentrated solution containing 25 IU/ml (0.48 g/l), supplied by Sandoz (Basle, Switzerland). In the described method, a felypressin stock standard solution [6] containing 5 mg/l was used. Prilocaine hydrochloride was obtained from Astra (Södertälje, Sweden). When testing the different stationary phases, a solution containing 36 mg/l of felypressin and 9.6 mg/l of prilocaine hydrochloride was prepared in deionized water. Citanest Octapressin injection solution was obtained from Astra.

Method

The assay of felypressin in the pharmaceutical formulation (Citanest Octapressin) was performed by the injection of undiluted sample into the chromatographic system. The different steps in the chromatographic procedure are described in Table I and a schematic diagram is given in Fig. 3.

The volumes of samples and standards injected were 20 μl and the flow-rates for both eluents were 1.0 ml/min. Detection was effected by post-column derivatization (flow-rate 0.25 ml/min) with fluorescamine and fluorescence detection (λ_{ex} = 390 nm, λ_{em} = 470 nm). For quantification, peak areas were compared with a calibration graph [0.3–0.7 mg/l of felypressin dissolved in 0.9% (w/v) sodium chloride solution].

RESULTS AND DISCUSSION

Choice of chromatographic system

On five different stationary phases (two C_{18}, two C_8 and one CN), the capacity factors (k') of felypressin and prilocaine were determined with variation of the pH between 3 and 7, using an eluent containing 20% (v/v) of acetonitrile. For the octadecyl- and octyl-bonded phases, the increase in k' for prilocaine was more pronounced than that for felypressin between pH 6 and 7, *i.e.*, the separation factor (α) increases. In this pH range felypressin was eluted first. On the nitrile phase, the retention order
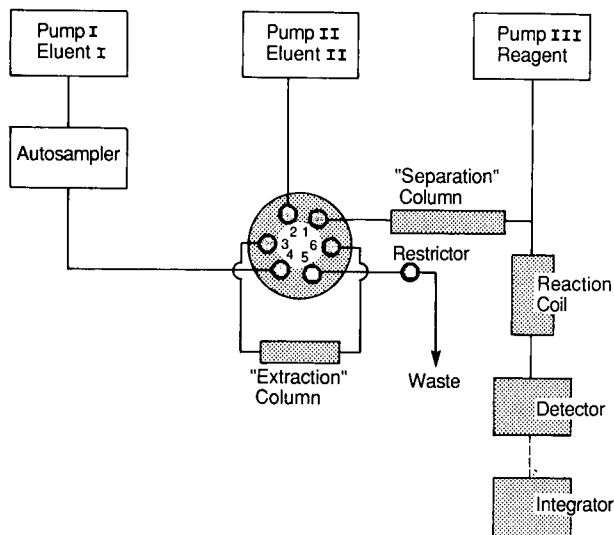
Fig. 3. Schematic diagram of the chromatographic system.

was changed and k' was less affected by pH. As the results were both unpredictable and irreproducible, no further experiments were done on this phase.

When varying the concentration of acetonitrile in the eluent, Superspher 60 RP-8e was selected as it gave the highest α value and good peak symmetry. Felypressin was more sensitive than prilocaine to variations in acetonitrile concentration and the retention order changed at a concentration about 18% (v/v). The effect of acetonitrile concentration is shown in Fig. 4. The large differences in the k' values of prilocaine and felypressin at concentrations below 14% (v/v) were utilized to remove prilocaine by the column-switching technique. Thus, felypressin can be extensively retained on a short extraction column, while e.g., large amounts of prilocaine can be removed as waste (Fig. 5).

By a subsequent increase in the acetonitrile concentration, felypressin can be eluted and chromatographed on a second column. When using the chromatographic procedure described in Table I, clean chromatograms and symmetrical peaks are obtained for both samples and standards (Fig. 6).

Detection

Detection was performed by post-column derivatization with fluorescamine and fluorescence detection. As this reagent reacts only with primary amines, a high selectivity is achieved and a detection limit of 0.6 pmol (signal-to-noise ratio $= 3$) is obtained. The reaction took place in a 5 m $\times$ 0.5 mm I.D. knitted Teflon tube [7]. To avoid the formation of bubbles when mixing the reagent and eluent, Brij-35 was included in the reagent [5].

Usually a pH above 8 is used for the reaction of fluorescamine with peptides. On increasing the reaction pH from 6 to 8, no differences were observed. This favours the use of pH 6 (eluent pH), as a higher pH requires an additional pump and leads to dilution of the sample.
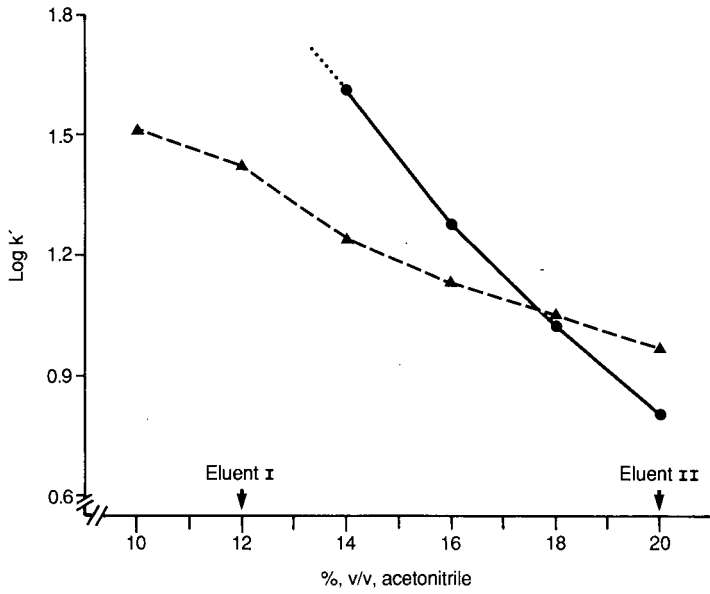
Fig. 4. Influence of eluent composition on the capacity factors of (●) felypressin and (▲) prilocaine. Eluent, acetonitrile in phosphate buffer (pH 6.0); ionic strength, 0.05; column, Superspher 60 RP-8e (50 × 4 mm I.D.), 4-μm particles.
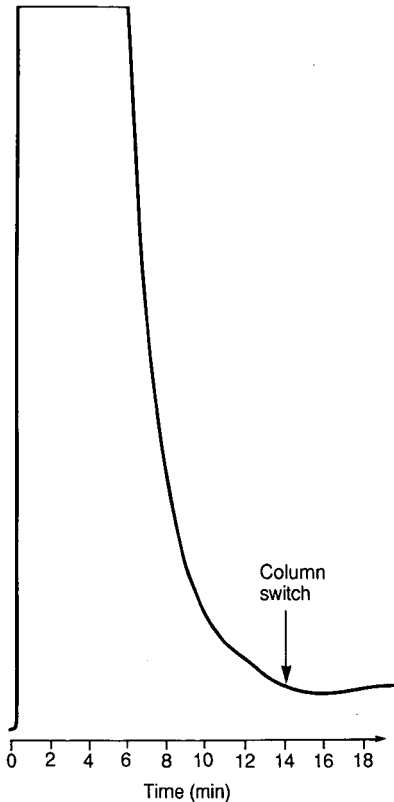
Fig. 5. UV trace (210 nm) from the extraction column. Eluent No. I (see Table I).
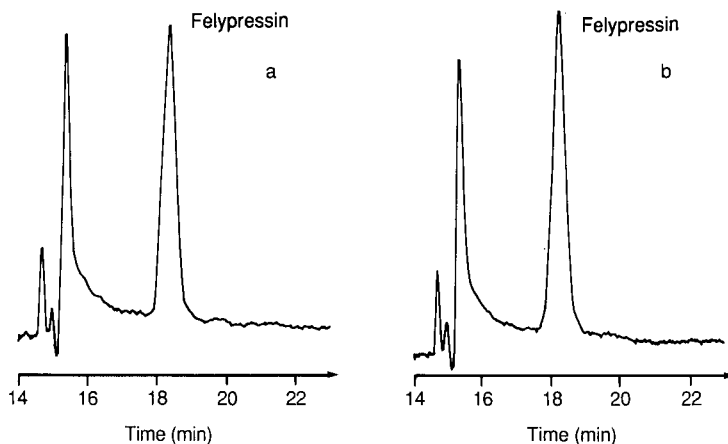
Fig. 6. Chromatograms after column switching of (a) standard and (b) sample solutions. About 10 ng of felypressin were injected.

Validation data

A calibration graph from five standard solutions, corresponding in concentration to 20–150% of the labelled amount of felypressin in a sample, was constructed. The correlation coefficient, r, was found to be 0.9998.

Six simulated samples were prepared and assayed according to the method. The mean recovery was found to be 101.8%.

The reproducibility (including day-to-day variations) of the method was 1.7% and 1.3% (relative standard deviation) for sample and standard, respectively. This precision was obtained only if special precautions to avoid adsorption to glass and plastic surfaces had been taken. Rinsing all glass and plastic ware with 1 mol/l acetic acid and deionized water and diluting all standards with 0.9% (w/v) sodium chloride solution minimize adsorption.

The selectivity of the method was tested on two closely related peptides, lypressin and ornipressin. Neither of them was detected, hence the method can be considered to be selective for felypressin. The proposed method is stability indicating, as degradation products are separated from intact felypressin.

As seen in Fig. 6, the peak symmetry and peak width from sample and standard were identical. After *ca.* 100 injections of a sample, the peak width was increased. Consequently, the extraction column should then be replaced.

CONCLUSION

An automated system which reduces sample handling to a minimum has been developed for the determination of felypressin in a pharmaceutical formulation. The running time with the proposed method is 30 min, including re-equilibration of the extraction column. Although this is a fairly long time, pre-extraction and precolumn derivatization procedures are eliminated [6].

REFERENCES

1 *U.S. Pharmacopeia XXII Revision*, U.S. Pharmacopeial Convention, Rockville, MD, 1989, p. 1443.
2 *British Pharmacopoeia 1988*, Vol. 2, H.M. Stationery Office, London, 1988, p. A173.
3 K. Krummen and R. W. Frei, *J. Chromatogr.*, 132 (1977) 429.
4 K. Krummen, F. Maxl and F. Nachtmann, *Pharm. Technol. Int.*, (1979) 37.
5 D. S. Brown and D. R. Jenke, *J. Chromatogr.*, 410 (1987) 157.
6 K. Gröningsson and M. Widahl-Näsman, *J. Chromatogr.*, 291 (1984) 185.
7 H. Engelhardt and U. D. Neue, *Chromatographia*, 15 (1982) 403.

Note

Separation and determination of Z and E isomers of dodecyl urocanate

MARIE CARMEN MONJE, ARMAND LATTES and MONIQUE RIVIÈRE*

Laboratoire IMRCP, URA CNRS 470, Université Paul Sabatier, 118 route de Narbonne, F-31062 Toulouse Cedex (France)

(First received March 6th, 1990; revised manuscript received June 26th, 1990)

(E)-Urocanic acid, a major metabolite of histidine [1,2] and a naturally occuring sunscreen, accumulates in the skin and is eventually excreted in sweat [3,4]. This compound, which undergoes $E \rightleftharpoons Z$ photoisomerization, is one of the major UV light absorbers in the epidermis [5,6]. Recent studies, however, have revealed additional photobiological properties, *i.e.*, photochemical binding to DNA and photoimmuno-suppressive activity for the Z isomer [7–10]. These observations rule against the use of urocanic acid as a sunscreen and led us to undertake a study of urocanic acid long-chain esters.
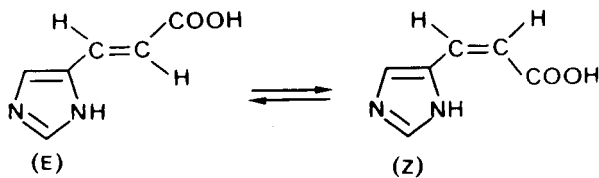
The separation of the E and Z isomers of urocanic esters has a twofold interest: photochemical, as it is necessary for the study of $E \rightleftharpoons Z$ isomerization and of the possible photocycloadditions; and biological, for the study of the influence of the configuration on the immunosuppressive properties.

Although separations of urocanic acid [11–14] and methyl urocanate isomers have been reported [15], those of for long-chain esters have not. We therefore set out to separate the E and Z isomers of n-dodecyl urocanate and to determine the proportions of mixtures of these compounds by chromatography.

EXPERIMENTAL

Instrumentation and procedure

Photoisomerization reactions were carried out in a Rayonet-type reactor (New England Ultraviolet) at 254 nm using 10-ml quartz tubes on a rotating rack.

Thin-layer chromatography (TLC) was done on 2.5 × 7.5 cm silica gel 60 Å plates (250-μm layer) (Whatman) with UV detection at 254 nm. The solvent was chloroform–methanol (95:5, v/v).

A 20 × 2 cm I.D. column of silica gel (250–400 mesh) (Fluka) was used for the preparative separation of the Z isomer from a 160-mg mixture of Z and E isomers (Z:E ≈ 75:25) using chloroform–methanol (95:5, v/v) as eluent. The elution was followed by TLC. The first isomer appeared after 75 ml of eluent and was pure in the twelve following 3.5 ml-fractions collected.

High-performance liquid chromatography (HPLC) was performed using a system consisting of a Millipore Waters unit (Model 510) with an automatic gradient controller, a Waters Assoc. 990 photodiode array detector and a Waters Assoc. μPorasil (10 μm) column (30 cm × 4 mm I.D.). The dectection wavelength was set at 310 nm, where both isomers absorb. The eluent was chloroform–ethanol (HPLC grade) (85:15, v/v) after having been filtered over Millipore membranes (0.22 μm). The flow-rate was of 0.7 ml/min.

UV spectra were recorded on a Hewlett-Packard HP 8451 A spectrophotometer. IR spectra were recorded on an FT-IR Perkin-Elmer 1760 X spectrophotometer. NMR spectra were recorded in deuterochloroform on a Bruker AC 80 apparatus.

Chemicals

(E)-Dodecyl urocanate was obtained by esterification [16] of urocanic acid (Aldrich). Its purity was checked by TLC (R_F = 0.21).

Photoisomerization was achieved by a 2-h irradiation, at 254 nm of a $6.5 \cdot 10^{-3}$ mol l^{-1} solution of 160 mg of (E)-dodecyl urocanate in 80 ml of butanol at 35°C.

After having evaporated the solvent, the separation of the Z isomer was performed by colum chromatography using the procedure described before. The twelve fractions containing the isomer eluted first were evaporated to give 110 mg of a solid of m.p. 61°C (uncorrected). This compound obtained in *ca.* 90% yield, was identified as the Z isomer by TLC [R_F (E) = 0.21; R_F (Z) = 0.44] and ^{1}H NMR spectroscopy: –CH=CH–COO(CH$_2$)$_{11}$CH$_3$: E isomer, δH_α = 6.73 ppm, δH_β = 7.58 ppm, $J(H_\alpha,H_\beta)$ = 16 Hz; Z isomer, δH_α = 5.60 ppm, δH_β = 6.83 ppm, $J(H_\alpha,H_\beta)$ = 13 Hz.

The UV spectra were recorded in butanol: E isomer, λ_{max} = 292 nm, ε = 19 200 l mol^{-1} cm^{-1}; Z isomer, λ_{max} = 302 nm, ε = 17 100 l mol^{-1} cm^{-1}.

The IR spectra were recorded in carbon tetrachloride: E isomer, ν_{NH}(free) = 3470 cm^{-1} (sharp band), ν_{NH}(bonded) = 3200–3425 cm^{-1} (intermolecular); Z isomer, ν_{NH}(bonded) = 3258 cm^{-1} (intramolecular hydrogen bond).

RESULTS AND DISCUSSION

The HPLC separation of an artificial mixture of (Z)- and (E)-dodecyl urocanate is shown in Fig. 1. Under the conditions described above, the elution times were 15.25 min and 6.75 min for the Z and E isomers, respectively. The weaker retention of the Z
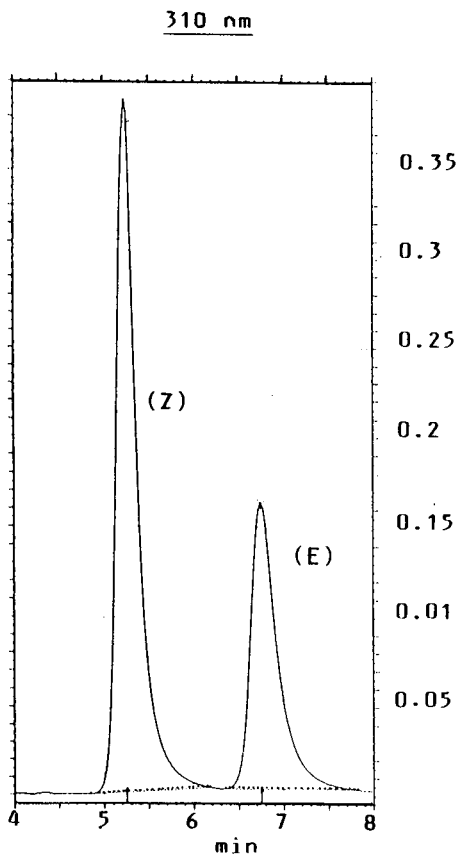
310 nm

Fig. 1. HPLC separation of an artificial mixture of (Z)- and (E)-dodecyl urocanate isomers. Column, μPorasil (10 μm) (30 cm × 4 mm I.D.); detection, absorption at 310 nm; mobile phase, chloroform–ethanol (85:15); flow-rate, 0.7 ml/min; temperature = 20°C; injection: 15 μl of an approximately 10^{-3} mol l^{-1} solution. Values on the y-axis are absorbance units.

isomer is probably related to the strong intramolecular hydrogen bond in this molecule, which is readily seen in infrared spectroscopy. This bond, already reported for methyl urocanate [17], is not disrupted in the long-chain ester.
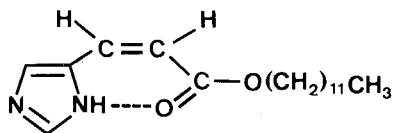
The peaks obtained in HPLC were assigned by analysing the previously identified pure isomers separately. Quantitative HPLC was then undertaken. Calibration was performed by plotting known concentrations of each isomer against peak area. Unlike urocanic acid [18], the isomers did not show a deviation from the Beer–Lambert law in the concentration range tested (seven concentrations from $4 \cdot 10^{-5}$ to

$5 \cdot 10^{-3}$ mol l^{-1}). This HPLC method was tested using two artificial mixtures of Z and E isomers, whose proportions were measured by weighing and chosen in the range expected in photochemical experiments ($45\% \leqslant Z \leqslant 75\%$). The results obtained, given in Table I, illustrate the precision of the method.

TABLE I

TEST OF HPLC ASSAY OF (E) AND (Z)-DODECYL UROCANATE

Mixture	$Z:E$ (weighing)	$Z:E$ (HPLC)^a
1 ($Z:E \approx 3$)	3.33 ± 0.03	3.35 ± 0.02
2 ($Z:E \approx 1$)	0.92 ± 0.01	0.91 ± 0.01

^{a} Values $\pm$ S.D. ($n = 4$).

Having confirmed the precision of the HPLC analysis for these compounds, we set out to analyse the mixture obtained after a 2-h irradiation of a $6.5 \cdot 10^{-3}$ mol l^{-1} solution of (e)-dodecyl urocanate in butanol. Eight tubes were used in the rotating rack and analysed separately (two measurements for each tube) by HPLC and ^{1}H NMR spectroscopy. The following results were obtained: $Z:E$ (HPLC) between 2.58 (72.1:27.9) and 2.62 (72.4:27.6) and $Z:E$ (^{1}H NMR) between 2.57 (72:28) and 3.00 (75:25). The results obtained by the two methods are close, but those given by HPLC are more reproducible.

We therefore decided to use HPLC to determine the photostationnary state of the photoisomerization of (E)-dodecyl urocanate in butanol ($6.5 \cdot 10^{-3}$ mol l^{-1}), and found that it was reached after 1 h of irridiation and corresponded to the ratio $Z:E = 2.6 \pm 0.02$.

CONCLUSION

The preparative method for the separation of (Z)- and (E)-dodecyl urocanate described has proved to be a readily applicable technique that allows the rapid production of large amounts of these two isomers. This will enable us to continue the study of the biological activities of these compounds, for instance the immunosuppression phenomenon. The quantitative analysis by HPLC of E and Z isomer mixtures greatly facilitates the study of the photoisomerization of dodecyl urocanate in a wide range of solvents and concentrations.

REFERENCES

1 A. H. Mehler and H. T. Tabor, *J. Biol. Chem.* 201 (1953) 775.
2 J. H. Anglin, Jr., D. H. Jones, T. Bever, Ph. Dand and M. A. Everett, *J. Invest. Dermatol.*, 46 (1966) 34.
3 H. P. Baden and M. A. Pathak, *J. Invest. Dermatol.*, 48 (1967) 11.
4 A. Zenisek and J. A. Kral, *Biochim. Biophys. Acta*, 12 (1953) 479.

5 J. H. Anglin Jr., *Cosmet. Toiletries*, 91 (1976) 53.

6 A. Zenisek, J. M. Hais and E. Marklova, *Parfums Cosmet. Aromes*, 24 (1978) 79.

7 H. Morrisson, B. Mauclair, R. N. Deibel, G. Pandey and W. M. Barid, *Photochem. Photobiol.*, 41 (1985) 251.

8 H. Morrisson, C. Bernasconi and G. Pandey, *Photochem. Photobiol.*, 38 (1983) 23.

9 E. C. De Fabo, F. P. Noonan, M. Fisher, J. Burns and H. Kaeser, *J. Invest. Dermatol.*, 80 (1983) 319.

10 T. G. Hamiott-Smith and W. J. Halliday, *Clin. Exp. Immunol.*, 82 (1988) 174.

11 H. Morrisson, D. Avnir and Th. Zarella, *J. Chromatogr.*, 183 (1980) 83.

12 J. C. Caron, B. Martin and B. Shroot, *J. Chromatogr.*, 230 (1980) 125.

13 W. Schwartz and Klaus Langer, *J. Chromatogr.*, 310 (1984) 188.

14 H. Norval, T. J. Simpson, E. Bardshiri and S. E. H. Howie, *Photochem. Photobiol.*, 49 (1989) 633.

15 H. Kimoto and S. Fujii, *J. Org. Chem.* 49 (1984) 1060.

16 M. C. Monje, A. Lattes and M. Rivière, *Bull. Soc. Chim. Fr.*, 127 (1990) 292.

17 R. Quinn, J. Mercer-Smith, J. N. Burstyn and J. Selverstone Valentine, *J. Am. Chem. Soc.*, 106 (1984) 4136.

18 H. Morrisson, D. Avnir, C. Bernasconi and G. Fagun, *Photochem. Photobiol.*, 32 (1980) 711.

Note

Rapid quantitative analysis of headspace components of green olive brine

ALFREDO MONTAÑO*, ANTONIO H. SANCHEZ and LUIS REJANO

Instituto de la Grasa y sus Derivados (CSIC), Apartado 1078, 41012 Seville (Spain)

(First received April 18th, 1990; revised manuscript received June 14th, 1990)

In order to study the complex biochemical transformations which take place during the controlled fermentation of vegetables, it is important to have analytical methods available that allow the determination of the main compounds involved. The sugars and the majority of organic acids (fructose, glucose, mannitol, sucrose, lactic acid, acetic acid, malic acid) can be satisfactorily determined by high-performance liquid chromatography [1]. Ethanol, another important component, can also be determined by this technique [2] but, owing to its volatility, gas chromatography (GC), and particularly the headspace technique (HSGC), is more appropriate [3]. This paper describes a simple, rapid method for the simultaneous determination of ethanol and other volatile components in brines of fermented vegetables by HSGC. The study was centred on green table olives, which, together with cucumbers, cabbages and peppers, account for the largest volume of vegetables and fruits commercially brined and fermented in the West [4].

EXPERIMENTAL

Reagents

Analytical-reagent grade anhydrous sodium sulphate (Panreac, Montplet and Esteban, Barcelona, Spain) was used as ionic reagent. Standard substances were obtained from Merck (Darmstadt, F.R.G.) and Fluka (Buchs, Switzerland). An aqueous solution containing 5.682 mg/ml of dioxane (Fluka) was used as an internal standard.

Preparation of the sample

Recovery and reproductibility studies were carried out with a fermentation brine from pickled green olives, prepared in our Department using the classical elaboration process [5]. At the time of this study, 6 months after brining, the latter had pH 4.50, free acidity (expressed as lactic acid) 0.60% and sodium chloride content 5.8%. Brine (1 ml) and internal standard solution (0.2 ml) were added to a 20-ml vial containing 1.0 g of anhydrous sodium sulphate. This ionic reagent was used to in-

crease the vapour pressure of volatile compounds in the brine. The vial was closed with a rubber stopper and aluminium cap and immediately placed in a thermostated bath at 60°C for 15 min. Next, a 0.1–0.2-ml sample of vapour was removed through the stopper, using a 0.5-ml gas-tight syringe (Hamilton 1750), and returned to the vial. This operation was repeated three more times, and finally the sample was injected into the gas chromatograph. After each injection, and immediately before making the next, the syringe was cleaned by removing the plunger and passing a current of nitrogen through the interior, at the same time warming the exterior with a hand drier.

Chromatographic conditions

A Perkin-Elmer 3920B gas chromatograph equipped with a flame ionization detector was used. A Supelcowax 10 fused-silica capillary column (30 m × 0.53 mm I.D., 1.0-μm film thickness, Supelco 2-5301) was used for analytical separations. The column was programmed from 50°C (held for 4 min) to 120°C at 8°C/min. The injection port was maintained at 150°C and the detector at 200°C. Nitrogen was used as carrier gas at a flow-rate of 9 ml/min. The chromatograms and peak areas were obtained from a Hewlett-Packard Model 3394A recording integrator.

Peak identification

The major peaks on the chromatograms were identified first by comparison of their retention times with those of authentic standards. The assignments were later confirmed using the syringe reaction technique of Hoff and Feit [6].

Quantification

The response factors of acetaldehyde, methanol, ethanol, 2-butanol and n-propanol with respect to the internal standard were determined from individual aqueous solutions at the following concentrations: acetaldehyde 0.187, methanol 8.656, ethanol 1.015, 2-butanol 0.329 and n-propanol 1.649 mg/ml. The same procedure was used as for the brine samples, placing 1 ml of solution in the 20-ml vial. The numerical values of the individual response factors (*RF*) determined from a minimum of three injections of each standard were 2.157, 0.329, 0.990, 4.038 and 2.238 for acetaldehyde, methanol, ethanol, 2-butanol and n-propanol, respectively, where

$$RF = AW'/WA'$$

A and *A'* are the total peak areas of component and internal standard, respectively, and *W* and *W'* are the weights of component (mg) and internal standard (mg) in the vial.

RESULTS AND DISCUSSION

Analysis of the headspace of the fermentation brine of pickled green olives as described gave the chromatogram shown in Fig. 1. The major peaks were identified as acetaldehyde, methanol, ethanol, 2-butanol and n-propanol. The presence of ethanol and acetaldehyde in olive brines has already been demonstrated by Fleming *et al.* [7] using HSGC–mass spectrometry. They also identified methyl sulphide and 2-butanol,
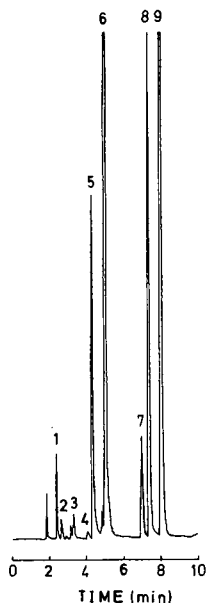
Fig. 1. Headspace gas chromatogram of fermentation brine from pickled green olive. Peaks: 1 = acetalde-hyde; 2 = methyl sulphide; 3 = acetone; 4 = ethyl acetate; 5 = methanol; 6 = ethanol; 7 = 2-butanol; 8 = *n*-propanol; 9 = dioxane (internal standard). See text for conditions.

although the latter only in "abnormal" brines. In previous studies, acetone and ethyl acetate were also identified, based on their retention times on three packed columns of different polarity [8]; these compounds were also found by Vlahov *et al.* [9] in brines of pickled green olives and natural black olives.

The wide-bore capillary column used in this work provides sharper and better separated peaks than a packed column and the problem of rapid loss of efficiency with packed columns [8] is eliminated.

The recoveries of different known amounts of compounds added to the fermentation brine of pickled green olives are given in Table I. The graph obtained on plotting the values added against those recovered was linear in all instances with coefficients of determination (R^2) of 0.992, 0.998, 0.999, 0.997 and 0.999 for acetalde-hyde, methanol, ethanol, 2-butanol and *n*-propanol, respectively. The precision of the method was measured from eight consecutive analyses of the same brine and the results are given in Table II.

The results were obtained using the individual response factors indicated under *Quantification*. We found that these factors did not show significant statistical differ-ences ($P < 0.05$) with respect to those calculated from a standard mixture of the five components. Consequently, quantification can be effected without any problems from such mixtures, as is usual in multi-component analyses of liquid samples by GC.

We conclude that the method described here permits the simultaneous, repro-ducible and accurate determination of the main volatile compounds in the headspace (aroma) of a fermentation brine of green olives. The advantages of this method are its

TABLE I

RECOVERY OF KNOWN AMOUNTS OF METHANOL, ETHANOL, n-PROPANOL, ACETALDEHYDE AND 2-BUTANOL ADDED TO GREEN OLIVE BRINE

Methanol		Ethanol		n-Propanol		Acetaldehyde		2-Butanol	
Added (mg/ml)	Recovery[a] (%)	Added (mg/ml)	Recovery[a] (%)	Added (mg/ml)	Recovery[a] (%)	Added (µg/ml)	Recovery[a] (%)	Added (µg/ml)	Recovery[a] (%)
0.32	113.4	0.34	99.6	0.15	99.9	10.3	103.9	32.9	112.5
0.64	96.4	0.56	95.6	0.29	108.7	18.7	101.0	68.8	104.7
1.08	103.4	1.02	103.9	0.43	113.9	37.8	89.7	99.6	98.4
2.17	104.5	2.02	102.7	0.61	114.5	67.2	101.3	199.2	104.9
	104.4 ± 2.6^{b}		100.4 ± 1.4^{b}		109.2 ± 2.9^{b}		99.0 ± 3.0^{b}		105.1 ± 3.1^{b}

[a] Each value is the mean of duplicate analyses.
[b] Mean ± standard error.

TABLE II

REPRODUCIBILITY OF THE HSGC METHOD

Compound	Concentration^a (mg/l)	Relative standard deviation (%)
Acetaldehyde	12.3 ± 1.1	8.9
Methanol	578.8 ± 12.1	2.1
Ethanol	523.1 ± 16.0	3.1
2-Butanol	16.4 ± 0.9	5.5
n-Propanol	154.7 ± 7.5	4.8

^{a} Mean $\pm$ S.D. of eight determinations using the same brine.

simplicity (sample preparation is minimal) and rapidity (the chromatographic analyses time is less than 10 min). In addition, because the matrix effects are similar, there should be no problem in applying this method to brines of black olives or other fermented vegetable products, such as cucumbers, cabbages and capers.

REFERENCES

1 R. F. McFeeters, R. L. Thompson and H. P. Fleming, *J. Assoc. Off. Anal. Chem.*, 67 (1984) 710.
2 R. Pecina, G. Bonn, E. Burtscher and O. Bobleter, *J. Chromatogr.*, 287 (1984) 245.
3 C. L. Mendenhall, J. MacGee and E. S. Green, *J. Chromatogr.*, 190 (1980) 197.
4 H. P. Fleming and R. F. McFeeters, *Food Technol.*, 35 (1981) 84.
5 M. J. Fernández-Diez, in H. J. Rehm and G. Reed (Editors), *Biotechnology*, Vol. 5, Verlag Chemie, Weinheim, 1983, Ch. 7, p. 379.
6 J. E. Hoff and E. D. Feit, *Anal. Chem.*, 36 (1964) 1002.
7 H. P. Fleming, J. L. Etchells and T. A. Bell, *J. Food Sci.*, 34 (1969) 419.
8 A. Montaño, unpublished results.
9 G. Vlahov, V. Marsilio and A. Brighigna, *Ann. Ist. Sper. Elaiotec.*, X (1984–1987).

Note

Capillary tube isotachophoretic separation of niacin derivatives

SHUNITZ TANAKA, TAKASHI KANETA and HITOSHI YOSHIDA*

Department of Chemistry, Faculty of Science, Hokkaido University, Sapporo 060 (Japan)

and

HIROKAZU OHTAKA

Department of Polymer Science, Faculty of Science, Hokkaido University, Sapporo 060 (Japan)

(First received February 12th, 1990; revised manuscript received May 23rd, 1990)

Niacin (nicotinic acid is a vitamin widely distributed in biological materials and food and is converted into the coenzyme nicotinamide adenine dinucleotide by biological reactions *in vivo* [1]. Niacin has many structural derivatives, some of which are converted into niacin *in vivo* and others being involved in the biosynthesis of niacin [2]. Some niacin derivatives have been determined by high-performance liquid chromatography or microbioassay [3]. However, a practical method for the simultaneous determination of various niacin derivatives is desirable in order to elucidate the metabolic system of niacine derivatives *in vivo*.

Capillary tube isotachophoresis (CITP) is an excellent separation method for many ionic compounds. Biologically important substances such as vitamins [4], amino acids [5,6] and nucleotides [7,8] have been separated and determined by CITP. Niacin and its derivatives all have a pyridine ring in their structure and act as weak bases. In order for niacin derivatives to migrate and be detected in CITP, it is necessary to protonate the pyridine ring so that they migrate as cationic species (pyridinium ion).

In this paper, the migration behaviour of niacin derivatives is described. Migration systems for some niacin derivatives with small mobilities were investigated. By selecting the optimum leading and terminating electrolytes, the niacin derivatives of weak bases were sufficiently protonated for migration. Six niacin derivatives could be separated using 40 mM potassium acetate as the leading electrolyte and 10 mM glycine as the terminating electrolyte.

EXPERIMENTAL

Apparatus

A Model IP-3A capillary tube isotachophoretic analyser (Shimadzu, Kyoto, Japan), equipped with a potential gradient detector and a column system consisting of

a PTFE preseparation capillary (80 × 0.7 mm I.D.) and a fused-silica analytical capillary column (170 × 0.2 mm I.D.), was used. The current was 15–60 μA after migration at 360 μA for 3–10 min. The capillary tube was filled with the leading and terminating electrolytes using a peristaltic pump.

Reagents

Potassium acetate, acetic acid, β-alanine, glycine, hydrochloric acid and Triton X-100 were of analytical-reagent grade from Wako (Osaka, Japan) and used without further purification.

Stock solutions of niacin derivatives were prepared by dissolving pyridine, nicotinamide (Wako), β-picoline, N-methylnicotinamide, 3-hydroxymethylpyridine, 3-acetylpyridine, isonicotinic acid hydrazide (Tokyo Kasei, Tokyo, Japan), thio-nicotinamide (Nacalai Tesque, Kyoto, Japan) and 6-aminonicotinamide (Sigma, St. Louis, MO, U.S.A.) in water.

Electrolytes

The three operational systems used are given in Table I. The leading electrolyte was prepared by diluting a stock solution of 1 M potassium acetate and 10% Triton X-100 and adjusting the pH by adding acetic acid. The terminating electrolyte for system I was prepared by dissolving β-alanine and adjusting the pH to 1.7 by adding hydrochloric acid. The terminating electrolyte for system II was prepared by dissolving glycine and adjusting the pH with hydrochloric acid to the same value as in system I. The terminating electrolyte for system III was acetic acid. In systems II and III, proton acts as the terminating ion.

TABLE I

OPERATING SYSTEMS

Parameter	Leading electrolyte	Terminating electrolyte		
		System I	System II	System III
Cation	K^+	β-Alanine	H^+	H^+
Counter ion	CH_3COO^-	Cl^-	Cl^-	CH_3COO^-
Concentration	10–50 mM	10 mM	10 mM	10 mM
Additive	0.1% Triton X-100	None	Glycine	None

RESULTS AND DISCUSSION

Niacin derivatives of β-picoline, 3-hydroxymethylpyridine, 6-aminonicotina-mide, isonicotinic acid hydrazide, nicotinamide, thionicotinamide, N-methylnicoti-namide and 3-acetylpyridine were used as samples and pyridine was added as it has a similar structure. All these substances have a pyridine ring and would be protonated to form cationic species. An acetate buffer of pH 4.0 was chosen as the leading electrolyte for protonation of the pyridine ring. With migration system I using β-alanine as the terminating ion, pyridine, β-picoline, 3-hydroxymethylpyridine and 6-aminonicotinamide migrated and could be separated. The order of migration seems

to depend on the dissociation constants of the substances. The other five substances, however, could not be detected with this migration system, because their effective mobilities are lower than that of the terminating ion. This situation could not be improved even by changing the pH of the leading electrolyte. Niacin could not be detected in a cationic system but could in an anionic system because it exists as an anionic species owing to the dissociation of its carboxyl group.

When glycine was used as the terminating electrolyte (system II), all the niacin derivatives could be detected in front of the terminating zone. Isonicotinic acid hydrazide, nicotinamide, thionicotinamide, N-methylnicotinamide and 3-acetylpyridine, however, were detected with a so-called "enforced zone", the effective mobility of which was lower than that of the terminating ion. A similar isotachopherogram to that with system II was also obtained with system III using acetic acid as the terminating electrolyte. With system I protonated β-alanine would act as the terminating ion, whereas with systems II and III proton itself would act as the terminating ion [9]. It is suggested that weak bases such as some niacin derivatives may be associated with proton in the terminating zone in addition to the leading zone and have a cationic charge. Consequently, they move back to the sample zone, and migrate in front of the terminating zone.

The relationship between the concentration of the leading ion and the R_E value (ratio of the potential gradient of the sample zone to that of the leading zone) of niacin derivatives and proton as terminating ion using system II is shown in Fig. 1. The R_E values of niacin derivatives remained almost unchanged at all concentrations of the leading ion, whereas the R_E value of the terminating ion increased with increasing concentration of the leading ion. The zones of isonicotinic acid hydrazide, nicoti-
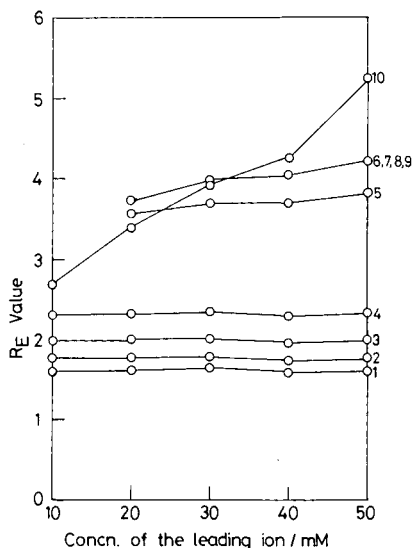

Fig. 1. Effect of the concentration of the leading ion on R_E values of niacin derivatives and the terminating ion. The pH was constant at 4.0. 1 = β-Picoline; 2 = pyridine; 3 = 3-hydroxymethylpyridine; 4 = 6-aminonicotinamide; 5 = isonicotinic acid hydrazide; 6 = nicotinamide; 7 = thionicotinamide; 8 = N-methylnicotinamide; 9 = 3-acetylpyridine; 10 = terminating ion.
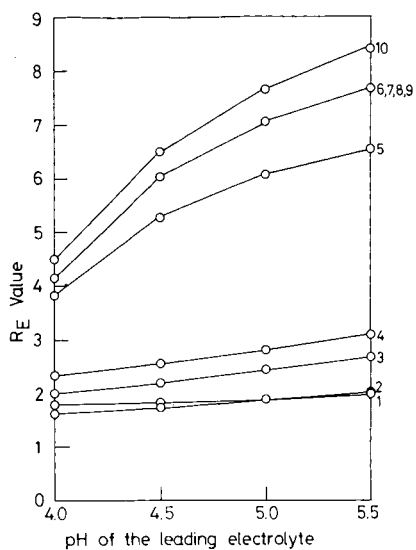
Fig. 2. Effect of pH of the leading electrolyte on R_E values of niacin derivatives and the terminating ion. The concentration of the leading ion was 40 mM. Line numbers as in Fig. 1.

namide, thionicotinamide, N-methylnicotinamide and 3-acetylpyridine were detected as an enforced zone when the concentration of the leading ion was up to 20 mM. However, when the concentration of the leading ion was 40 mM, the effective mobility
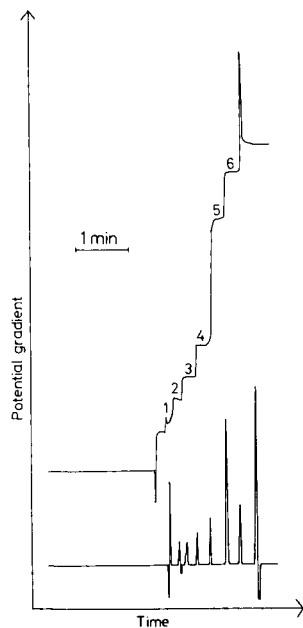
Fig. 3. Isotachopherogram of niacin derivatives. Electrolyte as in Fig. 1, except that the concentration of the leading ion was 40 mM. Numbers as in Fig. 1.

of the terminating ion became lower than that of sample ion and a normal isotachopherogram was obtained. This shows that the effective mobility of proton as terminating ion is controlled by the acid–base equilibrium with acetate ion as the counter ion of the leading electrolyte. Therefore, an increase in the concentration of the leading electrolyte decreases the effective mobility of proton as the terminating ion.

The relationship between the pH of the leading electrolyte and the R_E values of niacin derivatives at a leading ion concentration of 40 mM is shown in Fig. 2. With increasing pH, the R_E values of the niacin derivatives increased. However, the difference in mobility between pyridine and β-picoline decreased. At pH 4.0, β-picoline, pyridine, 3-hydroxymethylpyridine, 6-aminonicotinamide and isonicotinic acid hydrazide could be separated. Nicotinamide, thionicotinamide, N-methylnicotinamide and 3-acetylpyridine could also be detected under these conditions but as a mixed zone, and their separation could not be improved by changing the pH of the leading electrolyte.

An isotachopherogram obtained using 40 mM potassium acetate and acetic acid as the leading electrolyte and 10 mM glycine and hydrochloric acid as the terminating electrolyte is shown in Fig. 3. Six niacin derivatives, of β-picoline, pyridine, 3-hydroxymethylpyridine, 6-aminonicotinamide, isonicotinic acid hydrazide and nicotinamide, could be clearly separated. The calibration graphs were linear over the sample amounts range 1–5 nmol.

REFERENCES

1 Tadashi Kobayashi (Editor), *Vitamin Handbook (in Japanese)*, Vol. 2, Kagaku Dojin, 1989, p. 71.
2 Tadashi Kobayashi (Editor), *Vitamin Handbook (in Japanese)*, Vol. 5, Kagaku Dojin, 1989, p. 136.
3 Tadashi Kobayashi (Editor), *Vitamin Handbook (in Japanese)*, Vol. 3, Kagaku Dojin, 1989, p. 101.
4 C. J. Holloway (Editor), *Analytical and Preparative Isotachophoresis*, Walter de Gruyter, Berlin, New York, 1984, p. 109.
5 F. M. Everaerts, J. L. Beckers and Th. P. E. M. Verheggen, *Isotachophoresis: Theory, Instrumentation and Applications*, Elsevier, Amsterdam, Oxford, New York, 1976, p. 311.
6 F. S. Stover, *J. Chromatogr.*, 470 (1989) 131.
7 J. L. Beckers and F. M. Everaerts, *J. Chromatogr.*, 71 (1972) 380.
8 I. Nukatsuka and H. Yoshida, *J. Chromatogr.*, 237 (1982) 506.
9 J. L. Beckers and F. M. Everaerts, *J. Chromatogr.*, 68 (1972) 207.

PUBLICATION SCHEDULE FOR 1990

Journal of Chromatography and Journal of Chromatography, Biomedical Applications

MONTH	J	F	M	A	M	J	J	A	S	O	N	D
Journal of Chromatography	498/1 498/2 499	500 502/1	502/2 503/1 503/2 504/1	504/2 505/1	505/2 506 507 508/1	508/2 509/1 509/2 510	511 512 513	514/1 514/2 515	516/1 516/2 517 518/1	518/2 519/1	519/2 520 521/1 521/2 522	523
Cumulative Indexes, Vols. 451–500		501										
Bibliography Section		524/1		524/2		524/3		524/4		524/5		524/6
Biomedical Applications	525/1	525/2	526/1	526/2 527/1	527/2	528/1 528/2	529/1	529/2 530/1	530/2	531	532/2 532/1 533	534

INFORMATION FOR AUTHORS

(Detailed *Instructions to Authors* were published in Vol. 513, pp. 413–416. A free reprint can be obtained by application to the publisher, Elsevier Science Publishers B.V., P.O. Box 330, 1000 AH Amsterdam, The Netherlands.)

Types of Contributions. The following types of papers are published in the *Journal of Chromatography* and the section on *Biomedical Applications:* Regular research papers (Full-length papers), Notes, Review articles and Letters to the Editor. Notes are usually descriptions of short investigations and reflect the same quality of research as Full-length papers, but should preferably not exceed six printed pages. Letters to the Editor can comment on (parts of) previously published articles, or they can report minor technical improvements of previously published procedures; they should preferably not exceed two printed pages. For review articles, see inside front cover under Submission of Papers.

Submission. Every paper must be accompanied by a letter from the senior author, stating that he is submitting the paper for publication in the *Journal of Chromatography*. Please do not send a letter signed by the director of the institute or the professor unless he is one of the authors.

Manuscripts. Manuscripts should be typed in double spacing on consecutively numbered pages of uniform size. The manuscript should be preceded by a sheet of manuscript paper carrying the title of the paper and the name and full postal address of the person to whom the proofs are to be sent. As a rule, papers should be divided into sections, headed by a caption (*e.g.*, Abstract, Introduction, Experimental, Results, Discussion, etc.). All illustrations, photographs, tables, etc., should be on separate sheets.

Introduction. Every paper must have a concise introduction mentioning what has been done before on the topic described, and stating clearly what is new in the paper now submitted.

Abstract. Full-length papers and Review articles should have an abstract of 50–100 words which clearly and briefly indicates what is new, different and significant. (Notes and Letters to the Editor are published without an abstract.)

Illustrations. The figures should be submitted in a form suitable for reproduction, drawn in Indian ink on drawing or tracing paper. Each illustration should have a legend, all the *legends* being typed (with double spacing) together on a *separate sheet*. If structures are given in the text, the original drawings should be supplied. Coloured illustrations are reproduced at the author's expense, the cost being determined by the number of pages and by the number of colours needed. The written permission of the author and publisher must be obtained for the use of any figure already published. Its source must be indicated in the legend.

References. References should be numbered in the order in which they are cited in the text, and listed in numerical sequence on a separate sheet at the end of the article. Please check a recent issue for the layout of the reference list. Abbreviations for the titles of journals should follow the system used by *Chemical Abstracts*. Articles not yet published should be given as "in press" (journal should be specified), "submitted for publication" (journal should be specified), "in preparation" or "personal communication".

Dispatch. Before sending the manuscript to the Editor please check that the envelope contains four copies of the paper complete with references, legends and figures. One of the sets of figures must be the originals suitable for direct reproduction. Please also ensure that permission to publish has been obtained from your institute.

Proofs. One set of proofs will be sent to the author to be carefully checked for printer's errors. Corrections must be restricted to instances in which the proof is at variance with the manuscript. "Extra corrections" will be inserted at the author's expense.

Reprints. Fifty reprints of Full-length papers, Notes and Letters to the Editor will be supplied free of charge. Additional reprints can be ordered by the authors. An order form containing price quotations will be sent to the authors together with the proofs of their article.

Advertisements. Advertisement rates are available from the publisher on request. The Editors of the journal accept no responsibility for the contents of the advertisements.

Chemometrics Tutorials

Collected from Chemometrics and Intelligent Laboratory Systems - An International Journal, Volumes 1-5

edited by **D.L. Massart**, *Brussels,* **R.G. Brereton**, *University of Bristol, Bristol, UK,* **R.E.Dessy**, *Blacksburg, VA,* **P.K. Hopke**, *Potsdam, NY,* **C.H. Spiegelman**, *College Station, TX,* **W. Wegscheider**, *Graz, Austria*

The journal *Chemometrics and Intelligent Laboratory Systems* has a specific policy of publishing tutorial papers, (i.e. articles aiming to discuss and illustrate the application of chemometric and other techniques) solicited from leading experts in the varied disciplines relating to this subject. This book comprises reprints of tutorials from the first 5 volumes of this journal, covering the period from late 1986 to mid 1989. The authors of the papers include analytical, organic and environmental chemists, statisticians, pharmacologists, geologists, geochemists, computer scientists and biologists, which reflects the strong interdisciplinary communication. The papers have been reorganized into major themes, covering most of the main areas of chemometrics. This book is intended both as a personal reference text and as a useful background for courses in chemometrics and laboratory computing.

Contents: **Computers in the laboratory.** 1. Scientific word processing *(R.E. Dessy).* 2. The LIMS infrastructure *(R.D. McDowall, J.C. Pearce and G.S. Murkitt).* 3. Scientific programming with GKS: advantages and disadvantages *(E. Flerackers).* **Expert systems.** 4. Dendral and Meta-Dendral - the myth and the reality *(N.A.B. Gray).* On Gray's interpretation of the Dendral project and programs: myth or mythunderstanding? *(B.G. Buchanan, E.A. Feigenbaum and J. Lederberg).* Response to comments by Buchanan, Feigenbaum and Lederberg *(N.A.B. Gray).* 5. Expert systems in synthesis planning: a user's view of the LHASA program *(T.V. Lee).* 6. PROLOG for chemists. Part 1 *(G.J. Kleywegt, H.-J. Luinge and B.-J.P. Schuman).* 7. PROLOG for chemists. Part 2 *(G.J. Kleywegt, H.-J. Luinge and B.-J.P. Schuman).* **Experimental design and optimization.** 8. Practical exploratory experimental designs *(E. Morgan, K.W. Burton and P.A. Church).* 9. Optimisation via Simplex. Part 1: Background, definitions and a simple application *(K.W.C. Burton and G. Nickless).* 10. Chemometrics and method

development in high-performance liquid chromatography. Part 1: Introduction *(J.C. Berridge).* 11. Chemometrics and method development in high-performance liquid chromatography. Part. 2: Sequential experimental designs *(J.C. Berridge).* **Signal processing, time series and continuous processes.** 12. Fourier transforms: use, theory and applications to spectroscopic and related data *(R.G. Brereton).* 13. Dispersion vs. absorption (DISPA): a magic circle for spectroscopic line shape analysis *(A.G. Marshall).* 14. Sampling theory *(G. Kateman).* **Multivariate and related methods.** 15. Principal component analysis *(S. Wold, K. Esbensen and P. Geladi).* 16. Multivariate data analysis: its methods *(M. Mellinger).* 17. Correspondence analysis: the method and its application *(M. Mellinger).* 18. Spectral map analysis: factorial analysis of contrasts, especially from log ratios *(P.J. Lewi).* 19. Similarities and differences among multivariate display techniques illustrated by Belgian cancer mortality distribution data *(A. Thielemans, P.J. Lewi and D.L. Massart).* 20. Some fundamental criteria for multivariate correlation methodologies *(O.H.J. Christie).* 21. Mixture analysis of spectral data by multivariate methods *(W. Windig).* 22. Interpretation of direct latent-variable projection methods and their aims and use in the analysis of multicomponent spectroscopic and chromatographic data *(O.M. Kvalheim).* 23. Soft modelling and chemosystematics *(N.B. Vogt).* 24. Multivariate analysis in geology and geochemistry: an introduction *(H.J.B. Birks).* 25. Multivariate analysis in geoscience: fads, fallacies and the future *(R.A. Reyment).* 26. Interpretation of lithogeochemistry using correspondence analysis *(M. Mellinger).* 27. Multivariate analysis of stratigraphic data in geology: a review *(H.J.B. Birks).* **Fuzzy methods.** 28. Fuzzy theory explained *(M. Otto).* Author Index. Subject Index.

Elsevier Science Publishers